NON-LINEAR PARAMETER ESTIMATION USING VOLTERRA SERIES

by

ANIMESH CHATTERJEE

DEPARTMENT OF MECHANICAL ENGINEERING

INDIAN INSTITUTE OF TECHNOLOGY KANPUR

JULY, 2001

NON-LINEAR PARAMETER ESTIMATION USING VOLTERRA SERIES

A Thesis Submitted
in Partial Fulfilment of the Requirements
for the Degree of
DOCTOR OF PHILOSOPHY

by

ANIMESH CHATTERJEE

to the

DEPARTMENT OF MECHANICAL ENGINEERING
INDIAN INSTITUTE OF TECHNOLOGY KANPUR
JULY, 2001

CERTIFICATE

It is certified that the work contained in the thesis titled, "**NONLINEAR PARAMET ESTIMATION USING VOLTERRA SERIES**" has been carried out under supervision and that this work has not been submitted elsewhere for the award of a degr

Dr. Nalinaksh S. V
Profes
Department of Mechanical Engineer
Indian Institute of Technology, Kanp

SYNOPSIS

Name of the student Animesh Chatterjee **Roll No** 9710561

Degree for which submitted Ph.D. **Department** Mechanical Engineering

Thesis Title Nonlinear Parameter Estimation using Volterra Series

Name of the thesis supervisor Dr. Nalinaksh S. Vyas

System identification is an inverse problem of determination of the mathematical structure of the physical system from measurements of the forcing functions induced upon it and the resultant response. Inverse problems in nonlinear analysis require techniques with rigourous theoretical base, which can provide valid routes to parameter estimation. The structure of the Volterra series (Volterra 1930, 1959), which models the relationship between system response and input in terms of a series of first and higher order convolution integrals, provides an analytical platform which can be utilized for parameter estimation.

In the present study, the structured Volterra response representation under harmonic excitation is employed to develop identification and parameter estimation procedures for nonlinear systems. Single and multi-degree of freedom systems have been considered. Single and multi-tone harmonic forcing functions have been employed for system excitation. Frequency domain transformation of Volterra kernels is carried out to obtain higher order Frequency Response Functions, which are interpreted and processed for system identification and estimation. Practical application of Volterra series, however poses two basic difficulties - convergence of the series and measurement of individual kernel functions (Christensen, 1968; Czarniak and Kudrewicz, 1984; Tomlinson et al., 1996). A major emphasis has been put in this work on issues related to convergence of the series, implicit errors and measurability of higher order response components.

Volterra series is a non-parametric form of response representation. Non-parametric identification concerns modeling in a function space by input-output mapping, for systems where sufficient information on the mathematical structure or class is not available. Parametric identification, on the other hand, refers to systems where sufficient *a-priori*

information about the mathematical structure of the class to which the system belongs, i available. Identification procedure, in such cases reduces to estimation of system parameter through a search in parameter space. A review of identification procedures in application involving networks and devices, has been done by Haber and Unbehauen (1990) for various classes of nonlinearity, such as Wiener model, Hammerstein model, Wiener-Hammerstein model etc. Research in system structure identification, for mechanical engineering applications is relatively scant. Most of the works available in literature (Rice and Fitzpatrick, 1988, 1991; Mottershed and Stanway, 1986; Bendat and Peirsol, 1986; Khan and Vyas, 1999) pertain to parameter estimation based on an assumption of polynomial nonlinearity or specific non-polynomial nonlinearity forms. Nayfeh (1985) has suggested a combination of perturbation and free vibration tests for identification of certain nonlinear characteristics such as hysteresis, presence of self-oscillatory terms etc. Bendat et al (1992) developed a general identification technique for measured input-output stochastic data for a wide range of nonlinearities such as Duffing oscillator, Van-der Pol oscillator, dead band and clearance nonlinaerity.

Discussions on Volterra kernel identification can be found in review papers by Hung and Stark (1977), Billings (1980), Haber and Unbehauen (1990). Volterra series involves convolution between the applied excitation and the kernels of the system. The first order kernel is same as impulse response function of a linear system. Higher order kernel functions are understood as multi-dimensional impulse response functions. A nonlinear system can be either characterised, in time domain, through kernel functions (Schetzen, 1965a, 1965b, 1974; Marmarelis and Naka, 1974; Korenberg, 1973) or through kernel transforms in frequency domain (Bedrosian and Rice, 1971; Baumgarter and Rugh, 1975; Boyd, Tang and Chua, 1983; Chua and Liao, 1989, 1991; Gifford and Tomlinson, 1989). The Wiener series (Wiener, 1958) attempts to circumvent the two basic difficulties, of convergence and measurement of Volterra kernels. Wiener functionals are orthogonal for white Gaussian excitation function and can be separated through cross-correlation techniques. However Wiener theory can only be applied for Gaussian inputs and the analysis requires to be done for a large number of input-output records for obtaining statistical averages of the estimates (Khan and Vyas, 1999).

The present study attempts to develop an identification and parameter estimation approach for nonlinear systems using Volterra series response representation under harmonic excitations. Response is measured in time domain and filtered to obtain various response harmonic amplitudes. Most nonlinear analysis problems consider only the Duffing oscillator as a representative case. In engineering analysis, it is however, also important to recognize the type of nonlinearity influencing the system. In the present work, an identification procedure based on response component separation of the Volterra series is suggested for classification between polynomial and non-polynomial form of nonlinearities. Distinction is further made between a symmetric and asymmetric form of nonlinearity. Higher order kernel transforms are investigated for general polynomial forms and a peak ratio algorithm is developed to identify the polynomial structure up to the cubic term. The procedures are illustrated with simulated numerical results.

Limited convergence is an inherent difficulty associated with the series and needs to be addressed rigorously, prior to its application to a physical system. The problem of convergence is addressed, in this study, in terms of convergence of individual frequency harmonics of the nonlinear response. Though the procedure is applicable to general polynomial form nonlinearity, it is illustrated for a Duffing oscillator subjected to harmonic excitation. A general and structured series expression is obtained for amplitudes of all response harmonics and convergence is investigated in terms of a non-dimensional nonlinear parameter. Critical values of this parameter, representing the upper limit of excitation level for the convergence, are defined for a wide range of excitation frequencies. Zones of convergence and divergence of the response series are presented graphically, for a range of the non-dimensional nonlinear parameter and the number of terms included in the approximation of a response harmonic. An algorithm based on ratio test is presented to compute the critical value of the non-dimensional nonlinear parameter. Results obtained from the suggested algorithm are found to be in close agreement with the exact values. The method gives better results compared to previous methods and has wider application in terms of excitation frequency. The procedure is also investigated for a two-degree-of-freedom system.

procedures are based on a recursive iteration technique and employ the fact that for suc systems higher order Volterra kernels can be sysnthesised from first order kernel Measurements are made for the first and higher order kernels. The higher order kernels are als synthesised mathematically in terms of the measured first order kernels and the unknow nonlinear parameters. Estimation of these nonlinear parameters is carried out throug comparison between synthesised and measured higher order kernels. The estimation procedur considers the response series representation up to a finite number of terms, which is decided b convergence requirements of Volterra series. The problem of low signal strength of highe harmonics is investigated and a measurability criterion is proposed for selection of excitatio level and range of excitation frequency. The procedure is illustrated through numerica simulations on a Duffing oscillator typically representing a rotor-bearing system.

Estimation procedures for single-degree-of-freedom systems with single-point excitation ar extended to multi-degree-of-freedom systems. These systems involve cross-kernel functions i addition to direct kernel functions (Worden et al., 1997). Kernel synthesis formulations fo higher order direct and cross-kernels are developed in matrix forms. Multi-point harmoni excitation is designed for measurement and estimation of kernel transforms. Using kerne transform synthesis formulations, the vector of nonlinear parameters and linear paramete matrices are estimated through recursive iteration procedure. The algorithm is structured an can be readily employed for design of experiments. Numerical studies have been carried out fo a typical two-degree-of-freedom nonlinear model representing a rotor-bearing system wit cross-coupled stiffness coefficients.

Experimental investigations and validation of the developed estimation algorithms have been carried out on a laboratory rotor-bearing test rig. Harmonic excitation is applied to the system through the bearing housing caps using an electro-dynamic shaker. Excitation and response signals are simultaneously measured and processed. Linear and nonlinear stiffness parameters are estimated and compared with approximate theoretical formulations and some previous experimental results.

parameters are estimated and compared with approximate theoretical formulations and some previous experimental results.

To summerise, a structured form of nonlinear identification and estimation procedure has been developed. System identification is carried out to distinguish polynomial form of nonlinearity from other forms. The form of the polynomial is also identified. Estimation of the parameters of polynomial form nonlinear system is carried out through a recursive iteration procedure. The procedures, though illustrated for a cubic nonlinearity, are general in application and can be extended to any form of polynomial nonlinearity. The procedures are extended for multi-degree-of-freedom systems. Practical problems such as convergence, presence of background noise and low signal strength of higher harmonics have been discussed and excitation levels and frequencies have been designed to address and overcome these problems.

ACKNOWLEDGEMENTS

I take this opportunity to express my deep sense of gratitude to my thesis supervisor, Prof. N. S. Vyas for his valuable guidance, constructive criticisms and constant encouragement throughout my thesis work. I must also thank him for providing me complete freedom with the computational and laboratory facilities.

I thank Prof. A.K. Mallik, with whom I have had some critical discussions in the area of nonlinear vibrations. My thanks should also go to Dr. V. Raghuram for his ready help in sorting out instrumentation hardware and computer problems. I also acknowledge financial support provided by the Propulsion Panel, Aeronautical Research and Development Board, Government of India, in carrying out the present work.

I am thankful to my senior research scholars, Dr. Goutam Chakraborty, Dr. Ahmad Ali Khan and Dr. Goutam Pohit for their help. I must also mention here that our discussions during the tea session in the college canteen, on several occasions, recharged me with new ideas and thinking.

Finally I am deeply indebted to my wife, Manimala, for her immense understanding and patience during those busy days.

ANIMESH CHATTERJEE

CONTENTS

LIST OF FIGURES

LIST OF TABLES

NOMENCLATURE

c	Damping coefficient
c_{xx}, c_{yy}	Direct damping coefficients in two-degree-of-freedom system
${}_{k}^{n}e$	Series approximation error in nth response harmonic for k number of terms
${}^{\kappa}e_{k}(nr)$	Series approximation error in nth response harmonic for k number of terms and for response coordinate $\kappa = x, y$
$f(t)$	Excitation force
$f_x(t), f_y(t)$	Excitation force along x-direction and y-direction respectively
$\bar{f}_x(t), \bar{f}_y(t)$	Non-dimensional excitation forces along x-direction and y-direction respectively
g	Bearing pre-load
$g[x(t)]$	General expression for the restoring force
$h_1(\tau_1)$	First order Volterra kernel
$h_1^{(j:\eta)}(\tau_1)$	First order Volterra kernel in multi-degree-of-freedom system between response at jth coordinate and excitation at η-coordinate.
$h_2(\tau_1, \tau_2)$	Second order Volterra kernel
$h_2^{(j:\eta_1\eta_2)}(\tau_1, \tau_2)$	Second order Volterra kernel in multi-degree-of-freedom system for response at jth coordinate and excitations at η_1 , η_2 - coordinate.
$h_n(\tau_1, \tau_2, ..., \tau_n)$	nth order Volterra kernel
k	Number of series terms
k_1	Linear stiffness coefficient
k_2	Square nonlinear stiffness coefficient
k_3	Cubic nonlinear stiffness coefficient
k_{xx}, k_{yy}	Direct linear stiffness coefficients along x and y coordinates
k_{xy}, k_{yx}	Cross linear stiffness coefficients between x and y coordinates

$k_{2x}^{(\eta_1\eta_2)}$	Second order nonlinear stiffness coefficients along x-coordinate
$k_{2y}^{(\eta_1\eta_2)}$	Second order nonlinear stiffness coefficients along y-coordinate
$k_{3x}^{(\eta_1\eta_2\eta_3)}$	Third order nonlinear stiffness coefficients along x-coordinate
$k_{3y}^{(\eta_1\eta_2\eta_3)}$	Third order nonlinear stiffness coefficients along y-coordinate
${}^{n}k_{crit}$	Limiting number of series term in nth harmonic for convergence
m	Mass of the system
m_x, m_y	Mass of the system along x-coordinate and y-coordinate
r	Non-dimensional frequency
$x(t), y(t)$	Response coordinates
$x_n(t)$	nth order response component in Volterra series
$x^{(j)}(t)$	Response along jth coordinate in multi-degree-of-freedom system
$x_n^{(j)}(t)$	nth order response component for jth coordinate
A, B, C	Excitation force amplitude
$H_1(\omega)$	First order Volterra kernel transform
$H_1^{(j:\eta)}(\omega)$	First order Volterra kernel transform in multi-degree-of-freedom system between jth response and excitation at η-coordinate
$H_2(\omega_1,\omega_2)$	Second order Volterra kernel transform
$H_2^{(j:\eta_1\eta_2)}(\omega_1,\omega_2)$	Second order Volterra kernel transform in multi-degree-of-freedom system for jth response and excitations at η and η_2-coordinate
$H_3(\omega_1,\omega_2,\omega_3)$	Third order Volterra kernel transform
$H_n(\omega_1,...,\omega_n)$	nth order Volterra kernel transform
$H_n^{(j:\eta_1\eta_2...\eta_n)}(\omega_1,...,\omega_n)$	nth order Volterra kernel transform for multi-degree-of-freedom system
$H_n[f(t)]$	nth order Volterra operator
$MI(m\omega)$	Measurability index of mth harmonic

$X(m\omega)$	mth harmonic response amplitude
$X^{(j)}(m_1\omega_1 + m_2\omega_2)$	Combination tone response harmonic amplitude at jth coordinate
$Z(r)$	Fourier transform of non-dimensional response $\eta(\tau)$
$Z(nr)$	nth order non-dimensional response harmonic amplitude
${}^{\kappa}Z(nr)$	nth order non-dimensional response harmonic amplitude for $\kappa = x, y$
${}_{k}Z(nr)$	Response series of $Z(nr)$ with k number of terms
${}^{\kappa}_{k}Z(nr)$	Response series of $Z(nr)$ with k number of terms for $\kappa = x, y$
β	Scaling parameter between cubic nonlinear stiffness coefficients along x and y coordinates.
ζ	Damping
ζ_{xx}, ζ_{yy}	Damping along x and y coordinates
$\eta(\tau)$	Non-dimensional response
$\eta'(\tau)$	Non-dimensional velocity
${}^{x}\eta(\tau)$, ${}^{y}\eta(\tau)$	Non-dimensional response along x and y coordinates respectively
${}^{\kappa}\eta(\tau)$	Non-dimensional response along $\kappa = x$ or y direction
λ_2	Second order non-dimensional nonlinear parameter
λ_3	Third order non-dimensional nonlinear parameter
λ^{L}_{ij}	Linear non-dimensional stiffness
$\lambda^{N}_{xx}, \lambda^{N}_{yy}$	Cubic nonlinear non-dimensional stiffness, direct term coefficient
$\lambda^{N}_{xy}, \lambda^{N}_{yx}$	Cubic nonlinear non-dimensional stiffness, cross-term coefficient
${}^{1}_{k}\lambda_{crit}$	Critical value of cubic nonlinear parameter for first harmonic
${}^{3}_{k}\lambda_{crit}$	Critical value of cubic nonlinear parameter for third harmonic
μ	Ratio of system mass along x-coordinate to y-coordinate
$\sigma_i(n\omega)$	ith series term in response harmonic series expression of $X(n\omega)$

${}^{\kappa}\sigma_i(m_1\omega_1 + m_2\omega_2)$	ith term in the response harmonic amplitude series for the combination tone $(m_1\omega_1 + m_2\omega_2)$, for $\kappa = x, y$-coordinate
τ	Non-dimensional time
ϕ_n	Phase angle of nth harmonic complex response amplitude
ω	Excitation frequency
ω_n	Natural frequency
$\omega_{p,q}$	A general higher order harmonic of ω
$\Gamma_3(\omega)$	Third order kernel factor

CHAPTER 1

INTRODUCTION

Inverse problems of system identification and parameter estimation are crucial in nonlinear analysis. Response behaviour of nonlinear systems under specific excitation conditions can be predicted accurately only when the system structure and the parameters are completely known. While extensive research has been carried out in identification and parameter estimation of linear systems, research on nonlinear system identification has been relatively less.

Identification in linear mechanical and structural engineering applications is equivalent to finding the coefficients of the mass-spring-damper mathematical models. Identification problem is more involved for a nonlinear system, due to existence of various forms of restoring and dissipative force nonlinearities in physical systems. Nonlinearity structure of these forces can be of a polynomial or non-polynomial form. The Duffing oscillator is a typical example of polynomial form of restoring force nonlinearity, whereas quadratic damping, hysteretic damping and fractional power stiffness in rolling element bearings are some of the examples of non-polynomial form of nonlinearity. A nonlinearity structure can be a symmetric function of displacement, as in Duffing oscillator or asymmetric as in the case of a bilinear oscillator. System definition problem of a nonlinear system, therefore, consists of (i) identification of the nonlinearity structure through the most appropriate mathematical model and (ii) subsequent estimation of the various parameters in the mathematical model. However, few reports are available in literature on the nonlinearity structure identification and most of the reported works suggest parameter estimation procedures based on some assumed nonlinearity model.

The objective of the present study is to employ the Volterra series to address problems of both -identification and estimation in nonlinear systems. Procedures based on analysis of higher order frequency response functions defined through Volterra series, are developed for classification of restoring force nonlinearity. The dissipative force is assumed to be

linear. Systems are classified as having either polynomial type nonlinearity, where the restoring or spring force can be represented by a polynomial with constant coefficients, or non-polynomial type, where the spring force does not fall into this category. For polynomial class of spring forces, the structure of the polynomial is further identified. Non-polynomial class of nonlinearities is not sub-classified further. Parameter estimation methods have been developed for systems with polynomial nonlinearity. The approach is based on estimation of first and higher order Volterra kernels in the frequency domain, and then employing their mutual relationships to extract values of nonlinear parameters. The estimates are refined through recursive iteration. The series was developed by Vito Volterra in the early part of twentieth century and later used by Wiener for nonlinear system analysis. Wiener also extended the Volterra series for stochastic input-output relationship mapping, through a set of orthogonal functionals known as Wiener G-functionals and the new series came to be known as Wiener series.

The structures of Volterra and Wiener series provide rigorous theoretical platforms for response analysis of a nonlinear system. Volterra series represents the response of a system by a series of first and higher order convolution integrals. Convolution is carried out between the applied excitation and the kernels of the system. The first order kernel is the same as impulse response function of a linear system. Higher order kernel functions are understood as multi-dimensional impulse response functions. Multi-dimensional Fourier transforms of these kernel functions are called kernel transforms. A nonlinear system can be characterised either in time domain through kernel functions or through kernel transforms in the frequency domain. Two basic difficulties associated with practical application of Volterra series are convergence of the series and measurement of individual kernel functions. These difficulties are circumvented in the Wiener series. Wiener functional are orthogonal for white Gaussian excitation function and can be separated through cross-correlation techniques. However Wiener theory can only be applied for Gaussian inputs and the analysis requires to be done for a large number of input-output records for obtaining statistical averages of the estimates.

The procedures in the present thesis employ harmonic excitation functions and involve analysis of response harmonic characteristics. Harmonic excitations are most common type of excitation and can easily be generated in laboratory or field. Response under applied harmonic excitations is measured and harmonic contents are filtered for further analysis. A detailed review of available literature on identification and estimation of nonlinear system with particular emphasis on Volterra and Wiener series is given in Chapter 2. Various methods suggested by researchers are discussed with their applicability and limitations.

An introduction to Volterra series response representation and method of harmonic probing is given in Chapter 3. Response structures under single-tone and multi-tone harmonic excitations are formulated in terms of first and higher order kernel transforms. Series form expressions for response harmonic amplitudes are extracted from the overall response representation.

Procedures developed for identification of the form of nonlinearity are presented in Chapter 4. Characteristics of the various component orders in the Volterra series and their frequency transforms are discussed and employed to distinguish between polynomial form and non-polynomial form of nonlinearities. The form of Volterra series components also provides information on whether the nonlinearity is symmetric with respect to deformation or not. Damping is assumed to be linear in the analysis. Higher order kernel transforms are investigated for general polynomial forms and a peak ratio algorithm is developed to identify the polynomial structure up to the cubic term.

The parameter estimation procedure for single-degree-of-freedom systems is presented in Chapter 5. First and higher order kernel transforms are estimated from the measured response harmonic amplitudes. Kernel synthesis formulations are employed to estimate nonlinear parameters. Estimated nonlinear parameters are then employed to refine the kernels and the recursive iteration process is continued till desired convergence is achieved. The kernels are approximated from the measured response by considering a finite number of terms of the infinite number of power terms of the Volterra series.

Convergence of the truncated series is a function of the response harmonic under consideration, amplitude and frequency of excitation force and the yet to be determined linear and nonlinear parameters of the system. Major emphasis has been laid, in the present study, on carrying out a detailed convergence study and appropriate design of experiments for parameter estimation. Additionally, a simple procedure based on a ratio test is also suggested to determine the optimum number of terms for series convergence. Measurability of higher harmonics is an associated problem, which is highlighted in the present study. The problem of low signal strength of higher harmonics is investigated and a measurability criterion is developed for selection of excitation level and range of excitation frequency. The procedure is illustrated with numerical simulations for a Duffing oscillator, with data typically representing a rotor-bearing system. The results highlight the accuracy of estimation, particularly of the nonlinear parameter and damping.

The concept of single-point excitation based Volterra series has been extended to multi-degree-of-freedom systems by Tomlinson et al., using direct and cross-kernel functions. This extended structure is employed in Chapter 6, for developing parameter estimation procedure for a multi-degree-of-freedom system. Kernel synthesis formulations for higher order direct and cross-kernel transforms are developed in matrix forms. Multi-point harmonic excitations are designed for measurement and estimation of the kernel transforms. Formulations for synthesis of higher order transforms from lower orders are developed and the nonlinear parameter vector and linear parameter matrices are estimated using recursive iteration technique. The algorithm is structured and presented in a generic form so that it can be employed for general multi-degree-of-freedom systems. Numerical studies have been carried out for a typical two-degree-of-freedom nonlinear model representing a rotor-bearing system with cross-coupled bearing stiffness coefficients. Experimental investigations are described in Chapter 7. The laboratory test rig, excitation procedure and instrumentation have been discussed. Estimated linear and nonlinear bearing stiffness parameters are validated through comparisons with available theoretical approximations and previous experimental investigations.

CHAPTER 2

LITERATURE REVIEW

Identification of dynamic systems from input-output data is of considerable importance in areas of applied mechanics, control engineering, chemical and biological processes. System response under dynamic conditions can be predicted reliably and accurately only if the system model is known in terms of its mathematical structure and physical parameters. The need and objective of system identification can be manifold. In control problems, the objective is often to design control strategies for a particular performance. In structural engineering, the purpose of identification is to analyze and predict the structural response under a wide variety of excitations. Identification can be at times, usefully employed to diagnose malfunctioning or to detect damages through changes in the system parameters.

Procedures for input-output analysis and identification of a linear dynamic system are by now well established. A large number of identification techniques have been developed such as Frequency Response Function and curve fitting method, Ewins (1984); time domain identification technique, Ibrahim (1973); method of spectral density functions, Bendat and Peirsol (1986); Instrumental variable method, Fritzen (1986). System modeling in linear form is widely used as in most practical situations, system response can be reasonably analysed and predicted by a linear model. However, many physical phenomena like multiple steady states, jump, limit cycles, sub-harmonic and super-harmonic resonances, self-excited oscillations etc. cannot be predicted or explained by linear analysis.

Characterisation of nonlinear dynamic systems, from input-output data, is broadly categorised into parametric and non-parametric identification (Astrom and Eykhoff, 1971; Hung and Stark, 1977; Billings, 1980). Parametric identification refers to systems where sufficient a-priori information about the mathematical structure of the class to

which the system belongs, is available. The identification procedure, in such cases reduces to estimation of system parameters through a search in parameter space. Non-parametric identification concerns modeling in a function space by input-output mapping, for systems where sufficient information on the mathematical structure or class is not available.

2.1 Non-Parametric Identification Procedures

The input-output mapping, under non-parametric methods, is done through a series of functionals or a series of orthogonal functions. In functional series representation, such as in Volterra series or Wiener series, identification consists of determining the kernels of the functionals either in time-domain or in the frequency-domain. In orthogonal series representation, such as in Restoring Force Mapping techniques, response variables are represented in terms of some orthogonal series and identification consists of determination of the coefficients of the terms in the series. These series are generally infinite in nature and are to be truncated to finite number of terms for the purpose of identification. Identification results improve in accuracy with increasing number of terms in the truncated series. However, computational effort makes it prohibitive to consider large number of terms and in most cases, identification is limited to first few series terms.

2.1.1 Restoring force Mapping Techniques

Masri and Caughy (1979) expanded the nonlinear restoring force in a series of Chebyshev polynomials in terms of the response variables, displacement and velocity. Assuming the mass of the system as known, inertia force was calculated from the measured acceleration. Restoring force was then obtained from the measured applied force and the computed inertia force. Nonlinear relationship between the restoring force and the response variables was obtained by fitting a surface using regression over the displacement-velocity plane. The procedure can be applied to a wide class of nonlinear systems and there is no restriction on the type of input excitation. The method was later extended, by Masri et al (1982), for multi-degree-of-freedom systems. Modal matrix was assumed to be known and was used to transform the restoring force functions into

generalised forces. Udwadia and Kuo (1981) used arbitrary orthogonal sets of functions for restoring force mapping on close coupled multi-degree-of-freedom systems such as multi-story buildings. The method, was further extended to cases of support excitation by Masri et al (1987), in which the restoring force was separated into linear and nonlinear part and only the nonlinear part was approximated by Chebyshev polynomial. Ibrahim and Yang (1988) used power series to represent the restoring force for branched multi-degree-of-freedom systems. The advantage of using power series mapping is that when the nonlinearity is indeed in polynomial form, the coefficients exactly match with the nonlinear parameters. Further work in this direction has been reported by Worden and Tomlinson (1989) and Al-Hadid (1989). Restoring force mapping technique provides identification methods for a wide class of nonlinear systems, but it suffers from the mean bias and drift error which are introduced during integration of acceleration data to obtain velocity and displacement records. The method is not suitable for simple polynomial nonlinearity, like Duffing oscillator, because non-parametric mapping involves relatively large set of coefficients to be determined for sufficiently accurate representation of such nonlinearities.

2.1.2 Volterra and Wiener Series

Volterra series (1930, 1959) represents the response of a system in a functional series form. The first term in the series is the well-known convolution integral used for input-output mapping of linear systems. Subsequent series terms consist of higher order convolution integrals operating on the input functions through higher order impulse response functions known as Volterra kernels. Frechet (1910) was first to explore the possibility of a continuous functional on a set of functions to be represented in a power series form. Vitto Volterra studied these functionals as early as 1913 and represented the input-output relationship of a general system in a functional series form, which later came to be known as Volterra series. The series was first applied for nonlinear system analysis by Norbert Wiener (1958). Two basic difficulties associated with practical application of Volterra series are convergence of the series and measurement of individual Volterra kernels of the given system. Measurement of individual kernels is possible only if the contribution of each of the Volterra operators can be separated from the total response.

Wiener circumvented these difficulties by constructing a new functional series with a set of orthogonal functionals known as Wiener G-functionals. These functionals are orthogonal with respect to Gaussian white noise excitation. Due to orthogonal property of the functional, Wiener kernels can be conveniently separated through cross-correlation techniques. Wiener kernels are related to Volterra kernels and once Wiener kernels are separated, Volterra kernels can be subsequently determined. Wiener series has improved convergence characteristics because the convergence of an orthogonal series is a convergence in mean and thus Wiener series describes a larger class of nonlinear systems (Schetzen, 1980).

Barret (1963) and Flake (1963) have presented various details on use of Volterra series in nonlinear system analysis. Brillinger (1970) defined higher order transfer functions for polynomial systems and outlined the method of estimating these transfer functions by multi-tone harmonic excitation and by Gaussian excitation using higher order cumulant spectra. Bedrosian and Rice (1971) illustrated frequency domain methods for response characterisation of nonlinear systems under harmonic excitation as well as random excitation along with the effect of noise on the measured response. Concepts of inverse functional and inverse operator were also introduced. Palm and Poggio (1977) derived rigorous results concerning conditions under which a nonlinear functional admits Volterra and Wiener representations. They also provided sufficient conditions for connection between Volterra and Wiener representation. Lesiak and Krener (1978) studied existence and uniqueness criteria of Volterra series. Yasui (1979) discussed a stochastic functional Fourier series for nonlinear system analysis. In analogy to Fourier coefficients, Fourier kernels are introduced and are determined through cross-correlation between the output and the orthogonal basis functions of the stochastic input. Possible links between the Fourier and Volterra series are investigated and relationship between Volterra and Wiener series is discussed for a subclass of nonlinear systems. Palm and Popel (1985) have elaborated on the scope and limitation of Volterra representation and Weiner-like identification of nonlinear systems with reference to polynomial systems and discontinuity in system characteristic functions. Bussang et al. (1974) have determined interaction of multiple input signals within a nonlinear system. They introduced the

concept of nonlinear transfer function and discussed determination of these nonlinear transfer functions by the method of harmonic probing. Various response characteristics observed in electrical and communication networks such as de-sensitisation, inter-modulation, compression etc were explained. Further work based on single-tone and multi-tone harmonic excitation was carried out by Weiner and Spina (1980), Victor and Shapley (1980) and Chua and Ushida (1981).

2.1.3 Convergence of Volterra Series

Although Volterra series provides a structured approach for nonlinear system analysis, its convergence problem puts severe limitations to its use. Volterra series is a power series in functionals and similar to a Taylor series, it suffers from the problem of limited convergence. Chrinstensen (1968) and Czarniak and Kudrewicz (1984) have studied the convergence characteristics of Volterra series. Sandberg (1992) has shown that a truncated Volterra series provides a uniform approximation to the infinite Volterra series on a ball of bounded input for a large class of systems. Tomlinson and Manson (1996) studied the convergence of first order FRF of a Duffing oscillator under harmonic excitation and presented a simple formula for determining the upper limit of excitation level. However the formula is valid only for excitation frequencies close to the system natural frequency.

2.1.4 Time-domain Identification of Volterra and Winer kernels

Katzenelson and Gould (1962) developed an iterative time-domain method for obtaining the kernels. The method seeks to identify the system equivalently in terms of the solution needed for an optimum filter. Schetzen (1965) presented a method for measuring the Volterra kernels as multi-dimensional impulse responses of a finite order nonlinear system. A method for synthesis of higher order Volterra kernels was presented in a subsequent paper by the same author (1965a). Harris and Lipidus (1967) used Wiener theory for identification and synthesis of nonlinear chemical reactor system with two level inputs. Gardiner (1966,1968) developed a method for separation of the response into first order and higher order response components. The method is based on measuring responses at different excitation levels and solving a system of algebraic equations, in

which response components are related to the measured response values at every time instant by a Vander-Monde matrix. Sandberg and Stark (1968) measured the kernels of pupillary system up to second order using Lee-Schetzen's cross-correlation technique as well as bi-pulse method. Simpson and Powers (1972) discussed a correlation technique with periodic input function, in which the response components and Volterra kernels are directly separated by taking multi-dimensional cross-correlation between the output and input over the periodic duration of the input function. A method of directly identifying the Volterra kernels using an exponentially decaying function multiplied by a bounded zero mean independent process, was developed by Korenberg (1973). Marmarelis and Naka (1973) presented two-input approach for kernel identification in the response of catfish retina. Hung and Stark (1977) gave a comprehensive review of various kernel identification methods.

Fakhouri (1980) and Billings and Fakhouri (1980) analysed a nonlinear feedback system and developed an identification algorithm for open and close loop nonlinear systems based on pseudo-random excitation. Ewen and Weiner (1980) identified second order kernels for a nonlinear system with finite number of power law devices. The system is excited by a sum of exponentially decaying signals and the measured input-output data are processed using pencil-of-functions approach of system identification. This results in a complete set of linear equations involving all the parameters, which then can be solved to obtain the second order kernel.

Fakhouri, Billings and Wormald (1981) discussed estimation errors in Volterra kernel identification procedures through correlation techniques. They derived expressions for variance of the first and second order correlation function estimates and found that the variance is dependent on the record length, mean level and power of the input and the structure of the system under investigation. Haber (1989) has discussed kernel estimation of the discrete Volterra series for quadratic block oriented models. Koukoulas and Kalouptsidis (1995) proposed an approach for identification of Volterra kernels based on cross-cumulants and their spectra, rather than cross-correlation. The input to the system is a stationary zero mean Gaussian random process that is not necessarily white. Using the

cross-cumulant of the output sequence with m copies of the input, it is shown that the cumulant operator of the m copies of the input with any Volterra operator of order less than m is equal to zero. Using properties of cumulants, formulae are derived for computation of the Volterra kernels in the time and frequency domains.

2.1.5 Frequency-Domain Identification of Volterra and Wiener Kernels

Frequency domain methods determine kernel transforms over the frequency space. Two types of excitation are used for kernel transform estimation - harmonic excitation and random excitation. Wiener kernel transforms can be identified only through random excitation whereas Volterra kernel transforms, can be estimated through use of both random and harmonic excitations.

Method of Stochastic Excitation: French and Butz (1973) developed a general frequency domain method for calculation of higher order Wiener kernels using exponential functions as a set of orthogonal functions for expanding the kernels. In another work, French and Butz (1974) developed an algorithm based on expansion of Wiener kernel in terms of Walsh functions. Orabi and Ahmadi (1987), Gifford and Tomlinson (1988) illustrated the technique of calculating higher order FRF's for nonlinear structural systems. They curve-fitted a nonlinear multi-degree-of-freedom parametric model to FRF data considering the measured FRFs as Volterra kernel transforms. Nam, Kim and Powers (1990) presented a frequency domain approach for identification of a discrete third order Volterra system with random input. A digital poly-spectral analysis algorithm is developed and used for identification and parameter estimation of a Duffing oscillator. Odiari and Ahmadi (1987) presented a Wiener-Harmite functional series expansion method for response analysis of nonlinear systems under random excitations. Odiari and Ewins (1992) have presented a frequency domain procedure for identifying the vibration parameters of nonlinear vibratory systems with particular emphasis on rotor-bearing systems. Khan and Vyas (1999, 2000a, 2000b) developed a general procedure for parameter estimation in a rotor-bearing system through Wiener kernel estimation using broad-band random excitation.

Method of Harmonic Probing: Bedrosian and Rice (1971) presented a detailed study on determination of higher order Volterra kernel transforms from the response under sinusoidal excitations. It was shown that for complete determination of *n*th order kernel transform, the excitation has to consist of *n* different frequencies. Subsequently a large number of works (Bussang et al., 1974; Chua and Ng., 1979, 1979a; Weiner and Spina, 1980; Rugh, 1980) were reported on nonlinear system analysis and response characterisation using sinusoidal excitations. Baumgarter and Rugh (1975) presented an identification method using steady-state frequency response data and nonlinear transfer functions, for a class of nonlinear systems composed of cascaded linear systems interconnected with integer power nonlinearirties. The method works on interpolation by polynomials with rational coefficients. An improvement on this work was suggested by Wysocki and Rugh (1976), where higher harmonics were also measured. Chua and Tang (1982) reported a procedure to determine the amplitude and frequency of sinusoidal nonlinear oscillator by solving a pair of algebraic nonlinear equations which were generated by a recursive algorithm. Boyd, Tang and Chua (1983) discussed a technique for extracting the second order kernel transform using multi-tone harmonic probing. Response components were separated using Gardiner's method and frequency domain analysis was carried out to obtain the second order Volterra kernel transforms. Although two-tone excitation can determine completely the entire set of second order kernel transforms, the authors used three-tone excitation and demonstrated how it can significantly reduce the number of experiments. The focus of the work was proper selection of tone frequencies, such that the combination frequencies do not overlap. Another approach for establishing a rationale for selecting the in-commensurate tone frequencies has been presented by Victor and Shapley (1980). Chua and Liao (1989) extended the kernel measurement procedure to third and higher order transforms. The authors also presented a procedure for estimating the highest significant order in a polynomial system (1991). Xiaojiang et al. (1990) developed a nonlinear modal parameter surface fitting method and used it to determine second order kernel transform of a square law nonlinear system. Storer and Tomlinson (1993) and Gifford (1993) discussed procedures for estimation and experimental measurement of higher order transfer functions with truncated response series. The procedures involved sinusoidal

excitation and *n*th order transfer function was obtained from *n*th harmonic response component neglecting the contributions from higher order terms. Lee (1997) extended the higher order transfer function identification to parameter estimation where first harmonic response components are extracted by order separation method and the second and third order transfer functions so obtained, are related to the first order transfer functions through the nonlinear parameters. Worden, Manson and Tomlinson (1997) extended the harmonic probing algorithm to multi-input Volterra series. Response structure was developed in terms of direct and cross-kernel transforms.

2.2 Parametric Identification Procedures

Parametric methods require *a-priori* knowledge of the mathematical structure and order of the system. In control systems, electrical and electronic networks can often be represented by block oriented models such as Hammersein model, Wiener model etc (Haber, 1989, 1990). In these models linear parts are separately connected to nonlinear elements by a multiplier. Methods for structure identification for these block orieneted models are generally based on characteristics of measured Volterra kernels. Marmarelis and Naka (1974) pointed out that if the two-dimensional kernel exists only at a main diagonal then the model is of Hammerstein type. Haber (1989) presented structure identification of various models such as Hammerstein, Wiener, Wiener-Hammerstein models through characteristics of measured Volterra kernels. An overview of various structure identification methods for block-oriented models can be found in the survey paper of Haber and Unbehauen (1990).

In mechanical and structural systems, nonlinearity can occur in stiffness forces or in damping forces. These nonlinearities are modeled generally through polynomial form, though non-polynomial forms such as drag force type quadratic damping, hysteretic damping, Coulomb damping, bilinear stiffness etc (Nayfeh, 1979; Choi, Miksad and Powers, 1985; Bendat and Piersol, 1986) are also observed in the physical systems. Neyfeh (1985) proposed a method to identify the nonlinear character of a system by perturbation and free vibration test. The method investigates the presence of self oscillatory terms or hysteresis by perturbing the system about its equilibrium positions.

For systems not showing these nonlinearities, form of damping is determined by free vibration test based on rate of amplitude decay. Bendat, Palo and Coppolino (1992) developed a general identification technique from measured input-output stochastic data for a wide range of nonlinearities including Duffing oscillator, Van-der Pol oscillator, dead band and clearance nonlinearity. The method is based on multiple input/single output linear analysis of reverse dynamic systems. Dimentberg and Sokolov (1991) presented methods for identification of restoring force nonlinearity from system response to a white noise excitation. The method is based on estimating probability density functions and spectral analysis of the response. Parameter estimation methods include direct approaches, linearisation techniques, filtering and state estimation methods, methods using higher order spectral density functions and Markov process approach. White noise excitation is used as input forcing function for statistical linearisation techniques, methods using spectral density functions and Markov process approach.

2.2.1 Filtering and State Estimation techniques

Many filtering and estimation techniques have been developed for obtaining the best estimate of the parameters defining state trajectories from noisy data. These techniques estimate the augmented state vector including the unknown parameters appearing in the governing equations. Various methods commonly used for estimation are least squares, maximum likelyhood and Kalman filter. Distefano and Rath (1975) applied this procedure to the identification of nonlinear structural seismic systems using least square method, whereas Yun and Shinozuka (1980) applied it to identification of multi-degree-of-freedom nonlinear systems using Kalman filter. These methods assume nominal values for the elements of the augmented state vector and a nominal trajectory. The augmented state vector is then perturbed and the trajectory is expanded in a Taylor series about the nominal trajectory. Deviations in the trajectory as a function of time are related to the perturbations in the augmented state through a transition matrix. In the works of Distefano and Rath, Yun and Shonozuka the nominal responses and transition matrices were determined by numerically integrating the governing nonlinear equations. As an alternative, Hanagud, Meyappa and Craig (1985) analytically determined the nominal response using the method of multiple scales. Mook (1989) presented a technique for

optimal estimation of state vector trajectory from noisy time-domain state vector measurements of a nonlinear dynamic system. McNiven and Matzen (1978) have employed the Gauss-Newton method to minimise an integral of the weighted squared output error function to determine the unknown parameters.

2.2.2 Linearisation Techniques

Linearisation techniques are based on the concept that a nonlinear system with small nonlinearity can be replaced by an equivalent linear model. For sinusoidal excitation linearisation methods generally leave the fundamental frequency component undisturbed in an equivalent linear system, but neglect higher harmonics. Ibanez (1988) used a describing function approach to obtain an approximate transfer function for the fundamental response harmonic component. Mottershed and Stanway (1986) presented an identification procedure for *p*th-power damping where governing equations were framed in state-space form and the state vector was linearised with respect to the unknown parameters by taking a first order Taylor series expansion of the state vector. Time series record of state vector consisting of displacement and velocity were measured at a number of time steps and least square error criterion was applied to estimate the parameters.

In case of random vibration, interpretation in terms of fundamental frequency and harmonics is not possible. Systems, under such condition, are linearised by replacing a nonlinear relation by an equivalent linear gain, while conserving in specific properties of the true nonlinear output. Broerson (1974) modeled the nonlinear terms in the governing equation with a series expansion of functions and determined the coefficients of the expansion by using correlation techniques. This approach is an extension of the method of statistical linearisation and uses random excitation as the input.

2.2.3 Markov Process Approach

A process, whose present probabilty distribution depends on only one previous time instant, is called a Markov process. The structure of a Markov process is completely determined, for all future times, by the distribution at some initial time and a transition

probabilty density function, which satisfies a linear partial differential equation known as the Fokker-Planck-Kolmogorov (Fokker, 1914; Planck, 1917; Kolmogorov, 1931) equation. Statistical response characteristics have been extensively studied, using F-P-K equation for nonlinear restoring forces and special forms of nonlinear damping, by Ariaratnam (1960), Caughy (1963) and Caughy and Ma (1983). F-P-K equations for nonlinear parameter estimation was employed by Tiwari and Vyas (1995, 1997, 1997a, 1998). They described procedures for estimation of nonlinear elastic parameters of bearings based on the analysis of random response signals measured from the bearing housing vibration. The procedure did not require *a-priori* knowledge of the random excitation force induced by bearing defects. The dynamics of rotor-bearing system was modeled as a Markov process and F-P-K equations were formulated and solved for the inverse problem of parameter estimation. The procedure was developed for cases of rigid rotors; single disc flexible rotors and multi-disc flexible rotors. The study was extended further to include harmonic excitation due to rotor unbalance. The algorithms were also verified experimentally, for a laboratory rotor-bearing test rig.

2.2.4 Spectral Density Function Approach

Linear system identification procedure, using spectral density functions, was extended by Bendat and Peirsol (1982) for a nonlinear system with square law nonlinearity. In this method the nonlinear model was first reconfigured into multi-input single output model in which additional input paths correspond to various nonlinearities. Higher order spectral density functions such as bi-spectral and tri-spectral density functions were defined for random input-output data and linear and nonlinear path transfer functions were obtained in terms of these spectral density functions. Bi-spectral density function represents frequency domain transformation of a square law nonlinear path. Similarly the tri-spectral density function represents the transformation of a cubic nonlinear path. Thus use of these higher order spectral density functions is limited to polynomial form of nonlinearity only. A case of drag force type nonlinearity in wave force experienced by offshore structures and moored vessels was studied by Bendat and Piersol (1986a) where the non-polynomial quadratic nonlinearity was replaced by statistically equivalent combination of linear and cubic nonlinear paths and then higher order spectral density functions were

used for equivalent parameter estimation. Identification procedures for a wide range of nonlinear elements using higher order spectral density functions can be found in the subsequent work of Bendat (1990). Rice and Fritzpatrick (1988, 1991) presented a spectral density approach based on 'reverse path analysis'. Transformation, along nonlinear paths was carried out in time domain followed by first order spectral density computation. The identification approach was further extended to two-degree-of-freedom systems with cubic nonlinearity (Rice and Fritzpatrick, 1991b). Richard and Singh (1998, 1999) also utilized the 'reverse path analysis' to formulate another procedure for identifying multi-degree-of-freedom systems and illustrated the method for three and five-degree-of-freedom systems with asymmetric and distributed nonlinearities. A critical study comparing the methods of Rice and Fritzpatrick with that of Richard and Singh has been recently reported by the latter authors (Richards and Singh, 2000).

2.2.5 Direct Approaches

Mohammad, Worden and Tomlinson (1992) presented a parametric method, which works directly with the differential equation. The forcing function and response (acceleration) are measured at each time step and velocity and displacement values are obtained through integration of acceleration data. These time series data, when put into the governing equation of motion, gi ve an over-determined system of equations in terms of unknown parameters, which are estimated through minimising the norm of residual error vector. However the method suffers from the practical limitation that all the response variables are to be measured simultaneously which is particularly difficult for multiple-degree-of–freedom systems. Also the displacement and velocity data, obtained through integration of acceleration records, are susceptible to drift and dc bias.

CHAPTER 3

VOLTERRA SERIES RESPONSE REPRESENTATION

Volterra series provides a platform for non-parametric input-output mapping of a physical system. It is a power series and a generalisation of the well-known convolution integral for linear systems. Volterra series components are evaluated through convolution of various orders of impulse response functions with corresponding orders of the forcing function. Volterra series is described in this chapter and the response representation characteristics for harmonic force functions are discussed. Both single-tone and multi-tone excitations are considered and higher order kernel synthesis formulations are developed for a single-degree-of-freedom system. It is shown that the harmonic response of a nonlinear system can be obtained in a structured form using the Volterra series. The structured form is to be utilsed further for nonlinearity identification and parameter estimation of a nonlinear system.

3.1 Volterra Series Response Representation

The functional series representation of the input-output relationship for a general physical system with $f(t)$ as input excitation and $x(t)$ as output response can be expressed as

$$x(t) = \int_{-\infty}^{\infty} h_1(\tau_1) f(t-\tau_1) d\tau_1 + \int_{-\infty}^{\infty}\int_{-\infty}^{\infty} h_2(\tau_1,\tau_2) f(t-\tau_1) f(t-\tau_2) d\tau_1 d\tau_2 + \int_{-\infty}^{\infty}\int_{-\infty}^{\infty}\int_{-\infty}^{\infty} h_3(\tau_1,\tau_2,\tau_3) f(t-\tau_1) f(t-\tau_2) f(t-\tau_3) d\tau_1 d\tau_2 d\tau_3 + \ldots. \quad (3.1)$$

$$= x_1(t) + x_2(t) + \ldots + x_n(t) + \ldots$$

with nth order response component, $x_n(t)$, given as

$$x_n(t) = \int_{-\infty}^{\infty} \ldots \int_{-\infty}^{\infty} h_n(\tau_1,\ldots,\tau_n) f(t-\tau_1) \ldots f(t-\tau_n) d\tau_1 \ldots d\tau_n \quad (3.2)$$

$h_n(\tau_1,...,\tau_n)$ are the Volterra kernels and for a physically realizable system

$h_n(\tau_1,...,\tau_n) = 0$ for $\tau_j < 0, \quad j = 1,2,....n$.

First order Volterra kernel, $h_1(\tau_1)$, is the familiar impulse response function of a linear system. Higher order kernels can be viewed as higher order impulse response functions, which serve to characterise the various orders of nonlinearity.

The response series (3.1) can be, alternately, expressed in operator form as

$$x(t) = \sum_{n=1}^{\infty} H_n[f(t)] \tag{3.3}$$

with *n*th order Volterra operator given as

$$H_n[f(t)] = \int_{-\infty}^{\infty} ... \int_{-\infty}^{\infty} h_n(\tau_1,...,\tau_n) f(t-\tau_1)...f(t-\tau_n) d\tau_1...d\tau_n$$

Volterra series is a power series with memory, which expresses the output $x(t)$ of a nonlinear system in powers of the input $f(t)$. This can be seen, by changing the input by a factor κ, which gives the output as

$$\begin{aligned} x(t) &= \sum_{n=1}^{\infty} H_n[\kappa f(t)] \\ &= \sum_{n=1}^{\infty} \kappa^n H_n[f(t)] \end{aligned} \tag{3.4}$$

The above is a power series in the amplitude factor κ.

Higher order Frequency Response Functions (FRFs) or Volterra kernel transforms can be defined as the multi-dimensional Fourier transforms of the higher order Volterra kernels as

$$H_n(\omega_1,\omega_2,...,\omega_n) = \int_{-\infty}^{\infty} \int_{-\infty}^{\infty} ... \int_{-\infty}^{\infty} h_n(\tau_1,\tau_2,...,\tau_n) \prod_{i=1}^{n} e^{-j\omega_i\tau_i} d\tau_1 d\tau_2 ... d\tau_n \tag{3.5}$$

such that

$$h_n(\tau_1,...,\tau_n) = \frac{1}{(2\pi)^n} \int_{-\infty}^{\infty} \int_{-\infty}^{\infty} ... \int_{-\infty}^{\infty} H_n(\omega_1,\omega_2,...,\omega_n) \prod_{i=1}^{n} e^{j\omega_i\tau_i} d\omega_1 d\omega_2 ... d\omega_n \quad (3.6)$$

First order kernel transform $H_1(\omega_1)$ is the familiar linear transfer function. Similarly, $H_n(\omega_1,\omega_2,...,\omega_n)$, is the transform of the *n*th order Volterra kernel $h_n(\tau_1,\tau_2,...,\tau_n)$ and can be seen to be analogous to an *n*th order transfer function.

The kernels can be taken to be symmetric without loss of generality, i.e., $h_2(\tau_1,\tau_2) = h_2(\tau_2,\tau_1)$ etc (Schetzen, 1980). Consequently, the kernel transforms are also symmetric, i.e., $H_2(\omega_1,\omega_2) = H_2(\omega_2,\omega_1)$. In general, an *n*th order kernel transform $H_n(\omega_1,...,\omega_n)$ is independent of the arrangement order of its arguments $\omega_1,...,\omega_n$. Volterra kernels characterise a nonlinear system in time domain, whereas Volterra kernel transforms represent a system in the frequency domain.

3.2 Response under Single-Tone Harmonic Excitation

A single-degree-of-freedom system, with general polynomial form of stiffness nonlinearity is considered.

$$m\ddot{x}(t) + c\dot{x}(t) + g[x(t)] = f(t). \quad (3.7)$$

For single-tone harmonic excitation

$$f(t) = A\cos\omega t = \frac{A}{2}e^{j\omega t} + \frac{A}{2}e^{-j\omega t} \quad (3.8)$$

and nonlinear term $g[x(t)]$ expressed in general polynomial form as

$$g[x(t)] = k_1x(t) + k_2x^2(t) + k_3x^3(t) + ... \quad (3.9)$$

using Volterra series representation (3.2), the response components are obtained as

$$x_1(t) = \frac{A}{2}H_1(\omega)e^{j\omega t} + \frac{A}{2}H_1(-\omega)e^{-j\omega t} \quad (3.10a)$$

$$x_2(t) = \frac{A^2}{2}H_2(\omega,-\omega) + \frac{A^2}{4}H_2(\omega,\omega)e^{j2\omega t} + \frac{A^2}{4}H_2(-\omega,-\omega)e^{-j2\omega t} \quad (3.10b)$$

$$x_3(t) = \frac{A^3}{8} H_3(\omega,\omega,\omega)e^{j3\omega t} + \frac{3A^3}{8} H_3(\omega,\omega,-\omega)e^{j\omega t} + \frac{3A^3}{8} H_3(\omega,-\omega,-\omega)e^{-j\omega t} + \frac{A^3}{8} H_3(-\omega,-\omega,-\omega)e^{-j3\omega t} \tag{3.10c}$$

The expression for the nth order response component can be developed as

$$x_n(t) = \left(\frac{A}{2}\right)^n \sum_{p+q=n} {}^nC_q \, H_n(\underbrace{\omega,\ldots,\omega}_{p \text{ times}},\underbrace{-\omega,\ldots,-\omega}_{q \text{ times}})e^{j(p-q)\omega t}, \quad 0 \le p \le n; \quad 0 \le q \le n$$

$$= \left(\frac{A}{2}\right)^n \sum_{p+q=n} {}^nC_q \, H_n^{p,q}(\omega)e^{j\omega_{p,q} t} \tag{3.11}$$

where the following brief notations have been used

$$H_n^{p,q}(\omega) = H_n(\underbrace{\omega,\ldots,\omega}_{p \text{ times}},\underbrace{-\omega,\ldots,-\omega}_{q \text{ times}}) \qquad \omega_{p,q} = (p-q)\omega$$

The total response of the system, can be then expressed as

$$x(t) = \sum_{n=1}^{\infty}\left(\frac{A}{2}\right)^n \sum_{p+q=n} {}^nC_q \, H_n^{p,q}(\omega)\, e^{j\omega_{p,q}t} \tag{3.12}$$

3.2.1 Response Harmonic Amplitudes

Combinations of different p and q result in various response harmonics at frequencies $\omega_{p,q} = \omega, 2\omega, 3\omega$ etc. and the response series given in (3.12) can be written in terms of its harmonics as

$$x(t) = X_0 + |X(\omega)|\cos(\omega t + \phi_1) + |X(2\omega)|\cos(2\omega t + \phi_2) + |X(3\omega)|\cos(3\omega t + \phi_3) + .. \tag{3.13}$$

where the response harmonic amplitudes, $X(n\omega)$, are obtained by collecting all the terms associated with the exponential $e^{j\omega_{p,q}t}$ in equation (3.12) for $\omega_{p,q} = (p-q)\omega = n\omega$ and are given by

$$X_0 = \sum_{n=1}^{\infty}\left(\frac{A}{2}\right)^{2n} {}^{2n}C_n H_{2n}^{n,n}(\omega)$$

$$X(n\omega)=\sum_{i=1}^{\infty}\sigma_i(n\omega) \qquad \text{and} \qquad \phi_n=\angle X(n\omega) \tag{3.14}$$

with

$$\sigma_i(n\omega)=2\left(\frac{A}{2}\right)^{n+2i-2}{}_{n+2i-2}C_{i-1}\,H_{n+2i-2}^{n+i-1,i-1}(\omega) \tag{3.15}$$

Equations (3.14, 3.15) show that odd harmonics are associated with odd order kernel transforms and even harmonics are associated with even order kernel transforms. A response harmonic series, $X(n\omega)$, always begins with nth order kernel transform in its first series term.

3.2.2 Synthesis of Higher Order Kernel Transforms

Limiting the polynomial nonlinearity in equation (3.9) up to the cubic term, i.e.,

$$g[x(t)]=k_1x(t)+k_2x^2(t)+k_3x^3(t) \tag{3.16}$$

and substituting equation (3.12) in the equation of motion (3.7), one obtains

$$\begin{aligned}&\sum_{n=1}^{\infty}\left(\frac{A}{2}\right)^n\sum_{p+q=n}{}^nC_q\,H_n^{p,q}(\omega)\,e^{j\omega_{p,q}t}\left[-m\omega_{p,q}^2+k_1+jc\omega_{p,q}\right]\\&+k_2\left[\sum_{n=1}^{\infty}\left(\frac{A}{2}\right)^n\sum_{p+q=n}{}^nC_q\,H_n^{p,q}(\omega)\,e^{j\omega_{p,q}t}\right]^2\\&+k_3\left[\sum_{n=1}^{\infty}\left(\frac{A}{2}\right)^n\sum_{p+q=n}{}^nC_q\,H_n^{p,q}(\omega)\,e^{j\omega_{p,q}t}\right]^3=\frac{A}{2}e^{j\omega t}+\frac{A}{2}e^{-j\omega t}\end{aligned} \tag{3.17}$$

Applying the method of harmonic probing (Bedrosian and Rice, 1971) and equating the coefficients of $\left(\frac{A}{2}\right)^n e^{j\omega_{p,q}t}$, n =1, 2, 3....., one obtains

$$H_1(\omega)=1/(-m\omega^2+k_1+jc\omega) \qquad \text{for } n=1 \tag{3.18a}$$

and

$$H_n^{p,q}(\omega) = -\frac{H_1(\omega_{p,q})}{{}^nC_q}\left[\begin{array}{l} k_2 \sum\limits_{\substack{p_i+q_i=n_i \\ n_1+n_2=n}} \left\{{}^{n_1}C_{q_1} H_{n_1}^{p_1,q_1}(\omega)\right\} * \left\{{}^{n_2}C_{q_2} H_{n_2}^{p_2,q_2}(\omega)\right\} + \\ k_3 \sum\limits_{\substack{p_i+q_i=n_i \\ n_1+n_2+n_3=n}} \left\{{}^{n_1}C_{q_1} H_{n_1}^{p_1,q_1}(\omega)\right\} * \left\{{}^{n_2}C_{q_2} H_{n_2}^{p_2,q_2}(\omega)\right\} * \left\{{}^{n_3}C_{q_3} H_{n_3}^{p_3,q_3}(\omega)\right\} \end{array}\right]$$

for $n > 1$ (3.18b)

Thus, a higher order kernel transform $H_n^{p,q}(\omega)$, can be synthesised from the lower order kernel transforms and the nonlinear parameters k_2 and k_3.

Equation (3.18b) is based on partitioning of the integer n into (i) two integers n_1 and n_2 satisfying the condition $n_1 + n_2 = n$ and then into (ii) three integers n_1, n_2 and n_3 satisfying the condition $n_1 + n_2 + n_3 = n$. The number of permutations of partitioning increases exponentially with increasing n, thus making the symbolic expression too long.

In practice, it is more convenient to compute the higher order kernel transforms numerically through step by step reduction with an algorithm for integer partitioning. For a typical Duffing oscillator with only the cubic nonlinearity term in the equation (3.16), i.e. when $k_2 = 0$, equation (3.18b) becomes

$$H_n^{p,q}(\omega) = -\frac{H_1(\omega_{p,q})}{{}^nC_q}\left[k_3 \sum_{\substack{p_i+q_i=n_i \\ n_1+n_2+n_3=n}} \left\{{}^{n_1}C_{q_1} H_{n_1}^{p_1,q_1}(\omega)\right\} * \left\{{}^{n_2}C_{q_2} H_{n_2}^{p_2,q_2}(\omega)\right\} * \left\{{}^{n_3}C_{q_3} H_{n_3}^{p_3,q_3}(\omega)\right\}\right] \quad (3.19)$$

It is obvious, that for $n = 2$, there does not exist any set of three nonzero positive integers n_1, n_2, n_3 which can meet the required condition $n_1 + n_2 + n_3 = n = 2$. Therefore, the second order kernel transform $H_2^{p,q}(\omega)$ reduces to zero for a Duffing oscillator. Similarly, other even order kernel transforms, $H_4^{p,q}(\omega), H_6^{p,q}(\omega)$ etc. also become zero for a Duffing oscillator.

3.3 Response under Multi-Tone Harmonic Excitation

For the nonlinear system described earlier in equation (3.7) and a typical three-tone excitation given by

$$f(t) = A\cos\omega_1 t + B\cos\omega_2 t + C\cos\omega_3 t \tag{3.20}$$

the Volterra Series response components, following equation (3.2), are obtained as

$$x_1(t) = \frac{A}{2}H_1(\omega_1)e^{j\omega_1 t} + \frac{B}{2}H_1(\omega_2)e^{j\omega_2 t} + \frac{C}{2}H_1(\omega_3)e^{j\omega_3 t}$$
$$+ \text{complex conjugate terms} \tag{3.21}$$

$$x_2(t) = \frac{A^2}{2}H_2(\omega_1,-\omega_1) + \frac{B^2}{2}H_2(\omega_2,-\omega_2) + \frac{C^2}{2}H_2(\omega_3,-\omega_3)$$
$$+ \frac{A^2}{4}H_2(\omega_1,\omega_1)e^{j2\omega_1 t} + \frac{B^2}{4}H_2(\omega_2,\omega_2)e^{j2\omega_2 t} + \frac{C^2}{4}H_2(\omega_3,\omega_3)e^{j2\omega_3 t}$$
$$+ \frac{AB}{2}H_2(\omega_1,\omega_2)e^{j(\omega_1+\omega_2)t} + \frac{BC}{2}H_2(\omega_2,\omega_3)e^{j(\omega_2+\omega_3)t} + \frac{AC}{2}H_2(\omega_1,\omega_3)e^{j(\omega_1+\omega_3)t}$$
$$+ \frac{AB}{2}H_2(\omega_1,-\omega_2)e^{j(\omega_1-\omega_2)t} + \frac{BC}{2}H_2(\omega_2,-\omega_3)e^{j(\omega_2-\omega_3)t} + \frac{AC}{2}H_2(\omega_1,-\omega_3)e^{j(\omega_1-\omega_3)t}$$
$$+ \text{complex conjugate terms} \tag{3.22}$$

$$x_3(t) = \left[\frac{3A^3}{8}H_3(\omega_1,\omega_1,-\omega_1) + \frac{3AB^2}{4}H_3(\omega_1,\omega_2,-\omega_2) + \frac{3AC^2}{4}H_3(\omega_1,\omega_3,-\omega_3)\right]e^{j\omega_1 t}$$
$$+ \left[\frac{3B^3}{8}H_3(\omega_2,\omega_2,-\omega_2) + \frac{3A^2B}{4}H_3(\omega_1,-\omega_1,\omega_2) + \frac{3BC^2}{4}H_3(\omega_2,\omega_3,-\omega_3)\right]e^{j\omega_2 t}$$
$$+ \left[\frac{3C^3}{8}H_3(\omega_3,\omega_3,-\omega_3) + \frac{3B^2C}{4}H_3(\omega_2,-\omega_2,\omega_3) + \frac{3A^2C}{4}H_3(\omega_1,-\omega_1,\omega_3)\right]e^{j\omega_3 t}$$
$$+ \frac{A^3}{8}H_3(\omega_1,\omega_1,\omega_1)e^{j3\omega_1 t} + \frac{B^3}{8}H_3(\omega_2,\omega_2,\omega_2)e^{j3\omega_2 t} + \frac{C^3}{8}H_3(\omega_3,\omega_3,\omega_3)e^{j3\omega_3 t}$$
$$+ \frac{3ABC}{4}H_3(\omega_1,\omega_2,\omega_3)e^{j(\omega_1+\omega_2+\omega_3)t} + \frac{3ABC}{4}H_3(\omega_1,\omega_2,-\omega_3)e^{j(\omega_1+\omega_2-\omega_3)t}$$
$$+ \frac{3ABC}{4}H_3(\omega_1,-\omega_2,\omega_3)e^{j(\omega_1-\omega_2+\omega_3)t} + \frac{3ABC}{4}H_3(\omega_1,-\omega_2,-\omega_3)e^{j(\omega_1-\omega_2-\omega_3)t}$$

$$+\frac{3A^2B}{8}H_3(\omega_1,\omega_1,\omega_2)e^{j(2\omega_1+\omega_2)t}+\frac{3A^2B}{8}H_3(\omega_1,\omega_1,-\omega_2)e^{j(2\omega_1-\omega_2)t}$$

$$+\frac{3A^2C}{8}H_3(\omega_1,\omega_1,\omega_3)e^{j(2\omega_1+\omega_3)t}+\frac{3A^2C}{8}H_3(\omega_1,\omega_1,-\omega_3)e^{j(2\omega_1-\omega_3)t}$$

$$+\frac{3B^2C}{8}H_3(\omega_2,\omega_2,\omega_3)e^{j(2\omega_2+\omega_3)t}+\frac{3B^2C}{8}H_3(\omega_2,\omega_2,-\omega_3)e^{j(2\omega_2-\omega_3)t}$$

$$+\frac{3AB^2}{8}H_3(\omega_1,\omega_2,\omega_2)e^{j(2\omega_2+\omega_1)t}+\frac{3AB^2}{8}H_3(-\omega_1,\omega_2,\omega_2)e^{j(2\omega_2-\omega_1)t}$$

$$+\frac{3BC^2}{8}H_3(\omega_2,\omega_3,\omega_3)e^{j(2\omega_3+\omega_2)t}+\frac{3BC^2}{8}H_3(-\omega_2,\omega_3,\omega_3)e^{j(2\omega_3-\omega_2)t}$$

$$+\frac{3AC^2}{8}H_3(\omega_1,\omega_3,\omega_3)e^{j(2\omega_3+\omega_1)t}+\frac{3AC^2}{8}H_3(-\omega_1,\omega_3,\omega_3)e^{j(2\omega_3-\omega_1)t}$$

$$+\text{ complex conjugate terms} \tag{3.23}$$

In general, the *n*th order response component can be expressed as

$$x_n(t)=\frac{1}{2^n}\sum_{\substack{p+q+s+u\\+v+w=n}}A^{p+q}B^{s+u}C^{v+w}\,{}^nC_{p,q,s,u,v,w}H_n^{p,q,s,u,v,w}(\omega)\,e^{j\omega_{p,q,s,u,v,w}t} \tag{3.24}$$

where

$${}^nC_{p,q,s,u,v,w}=\frac{n!}{p!\,q!\,s!\,u!\,v!\,w!},\qquad \omega_{p,q,s,u,v,w}=(p-q)\omega_1+(s-u)\omega_2+(v-w)\omega_3$$

and

$$H_n^{p,q,s,u,v,w}(\omega)=H_n(\underbrace{\omega_1,\ldots,\omega_1}_{p\text{ times}},\underbrace{-\omega_1,\ldots,-\omega_1}_{q\text{ times}},\underbrace{\omega_2,\ldots,\omega_2}_{s\text{ times}},\underbrace{-\omega_2,\ldots,-\omega_2}_{u\text{ times}},\underbrace{\omega_3,\ldots,\omega_3}_{v\text{ times}},\underbrace{-\omega_3,\ldots,-\omega_3}_{w\text{ times}})$$

The expression for the total response can be then written as

$$x(t)=\sum_{n=1}^{\infty}\frac{1}{2^n}\sum_{\substack{p+q+s+u\\+v+w=n}}A^{p+q}B^{s+u}C^{v+w}\,{}^nC_{p,q,s,u,v,w}H_n^{p,q,s,u,v,w}(\omega)\,e^{j\omega_{p,q,s,u,v,w}t} \tag{3.25}$$

Substituting response series of equation (3.25), in the equation of motion (3.7), with polynomial nonlinearity given by (3.16), and equating the coefficients of $\frac{AB}{2}e^{j(\omega_1+\omega_2)t}$, one obtains

$$H_2(\omega_1,\omega_2) = -k_2 H_1(\omega_1)H_1(\omega_2)H_1(\omega_1+\omega_2) \tag{3.26a}$$

which gives the general synthesis formulation of a second order kernel transform.

Similarly, equating the coefficients of $\frac{3ABC}{4}e^{j(\omega_1+\omega_2+\omega_3)t}$, the third order kernel transform can be synthesized from the first order kernel as

$$H_3(\omega_1,\omega_2,\omega_3) = H_1(\omega_1)H_1(\omega_2)H_1(\omega_3)H_1(\omega_1+\omega_2+\omega_3)* \left[\frac{2}{3}k_2^2\{H_1(\omega_1+\omega_2)+H_1(\omega_2+\omega_3)+H_1(\omega_1+\omega_3)\}-k_3\right] \tag{3.26b}$$

3.3.1 Response Harmonic Content

It can be seen from equation (3.25) that the response $x(t)$, under multi-tone excitation in addition to the harmonics at the probing frequencies $\omega_1, \omega_2, \omega_3$ etc., contains harmonics at higher order combination frequencies given by $m_1\omega_1 + m_2\omega_2 + m_3\omega_3 + \ldots$, where $m_1, m_2, m_3, \ldots$ are integers and can be either positive or negative.

It is also to be noted that, the first order response component, $x_1(t)$, contains only the fundamental harmonics (equation 3.21), while higher order response components contain multiple harmonics and combination tones (equations 3.22, 3.23). The number of combination tones or harmonics increases in a response component with its order. For a general multi-tone excitation having n number of probing frequencies, the number of harmonics contained in various response components (up to third order) are tabled below.

Table: 3.1 Harmonics in various response components

Response Component	Combination tone types	Number in each type	Total Number of harmonics
$x_1(t)$	ω_i	n	n
$x_2(t)$	$2\omega_i$	n	
	$\omega_i \pm \omega_j$	$n(n\text{-}1)$	n^2
$x_3(t)$	ω_i	n	
	$3\omega_i$	n	
	$2\omega_i + \omega_j$	$2n(n\text{-}1)$	$2n^2$, for $n=2$
	$\omega_i \pm \omega_j \pm \omega_k$ (for $n>2$ only)	$4\ {}^nC_3$	$\frac{2n^3+4n}{3}$, for $n>2$

Harmonic contents in higher order response components can be similarly worked out.

3.3.2 First Appearance of a Harmonic

The expression (3.24), for the nth order response component $x_n(t)$, reveals that a particular combination tone of frequency equal to $m_1\omega_1 + m_2\omega_2 + m_3\omega_3 + \ldots$, appears for the first time in the nth order response component $x_n(t)$ where $n = |m_1| + |m_2| + |m_3| + \ldots$ and then it appears in every alternate successive response component $x_{n+2i}(t)$. Also, a harmonic of the form $m_1\omega_1 + m_2\omega_2 + m_3\omega_3 + \ldots$ is associated with the kernel transforms of order n, n+2, n+4 etc.

3.3.3 Response Amplitude of a Harmonic

Response harmonic amplitude representation for a multi-tone excitation involves large number of tones. For a typical three-tone excitation, using equation (3.25), the response amplitude $X(m_1\omega_1 + m_2\omega_2 + m_3\omega_3)$ can be written in a series form as

$$X(m_1\omega_1 + m_2\omega_2 + m_3\omega_3) = \sum_{i=1}^{\infty} \sigma_i(m_1\omega_1 + m_2\omega_2 + m_3\omega_3) \tag{3.27}$$

with

$$\sigma_i(m_1\omega_1 + m_2\omega_2 + m_3\omega_3) = \frac{1}{2^{n+2i-3}} \sum_{\substack{i_1+i_2 \\ +i_3=i-1}} A^{m_1+2i_1} B^{m_2+2i_2} C^{m_3+2i_3} * {}^{n}C_{m_1+i_1,i_1,m_2+i_2,i_2,m_3+i_3,i_3} * H_{n+2i-2}^{m_1+i_1,i_1,m_2+i_2,i_2,m_3+i_3,i_3}(\omega) \tag{3.28}$$

where $n = |m_1| + |m_2| + |m_3|$

Application of equation (3.27) requires, for uniqueness, that among the set of combination tones under consideration, two combination tones should not be equal to each other or to any of the fundamental probing frequencies (Boyd et al 1983).

3.4 Remarks

The Volterra series provides a structured form response representation for a nonlinear system. The series is constituted of the first and higher order components. The first order component is associated to the linear part of the system. The higher order components are contributed by the nonlinear parameters of the system. The first order component involves the impulse response function, while higher order kernels can be viewed as multi-dimensional impulse response functions. Odd order response components display only odd harmonics in the frequency domain, while even order components of the response display only even harmonics. These characteristics of the Volterra series are employed further for nonlinearity characterization and estimation.

CHAPTER 4

NONLINEARITY STRUCTURE CLASSIFICATION

The Volterra series structure discussed in the previous chapter is utilized to develop a nonlinearity classification scheme. System nonlinearity is distinguished between polynomial and non-polynomial forms. A procedure for classification of nonlinearity structure into symmetric and asymmetric forms, is also presented. Further, for polynomial form nonlinearities, the polynomial structure is also identified using properties of higher order kernel transforms. The procedures have been illustrated through numerical simulation.

4.1 Ordered Component Separation Technique

For a single degree of freedom system,

$$m\ddot{x}(t) + c\dot{x}(t) + g[x(t)] = f(t) \tag{4.1}$$

with harmonic excitation $f(t) = A\cos\omega t$, the first three response components given in equation (3.10) are rewritten below.

$$x_1(t) = \frac{A}{2}H_1(\omega)e^{j\omega t} + \frac{A}{2}H_1(-\omega)e^{-j\omega t} \tag{4.2a}$$

$$x_2(t) = \frac{A^2}{2}H_2(\omega,-\omega) + \frac{A^2}{4}H_2(\omega,\omega)e^{j2\omega t} + \frac{A^2}{4}H_2(-\omega,-\omega)e^{-j2\omega t} \tag{4.2b}$$

$$x_3(t) = \frac{A^3}{8}H_3(\omega,\omega,\omega)e^{j3\omega t} + \frac{3A^3}{8}H_3(\omega,\omega,-\omega)e^{j\omega t} + \frac{3A^3}{8}H_3(\omega,-\omega,-\omega)e^{-j\omega t} + \frac{A^3}{8}H_3(-\omega,-\omega,-\omega)e^{-j3\omega t} \tag{4.2c}$$

A characteristic feature of the response components above is that odd harmonics appear only in odd order response components and even harmonics appear only in even order response components.

An odd order response component $x_{2m+1}(t)$ comprises of odd harmonics $\omega, 3\omega, ..., (2m+1)\omega$, while an even order response component $x_{2m}(t)$ contains a constant d.c. term and even harmonics $2\omega, 4\omega, ..., 2m\omega$.

These structural characteristics of Volterra series response components are employed here for nonlinearity identification. The procedure is based on separating the first few response components by a method originally suggested by Gardiner (1968) and then used in a matrix form by Simpson and Powers (1972).

If $x_{(\alpha)}(t)$, $x_{(\beta)}(t)$ and $x_{(\gamma)}(t)$ are the measured responses for three different cases of system excitation $f(t) = \alpha \cos \omega t$, $f(t) = \beta \cos \omega t$ and $f(t) = \gamma \cos \omega t$, respectively, then

$$\begin{bmatrix} x_{(\alpha)}(t) \\ x_{(\beta)}(t) \\ x_{(\gamma)}(t) \end{bmatrix} = \begin{bmatrix} \alpha & \alpha^2 & \alpha^3 \\ \beta & \beta^2 & \beta^3 \\ \gamma & \gamma^2 & \gamma^3 \end{bmatrix} \begin{bmatrix} x_1(t) \\ x_2(t) \\ x_3(t) \end{bmatrix} + \begin{bmatrix} e_1 \\ e_2 \\ e_3 \end{bmatrix} \tag{4.3}$$

Response components $x_1(t), x_2(t), x_3(t)$ can be estimated from the above relationship. e_i are the truncation errors which are generally neglected while solving equation (4.3).

4.2 Identification of Polynomial Nonlinearity Form

Frequency domain analysis of the response components is carried out to distinguish a polynomial form of the nonlinear restoring force $g[x(t)]$, in the governing equation (4.1), from non-polynomial forms (e.g. bilinear, coulomb, *p*-th power type etc.).

For a system with a general polynomial form of nonlinearity

$$g[x(t)] = k_1 x(t) + k_2 x^2(t) + k_3 x^3(t) \tag{4.4}$$

the response spectrum is typically shown in Figure 4.1(a). The non-dimensional response $\eta(\tau) = x(t)/(A/k_1)$ has been numerically simulated, through a fourth order Runge-Kutta

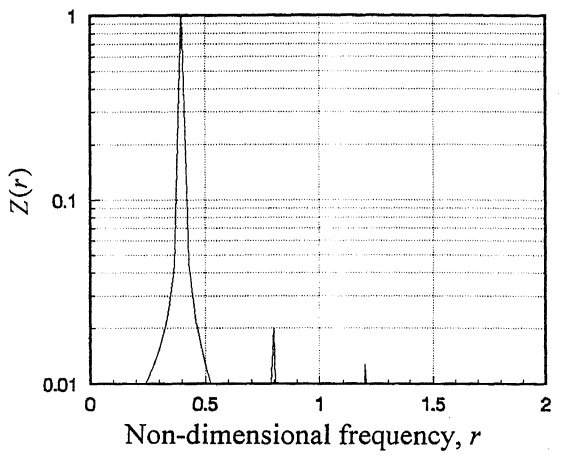

a) Total response

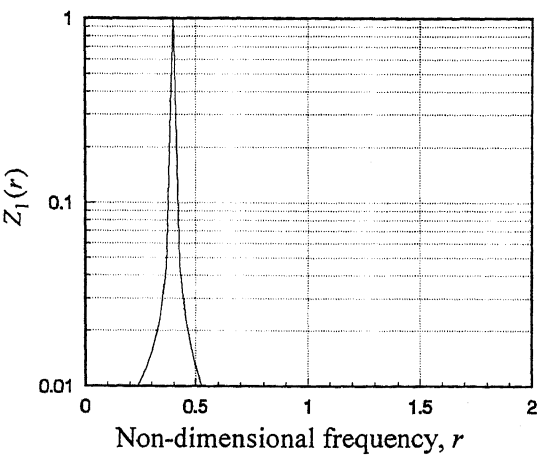

b) First order response component

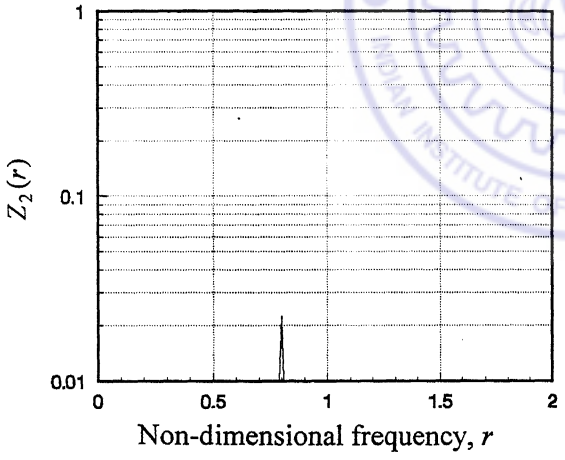

c) Second order response component

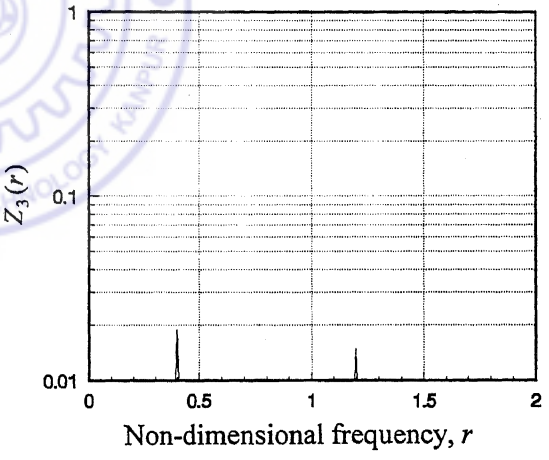

d) Third order response component

Figure 4.1 Response component spectra for $g[x(t)] = k_1 x(t) + k_2 x^2(t) + k_3 x^3(t)$

algorithm, for a set of non-dimensional parameters: $r = \omega / \sqrt{k_1 / m}$ =0.4; $\varsigma = c / 2\sqrt{k_1 m}$ =0.01; $\lambda_2 = k_2 A / k_1^2$ =0.01; $\lambda_3 = k_3 A^2 / k_1^3$ =0.015, where the non-dimensional time $\tau = \sqrt{k_1 / m}\, t$. The response components, $\eta_1(\tau), \eta_2(\tau), \eta_3(\tau)$ are separated using the order component separation technique of equation (4.3). Figures 4.1(b),(c),(d), respectively show the Fourier transforms $Z_1(r)$, $Z_2(r)$ and $Z_3(r)$ of the response components $\eta_1(\tau), \eta_2(\tau), \eta_3(\tau)$.

It can be seen that the first response component spectrum, $Z_1(r)$, contains only the first harmonic at r = 0.4, second response component spectrum, $Z_2(r)$, contains the second harmonic at $2 \times r = 0.8$ alone, while the third response component spectrum, $Z_3(r)$, contains the first and third harmonics. This observation is in confirmation with the structure of order components as given in equations (4.2). However a non-polynomial form of nonlinearity, gives results, which are in violation of equations (4.2). Figure 4.2(a) gives the Fourier transform of the simulated response for a system with nonlinearity given by

$$g[x(t)] = kx(t)|x(t)| \tag{4.5}$$

It is to be noted that a nonlinearity of above type can be expressed as a polynomial, with constant coefficients only for a constant range of response amplitude. The coefficients of the polynomial approximations, in general are functions of response amplitudes. The Fourier transforms (Figures 4.2.a-d) of the response components, in this case do not show the kind of structured behaviour, as seen in the case of polynomial nonlinearity (Figures 4.1.b-d. Similar disorder is observed in the case of a bilinear form of nonlinear function, given by

$$g[x(t)] = kx(t) \tag{4.6}$$

with the dual stiffness values $k = c_1$ for $x(t) \geq 0$ and $k = c_2$ for $x(t) < 0$. The Fourier transforms of the overall non-dimensional response $\eta(\tau)$ and the first response components $\eta_1(\tau)$ are shown in Figures 4.3(a),(b), for $c_1 = 0.9, c_2 = 1.0$ and non-

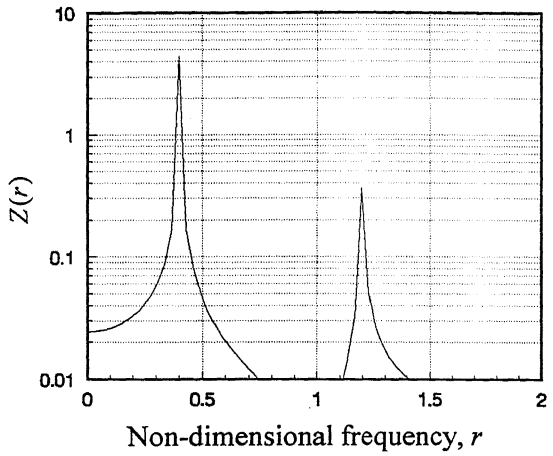

a) Total response

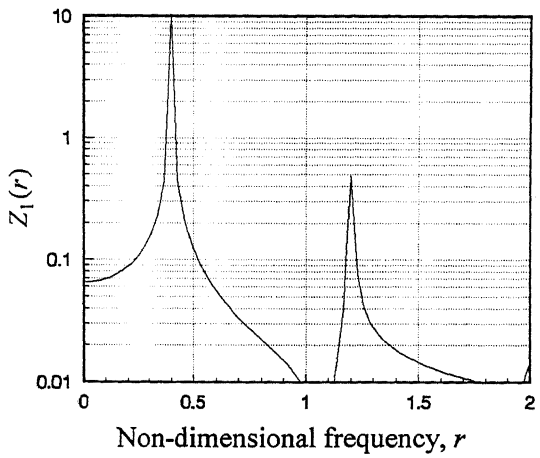

b) First order response component

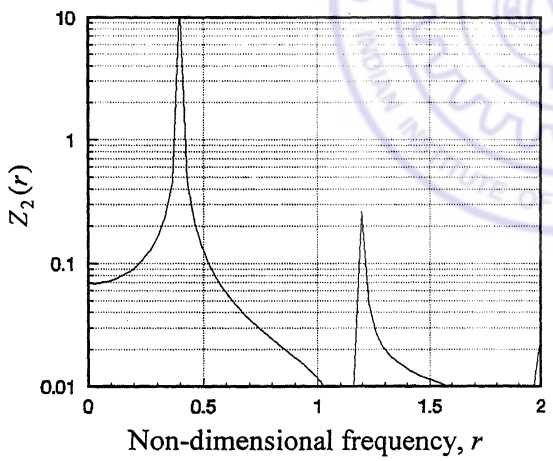

c) Second order response component

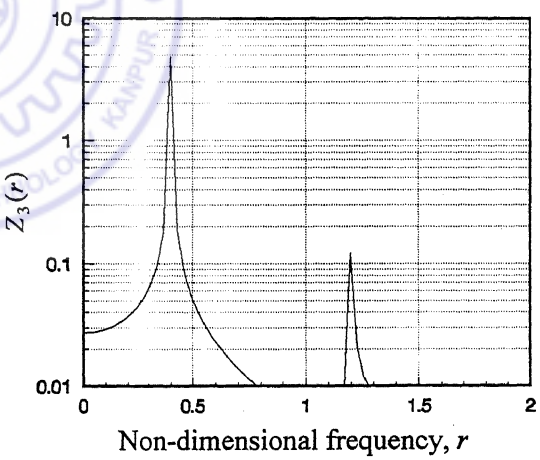

d) Third order response component

Figure 4.2 Response component spectra for $g[x(t)] = kx(t)|x(t)|$

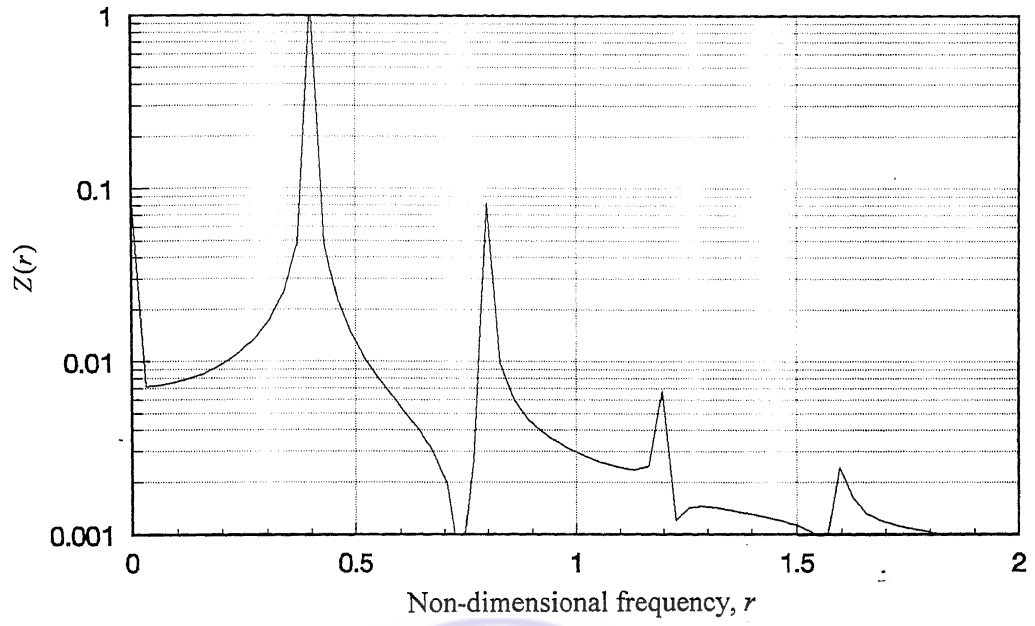

a) Total response

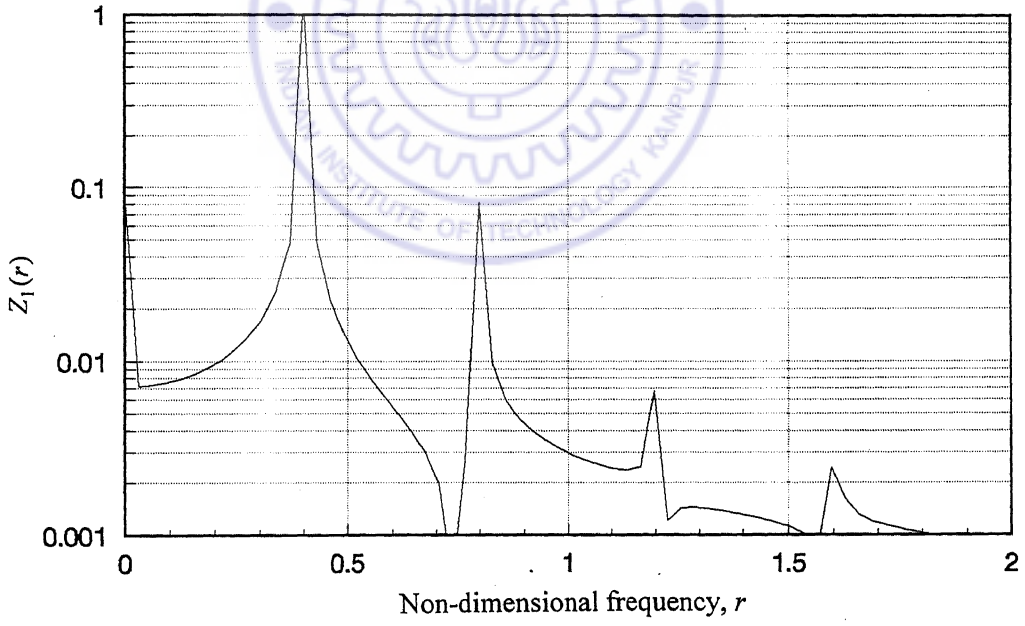

b) First order response component

Figure 4.3 Response component spectra for $g[x(t)] = kx(t)$; $k = 0.9$, for $x(t) \geq 0$; $k = 1.0$ for $x(t) < 0$

dimensional frequency equal to 0.4. However the second and third order components, $\eta_2(\tau)$ and $\eta_3(\tau)$ are found to be zero. Other commonly occurring non-polynomial forms of nonlinearity, where the damping and stiffness forces take the form $a\left[x^2(t)-1\right]\dot{x}(t)$ (Van-der Pol Oscillator); $c\dot{x}(t)+k_1x(t)\pm F_d$ (Coulomb Damper); $\beta\dot{x}(t)\left|\dot{x}(t)\right|+k_1x(t)$ (Quadratic Damping); $c\dot{x}(t)+kx^p(t)\mathrm{sgn}(x)$ (for a fractional power p, as in rolling element bearings) also do not exhibit an ordered form, as discussed earlier, when their response is treated as a Volterra series comprising of various ordered components.

These observations can be explained by the fact that, the procedure for ordered component separation remains valid only if the system kernels are amplitude independent. For a polynomial form of nonlinearity, the system kernels are independent of response amplitude and function of system parameters only. This is seen from the first order kernel transform expressions given in equation (3.18a) and the synthesis formulation for higher order kernel transforms given in equation (3.18b). While, the first order kernel transform is a function of the system's linear parameters alone (in addition to the excitation frequency), the higher order kernel transforms $H_n^{p,q}(\omega)$ are functions of lower order kernel transforms and nonlinear parameters. For non-polynomial nonlinearity, such expression of kernels in amplitude independent form is not possible. An equivalent polynomial form, in such cases, gives rise to amplitude dependent system parameters through its coefficients. This results in amplitude dependent kernel transforms. Subsequently, application of the method of ordered component separation, which involves variation of the excitation amplitude, gives inconsistent results.

These observations constitute the identification procedure for polynomial form of nonlinearity, whereby a given system can be subjected to a sinusoidal excitation and the response $x(t)$ is assumed to be a result of the convolution of applied force with the first and higher order Volterra kernels. Volterra series response components $x_1(t), x_2(t), x_3(t)$ can be extracted through equation (4.3). Compliance of the Fourier transforms of these response components with the harmonic component structure of equation (4.2) can be

checked. The system can be classified as having a polynomial form of nonlinearity in its restoring force if an odd order response component, $x_{2m+1}(t)$, contains only odd harmonics $\omega, 3\omega, ..., (2m+1)\omega$, while an even order response component $x_{2m}(t)$, if present, comprises of even harmonics $2\omega, 4\omega, ..., 2m\omega$ alone. If the spectra of the response components do not exhibit above ordered characteristics, the system nonlinearity can not be classified as polynomial form.

4.3 Distinction between Symmetric and Asymmetric Polynomial Forms

A polynomial form of nonlinearity, can be further identified as symmetric or asymmetric, through analysis of the even and odd harmonic of the response components. For a symmetric nonlinearity (e.g. as in Duffing oscillator), where

$$g[x(t)] = -g[-x(t)], \tag{4.7}$$

only odd orders $x_{2m+1}(t)$ of the response $x(t)$ exist. The even orders $x_{2m}(t)$ are zero. Expressing a symmetric form polynomial nonlinearity of the restoring force in a system through

$$m\ddot{x}(t) + c\dot{x}(t) + k_1 x(t) + k_3 x^3(t) + k_5 x^5(t) + ... = f(t), \tag{4.8}$$

and multiplying the above equation (4.8) by –1, one gets

$$-m\ddot{x}(t) - c\dot{x}(t) - k_1 x(t) - k_3 x^3(t) - k_5 x^5(t) - ... = -f(t) \tag{4.9}$$

Noting that , $-x^{2m+1}(t) = [-x(t)]^{2m+1}$, above equation (4.9) can be rewritten as

$$m[-\ddot{x}(t)] + c[-\dot{x}(t)] + k_1[-x(t)] + k_3[(-x(t))^3] + k_5[(-x(t))^5] + ... = -f(t) \tag{4.10}$$

If $\bar{x}(t)$ be the response for a negative excitation, $-f(t)$, so that the governing equation is,

$$m\ddot{\bar{x}}(t) + c\dot{\bar{x}}(t) + k_1\bar{x}(t) + k_3\bar{x}^3(t) + k_5\bar{x}^5(t) + ... = -f(t) \tag{4.11}$$

comparison of (4.8) and (4.11) gives

$$x(t) + \bar{x}(t) = 0 \tag{4.12}$$

i.e. for a symmetric nonlinear system, the sum of response under excitations $f(t)$ and $-f(t)$ become zero. However, a system with asymmetric nonlinearity with atleast an even power term $k_{2m}x^{2m}(t)$ in its governing equation, provides $[-x(t)]^{2m} = [x(t)]^{2m}$,

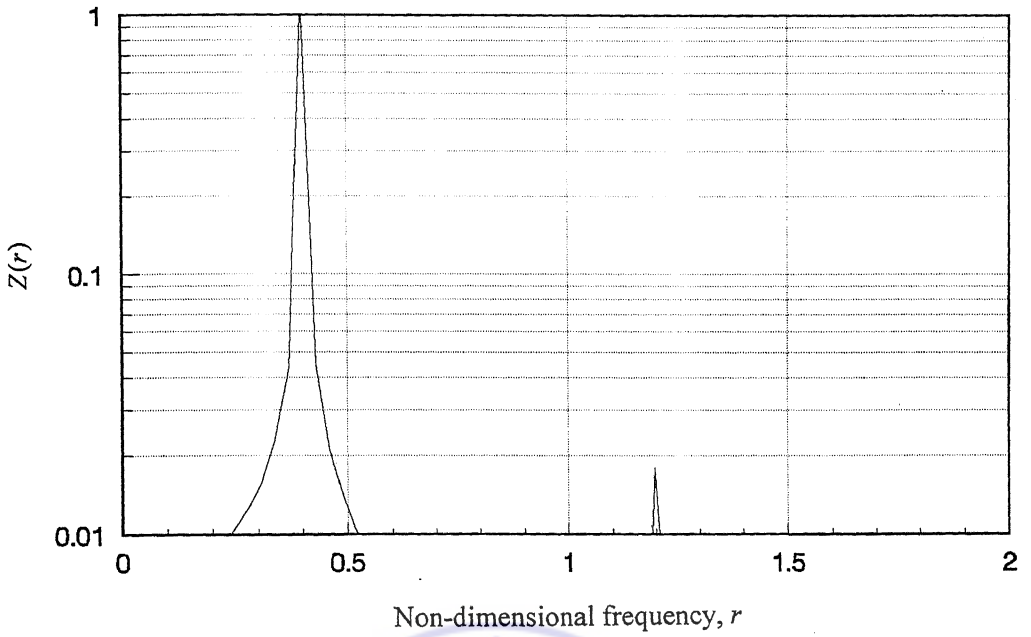

Figure 4.4 Response spectrum for $g[x(t)] = k_1 x(t) + k_3 x^3(t)$

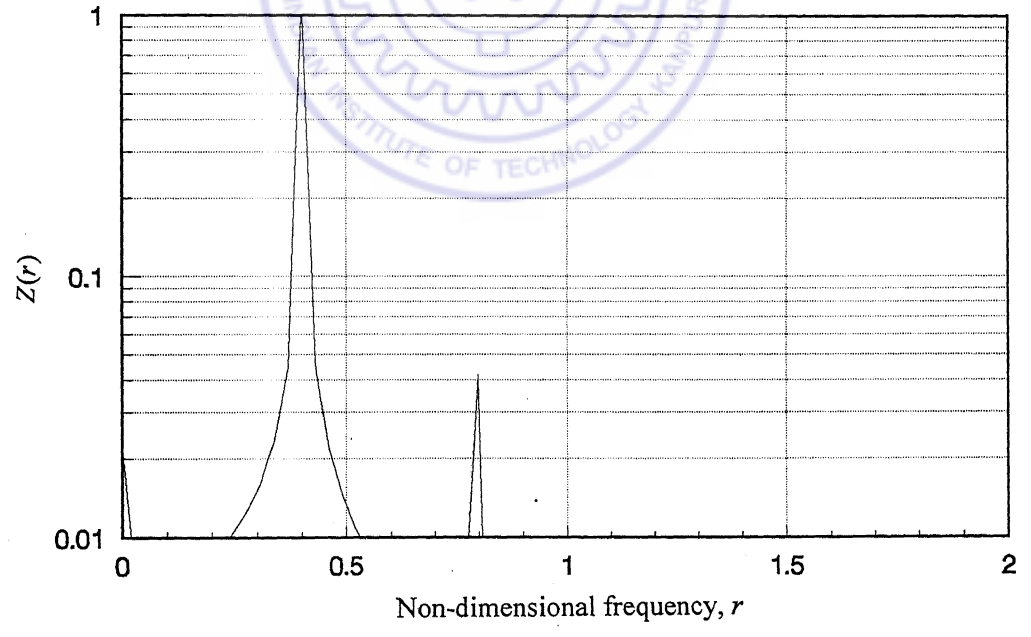

Figure 4.5 Response spectrum for $g[x(t)] = k_1 x(t) + k_2 x^2(t)$

leading to $x(t)+\bar{x}(t)\neq 0$. Substituting $\kappa=1$ in equation (3.4), for excitation $f(t)$ one obtains

$$x(t)=x_1(t)+x_2(t)+x_3(t)+... \tag{4.13}$$

Similarly, substitution of $\kappa=-1$ in equation (3.4) for excitation $-f(t)$ gives

$$\bar{x}(t)=-x_1(t)+x_2(t)-x_3(t)+... \tag{4.14}$$

Application of condition in equation (4.12) for a symmetric polynomial nonlinearity gives

$$x_2(t)+x_4(t)+...=0 \tag{4.15}$$

As the above equation is to be satisfied for all excitation levels, it implies that

$$x_2(t)=0,\quad x_4(t)=0,...$$

Now, since even order harmonic of the excitation frequency ω appear only in even order response components $x_2(t), x_4(t),...$ (equation (4.2)), the above leads to the conclusion that the response $x(t)$, of a system with symmetric polynomial nonlinearity will be devoid of any even order harmonics of the excitation frequency. The Fourier spectrum $Z(r)$ of the non-dimensional response $\eta(\tau)$ for a Duffing oscillator (symmetric polynomial nonlinearity) has been shown in Figure 4.4 . The spectrum is characterised by the presence of odd harmonics only. Even harmonic will, however, appear in response of asymmetric nonlinear systems (Figure 4.5).

4.4 Identification of the Series Structure of Polynomial Nonlinearity

Identification of the structure of polynomial series representing the nonlinear stiffness function $g[x(t)]$ is carried out through probing higher order Volterra kernel transforms of the system, which are obtained through subjecting the system to multi-tone excitation forces. Such multi-harmonic signals can be readily simulated on a computer. An electrodynamic shaker, connected to the computer through an analog to digital card and an amplifier can be employed to provide excitation to the system. The present analysis is restricted to a third degree polynomial, i.e.

$$g[x(t)]=k_1x(t)+k_2x^2(t)+k_3x^3(t) \tag{4.16}$$

Identification is made between following cases:

(i) $k_2 = 0$ and $k_1, k_3 \neq 0$

(ii) $k_3 = 0$ and $k_1, k_2 \neq 0$

(iii) $k_1, k_2, k_3 \neq 0$

Considering a three-tone excitation

$f(t) = A\cos\omega_1 t + B\cos\omega_2 t + C\cos\omega_3 t$

in equation (4.1), with

$g[x(t)] = k_1 x(t) + k_2 x^2(t) + k_3 x^3(t)$

the response harmonic amplitudes at fundamental and combination tones of various response components can be obtained (following equations 3.21-3.23) as

$$X_1(\omega_1) = AH_1(\omega_1) \tag{4.17a}$$

$$X_2(\omega_1 + \omega_2) = ABH_2(\omega_1, \omega_2) \tag{4.17b}$$

$$X_3(\omega_1 + \omega_2 + \omega_3) = \frac{3ABC}{2} H_3(\omega_1, \omega_2, \omega_3) \tag{4.17c}$$

Equations (4.17) provide the basis for estimating the first and higher order kernel transforms as

$$H_1(\omega_1) = X_1(\omega_1)/A \tag{4.18a}$$

$$H_2(\omega_1, \omega_2) = X_2(\omega_1 + \omega_2)/AB \tag{4.18b}$$

$$H_3(\omega_1, \omega_2, \omega_3) = \frac{X_3(\omega_1 + \omega_2 + \omega_3)}{(3ABC/2)} \tag{4.18c}$$

It is to be noted here, that above equations are based on the condition that the second order frequency combination $(\omega_1 + \omega_2)$ is distinct in its value from other second order frequency combinations. Similarly the third order frequency combination $(\omega_1 + \omega_2 + \omega_2)$ should be distinct in its value from all other third order frequency combinations. Although this condition is generally satisfied over the frequency range, there may be certain frequency sets $(\omega_1, \omega_2, \omega_3)$ for which the frequency combination $(\omega_1 + \omega_2)$ or $(\omega_1 + \omega_2 + \omega_2)$ may become commensurate with some other frequency combinations. In

such cases the second and third order kernel transforms can be obtained through summing up the contributing terms from all commensurate frequency combinations.

Figures 4.6 and 4.7 show the second and third order kernel transforms $H_2(\omega_1,\omega_2)$ and $H_3(\omega_1,\omega_2,\omega_3)$ obtained from the numerically simulated response to the three-tone excitation for the three cases of polynomial structures mentioned above. (These kernel transforms have been plotted for a range of ω_1/ω_n and ω_2/ω_n, keeping ω_3/ω_n fixed at a value of 0.6). It is simple to distinguish the first case ($k_2 = 0$ and $k_1, k_3 \neq 0$) from the other two, by noting that the second order Volterra kernel $H_2(\omega_1,\omega_2)$, is identically equal to zero, over the entire frequency range in this case, as seen from synthesised expressions of higher order kernel transforms given in equation (3.26), which are rewritten here for easy reference.

$$H_2(\omega_1,\omega_2) = -k_2 H_1(\omega_1)H_1(\omega_2)H_1(\omega_1+\omega_2) \tag{4.19}$$

$$H_3(\omega_1,\omega_2,\omega_3) = H_1(\omega_1)H_1(\omega_2)H_1(\omega_3)H_1(\omega_1+\omega_2+\omega_3)* \left[\frac{2}{3}k_2^2\{H_1(\omega_1+\omega_2)+H_1(\omega_2+\omega_3)+H_1(\omega_1+\omega_3)\}-k_3\right] \tag{4.20}$$

The equations (4.19, 4.20) above can also be referred to similarly recognise second order combination peaks at $\omega_1+\omega_2=\omega_n$, $\omega_2+\omega_3=\omega_n$ and $\omega_2+\omega_3=\omega_n$, in the third order kernel transform map of $H_3(\omega_1,\omega_2,\omega_3)$ for cases ii) and iii). These combination peaks can be seen to be absent in case i). These characteristics distinguish the symmetric case i) from cases ii) and iii).

Distinction can be made between the cases ii) and iii) by further investigating the third order kernel transform, $H_3(\omega_1,\omega_2,\omega_3)$. Figures 4.8(a),(b) show the third order kernel transform $H_3(\omega_1,\omega_2,\omega_n)$, with $\omega_3=\omega_n$, for cases (ii) and (iii) respectively. Both plots show peak values of the kernel transform at frequency combinations

(a) $\omega_1=\omega_n$, $\omega_2=\omega_n$

(b) $\omega_1=\omega_n$, $\omega_2=0$

(c) $\omega_1=0$, $\omega_2=\omega_n$

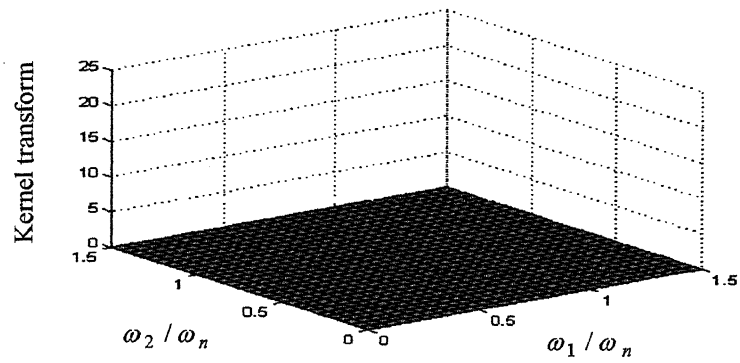

a) Case i): $k_2 = 0.0,\ k_3 = 0.01$

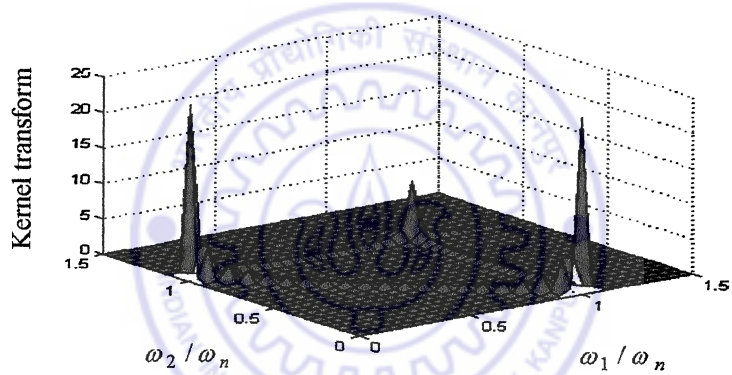

b) Case ii): $k_2 = 0.01,\ k_3 = 0.0$

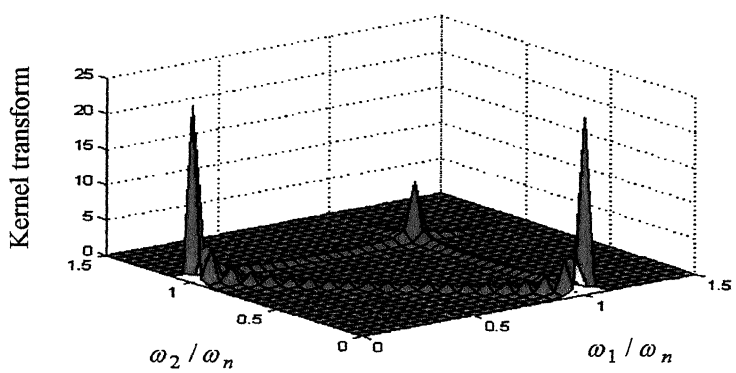

c) Case iii): $k_2 = 0.01,\ k_3 = 0.0001$

Figure 4.6 Second order kernel transform $H_2(\omega_1, \omega_2)$ for various series structures.

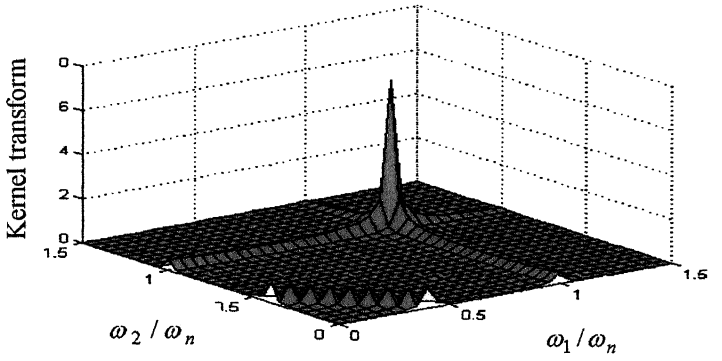

Case i): $k_2 = 0.0,\ k_3 = 0.01$

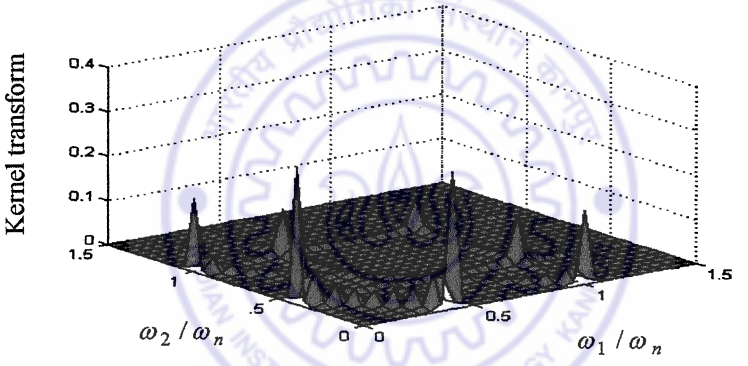

Case ii): $k_2 = 0.01,\ k_3 = 0.0$

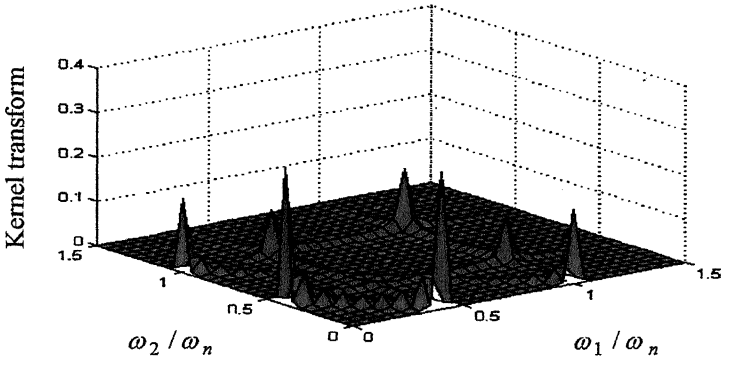

Case iii): $k_2 = 0.01,\ k_3 = 0.0001$

Figure 4.7: Third order kernel transform $H_3(\omega_1, \omega_2, \omega_3)$ for various series Structures. $[\omega_3 / \omega_n = 0.6]$

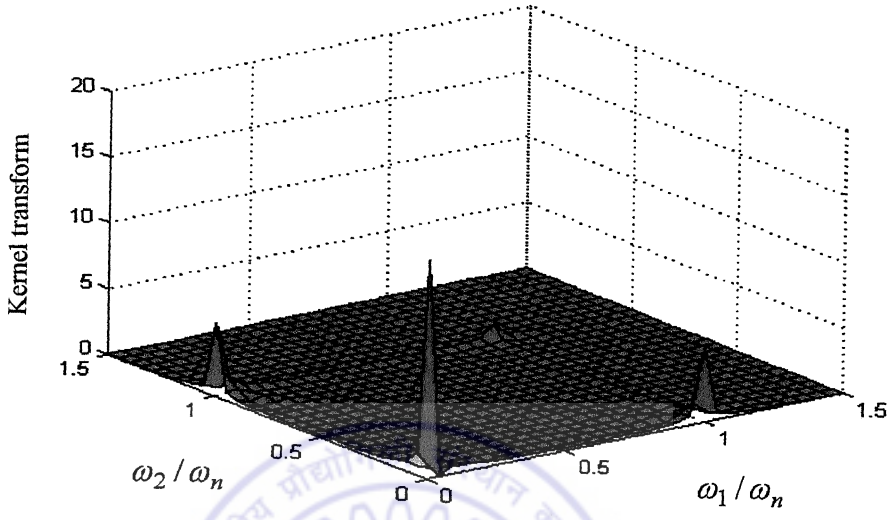

a) Case ii): $[k_2 = 0.01,\ k_3 = 0.0]$

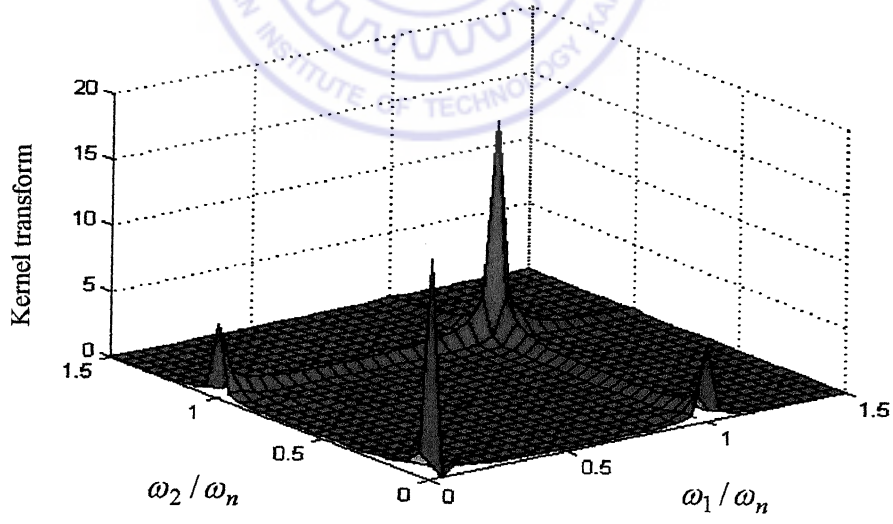

b) Case iii): $k_2 = 0.01,\ k_3 = 0.001$

Figure 4.8: Third order kernel transform $H_3(\omega_1, \omega_2, \omega_n)$ for cases ii) and iii).

It is to be noted that the peaks in cases (b) and (c) are identical due to reasons of symmetry. Distinction can be made between cases (ii) and (iii) by a comparison between the peaks of cases (b) or (c) with that occurring at the frequency combination (a). Using equation (4.20), the ratio of these peak values becomes

$$\frac{H_3(0,\omega_n,\omega_n)}{H_3(\omega_n,\omega_n,\omega_n)} = \frac{H_1(0)H_1(2\omega_n)\left[\{4H_1(\omega_n)+2H_1(2\omega_n)\}-k_1k_3/k_2^2\right]}{H_1(\omega_n)H_1(3\omega_n)\left[6H_1(2\omega_n)-k_1k_3/k_2^2\right]} \tag{4.21}$$

For $k_3 = 0$, the peak ratio becomes

$$\frac{H_3(0,\omega_n,\omega_n)}{H_3(\omega_n,\omega_n,\omega_n)} = \frac{H_1(0)H_1(2\omega_n)\left[\{4H_1(\omega_n)+2H_1(2\omega_n)\}\right]}{H_1(\omega_n)H_1(3\omega_n)\left[6H_1(2\omega_n)\right]} \tag{4.22}$$

Noting that for small damping, $H_1(\omega_n) >> H_1(2\omega_n)$, equation (4.22) can be further simplified as

$$\frac{H_3(0,\omega_n,\omega_n)}{H_3(\omega_n,\omega_n,\omega_n)} \approx \frac{H_1(0)H_1(2\omega_n)\left[4H_1(\omega_n)\right]}{H_1(\omega_n)H_1(3\omega_n)\left[6H_1(2\omega_n)\right]} \approx 5.33 \tag{4.23}$$

Similarly for $k_2 = 0$, and assuming damping to be very small

$$\frac{H_3(0,\omega_n,\omega_n)}{H_3(\omega_n,\omega_n,\omega_n)} = \frac{H_1(0)H_1(2\omega_n)}{H_1(\omega_n)H_1(3\omega_n)} \approx 5.33\zeta \tag{4.24}$$

Thus the peak ratio will vary between a maximum value of 5.33 for $k_3 = 0$ to a low value of 5.33ς for $k_2 = 0$. This can be seen in Figure 4.9, in which the peak ratio $\frac{H_3(0,\omega_n,\omega_n)}{H_3(\omega_n,\omega_n,\omega_n)}$ is plotted as a function of non-dimensional stiffness ratio k_1k_3/k_2^2, for a typical damping $\varsigma = 0.01$. It can be seen that the peak ratio is high and nearly constant at 5.33 up to a value of k_1k_3/k_2^2 equal to 0.01 and a system showing such characteristic can be deemed to be belonging to case ii), with the cubic term zero. The peak ratio is low and nearly constant at 0.0533 for value of k_1k_3/k_2^2 larger than 1000.0, categorising the system to case i). System giving values of this peak ratio somewhere in between can be seen to belong to case (iii), where both square and cubic powers of $x(t)$ are present in the nonlinear restoring force function.

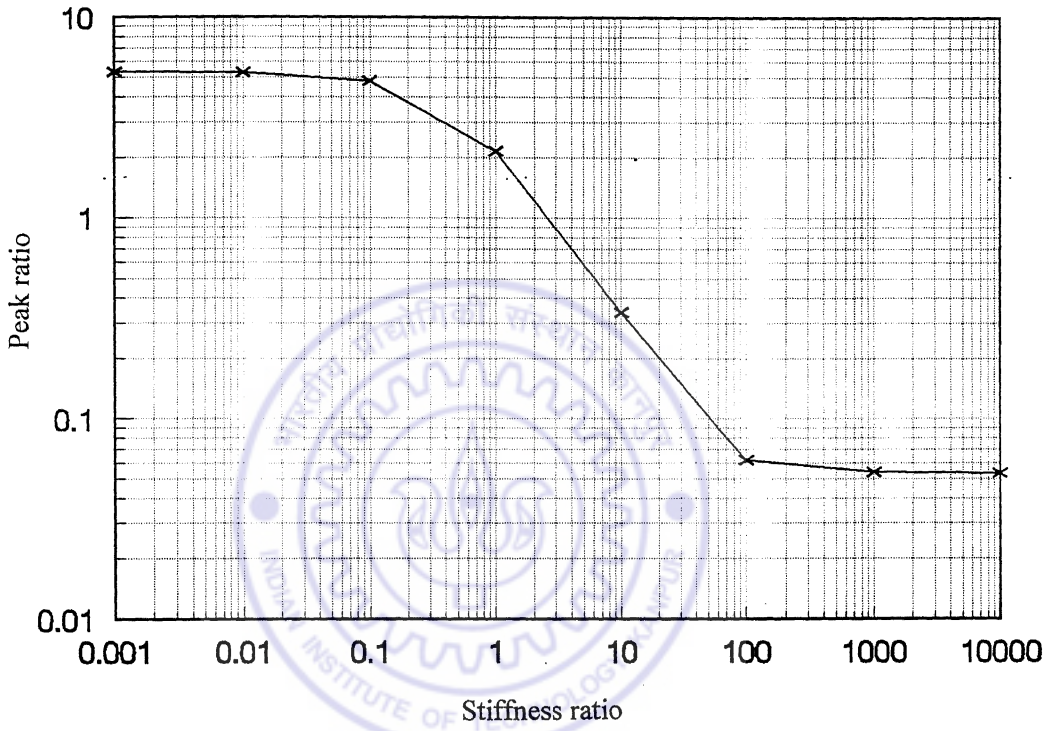

Figure 4.9 Variation in peak ratio, $H_3(0,\omega_n,\omega_n)/H_3(\omega_n,\omega_n,\omega_n)$ with non-dimensional Stiffness ratio, k_1k_3/k_2^2.

To obtain the peak ratio experimentally, response harmonic amplitude component $X_3(2\omega_n)$ is filtered from the third order response component $x_3(t)$ by employing a three tone excitation $f(t) = A\cos\omega_1 t + B\cos\omega_2 t + C\cos\omega_3 t$ with $\omega_1 = 0$, $\omega_2 = \omega_n$, $\omega_3 = \omega_n$. Similarly response harmonic amplitude component $X_3(3\omega_n)$ is filtered from $x_3(t)$ for the case $\omega_1 = \omega_n, \omega_2 = \omega_n, \omega_3 = \omega_n$. Considering the fact that these response harmonics can be generated by several commensurate frequency combinations, the amplitudes are related to the third order kernel transforms, through summing up all the coefficients contributed by each commensurate frequency combination, using equation (3.23), as

$$X_3(2\omega_n) = \left[\frac{3ABC}{2} + \frac{3ABC}{2} + \frac{3AB^2}{4} + \frac{3AC^2}{4} + \frac{3AB^2}{4} + \frac{3AC^2}{4}\right] H_3(0,\omega_n,\omega_n)$$
$$= \left[3ABC + \frac{3AB^2}{2} + \frac{3AC^2}{2}\right] H_3(0,\omega_n,\omega_n) \qquad (4.25)$$

and

$$X_3(3\omega_n) = \left[\begin{array}{l} \frac{A^3}{4} + \frac{B^3}{4} + \frac{C^3}{4} + \frac{3ABC}{2} + \frac{3AB^2}{4} + \frac{3AC^2}{4} \\ + \frac{3A^2B}{4} + \frac{3A^2C}{4} \frac{3B^2C}{4} + \frac{3BC^2}{4} \end{array}\right] H_3(\omega_n,\omega_n,\omega_n) \qquad (4.26)$$

Thus the kernel transforms $H_3(0,\omega_n,\omega_n)$ and $H_3(\omega_n,\omega_n,\omega_n)$ can be obtained from equations (4.25, 4.26) above and the peak ratio can be computed for determining the polynomial structure among the cases (i), (ii) and (iii).

4.5 Remarks

The nonlinearity identification scheme is restricted to making distinctions between polynomial and non-polynomial forms and further between symmetric and asymmetric polynomial forms and their series structure. Classification within non-polynomial forms has not been attempted. The possibility of employing time Volterra kernels for such classification however, can be explored.

CHAPTER 5

PARAMETER ESTIMATION IN SINGLE-DEGREE-OF-FREEDOM SYSTEMS

The parameter estimation procedure has been developed for systems containing polynomial form of nonlinearity. For such systems, as seen in Chapter 3, higher order Volterra kernel transforms can be synthesised in terms of the first order kernel transforms and the nonlinear parameters of the polynomial. The synthesis relationships along with measurements of the first and higher order kernels can be employed to determine the unknown parameters. Volterra series, being an infinite power series, however, suffers from the inherent limitation of truncation error and convergence. Emphasis has been laid here on addressing these issues rigorously, while making measurements for the higher order Frequency Response Functions (FRFs). The quality of FRF measurements and subsequent processing is a function of system nonlinearity, which is unknown. The convergence of the series can also be ascertained only if the magnitude of nonlinearity is known. A procedure based on recursive iteration is therefore suggested in this chapter to deal with these aspects in an integral manner. Harmonic excitation is employed and measurements of the first and higher order response harmonics are obtained. Single term approximations are initially applied to these measurements to obtain preliminary estimates of the kernels. The number of terms is increased up to the convergence threshold in the approximations through recursive iteration to refine the estimates. A detailed convergence analysis of response harmonic series is presented and a critical non-dimensional nonlinear parameter is defined as a function of excitation level, excitation frequency and number of series terms. A method of selecting the excitation levels is suggested for minimum error in the response harmonic series approximation. Signal strength and series approximation error of higher order response harmonics is investigated over the frequency space and a guideline is developed for selecting the excitation frequencies. The procedure is illustrated with numerical simulations.

5.1 Recursive Iteration

A single-degree-of-freedom system with polynomial form of nonlinearity under single-tone harmonic excitation is considered. The governing equation is

$$m\ddot{x}(t) + c\dot{x}(t) + g[x(t)] = A\cos\omega t \tag{5.1}$$

with

$$g[x(t)] = k_1 x(t) + k_2 x^2(t) + k_3 x^3(t) + \ldots$$

Considering the response harmonic series (3.14) up to a finite number of terms, k, and rearranging for the first three response harmonics, one obtains

$$H_1(\omega) \approx \frac{1}{A}\left[X(\omega) - \sum_{i=2}^{k} \sigma_i(\omega) \right] \tag{5.2a}$$

$$H_2(\omega,\omega) \approx \frac{2}{A^2}\left[X(2\omega) - \sum_{i=2}^{k} \sigma_i(2\omega) \right] \tag{5.2b}$$

$$H_3(\omega,\omega,\omega,) \approx \frac{4}{A^3}\left[X(3\omega) - \sum_{i=2}^{k} \sigma_i(3\omega) \right] \tag{5.2c}$$

The higher order kernel transforms, $H_2(\omega,\omega)$ and $H_3(\omega,\omega,\omega)$ are related to the first order kernel transform and nonlinear parameters (using equation 3.18b) as

$$H_2(\omega,\omega) = -k_2 H_1^2(\omega) H_1(2\omega) \tag{5.3a}$$

$$H_3(\omega,\omega,\omega) = H_1^3(\omega) H_1(3\omega)\left[2k_2^2 H_1(2\omega) - k_3\right] \tag{5.3b}$$

The truncated series $\sum_{i=2}^{k} \sigma_i(n\omega)$ in equations (5.2) are computed at every step of iteration with the estimated values of first order kernel transforms, $H_1(\omega)$, and nonlinear parameters, k_2 and k_3, obtained from the previous step. Employing equation (5.2), linear and nonlinear parameters are re-estimated and the iteration is continued till the estimates converge within a specified limit. For a typical cubic nonlinearity case with $g[x(t)] = k_1 x(t) + k_3 x^3(t)$, the parameter estimation algorithm involves the following steps.

Step-I: System is excited at frequencies, ω_i, with ω_i varying over a frequency range encompassing the natural frequency, ω_n, of the system. First response harmonic amplitude, $X(\omega_i)$, is filtered from the overall response, $x(t)$, which gives the preliminary estimate of first order kernel transform as

$$H_1(\omega_i) = X(\omega_i)/A_i \quad , \qquad i = 1,....N \tag{5.4}$$

A curve fitting procedure (Ewins, 1984) is employed to obtain the best fit FRF curve and preliminary estimation of linear parameters is made.

Step-II: System is excited at frequencies, ω_j, $j = 1,2,...N$, where the third response harmonic, $X(3\omega_j)$, is distinct and measurable (As shown in next section, the third response harmonic becomes distinct around one-third of natural frequency). Employing equation (5.2c), preliminary estimate of nonlinear parameter, k_3, is obtained through regression between the estimated third order kernel transform and its synthesised kernel factor, $\Gamma_3(\omega_j)$, using the following relationship

$$H_3(\omega_j, \omega_j, \omega_j) = k_3 \Gamma_3(\omega_j) \tag{5.5}$$

where

$$\Gamma_3(\omega_j) = -H_1^3(\omega_j) H_1(3\omega_j) \tag{5.6}$$

Step-III: The series $\sum_{i=2}^{k} \sigma_i(\omega)$ is computed with the $H_1(\omega)$ values taken from the best fit curve estimated in Step-I and the nonlinear parameter, k_3, estimated in Step-II and substituted in equation (5.2a) to obtain new estimates of linear parameters.

Step-IV: The series $\sum_{i=2}^{k} \sigma_i(3\omega)$ is computed and substituted in equation (5.2c) to re-estimate the nonlinear parameter k_3.

Iteration is continued till the estimate of nonlinear parameter, k_3, converges within a specified limit. The algorithm is general in nature and can be readily extended to a system

with square or combined square and cubic form of nonlinearity. However, for accurate and convergent parameter estimation the following issues need to be addressed

i) selection of appropriate excitation levels, A_i, in equation (5.4) for error minimization in first response harmonic measurement,

ii) selection of limiting number of terms, k, in the equations (5.2a,c) for convergent Volterra series application,

iii) selection of appropriate excitation frequency and amplitude for good measurability of higher response harmonics.

In the following sections, a detailed error analysis and convergence study is carried out to address the first two issues mentioned above. Measurability of the higher response harmonic signals is then studied for deciding the excitation frequency and excitation level.

5.2 Convergence and Error Analysis

The convergence study has been restricted to the case of a Duffing oscillator under a single-tone harmonic excitation

$$m\ddot{x}(t) + c\dot{x}(t) + k_1 x(t) + k_3 x^3(t) = A\cos\omega t \tag{5.7}$$

Defining non-dimensional parameters

$$\tau = \omega_n t \qquad \omega_n = \sqrt{k_1/m} \qquad \varsigma = c/2m\omega_n \qquad \eta = x/X_{st}$$

$$X_{st} = A/k_1 \qquad \lambda_3 = k_3 A^2/k_1^3 \qquad r = \omega/\omega_n$$

equation (5.7) is rewritten as

$$\eta''(\tau) + 2\varsigma\,\eta'(\tau) + \eta(\tau) + \lambda_3\eta^3(\tau) = \cos r\tau \tag{5.8}$$

$(')$ denotes differentiation with respect to τ. The non-dimensional response $\eta(\tau)$ can be expressed as

$$\eta(\tau) = |Z(r)|\cos(r\,\tau + \psi_1) + |Z(3r)|\cos(3r\tau + \psi_3) + |Z(5r)|\cos(5r\tau + \psi_5) + \ldots \tag{5.9}$$

with nth response harmonic amplitude, $Z(nr)$, given by

$$Z(nr) = \sum_{i=1}^{\infty} \sigma_i(nr) \tag{5.10}$$

The individual series term, $\sigma_i(nr)$, becomes

$$\sigma_i(nr) = 2\left(\frac{1}{2}\right)^{n+2i-2} {}_{n+2i-2}C_{i-1}\, H_{n+2i-2}^{n+i-1,i-1}(r) \tag{5.11}$$

The non-dimensional synthesis equations, for higher order kernel transforms $H_{n+2i-2}^{n+i-1,i-1}(r)$, following the harmonic probing procedure (equation 3.18) become

$$H_1(r) = 1/(-r^2 + 1 + j2\varsigma r) \qquad \text{for } n = 1 \tag{5.12a}$$

and

$$H_n^{p,q}(r) = -\frac{\lambda_3 H_1(r_{p,q})}{{}^nC_q} \sum_{\substack{p_i+q_i=n_i \\ n_1+n_2+n_3=n}} \left\{{}^{n_1}C_{q_1} H_{n_1}^{p_1,q_1}(r)\right\} * \left\{{}^{n_2}C_{q_2} H_{n_2}^{p_2,q_2}(r)\right\} * \left\{{}^{n_3}C_{q_3} H_{n_3}^{p_3,q_3}(r)\right.$$

$$\text{for } n > 1 \tag{5.12b}$$

Since practical estimation of a response harmonic, incorporates only a finite number of terms of the series (5.10), convergence of the response harmonic is specific to the number of terms included in the analysis. Confining the power series to include a finite number of terms, *k*, the approximation for the *n*th harmonic can be denoted as

$${}_kZ(nr) = \sum_{i=1}^{k} \sigma_i(nr) \tag{5.13}$$

and the relative error between the above approximation and the exact value of the response amplitude of the *n*th harmonic is

$${}_k^n e = \left|[Z(nr) - {}_kZ(nr)]/Z(nr)\right| \tag{5.14}$$

For absolute convergence of a series, its succeeding terms should continuously decrease. However, the response series, $Z(nr)$, exhibits conditional convergence characteristics and the error, ${}_k^n e$, is seen to depend on the number of series terms, *k*, excitation frequency ratio, *r*, and on the non-dimensional nonlinear parameter λ_3.

5.2.1 Convergence Analysis

The response $\eta(\tau)$ of the governing equation (5.8) is computed numerically in non-dimensional form, through fourth order Runge-Kutta method. Amplitudes of various response harmonics $Z(r)$, $Z(3r)$ etc are obtained through harmonic filtering of the response $\eta(\tau)$. This is termed as 'exact' response. Figures 5.1 (a), (b) typically show the non-dimensional response $\eta(\tau)$ and the exact response harmonic amplitudes for non-dimensional frequency $r = 0.35$ and non-dimensional nonlinear parameter $\lambda_3 = 0.04$. The Volterra series response is synthesized by considering the series in equation (5.10) up to k number of terms. Each series term, $\sigma_i(nr)$, $i = 1,2,...,k$ is computed from equation (5.11), in which the higher order kernel transforms $H_{n+2i-2}^{n+i-1,i-1}(r)$ are obtained by step-by-step reduction into lower order transforms using (5.12b). The series form of response amplitude $Z(r)$, following equations (5.10, 5.11 and 5.12b), becomes

$$\begin{aligned} Z(r) &= H_1(r) + \frac{3}{4}H_3(r,r,-r) + \frac{5}{8}H_5(r,r,r,-r,-r) + \ldots \\ &= H_1(r) - \frac{3}{4}\lambda_3 H_1^3(r)H_1(-r) + \lambda_3^2\left[\begin{array}{l} \frac{9}{16}H_1^4(r)H_1^3(-r) + \frac{9}{8}H_1^5(r)H_1^2(-r) \\ +\frac{3}{16}H_1^4(r)H_1^2(-r)H_1(3r) \end{array}\right] + \ldots \end{aligned} \quad (5.15)$$

Similarly series form of response harmonic amplitude $Z(3r)$ becomes

$$\begin{aligned} Z(3r) &= \frac{1}{4}H_3(r,r,r) + \frac{5}{16}H_5(r,r,r,r,-r) + \ldots \\ &= -\frac{\lambda_3}{4}H_1^3(r)H_1(3r) + \lambda_3^2\left[\begin{array}{l} \frac{9}{16}H_1^5(r)H_1(-r)H_1(3r) \\ +\frac{3}{8}H_1^4(r)H_1(-r)H_1^2(3r) \end{array}\right] + \ldots \end{aligned} \quad (5.16)$$

Convergence of Volterra series representation of overall response $\eta(\tau)$ is shown in Figure 5.2 (a), (b) through phase-plane plots for first two terms for a typical non-dimensional frequency $r = 0.6$ and for two different values of nonlinear parameter $\lambda_3 = 0.05$ and $\lambda_3 = 0.1$. These response components are constructed using

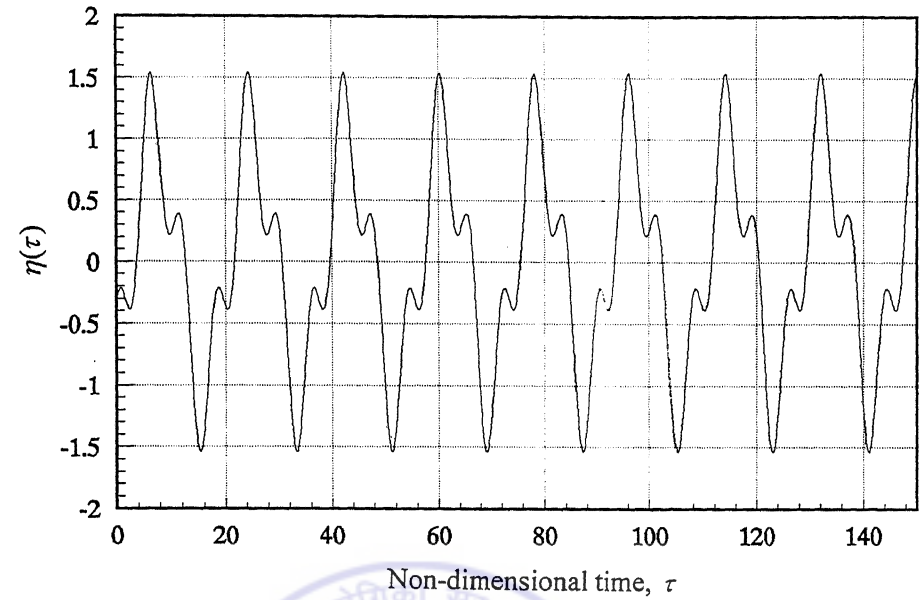

a) Response $\eta(\tau)$

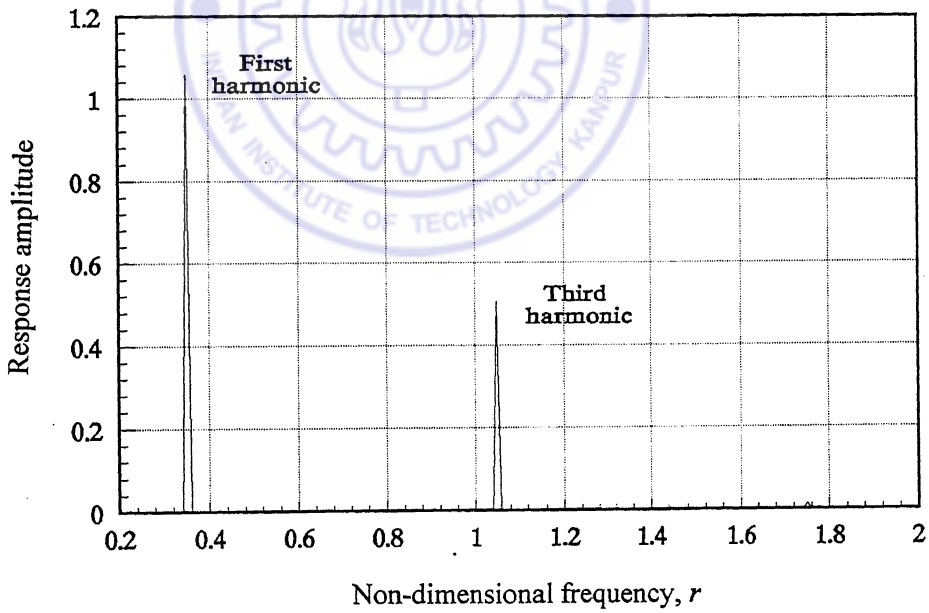

b) Response spectrum of $\eta(\tau)$

Figure 5.1 Typical non-dimensional response, $\eta(\tau)$ and its dominant harmonic amplitudes. ($\lambda_3 = 0.04$, excitation frequency $r = 0.35$)

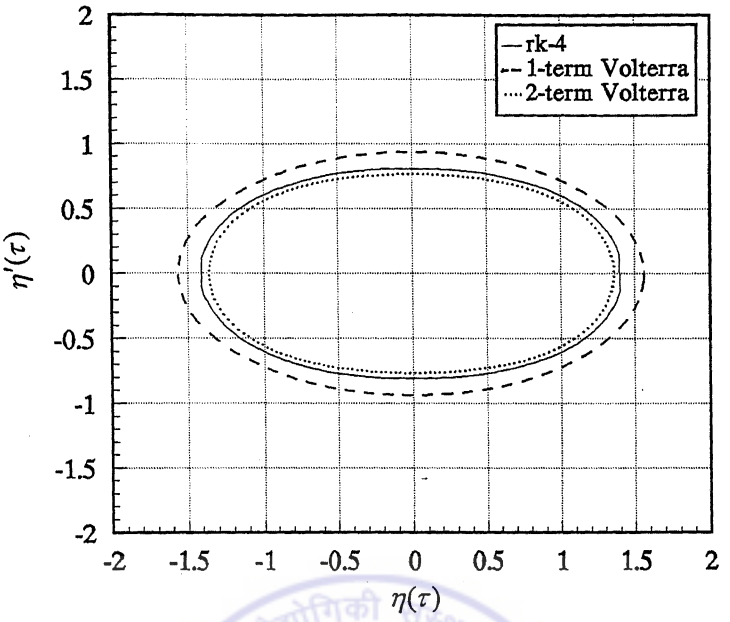

a) $r = 0.6$ and $\lambda_3 = 0.05$.

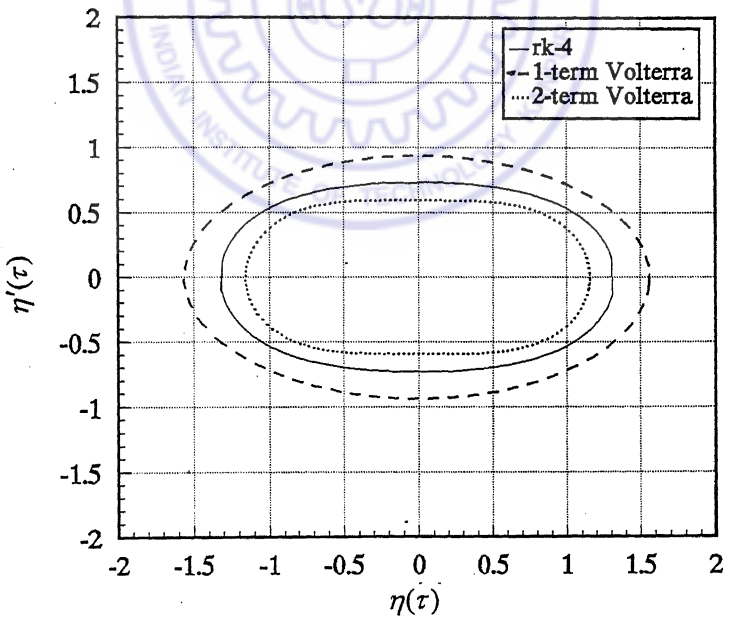

b) $r = 0.6$ and $\lambda_3 = 0.1$.

Figure 5.2 Phase-plane trajectories of response, $\eta(\tau)$

$$\eta(\tau) = \eta_1(\tau) + \eta_3(\tau) + \ldots \tag{5.17}$$

with

$\eta_1(\tau) = \sigma_1(r)e^{jr\tau}$ + complex conjugate term

$\eta_3(\tau) = \sigma_1(3r)e^{j3r\tau} + \sigma_2(r)e^{jr\tau}$ + complex conjugate terms

where $\sigma_1(r), \sigma_1(3r)$ and $\sigma_2(r)$ are defined in equation (5.11).

Convergence of the Volterra series response can be graphically represented by the proximity of the trajectory to that of response obtained from numerical integration. It can be seen that the phase plot of a two-term series is closer to the exact one than the single-term series, indicating a converging trend. A comparison of Figures 5.2 (a) and 5.2 (b) shows that better convergence is obtained with a lower value of λ_3. However, the phase-plane comparison can be used for convergence study of overall response only.

Convergence of individual response harmonic amplitudes, $Z(nr)$, is analysed by computing the relative errors ${}^n_k e$ using equation (5.14) for various values of non-dimensional nonlinear parameter λ_3. The variation of relative errors, ${}^1_k e$ and ${}^3_k e$, between the 'exact' and k-term approximations of the harmonics for various values of k and non-dimensional non-linear parameter, λ_3, have been plotted in Figures 5.3 (a) and 5.3 (b) for a typical non-dimensional excitation frequency, $r = 0.6$. The errors can be seen to decrease up to a certain number of terms in the approximation, beyond which they display an increasing trend. The number of terms up to which the error, for the nth harmonic and a given λ_3, shows a decreasing trend can be denoted as ${}^n k_{crit}$. It can be observed that for $\lambda_3 = 0.08$, ${}^1 k_{crit} = 4$ in the case of the 1st harmonic and the optimum number of terms in the response series should be four. Similarly three term series is optimum for representing the 3rd harmonic.

Approximation errors have been shown as a function of the nonlinear parameter λ_3, for $k = 1$ to 4, in Figures 5.4(a), (b). The plots in Figures 5.3 and 5.4 can be utilised to define

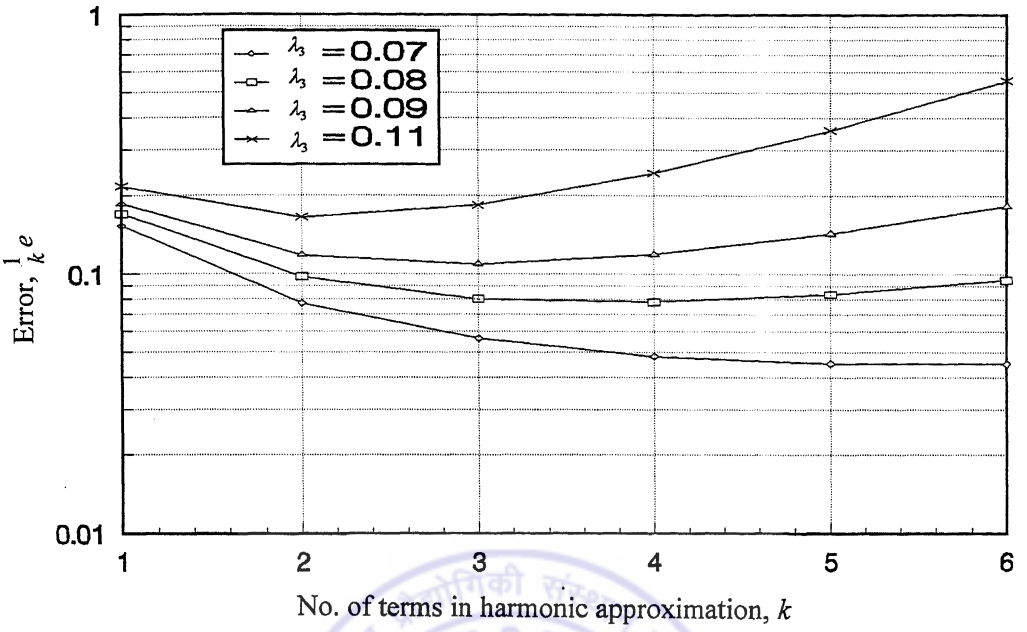

a) 1st harmonic.

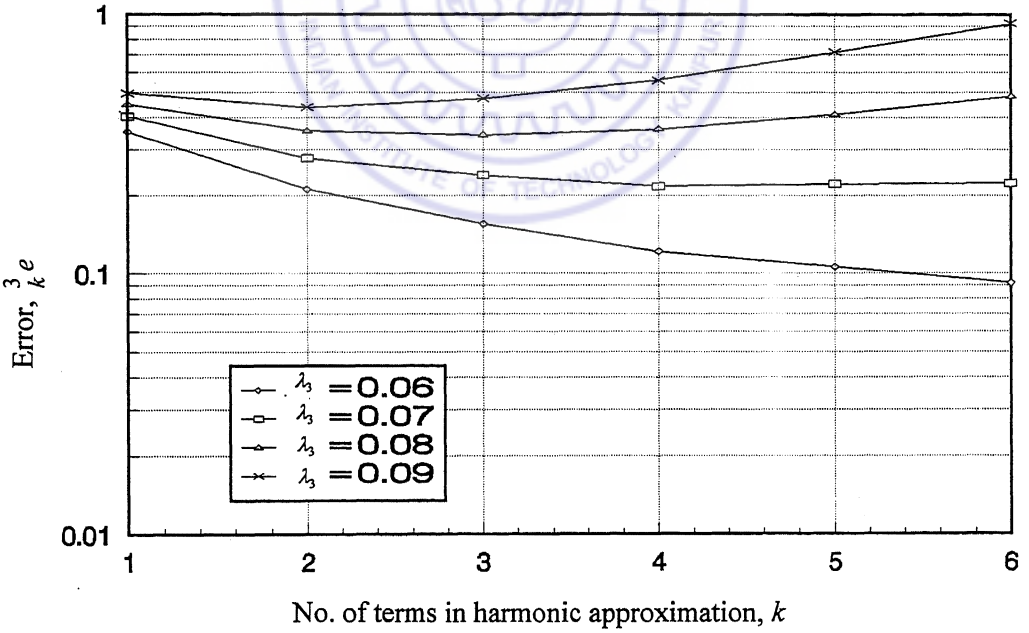

b) 3rd harmonic.

Figure 5.3 Error variation with the number of approximation terms, k. ($r = 0.6$)

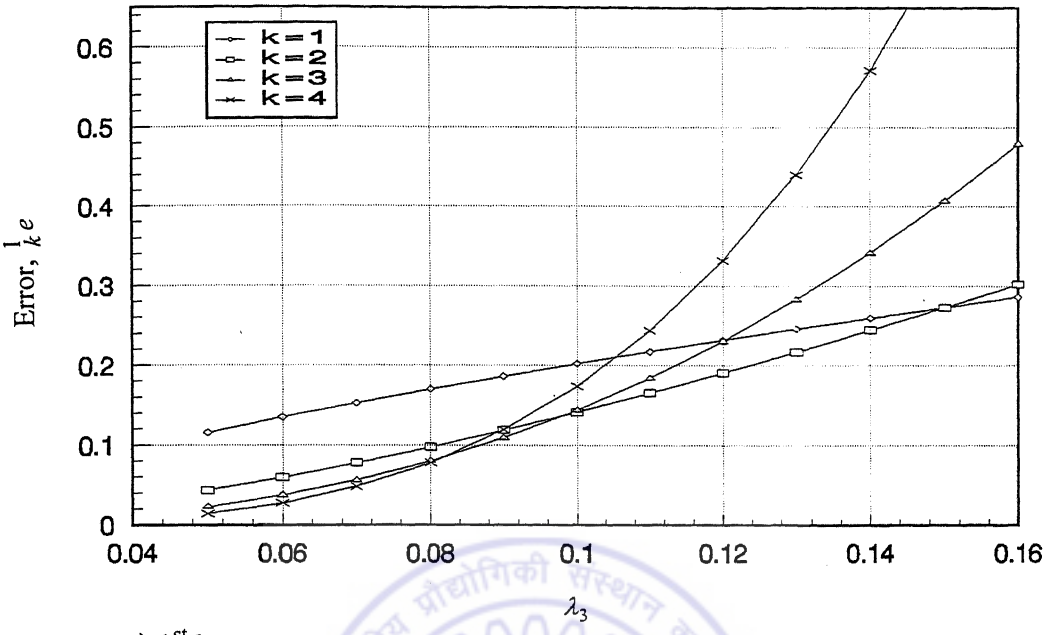

a) 1st harmonic.

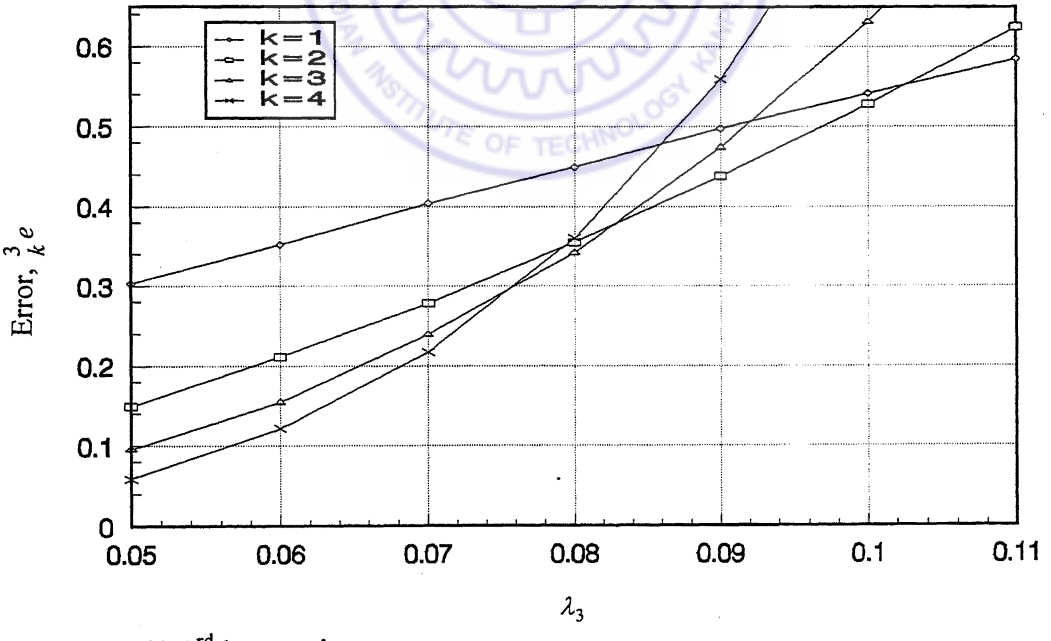

b) 3rd harmonic.

Figure 5.4 Relative errors in response harmonics for various values of non-dimensional parameter λ_3 . ($r = 0.6$)

a critical value ${}^{n}_{k}\lambda_{crit}$, of the non-dimensional nonlinear parameter, to get convergence in a k-term approximation of the nth harmonic. It should be noted that the non-dimensional nonlinear parameter λ_3, involves the nonlinear stiffness term k_3 as well as the harmonic force amplitude A. Critical values ${}^{n}_{k}\lambda_{crit}$, can be suitably employed to decide the excitation levels in experiments.

The critical value, ${}^{n}_{k}\lambda_{crit}$, can be defined as the maximum value of λ_3, for which ${}^{n}_{k}e \leq {}^{n}_{k-1}e$. For a four term approximation of the 1st harmonic, the critical value ${}^{1}_{4}\lambda_{crit}$, of the nonlinear parameter is seen to be 0.082 (Figure 5.4a), while for a three term approximation ${}^{1}_{3}\lambda_{crit} = 0.098$ (Figure 5.4a). Similarly, for four-term approximation of the 3rd harmonic, the critical value ${}^{3}_{4}\lambda_{crit}$ is 0.075 and for three term approximation ${}^{3}_{3}\lambda_{crit}$ is 0.083 (Figure 5.4b).

The critical values ${}^{1}_{k}\lambda_{crit}$ and ${}^{3}_{k}\lambda_{crit}$ (for harmonics $n = 1$ and 3) are plotted in Figures 5.5(a), (b) respectively, for k ranging from 2 to7. As shown, these figures help to define the zones of convergence and divergence of a response harmonic as a function of the non-dimensional parameter λ_3 and the number of terms, k, in the approximation. As an example, if the value of the non-dimensional nonlinear parameter λ_3, of a given system is 0.1, then only the first three terms, i.e. $k = 3$, in the approximation, will give a converging solution for the 1st harmonic (Figure 5.5a). For a lower value of $\lambda_3 = 0.07$, converged solution is obtained till six terms ($k = 6$) in the approximation. Similar pattern can be observed in the case of the 3rd harmonic, given in Figure 5.5(b). It is obvious that better accuracy can be obtained with lower values of λ_3, since more number of terms can be included in the approximation of the response harmonics. Figures 5.3, 5.4 and 5.5 pertain to a non-dimensional excitation frequency, $r = 0.6$. The excitation frequency is varied over a range and the critical values of λ_3 are plotted for k, ranging from 2 to 7, in Figures 5.6a-f for the 1st harmonic and Figures 5.7a-e for the 3rd harmonic. It can be seen

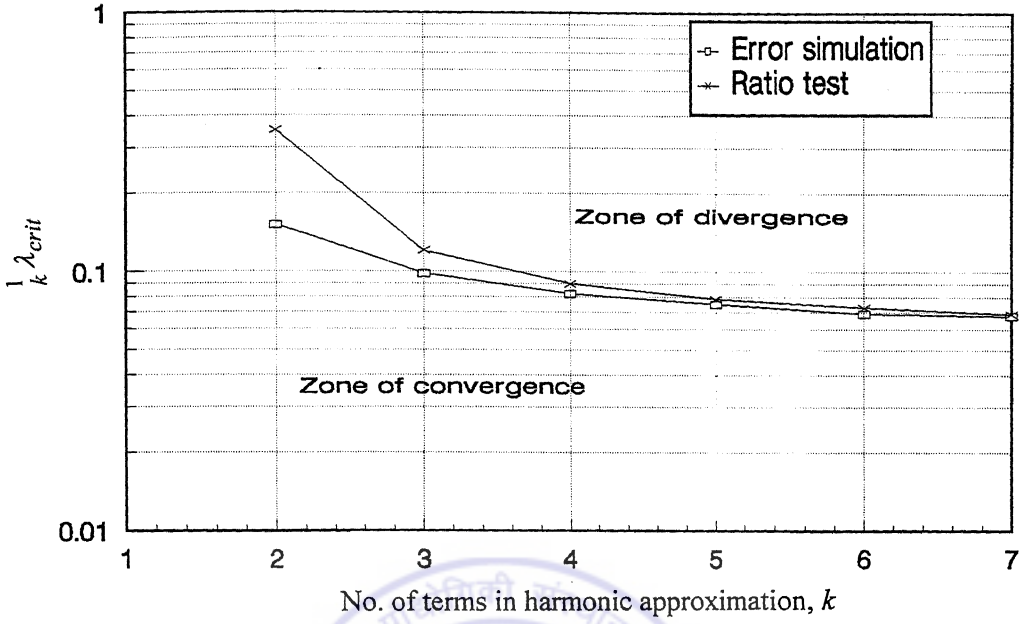

a) 1st harmonic.

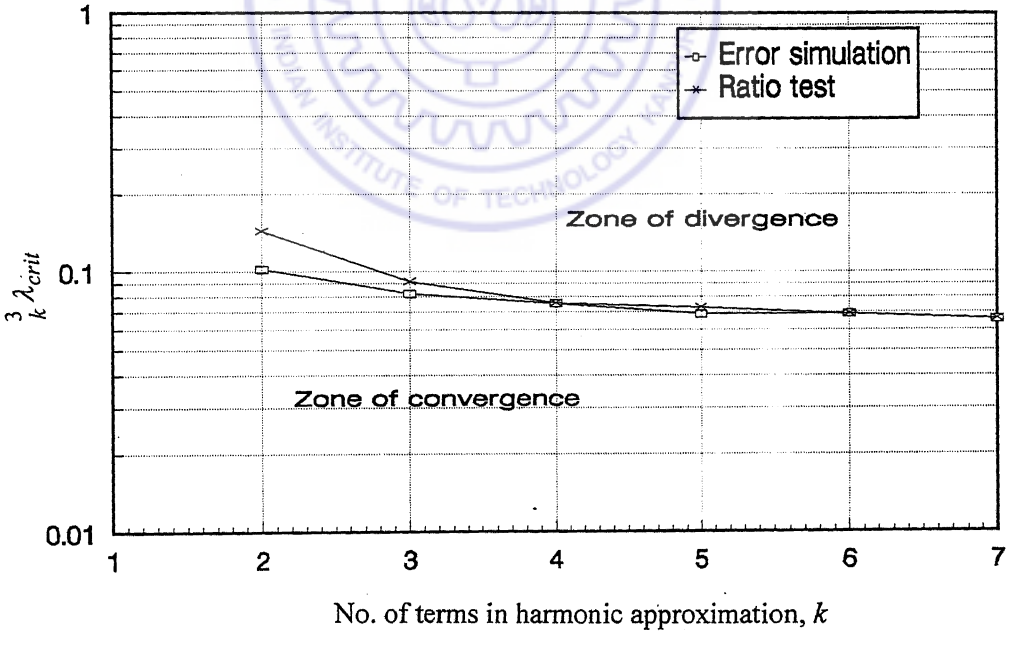

b) 3rd harmonic.

Figure 5.5 Zones of convergence and divergence, ($r = 0.6$).

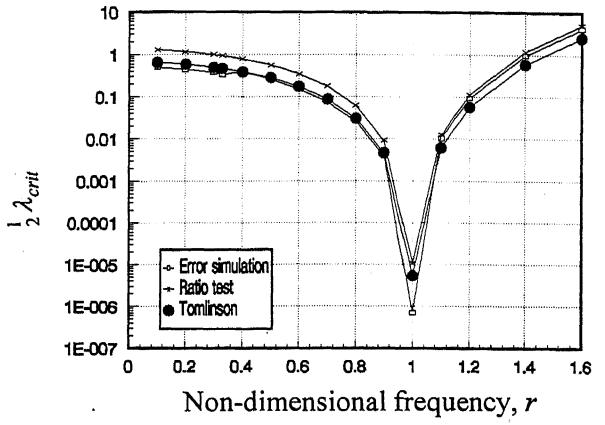

(a) $k = 2$

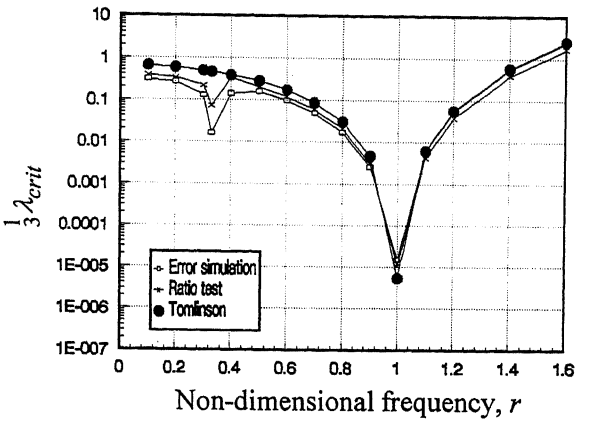

(b) $k = 3$

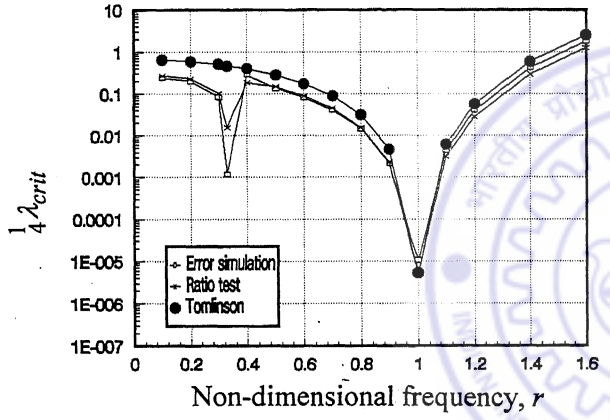

(c) $k = 4$

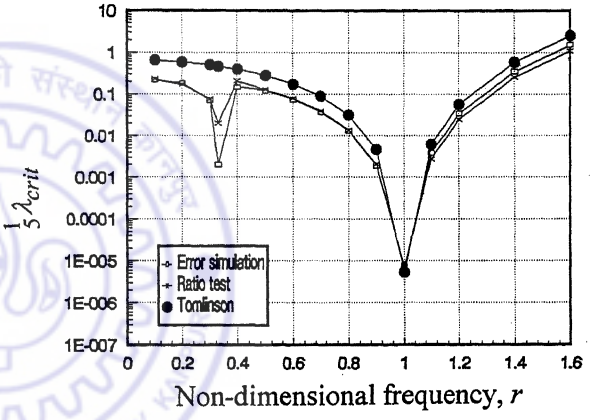

(d) $k = 5$

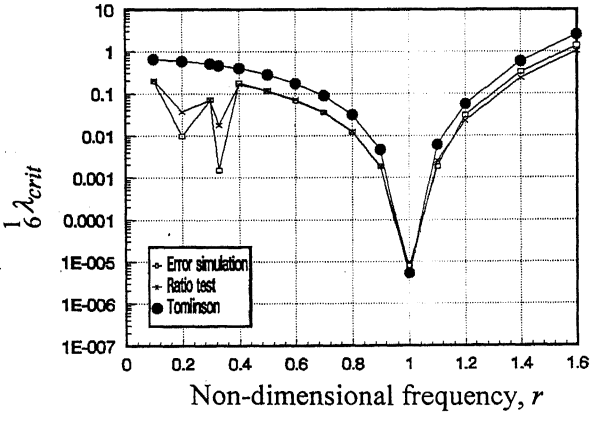

(e) $k = 6$

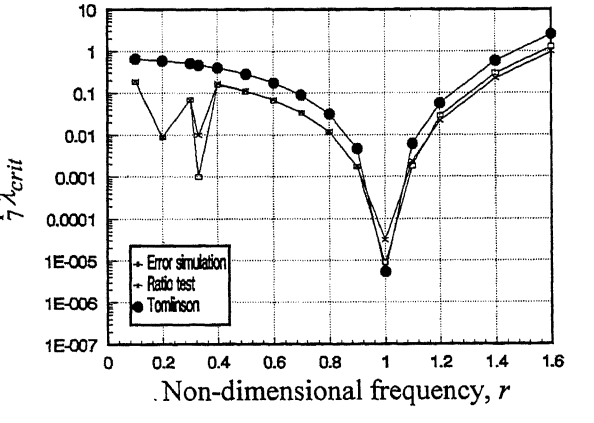

(f) $k = 7$

Figure 5.6 Variation of critical non-dimensional parameter, $\frac{1}{k}\lambda_{crit}$, with the non-dimensional frequency, r.

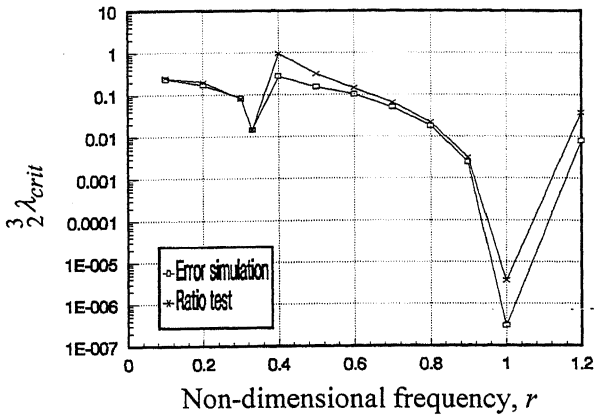

(a) $k = 2$

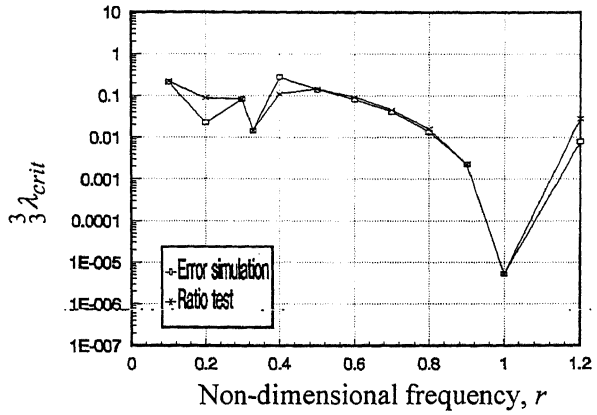

(b) $k = 3$

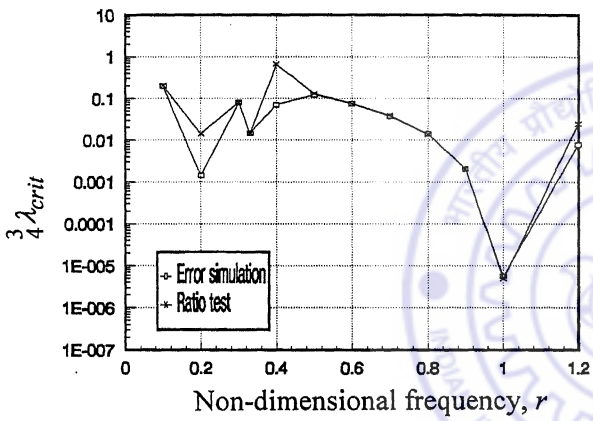

(c) $k = 4$

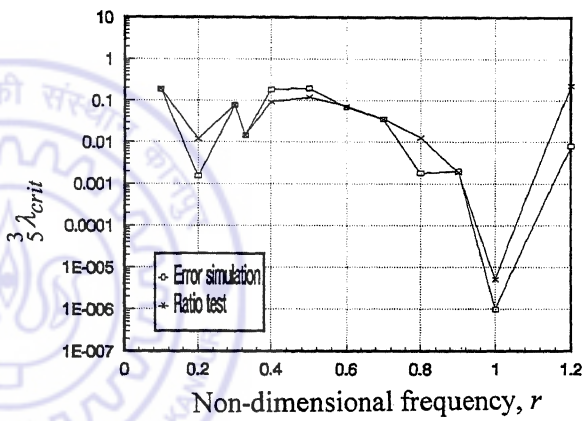

(d) $k = 5$

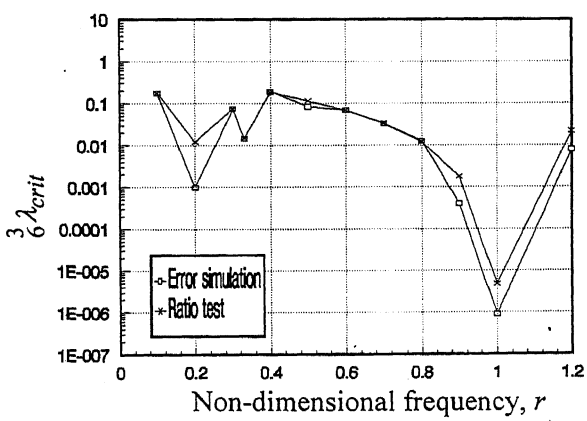

(e) $k = 6$

Figure 5.7 Variation of critical non-dimensional parameter, ${}^{3}_{k}\lambda_{crit}$, with the non-dimensional frequency, r.

that approximations with low values of k either completely miss out on the 1/3 and 1/5 subharmonics at r = 0.33 and r = 0.2, respectively, or give non-converging solutions. Critical values ${}^{n}_{k}\lambda_{crit}$ can be seen to be low at these frequencies. This fact is discussed in the next section.

5.2.2 Ratio Test for Convergence

The procedure for finding the critical value, of the non-dimensional parameter, through numerical simulation, needs iterative computation over a large number of values of λ_3. Alternately, ${}^{n}_{k}\lambda_{crit}$ can be determined through application of a simple ratio test to the power series (5.10). The critical non-dimensional parameter, ${}^{n}_{k}\lambda_{crit}$, can be defined, for a k-term approximation of the nth harmonic, as the limiting value of λ_3, for which

$$\left|\frac{\sigma_k(nr)}{\sigma_{k-1}(nr)}\right| = 1.0 \tag{5.18}$$

Application of the above with equation (5.11) gives

$$\left|\frac{1}{4}\frac{{}^{n+2k-2}C_{k-1}H^{n+k-1,k-1}_{n+2k-2}(r)}{{}^{n+2k-4}C_{k-2}H^{n+k-2,k-2}_{n+2k-4}(r)}\right| = 1 \qquad \text{for } \lambda_3 = {}^{n}_{k}\lambda_{crit} \tag{5.19}$$

Employing equation (5.12b), to express the higher order kernels, in the above, in terms of lower ones, the ratio can be seen to be a function g_k, of the kernel transforms $H_1(r), H_1(3r), H_1(5r)$ ...etc., and proportional to λ_3, i.e.

$$\left|\frac{1}{4}\frac{{}^{n+2k-2}C_{k-1}H^{n+k-1,k-1}_{n+2k-2}(r)}{{}^{n+2k-4}C_{k-2}H^{n+k-2,k-2}_{n+2k-4}(r)}\right| = \lambda_3\, g_k[H_1(r), H_1(3r), H_1(5r).....] \tag{5.20}$$

providing ${}^{n}_{k}\lambda_{crit}$ as

$${}^{n}_{k}\lambda_{crit} = 1/\, g_k[H_1(r), H_1(3r), H_1(5r).....] \tag{5.21}$$

Using equations (5.19) and (5.20), ${}^{n}_{k}\lambda_{crit}$ can be computed as

$$ {}^{n}_{k}\lambda_{crit} = \left| 4 \frac{{}^{n+2k-4}C_{k-2} H^{n+k-2,k-2}_{n+2k-4}(r)}{{}^{n+2k-2}C_{k-1} H^{n+k-1,k-1}_{n+2k-2}(r)} \right|_{\lambda_3=1} \tag{5.22} $$

For the 1st and 3rd harmonics, putting $n = 1$ and $n = 3$, one obtains

$$ {}^{1}_{k}\lambda_{crit} = \left| 4 \frac{{}^{2k-3}C_{k-2} H^{k-1,k-2}_{2k-3}(r)}{{}^{2k-1}C_{k-1} H^{k,k-1}_{2k-1}(r)} \right|_{\lambda_3=1} \tag{5.23} $$

$$ {}^{3}_{k}\lambda_{crit} = \left| 4 \frac{{}^{2k-1}C_{k-2} H^{k+1,k-2}_{2k-1}(r)}{{}^{2k+1}C_{k-1} H^{k+2,k-1}_{2k+1}(r)} \right|_{\lambda_3=1} \tag{5.24} $$

(the sub-script on the right hand side of the above expression denotes that the ratio has been computed at a value of $\lambda_3 = 1$)

The value of ${}^{n}_{k}\lambda_{crit}$ obtained from ratio test is an approximation of its correct value, which is obtained through the error divergence criterion, discussed earlier and illustrated through numerical simulation. However, the approximation of ${}^{n}_{k}\lambda_{crit}$ through the ratio test is fairly good and has been shown, along with the numerically simulated one, in Figures 5.6a-f and 5.7a-e, for the 1st and 3rd harmonic respectively. As k increases, the critical value ${}^{n}_{k}\lambda_{crit}$ obtained from ratio test gets closer to the exact one obtained from error simulation. For $k > 3$ ratio test gives very accurate results over a wide range of excitation frequencies. The ratio test also helps to understand the low values of ${}^{n}_{k}\lambda_{crit}$ at the natural frequencies and sub-harmonics. It can be seen, from equation (5.11) that the ratio $\left| \frac{\sigma_k(nr)}{\sigma_{k-1}(nr)} \right|$ is of the order of $\lambda_3 |H_1(nr)|^3$ and the term $|H_1(nr)|$ assumes a large value for $r = 1/n$, making ${}^{n}_{k}\lambda_{crit}$ too small to satisfy convergence criterion given by equation (5.19). Figure 5.6 also shows a comparison with the results of Tomlinson (1996), who carried out a ratio test on truncated expansion of equation (5.10) for higher order kernel transforms. Tomlinson's formula gives reasonable values of the critical parameter only at $r = 1$ and for $k = 2$, i.e, for a two-term series approximation. Away

from natural frequency and for $k > 2$ the results deviate considerably from the exact ones, since Tomlinson 's formula employs a truncated form of σ_i, by considering their first terms alone. However, subsequent terms of σ_i can be of the same order as its first term, as they may involve kernels of the same order. Also, Tomlinson computed the error by averaging over a range of excitation frequencies. Such averaging may entail a large error, since the kernels are frequency sensitive and the critical value of the nonlinear parameter λ_3 should be treated as specific to the excitation frequency. Moreover, Tomlinson's analysis was restricted to the first harmonic $Z(r)$ and its convergence was taken to conclude the convergence of the Volterra series.

5.2.3 Error Analysis

Convergence analysis gives the limiting number of terms in the Volterra series for convergence. The consequent error in the estimates is dependent on this truncation and is a function of the excitation frequency and amplitude. Figure 5.8(a) shows the error variation, for a two-term approximation in the first harmonic amplitude $Z(r)$, over a frequency range, for constant excitation levels (i.e. for constant λ_3 values). It can be seen that the error increases with the increase in excitation amplitude and becomes very large near the natural frequency (i.e., $r = \omega/\omega_n = 1$). Figure 5.8(b) shows error for different number of terms in the series for a given excitation level, $\lambda_3 = 0.005$. It is seen that the high error near natural frequency increases further with more terms in the series. This is because the excitation level selected in this case is high and correspondingly λ_3 is higher than the critical value near natural frequency (Figure 5.6). Similar error characteristics for third harmonic amplitude $Z(3r)$ are shown in Figure 5.9.

Reduction of the error in the vicinity of the natural frequency of the system would require a reduction in the amplitude of the excitation force. Variation of the excitation amplitude over the frequency range in such a manner that a constant error level is maintained throughout the frequency range can be suggested for consistency in results. Figure 5.10 shows the required variation of excitation level in terms of the non-dimensional nonlinear

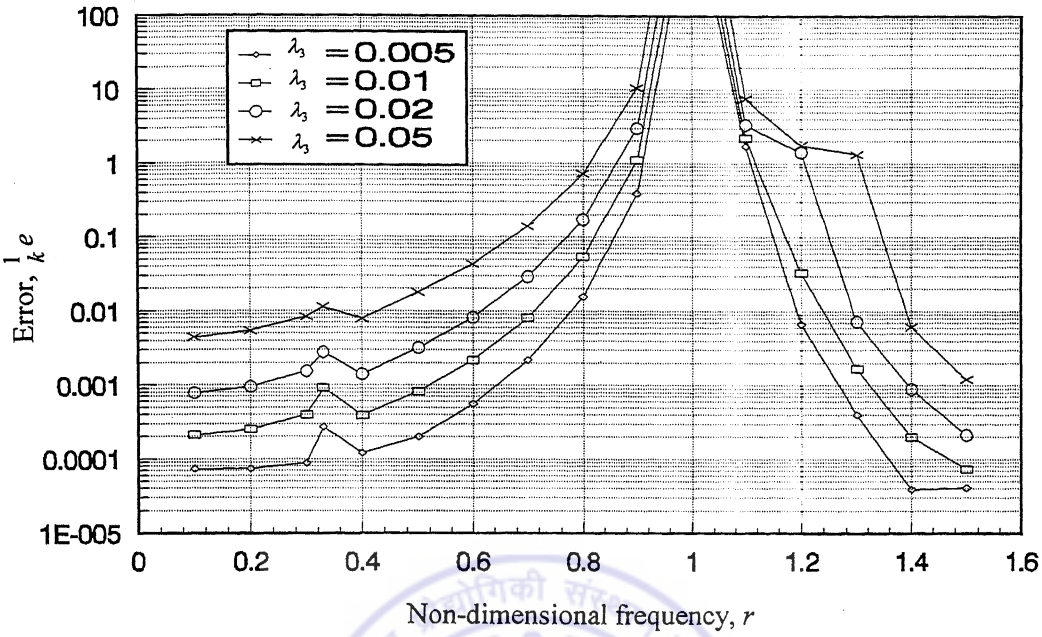

a) $[k=2]$.

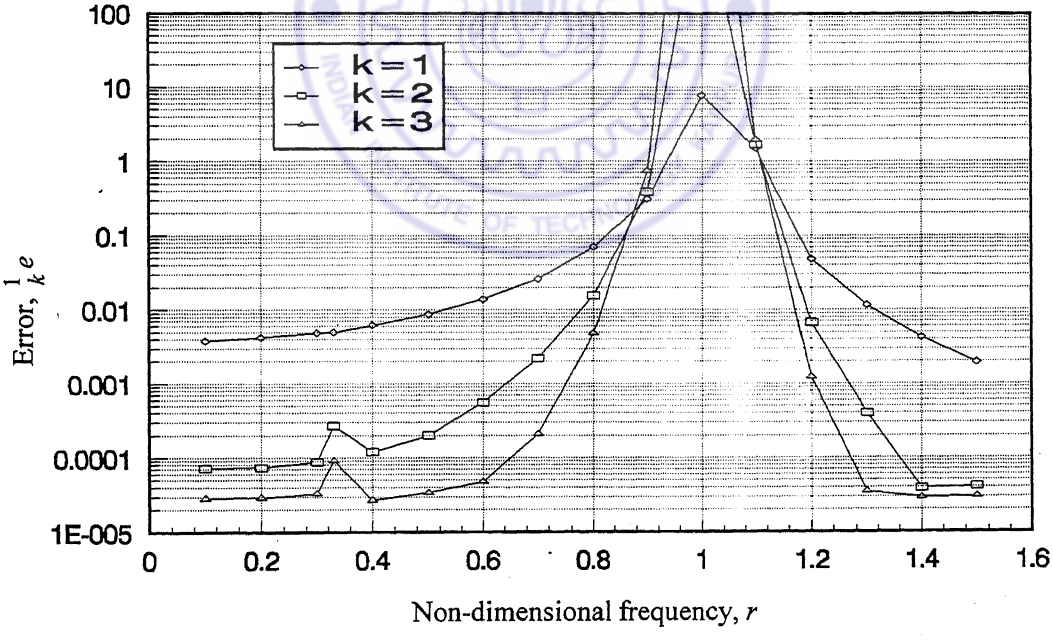

b) $\lambda_3 = 0.005$

Figure 5.8 Variation of approximation error in first response harmonic.

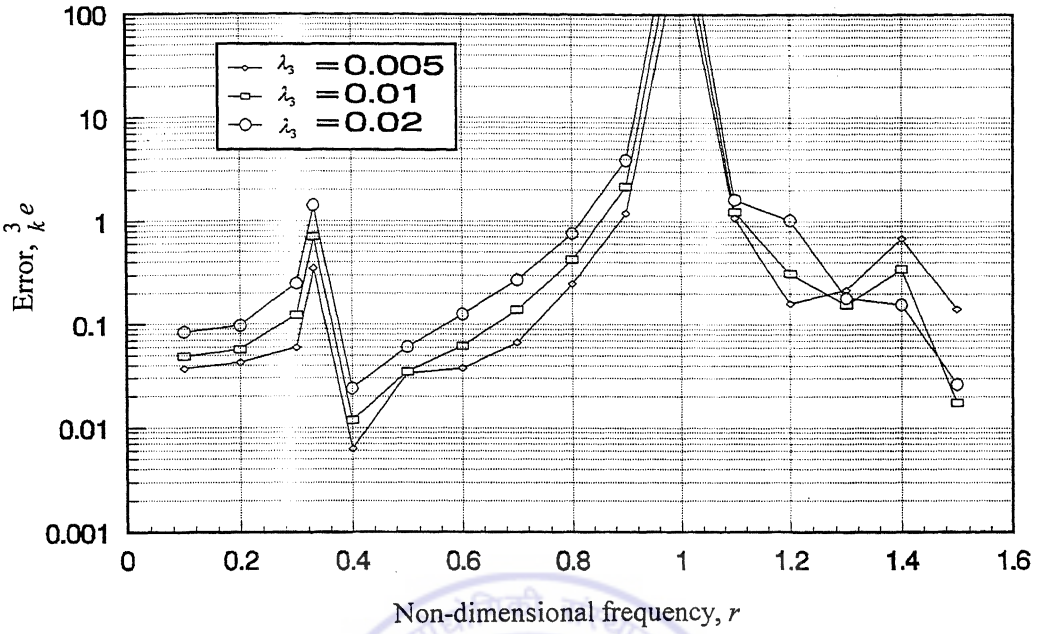

a) $[k=1]$.

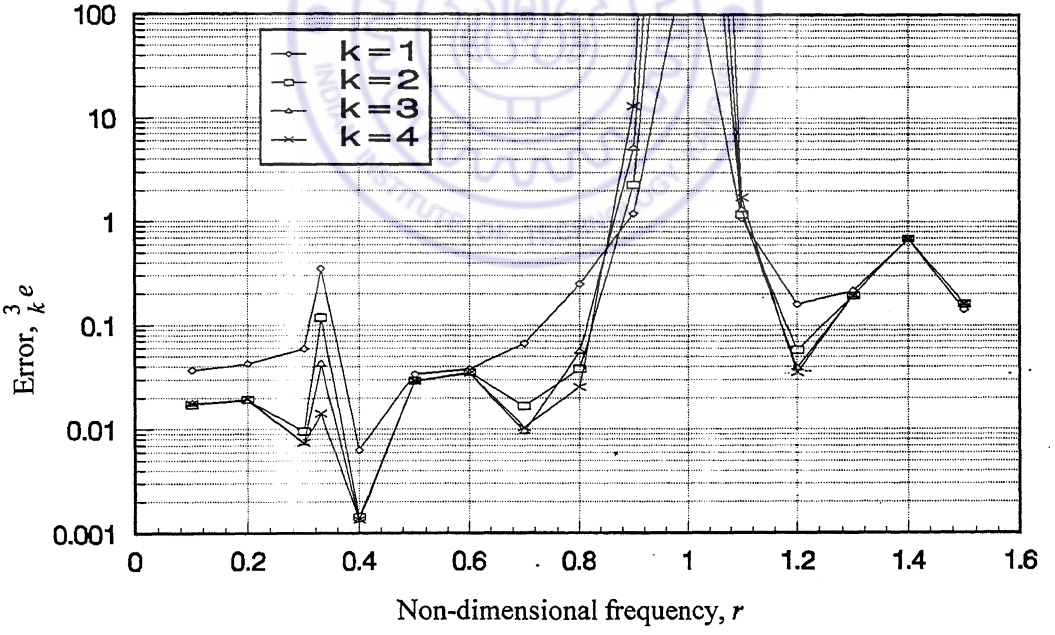

b) $\lambda_3 = 0.01$

Figure 5.9 Variation of approximation error in third response harmonic.

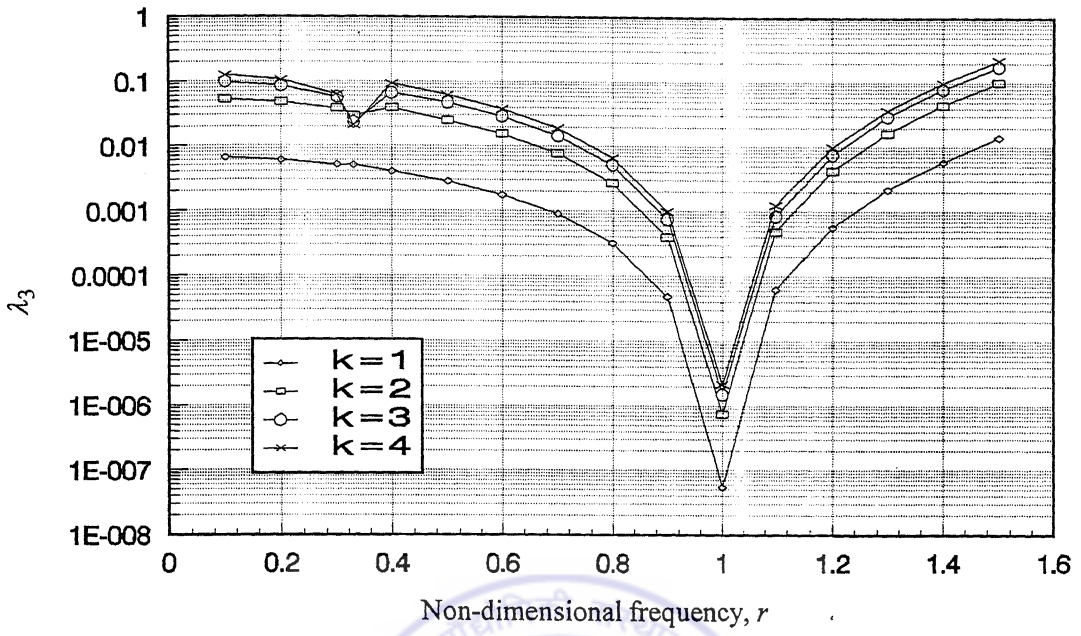

a) Error limit = 0.005

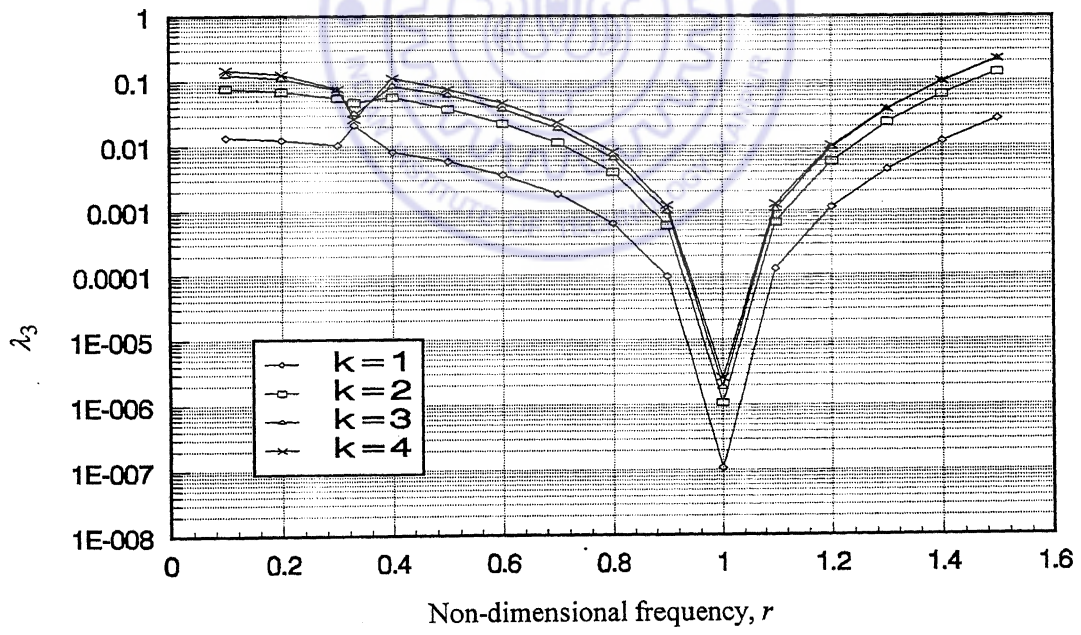

b) Error limit = 0.01

Figure 5.10 Variation in excitation level for constant error

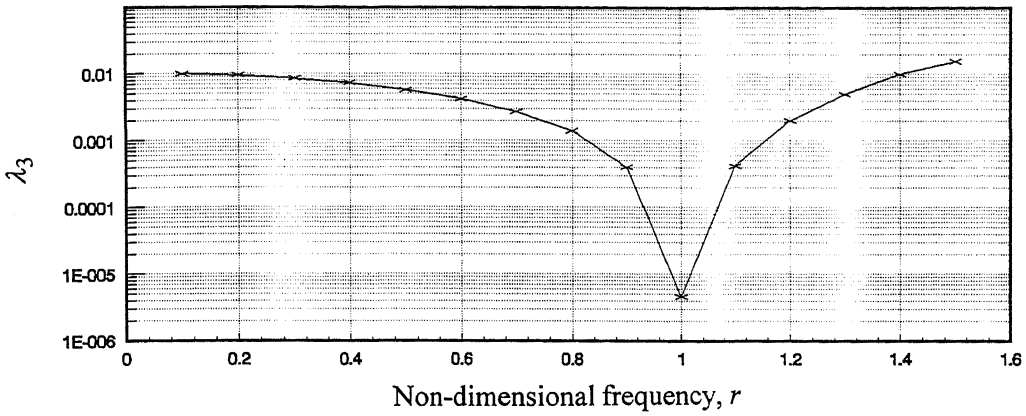

Figure 5.11(a) Excitation level for constant response harmonic amplitude, $Z(r)$

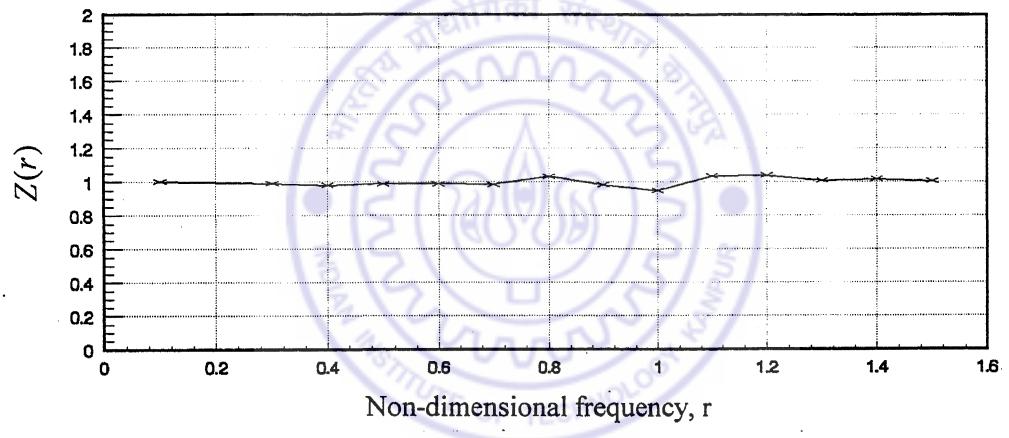

Figure 5.11(b) Response harmonic amplitude, $Z(r)$

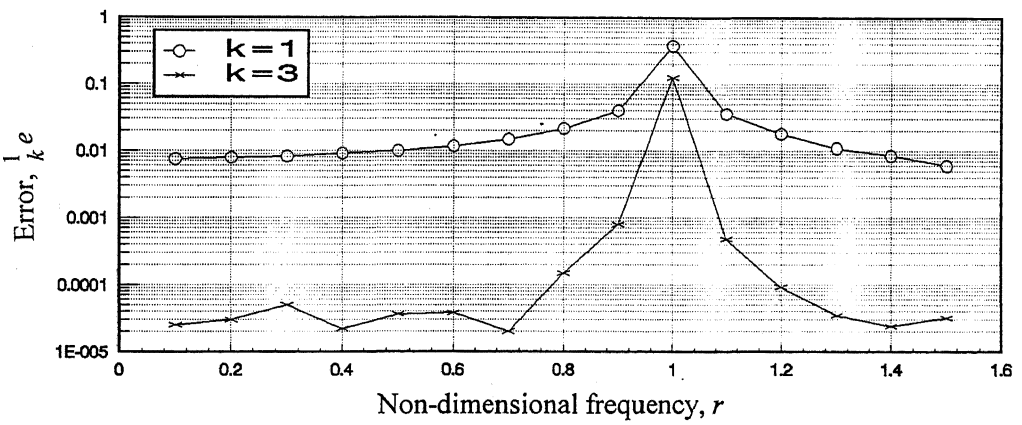

Figure 5.11(c) Series approximation error for excitation level with constant $Z(r)$

parameter λ_3 over the frequency range for constant approximation error in the first response harmonic series. Obtaining such a plot during a practical application for parameter estimation is difficult for it requires *a-priori* knowledge of the nonlinear parameter itself. However, the excitation amplitude can be varied over the frequency range such that the first harmonic response amplitude is maintained constant. Figure 5.11(a) typically shows such a variation of excitation amplitude for obtaining constant response harmonic amplitude. The consequent response is depicted in Figure 5.11(b) and Figure 5.11(c) shows the resultant error for different number of series terms. It can be observed that while the error is relatively higher near the natural frequency (10% error with k=3), it is significantly less in compared to what would have resulted for the constant excitation level case of Figure 5.8.

5.3 Measurability of Higher Order Response Harmonics

Higher order response harmonics for weakly nonlinear systems will be of much lower amplitude compared with the fundamental harmonic. These higher order harmonics may not be significantly stronger than background vibration or measurement noise. This is illustrated in Figures 5.12 (a), where non-dimensional third order response harmonic amplitude $Z(\omega_1+\omega_2+\omega_3)$ is plotted for a range of ω_1 and ω_2, while maintaining a constant $\omega_3/\omega_n = 0.2$. It can be seen that the third order harmonic $Z(\omega_1+\omega_2+\omega_3)$ is distinct along the line A representing the frequency combinations $\omega_1+\omega_2+\omega_3=\omega_n$. On other regions of the frequency floor the response strength is significantly small. Better signal/noise ratio would therefore be achieved for the third order harmonic measurements, if carried out along the line A, indicated in Fig. 5.12 (a).

A single-term approximation of the non-dimensional response harmonic $Z(\omega_1+\omega_2+\omega_3)$ can be obtained as

$$Z(\omega_1+\omega_2+\omega_3) \approx \frac{3}{2} H_3(\omega_1/\omega_n, \omega_2/\omega_n, \omega_3/\omega_n) \qquad (5.25)$$

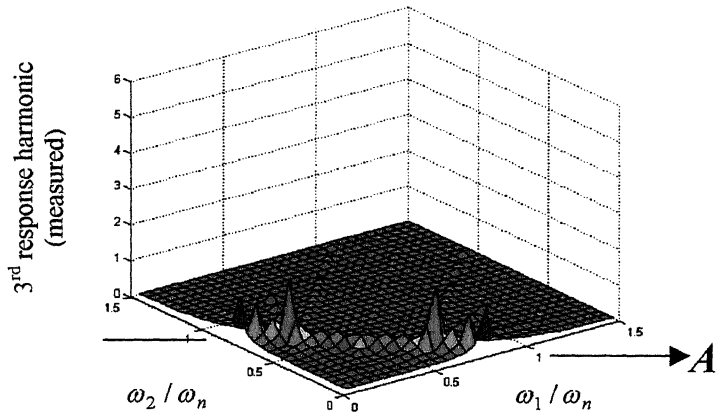

a) Exact response harmonic amplitude

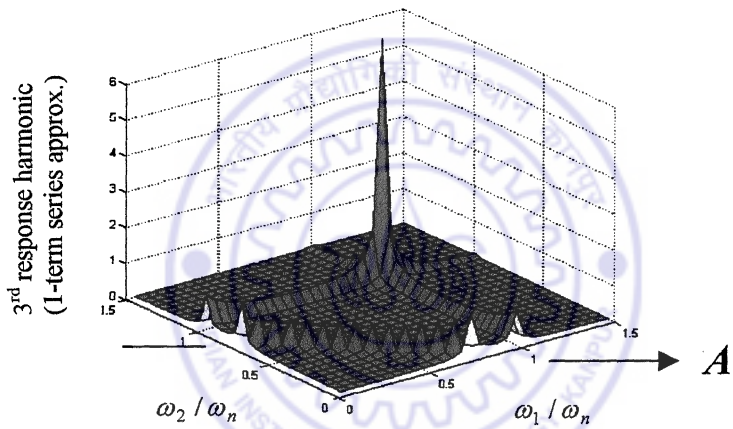

b) Single-term series approximation

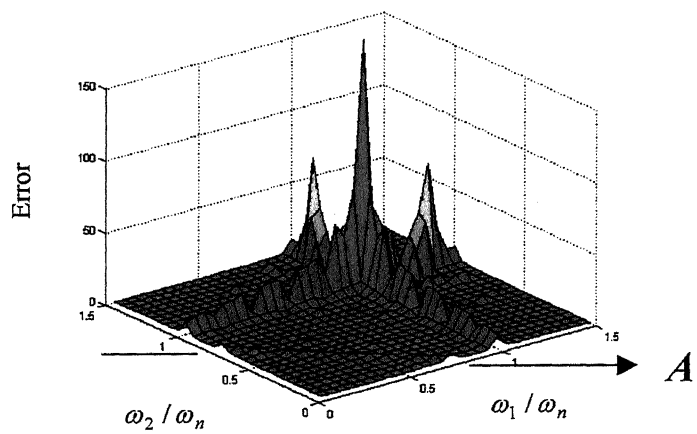

c) Error in single-term series approximation

Figure 5.12 Third harmonic amplitude, $Z(\omega_1 + \omega_2 + \omega_3)$ and error in single-term series approximation. $[\omega_3 / \omega_n = 0.2;\ \lambda_3 = 0.01]$

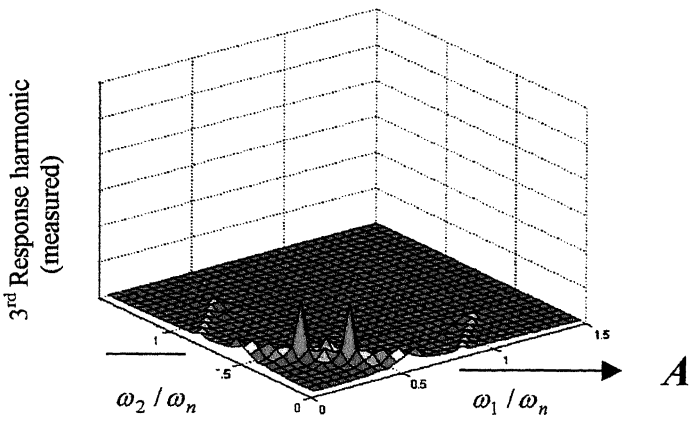

a) Exact response harmonic amplitude

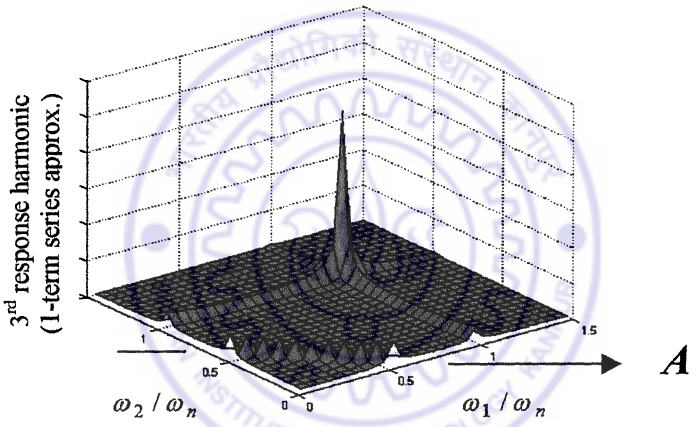

b) Single-term series approximation

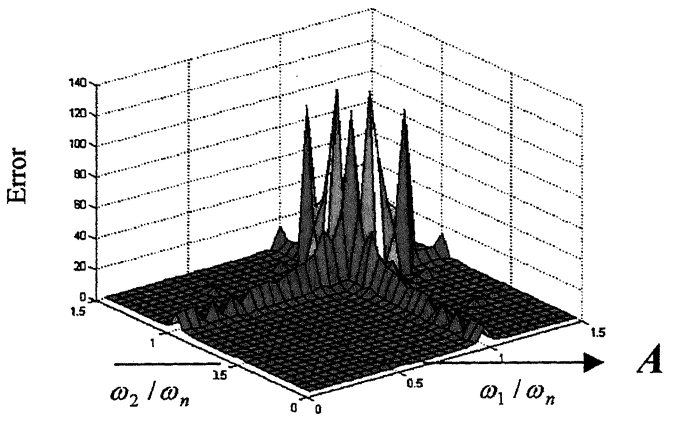

c) Error in single-term series approximatior

Figure 5.13 Third response harmonic amplitude, $Z(\omega_1 + \omega_2 + \omega_3)$ and error in single-term series approximation. $[\omega_3 / \omega_n = 0.4;\ \lambda_3 = 0.01]$

Denoting non-dimensional frequencies

$r_1 = \omega_1 / \omega_n$, $r_2 = \omega_1 / \omega_n$ and $r_3 = \omega_1 / \omega_n$

equation (5.25) becomes

$$Z(\omega_1 + \omega_2 + \omega_3) \approx \frac{3}{2} H_3(r_1, r_2, r_3)$$

where the third order kernel transform can be synthesized, similar to equation (3.26), for a Duffing oscillator) as

$$H_3(r_1, r_2, r_3) = -\lambda_3 H_1(r_1) H_1(r_2) H_1(r_3) H_1(r_1 + r_2 + r_3)$$

with the non-dimensional first order kernel transforms given by equation (5.12a). The single-term approximation of the third harmonic has been plotted in Figure 5.12 (b) over the frequency range. Comparison between Figures 5.12 (a), (b) shows a good correlation along the frequency combination line *A*. Figure 5.12 (c) gives the error between the 'exact' response of Figure 5.12 (a) and the single term approximation of Figure 5.12 (b). The parameter estimation procedure suggested in the earlier section involves equating these two figures for extraction of the nonlinear term. It is apparent that the estimation error can be kept low, while maintaining high signal/noise ratio if measurements are made along line *A* representing the frequency combinations $\omega_1 + \omega_2 + \omega_3 = \omega_n$. Figures 5.13 (a), (b), (c) show similar results for frequency ratio $\omega_3 / \omega_n = 0.4$.

In case of single-tone excitation, it is obvious from above that third order response harmonic, $X(3\omega)$, should be measured at or close to $3\omega = \omega_n$, i.e., $\omega = \omega_n / 3$. The measurability of the third response harmonic in case of a Duffing oscillator under single tone excitation is shown in Figure 5.14 (a), (b). This has been done by defining a parameter as Measurability Index, $MI(m\omega)$, which is the ratio of *m*th response harmonic amplitude to the first harmonic amplitude, i.e.,

$$MI(m\omega) = X(m\omega) / X(\omega) \qquad (5.26)$$

Measurability is maximum at one-third of the natural frequency and this maximum value can be termed as Peak Measurability Factor. Figures 5.14 (a), (b) also show the dependence of Peak Measurability Factor on excitation amplitude and damping.

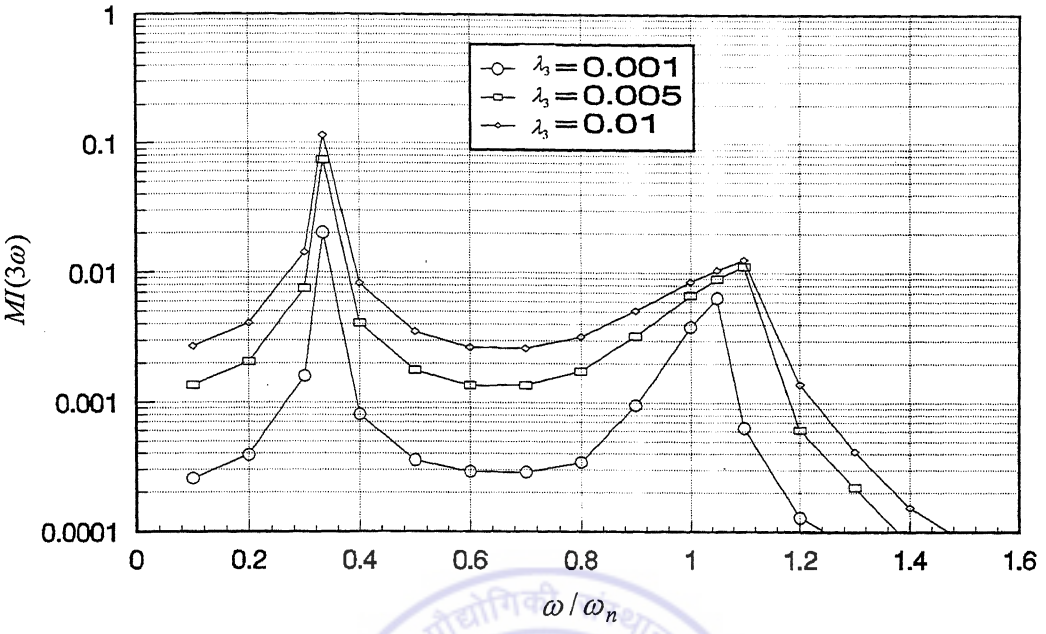

a) for different excitation levels with $\zeta = 0.01$

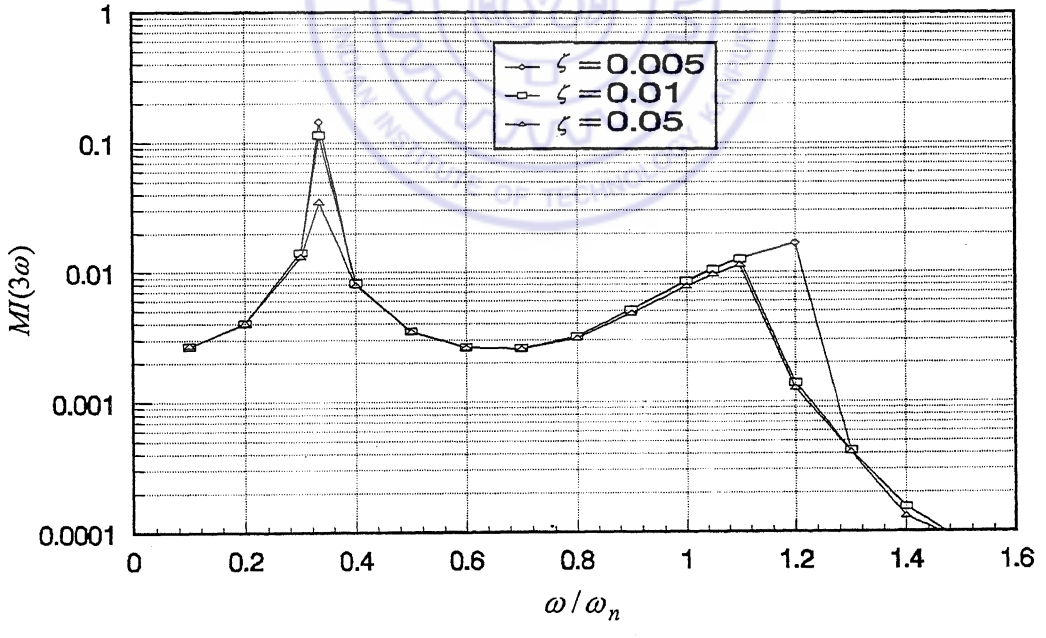

b) for different damping with $\lambda_3 = 0.01$

Figure 5.14 Measurability index, $MI(3\omega)$

From Figure 5.7, for a k-term series approximation of $X(3\omega)$, the critical value ${}^{3}_{k}\lambda_{crit}$ is found to be of the order of 0.01 for $1 \le k \le 5$ ($\zeta = 0.01$). It can be seen from Figure 5.14(a) that the excitation level corresponding to this critical value of λ_3, gives a measurability as high as 10%. Figure 5.9(b) shows that at this excitation level ($\lambda_3 = 0.01$), error in $X(3\omega)$ approximation can be reduced to 3% for three-term series and to 1% for a four term series. It is suggested to measure the third harmonic at a set of frequencies very close to one-third natural frequency and on both side of it. The excitation level is kept constant for this close frequency band and can be set to a desired peak measurability.

5.4 Detection of the Sign of Nonlinear Parameter

The nonlinear parameter k_3 is obtained through the linear regression of equation (5.5). The regression is done with the magnitude of the complex quantities and hence the estimated values represent only the magnitude of the nonlinear parameters and not their sign. Sign of the nonlinear parameter, k_3, can be detected through observations of change of sign of real part of measured third harmonic amplitudes during transition of excitation frequency across one-third of the natural frequency. Rewriting equation (5.6) for synthesis of the kernel factor

$$\Gamma_3(3\omega) = -H_1^3(\omega)H_1(3\omega), \qquad (5.27)$$

one can note that since for $\omega < \omega_n/3$, both $H_1(\omega)$ and $H_1(3\omega)$ have positive real parts (equations 3.18a) the kernel factor $\Gamma_3(3\omega)$ will have a negative real part. Consequently, the estimated third order kernel transform $H_3(\omega,\omega,\omega)$ given by (equation 5.5) will also have a negative real part for positive k_3. For $\omega_n > \omega > \omega_n/3$, $H_1(\omega)$ will have a positive real part while the real part of $H_1(3\omega)$ will bear negative sign. The kernel factor $\Gamma_3(3\omega)$ and $H_3(\omega,\omega,\omega)$ consequently, will have a positive real part for positive value of the nonlinear parameter k_3.

5.5 Illustration

The parameter estimation procedure is numerically illustrated here for a Duffing oscillator given by equation (5.7), with following parameters

$k_1 = 1.0\times10^7$ N/m $\quad m = 1.0$ kg $\quad c = 64.3$ Ns/m $\quad k_3 = 1.0\times10^{19}$ N/m^3.

The above stiffness parameters are selected to correspond to a typical rotor bearing system with rolling element bearings (Khan, 1999) and the damping coefficient is selected to correspond 1% damping ratio (i.e. $\zeta = 0.01$).

5.5.1 Preliminary Linear Estimates

Numerical simulation is carried out by solving the equation of motion (5.7), using 4th order Runge-Kutta integration algorithm to obtain the response, $x(t)$. Response harmonics $X(\omega)$ and $X(3\omega)$ are separated by harmonic filtering. The first response harmonic, $X(\omega)$, is measured with excitation level adjusted so as to give a constant response amplitude of 1.0×10^{-7} m. A wide range of excitation frequency is considered from 50Hz to 750Hz, covering the natural frequency $\omega_n = 503$ Hz. Figure 5.15(a) shows the excitation amplitude employed at various frequencies to obtain the constant harmonic amplitude $X(\omega)$ shown in Figure 5.15 (b). Preliminary estimate of the first order kernel $H_1(\omega)$ from $X(\omega)$ using equation (5.2a) is plotted in Figure 5.15(c). Linear parameters are estimated through curve fitting equation (3.18a) over the estimated $H_1(\omega)$ values. The preliminary estimates are

$k_1 = 1.0074\times10^7$ N/m, $\quad m = 0.9999$ kg, $\quad \varsigma = 0.01055$.

5.5.2 Nonlinear Estimates

For estimation of nonlinear parameters, the plot of third harmonic Peak Measurability Factor is obtained for various excitation amplitudes (Figure 5.16a). Peak Measurability Factors are typically chosen as 2%, 5% and 10% and the excitation force amplitudes required for these measurabilities of the third harmonic are read from Figure 5.16 (a) to be 0.35N, 0.565N and 0.875N respectively. The recursive iteration method is illustrated

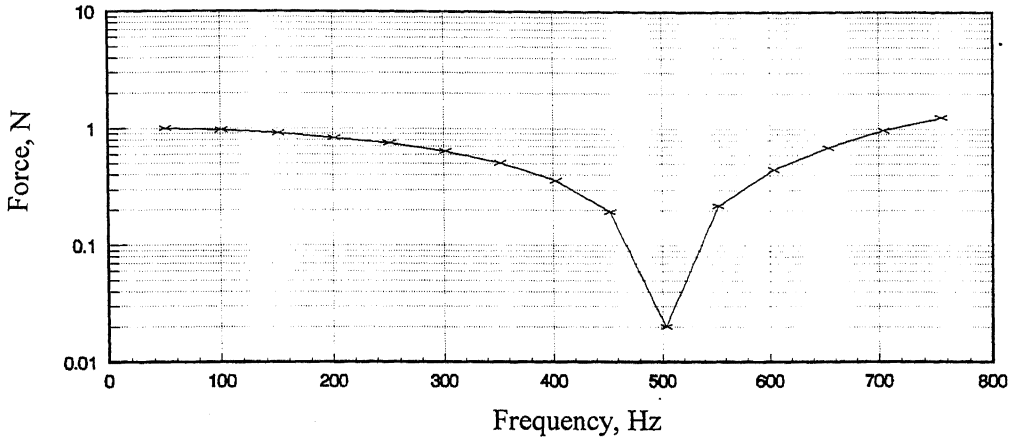

Figure 5.15(a) Variation in excitation level for constant response harmonic amplitude $X(\omega) = 1.0 \times 10^{-7}$ m

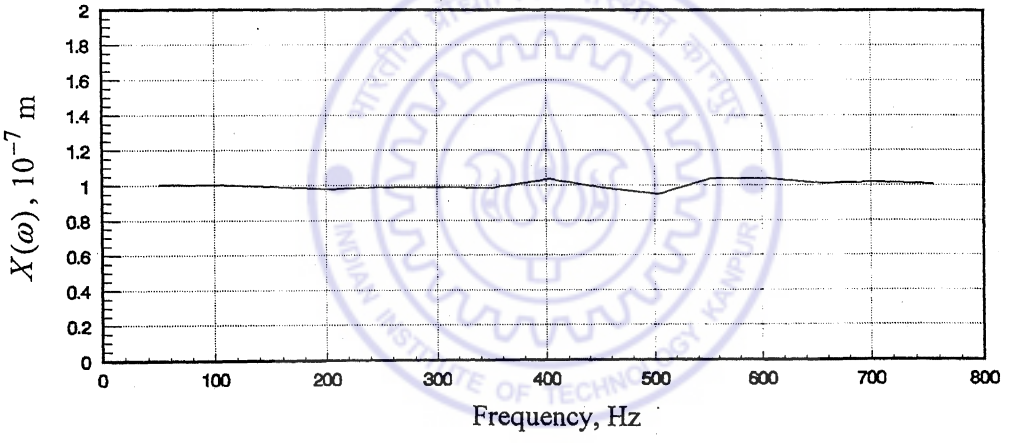

Figure 5.15(b) Measured response harmonic amplitude, $X(\omega)$

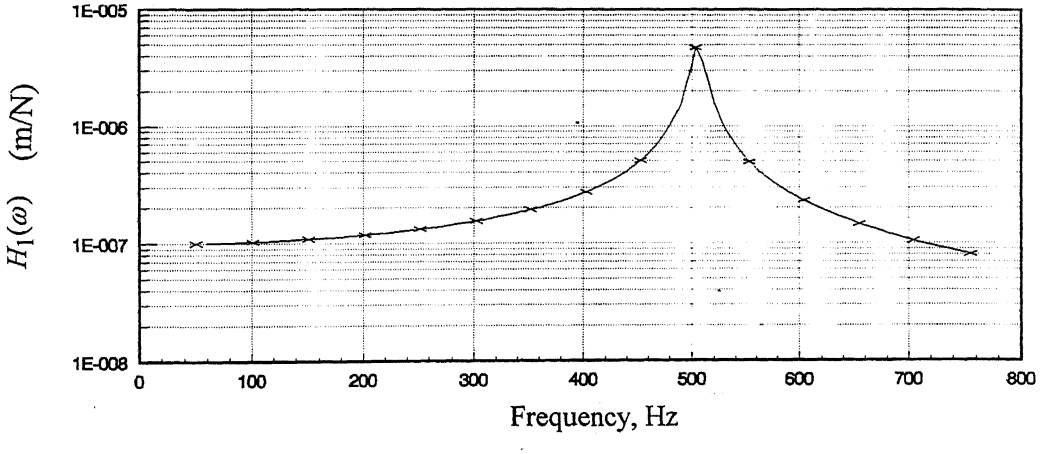

Figure 5.15(c) Preliminary estimates of first order kernel transform, $H_1(\omega)$

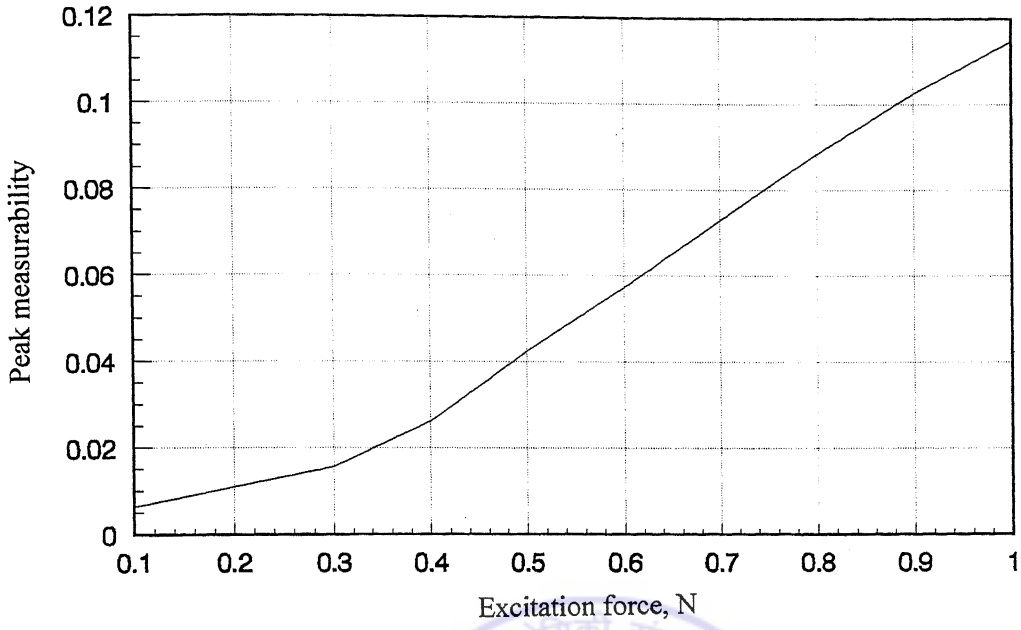

Figure 5.16(a) Peak Measurability Factor at different excitation levels.

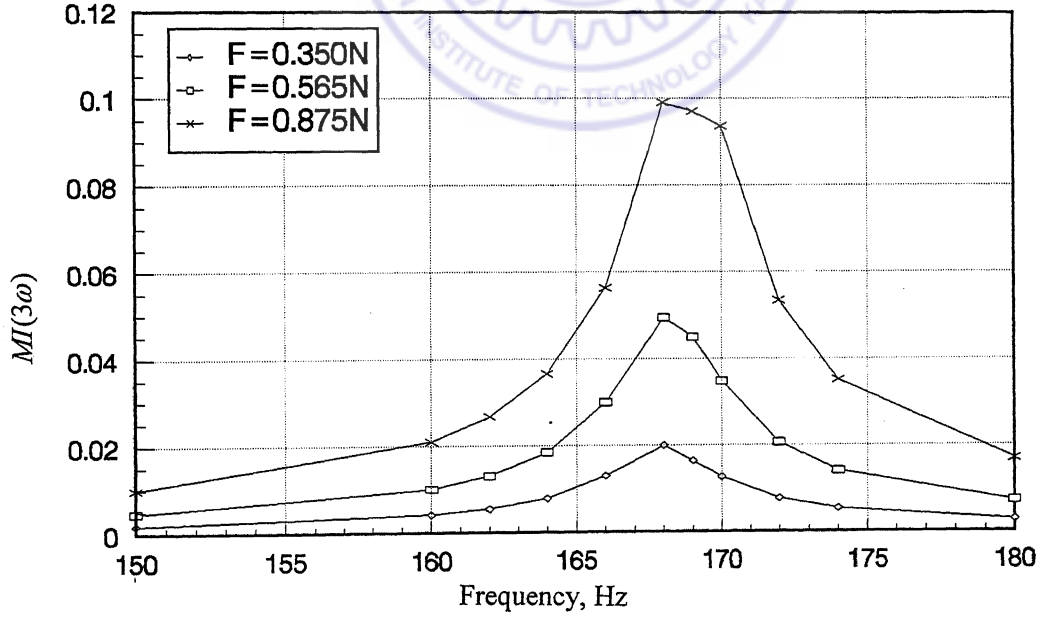

Figure 5.16(b) Variation in Measurability index, $MI(3\omega)$ around $\omega_n/3$.

for the three cases of measurability chosen above. Four excitation frequencies (164.0 Hz, 166.0 Hz, 170.0 Hz and 172.0 Hz) are selected close to one-third of the natural frequency ($\omega_n/3 = 167.7\,\text{Hz}$) for the measurement of third response harmonic. Figure 5.16 (b) shows the measurability variation in the neighborhood of this band of frequencies.

Case (i) (2% peak measurability; Force Amplitude = 0.35N)

Harmonic excitation of amplitude 0.35N is applied at the four selected frequencies and third response harmonic amplitude $X(3\omega)$ filtered from the response is shown in Figures 5.17 (a-d). Preliminary estimation in accordance with equations (5.5) and (5.6), gives the value of the nonlinear parameter, $k_3 = 1.0332\times10^{19}\,\text{N/m}^3$. This estimate is in error by 3.32%. With subsequent iterations, this estimate converges to a value $k_3 = 1.0053\times10^{19}\,\text{N/m}^3$. The convergence pattern is displayed in Figure 5.18 (a). (Iteration is stopped when the change in successive estimates of k_3 becomes less than 0.1%). Significant improvement in the estimated value is achieved with iterations, whereby the error can be seen to come down from 3.32% to 0.53%. The final estimate of the first order kernel transform, $H_1(\omega)$, is shown in Figure 5.18 (b) and the estimated linear parameters are:

$k_1 = 0.9998\times10^7\,\text{N/m}$ $\quad m = 0.9999\,\text{kg}$ $\quad \varsigma = 0.01024$

Case (ii): (5% peak measurability; Force Amplitude = 0.565N)

Figures 5.19(a-d) show the response spectrum at the four frequencies selected for measurements. The estimate for the nonlinear parameter k_3, in this case, converges from a preliminary value of $1.0309\times10^{19}\,\text{N/m}^3$ to a final value of $1.0065\times10^{19}\,\text{N/m}^3$, as shown in Figure 5.20 (a). The errors are 3.09% - for the preliminary value and 0.65% - for the final value. The final estimate of first order kernel transform, $H_1(\omega)$, is shown in Figure 5.20(b) and the estimated linear parameters are

$k_1 = 0.9998\times10^7\,\text{N/m}$ $\quad m = 0.9999\,\text{kg}$ $\quad \varsigma = 0.01023$

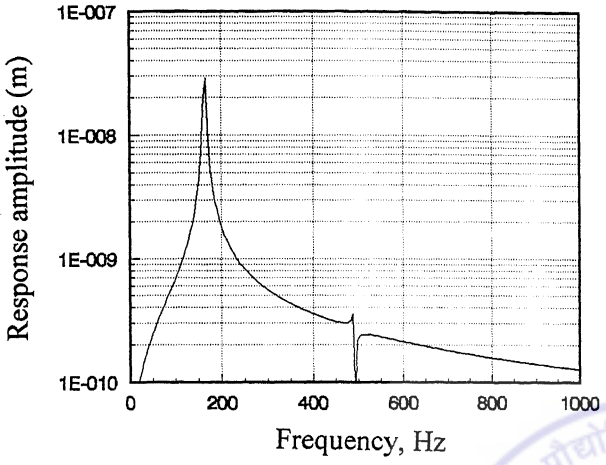

a) Excitation at 164 Hz.

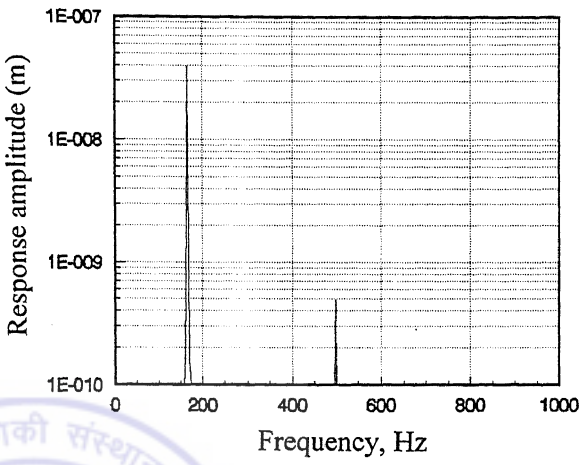

b) Excitation at 166 Hz.

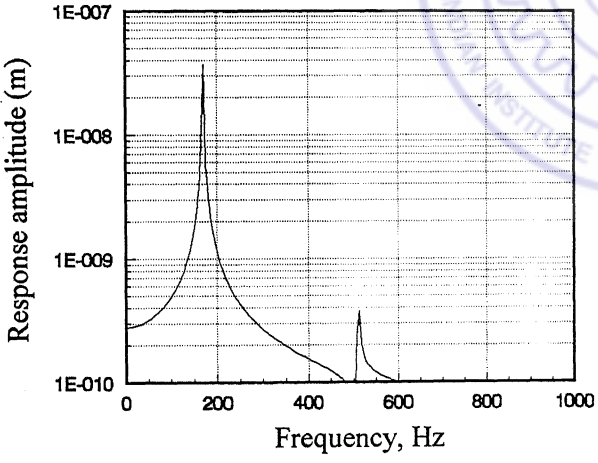

c) Excitation at 170 Hz

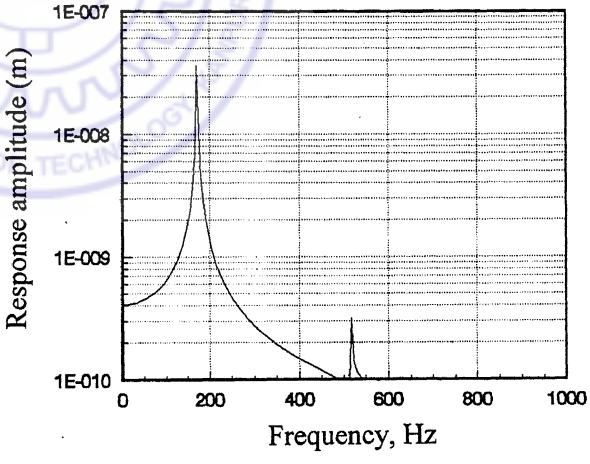

d) Excitation at 172 Hz.

Figure 5.17 Response spectra with force amplitude = 0.35N.
[Case (i): 2% peak measurability]

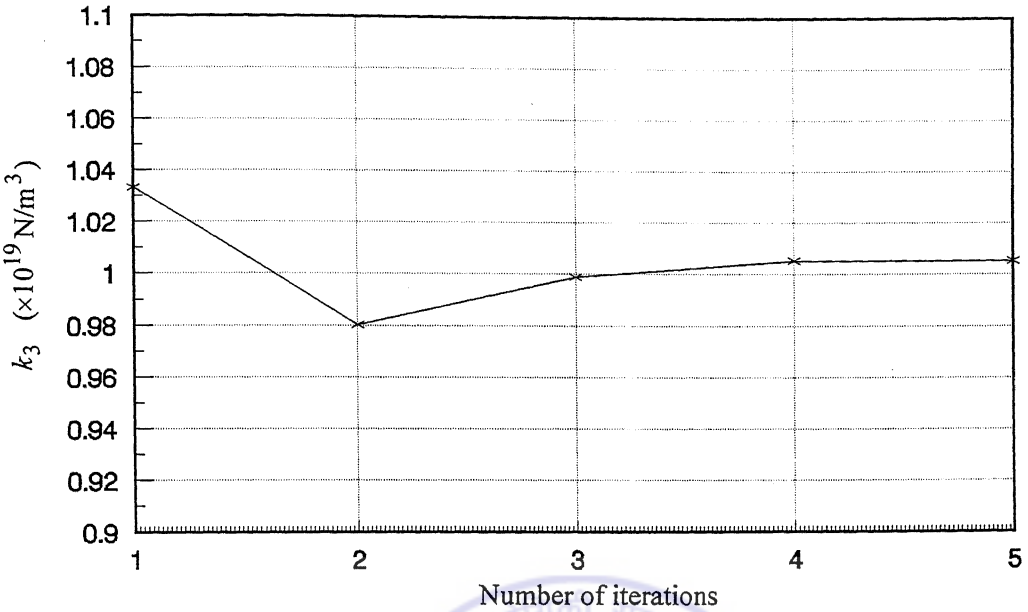

Figure 5.18(a) Iterative estimates of k_3

[Case (i) : 2% peak measurability]

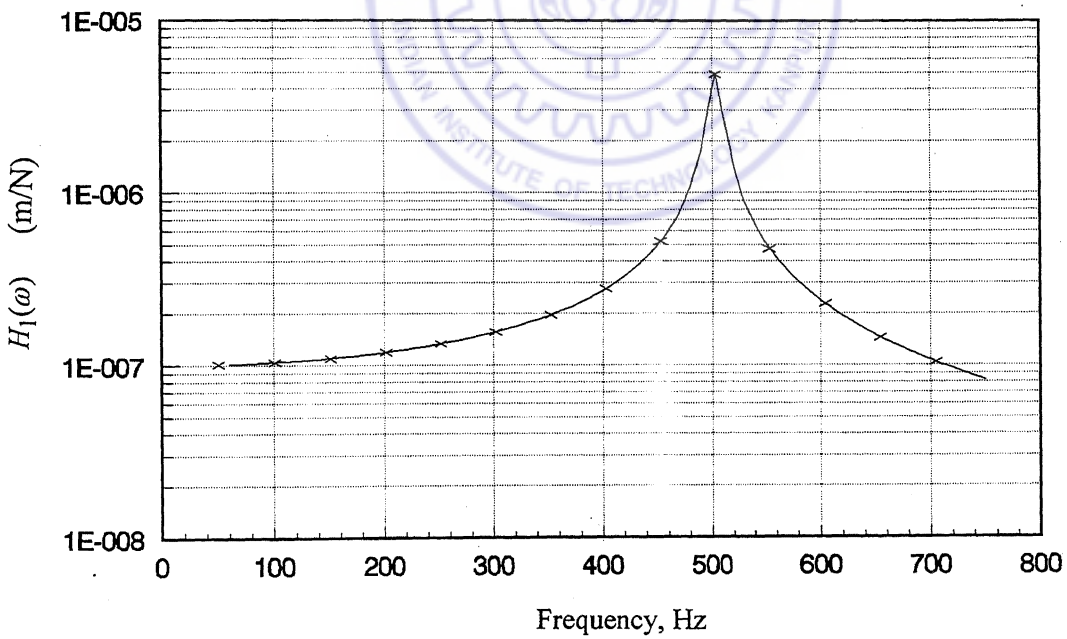

Figure 5.18(b) Final estimate of first order kernel transform, $H_1(\omega)$
[Case (i): 2% peak measurability]

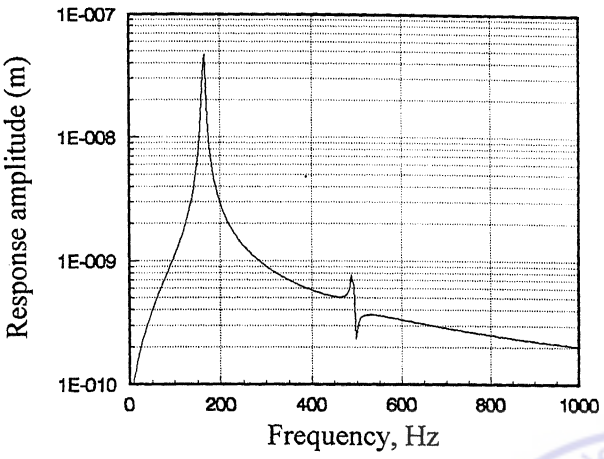

a) Excitation at 164 Hz.

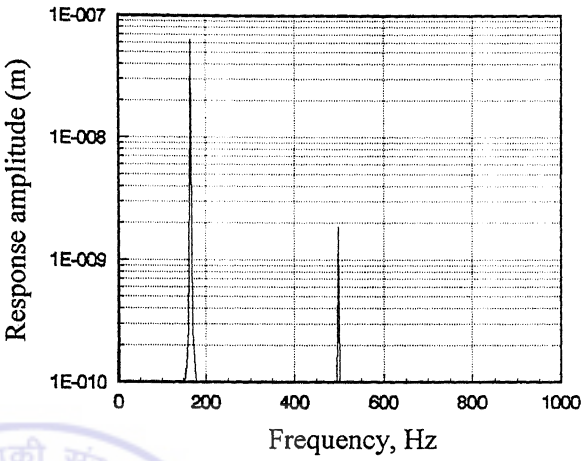

b) Excitation at 166 Hz.

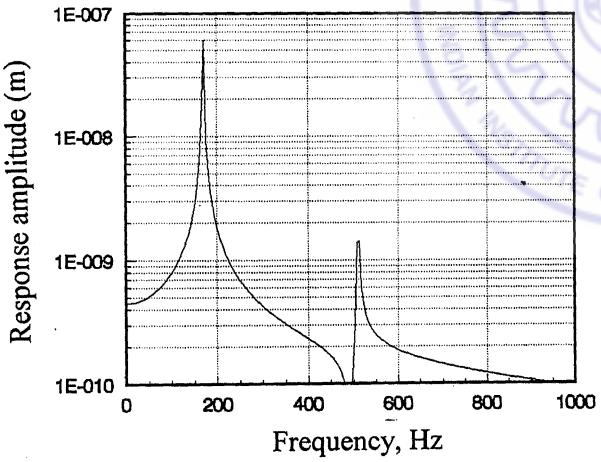

c) Excitation at 170 Hz

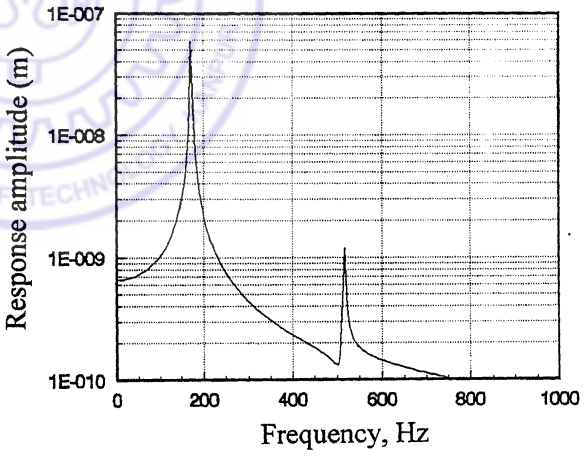

d) Excitation at 172 Hz.

Figure 5.19 Response spectra with force amplitude = 0.565N.
[Case (ii): 5% peak measurability]

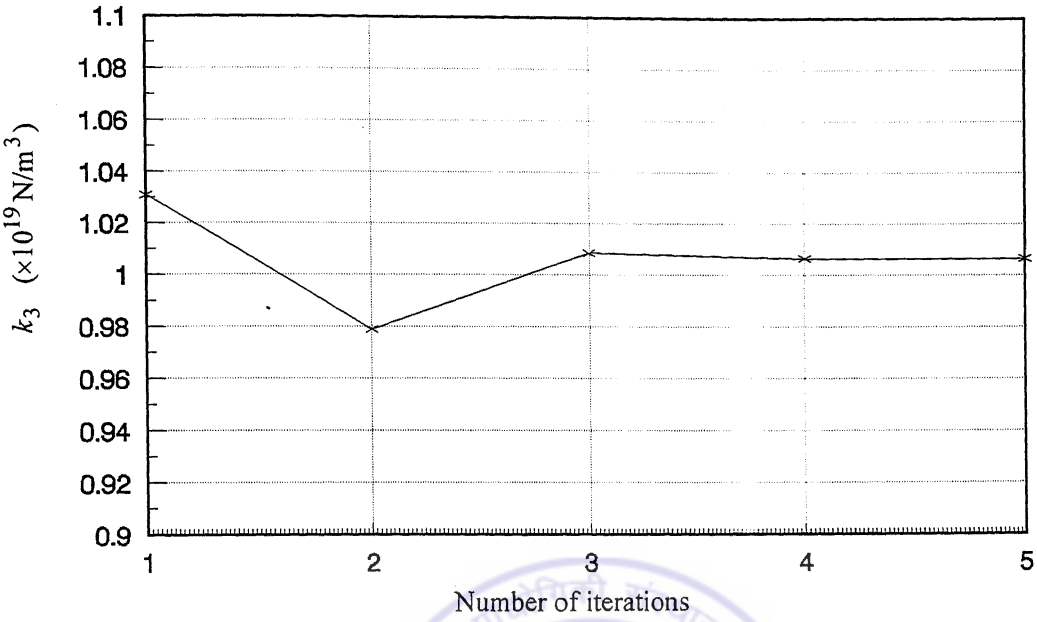

Figure 5.20(a) Iterative estimates of k_3

[Case (ii): 5% peak measurability]

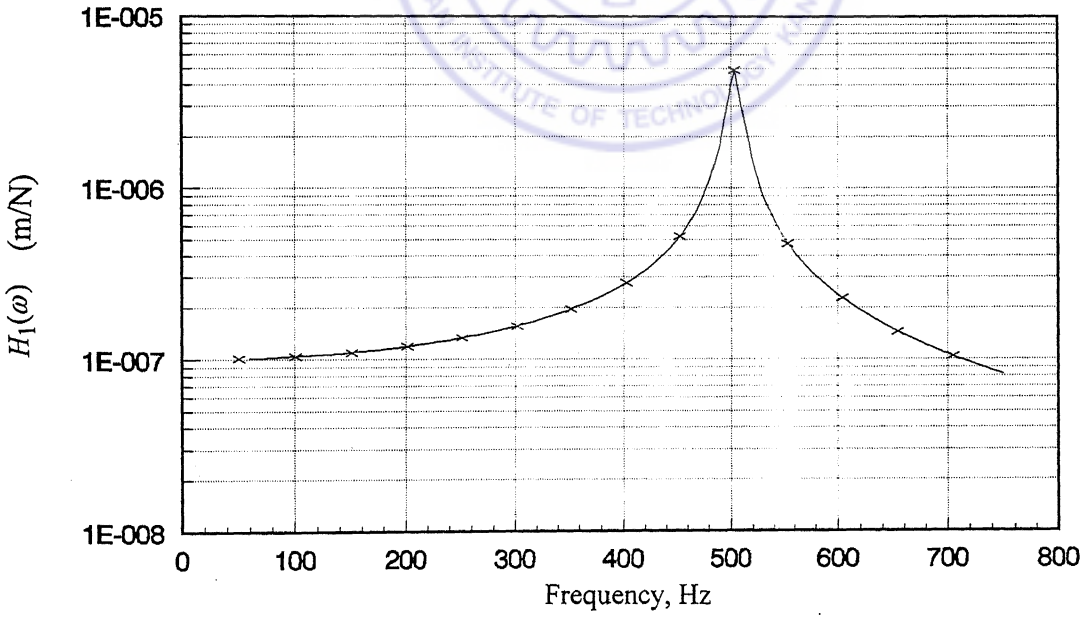

Figure 5.20(b) Final estimate of first order kernel transform, $H_1(\omega)$

(Case (ii): 5% peak measurability)

Case (iii): (10% peak measurability; Force Amplitude = 0.875N)

Figures 5.21 (a-d) show the response spectrum at the four selected frequencies. Estimate of the nonlinear parameter k_3 converges from an initial value of 1.0520×10^{19} N/m^3 to a final value of 1.0146×10^{19} N/m^3 as shown in Figure 5.22 (a). The estimation error is 5.2% for the preliminary value and 1.46% for the final value. The final estimation of first order kernel transform is shown in Figure 5.22 (b) and the estimated linear parameters are

$k_1 = 0.9996\times10^7$ N/m $\qquad$ $m = 0.9999$ kg $\qquad$ $\varsigma = 0.01029$

The summary of the results in the three cases is given in Table 5.1.

Table 5.1 Estimates under different measurability conditions

	k_1 $\times10^7$ N/m	m kg	ς	k_3 $\times10^{19}$ N/m^3
Preliminary estimates	1.0074	0.9999	0.01055	1.0332, 1.0309, 1.0520
Final estimates Case (i)	0.9998	0.9999	0.01024	1.0053
Final estimates Case (ii)	0.9998	0.9999	0.01023	1.0065
Final estimates Case (iii)	0.9996	0.9999	0.01029	1.0146

It is evident that while significant improvement in estimates is achieved with iteration, the error is strongly linked to the excitation amplitude used in third harmonic measurement. A higher excitation level (Force Amplitude = 0.875 N), while providing a better measurability of 10% also gives a relatively high error of 1.46%. The excitation amplitude of 0.35 N gives relatively less error of 0.53%, but reduces the measurability of third harmonic to 2%. Estimates of mass and stiffness parameters do not show any significant trend with iterations. Damping estimates, however get refined with iteration. These improvements in damping estimates play a numerically critical role during the estimation of the nonlinear parameter k_3.

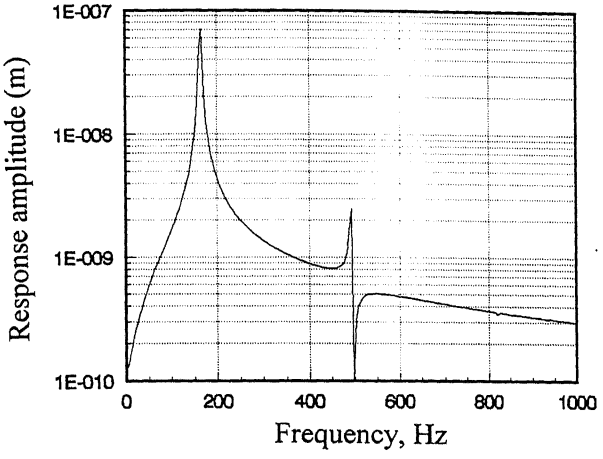

a) Excitation at 164 Hz.

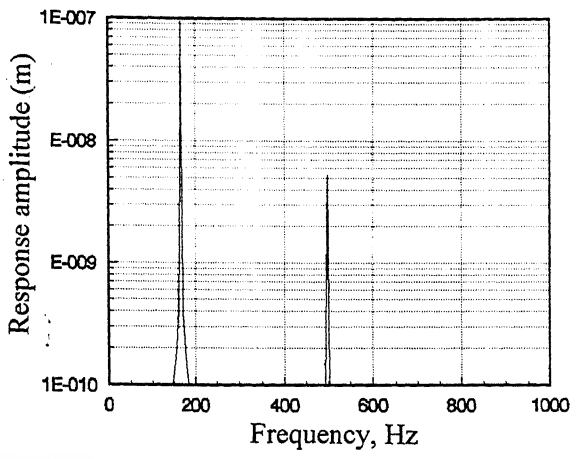

b) Excitation at 166 Hz.

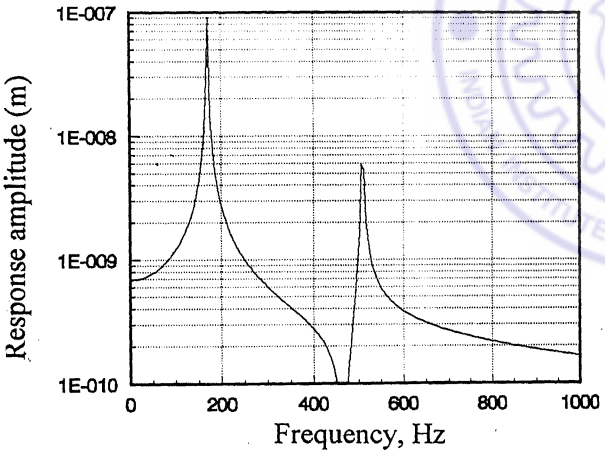

c) Excitation at 170 Hz

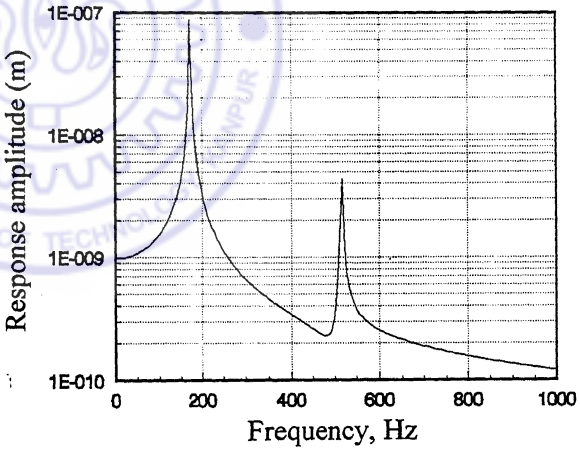

d) Excitation at 172 Hz.

Figure 5.21 Response spectra with force amplitude = 0.875N.
[Case (iii): 10% peak measurability]

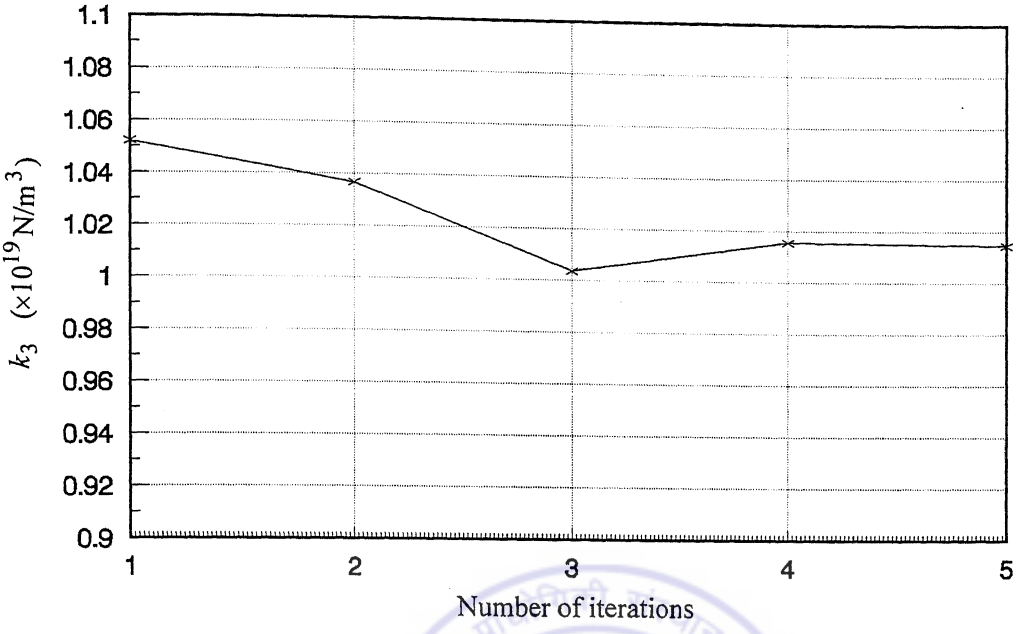

Figure 5.22(a) Iterative estimation of k_3
[Case (iii): 10% peak measurability]

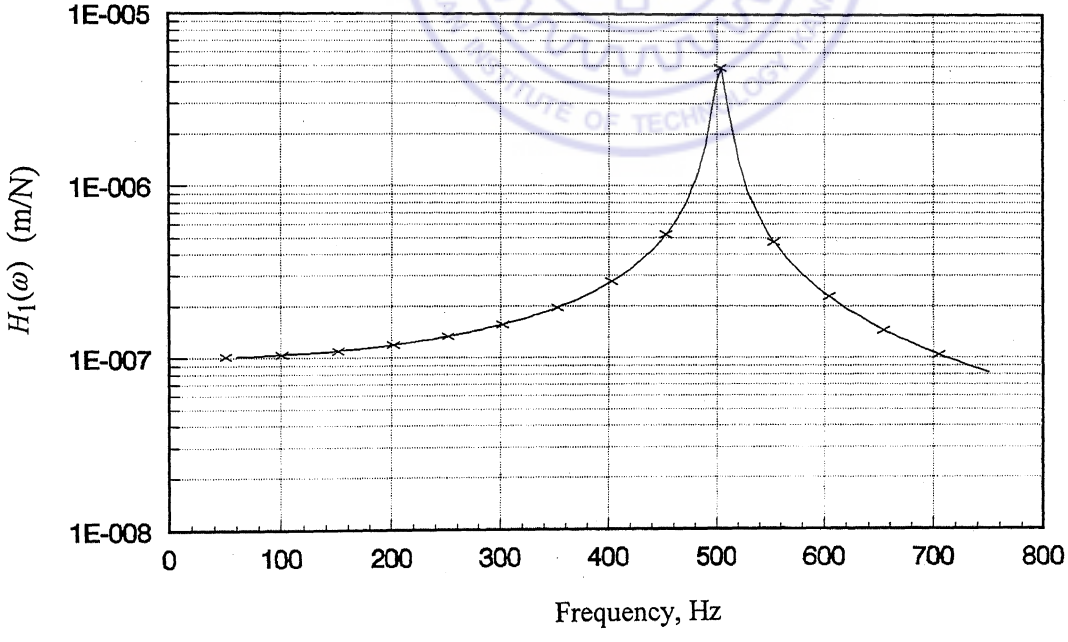

Figure 5.22(b) Final estimate of first order kernel transform, $H_1(\omega)$
[Case (iii): 10% peak measurability]

5.5.3 Convergence Problem at Higher Response Levels

Accuracy of estimates gets improved if more number of terms can be included in the approximation of a harmonic (equations 5.2). The number of terms, in the approximation is however limited by the convergence criterion. Consider two experiments – (i) a case where the response amplitude, $X(\omega)$, is maintained constant at 1.0×10^{-7} m, throughout the frequency range of measurement, (ii) $X(\omega)$, is maintained constant at 2.0×10^{-7} m. For the two cases, the required force amplitude variation with frequency is plotted in Figure 5.23. The force amplitude variation required for achieving convergence with a four-term approximation of $X(\omega)$ is also shown in Figure 5.23. It can be seen that for the first experiment with lower constant response level, the excitation amplitude employed is less than the critical limit throughout the frequency range, indicating that recursive iteration could employ at least four series terms for all the excitation frequencies. Consequently the estimation accuracy is expected to be good, as seen in the previous section. For the second experiment, with a higher value of response level at 2.0×10^{-7} m, the series does not converge at the natural frequency ($\lambda_3 > \frac{1}{4}\lambda_{crit}$). The final estimate of the nonlinear parameter in this case (under 2% measurability condition) is found to be $k_3 = 1.2468\times10^{19}$ N/m^3 and the error is 24%. Thus the error in the nonlinear parameter estimate is strongly related to the convergence criterion discussed in section 5.2.

5.5.4 Influence of Measurement Noise

To investigate the robustness of the iterative procedure against the external noise, white noise is generated and added to the response time history. Noise to signal ratio is typically selected as 5%. Figure 5.24(a) shows a typical response time history for response level of 1.0×10^{-7} m and Figure 5.24(b) shows a randomly varying white noise with noise to signal ratio of 5%. The combined time history is shown in Figure 5.24(c). The noisy response data are then processed for the estimation of the parameters. Linear parameters are found to be

$k_1 = 0.9998\times10^{7}$ N/m $m = 0.9999$ kg $\varsigma = 0.01028$

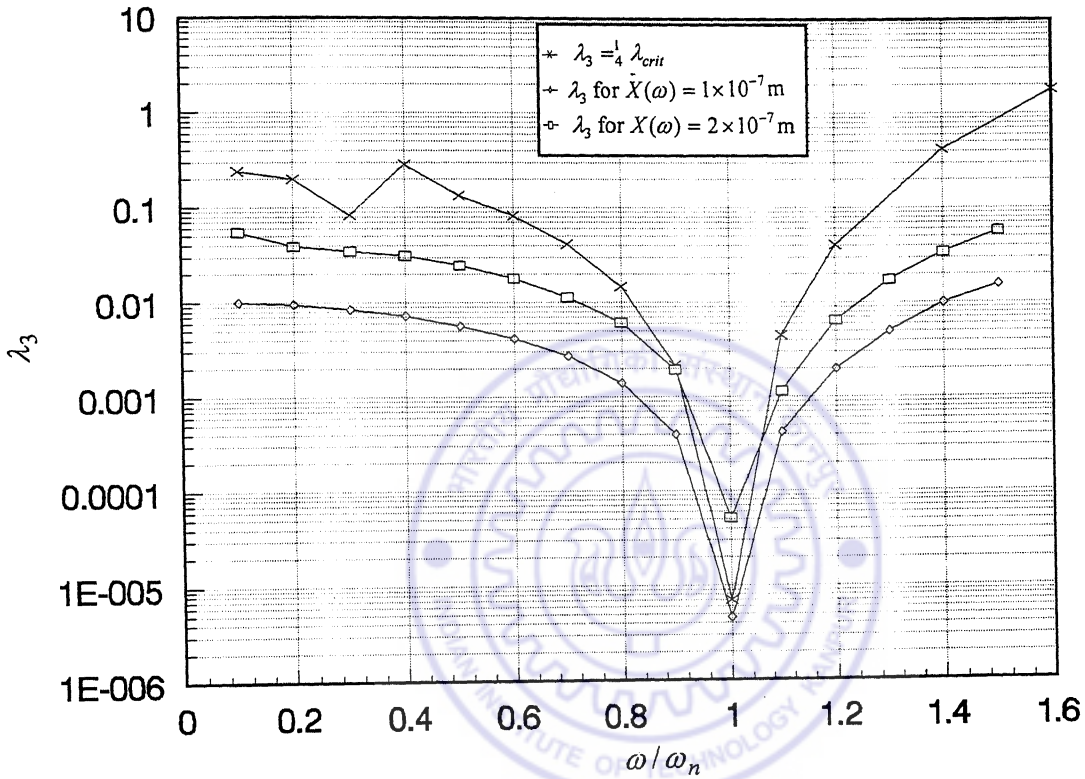

Figure 5.23 Comparison of variations in non-dimensional excitation amplitude, (λ_3)

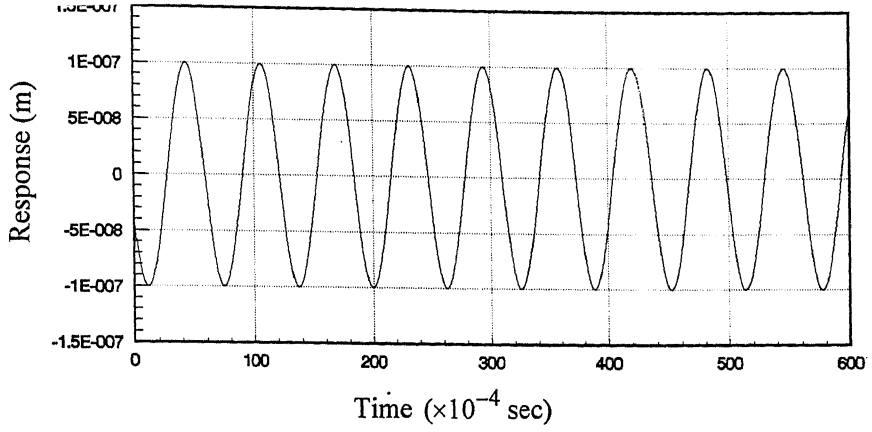

a) Response without noise.

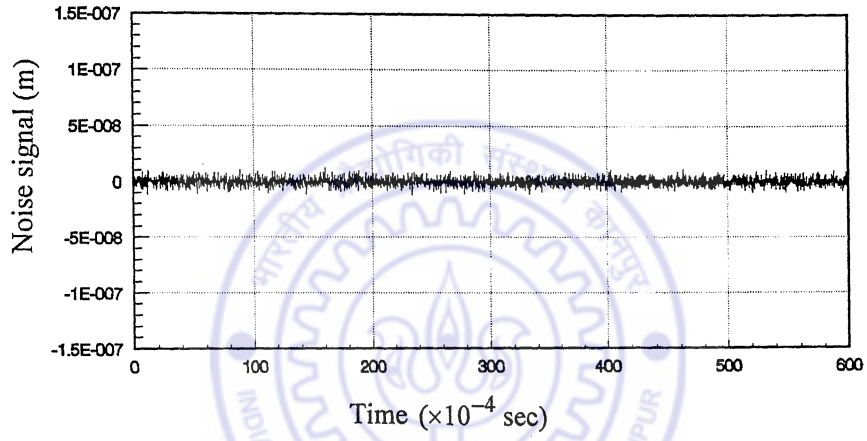

b) Noise signal

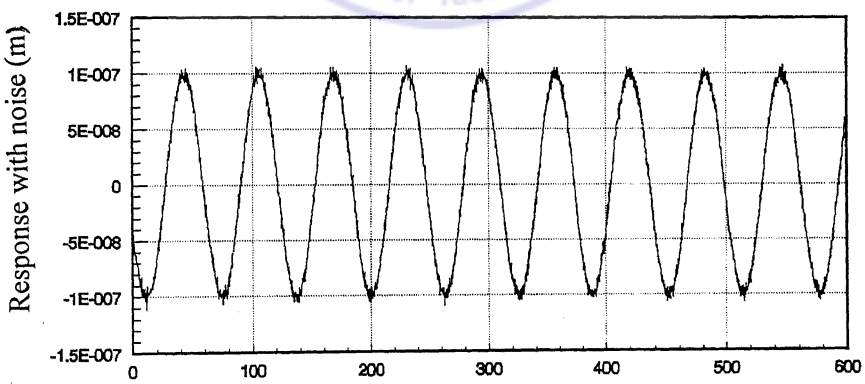

c) Response with 5% noise.

Figure 5.24 Response measurement in presence of noise. (noise to signal ratio 5%)

Estimated values of the nonlinear param eter k_3, in presence of 5% noise, under different measurability conditions are tabled below along with the estimation values under zero noise condition obtained in section 5.5.2.

Table 5.2 Effect of noise in parameter estimation

Measurability Condition	k_3, $\times 10^{19}$ N/m^3 with 5% noise	k_3, $\times 10^{19}$ N/m^3 with zero noise
Case (i)	1.0069	1.0053
Case (ii)	1.0080	1.0065
Case (iii)	1.0150	1.0146

The results in the above table indicate the robustness of the estimation algorithm in the presence of measurement noise.

5.6 Comparison with Response Component Separation Method

A comparison of the present procedure is made with the parameter estimation method suggested by Lee (1997), which is based on Response Component Separation technique, discussed earlier in section 4.1. The individual response components $x_1(t), x_2(t), x_3(t)$..... (equation 4.2),are separated from the overall response $x(t)$, employing equation (4.3). The first order kernel transform, $H_1(\omega)$ and third order kernel transform $H_3(\omega,\omega,\omega)$ are respectively estimated from the first harmonic content of response component $x_1(t)$ and third harmonic content of response component $x_3(t)$, using the following relationships.

$$H_1(\omega) = X_1(\omega)/A$$
$$H_3(\omega,\omega,\omega) = (4/3A^3)X_1(3\omega) \qquad (5.28)$$

The nonlinear parameter is estimated through regression between measured third order kernel transform, $H_3(\omega,\omega,\omega)$ and the third order kernel factor $\Gamma_3(3\omega)$, which is synthesised (equation 5.6) with the estimated first order kernel transforms, $H_1(\omega)$. The relationships (5.28) employed by Lee are based on single-term series approximations, and

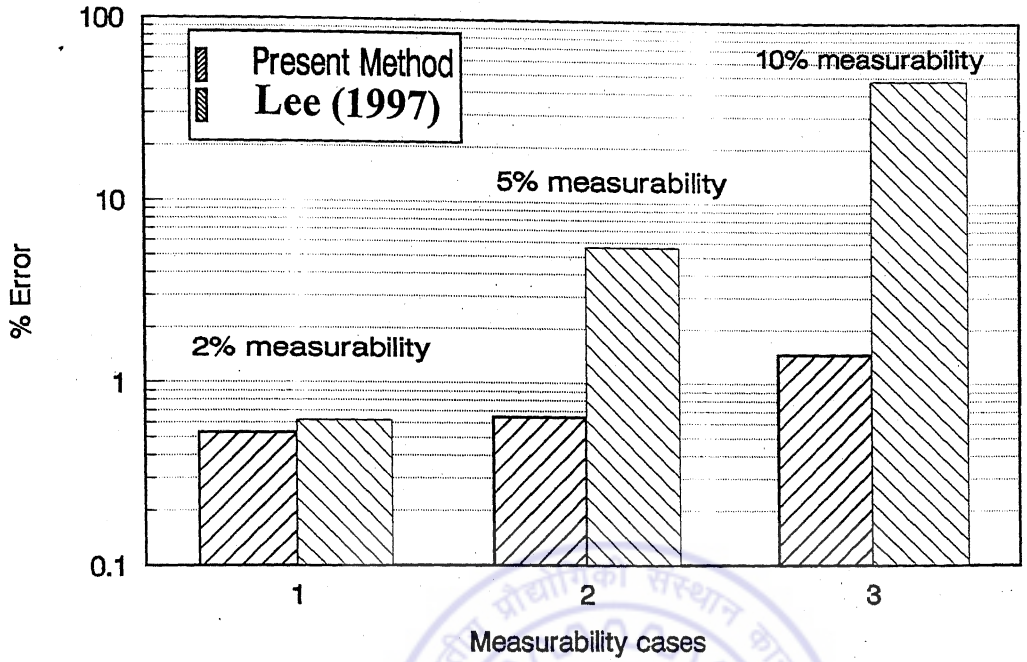

a) Without noise

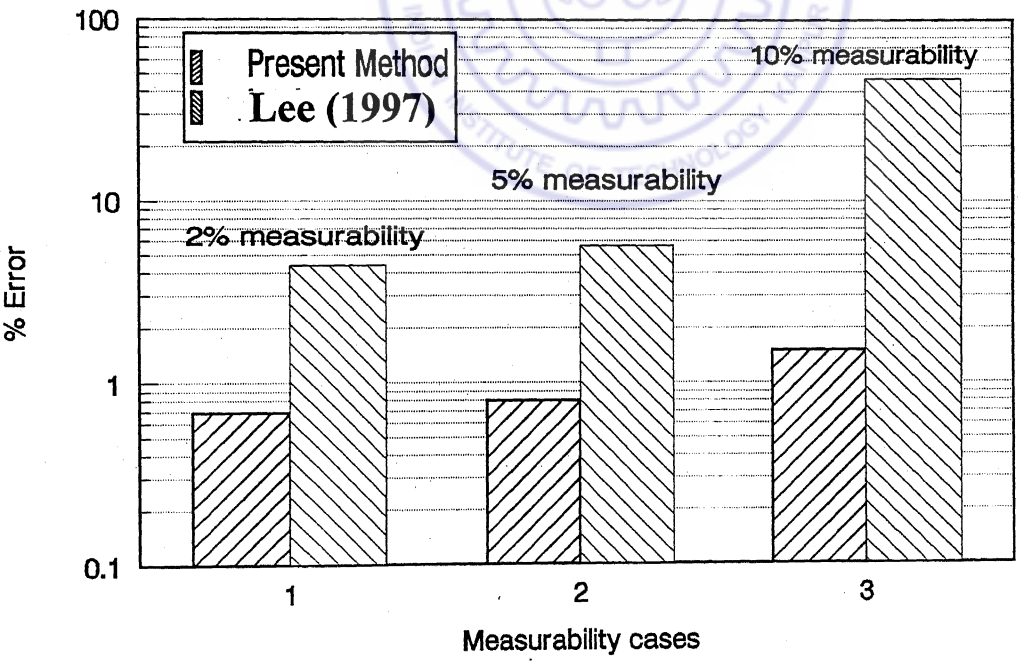

b) With 5% noise

Figure 5.25 Error comparison in final estimates of nonlinear parameter, k_3

the results obtained through this method (Table 5.3) contain high error. These results along with results obtained through the procedure developed in the present study (Table 5.2) are plotted in Figure 5.25.

Table 5.3 Estimate of nonlinear parameter by response component separation

Measurability Condition	k_3, $\times 10^{19}$ N/m^3 with 5% noise	k_3, $\times 10^{19}$ N/m^3 with zero noise
Force Amplitude = 0.35N	1.04414	0.9938
Force Amplitude = 0.565N	1.0566	1.0565
Force Amplitude = 0.875N	1.4707	1.4791

5.7 Remarks

The parameter estimation procedure based on recursive evaluation of Volterra kernels, presented in this chapter, can be expected to yield good nonlinear estimates, with suitably designed experiments where excitation amplitudes and frequencies are chosen according to the discussed guidelines. The estimation algorithm is robust against random measurement noise and is more accurate than the response component separation method.

CHAPTER 6

PARAMETER ESTIMATION IN MULTI-DEGREE-OF-FREEDOM SYSTEMS

Analysis of multi-degree of freedom systems and output measurement, which involve multiple stations, require concepts of cross-kernels (Worden and Tomlinson, 1997), in addition to the direct kernels, as employed for single-degree of-freedom systems. In this chapter, Volterra series response representation for a multi-degree-of-freedom system, under a set of harmonic excitations, is developed. Generic expressions for response harmonic amplitudes are presented and kernel synthesis formulations are developed. It is shown that higher order direct and cross-kernel transforms are functions of the first order kernel transforms and the set of nonlinear parameters, for systems with polynomial form nonlinearity. The parameter estimation procedure based on recursive iteration, developed for a single-degree-of-freedom system, is extended and illustrated here for a two-degree-of-freedom system with square and cubic stiffness nonlinearity. Numerical simulations and error analysis are presented for typical rotor bearing system parameters. Estimation is carried out for various combinations of linear and nonlinear parameters.

6.1 Response Representation of Multi-Degree-of-Freedom System

For a multi-degree-of-freedom system, acted upon by forces $f_a(t), f_b(t),...$ at points $a, b,...$ the response at a station, j, is given by

$$x^{(j)}(t) = x_1^{(j)}(t) + x_2^{(j)}(t) + x_3^{(j)}(t) + ... \tag{6.1}$$

where, $x_n^{(j)}(t)$ is the nth order response component at the jth station. First order response component at the jth station is formed as a summation of responses due to all the first order components resulting from each individual force and is expressed as

$$x_1^{(j)}(t) = x_1^{(j:a)}(t) + x_1^{(j:b)}(t) + ... \tag{6.2}$$

with

$$x_1^{(j:a)}(t) = \int_{-\infty}^{\infty} h_1^{(j:a)}(\tau_1) f_a(t-\tau_1) d\tau_1 , \qquad x_1^{(j:b)}(t) = \int_{-\infty}^{\infty} h_1^{(j:b)}(\tau_1) f_b(t-\tau_1) d\tau_1 \quad \text{etc.}$$

The first order component can, therefore, be written as

$$x_1^{(j)}(t) = \sum_{\eta=a,b,\ldots} \int_{-\infty}^{\infty} h_1^{(j:\eta)}(\tau_1) f_\eta(t-\tau_1) d\tau_1 \tag{6.3}$$

The kernels $h_1^{(j:\eta)}(\tau_1)$ for $\eta = a,b,\ldots$ etc. represent the linear impulse response functions, and the corresponding kernel transforms are

$$H_1^{(j:\eta)}(\omega_1) = \int_{-\infty}^{\infty} h_1^{(j:\eta)}(\tau_1) e^{-j\omega_1\tau_1} d\tau_1 \tag{6.4}$$

The second order response component $x_2^{(j)}(t)$ is given by

$$x_2^{(j)}(t) = \sum_{\eta_1=a,b,\ldots} \sum_{\eta_2=a,b,\ldots} \int_{-\infty}^{\infty} \int_{-\infty}^{\infty} h_2^{(j:\eta_1\eta_2)}(\tau_1,\tau_2) f_{\eta_1}(t-\tau_1) f_{\eta_2}(t-\tau_2) d\tau_1 d\tau_2 \tag{6.5}$$

Kernels $h_2^{(j:\eta_1\eta_2)}(\tau_1,\tau_2)$, for $\eta_1 = \eta_2$, are called second order direct kernels whereas for $\eta_1 \neq \eta_2$, they are called second order cross-kernels. Fourier transforms of these direct and cross-kernels give the respective direct and cross-kernel transforms as

$$H_2^{(j:\eta_1\eta_2)}(\omega_1,\omega_2) = \int_{-\infty}^{\infty} \int_{-\infty}^{\infty} h_2^{(j:\eta_1\eta_2)}(\tau_1,\tau_2) e^{-j(\omega_1\tau_1+\omega_2\tau_2)} d\tau_1 d\tau_2 \qquad \text{for } \eta_1,\eta_2 = a,b,\ldots \tag{6.6}$$

Proceeding similarly the general *n*th order response component can be written as

$$x_n^{(j)}(t) = \sum_{\eta_1=a,b,\ldots} \sum_{\eta_2=a,b,\ldots} \cdots \sum_{\eta_n=a,b,\ldots} \int_{-\infty}^{\infty} \int_{-\infty}^{\infty} \cdots \int_{-\infty}^{\infty} h_n^{(j:\eta_1\eta_2\ldots\eta_n)}(\tau_1,\ldots,\tau_n) f_{\eta_1}(t-\tau_1)\ldots f_{\eta_n}(t-\tau_n) d\tau_1\ldots d\tau_n \tag{6.7}$$

where the kernels $h_n^{(j:\eta_1\ldots\eta_n)}(\tau_1,\ldots,\tau_n)$ represent the *n*th order direct and cross kernel functions. The *n*th order kernel transforms are

$$H_n^{(j:\eta_1\ldots\eta_n)}(\omega_1,\ldots,\omega_n) = \int_{-\infty}^{\infty} \cdots \int_{-\infty}^{\infty} h_n^{(j:\eta_1\ldots\eta_n)}(\tau_1,\ldots,\tau_n) e^{-j(\omega_1\tau_1+\ldots+\omega_n\tau_n)} d\tau_1\ldots d\tau_n \tag{6.8}$$

For m number of inputs, there would be m^n number of nth order kernels for each measurement location j and a system with N degrees-of-freedom would be characterised by a set of Nm^n number of nth order kernels. This shows that analysis of multi-degree-of-freedom systems with multi-input excitation involves a large number of kernels. However the number of kernels can be significantly reduced using symmetry considerations as

$$h_2^{(j:ab)}(\tau_1,\tau_2)+h_2^{(j:ba)}(\tau_1,\tau_2)\rightarrow 2h_2^{(j:ab)}(\tau_1,\tau_2)$$

$$h_3^{(j:aab)}(\tau_1,\tau_2,\tau_3)+h_3^{(j:baa)}(\tau_1,\tau_2,\tau_3)+h_3^{(j:aba)}(\tau_1,\tau_2,\tau_3)\rightarrow 3h_3^{(j:aab)}(\tau_1,\tau_2,\tau_3)$$

and so on. The rule of symmetry is also applied to the kernel transforms and all kernel transforms with same set of frequency arguments are considered identical irrespective of the order of arrangement of the arguments.

6.2 Response Structure under Harmonic Excitation

A multi-degree-of-freedom system with two inputs $f_a(t)$ and $f_b(t)$ is considered here for general illustration of the response characteristics. For harmonic excitations

$f_a(t)=A\cos\omega_1 t$, $f_b(t)=B\cos\omega_2 t$

the response components at a coordinate, j, are obtained, using equations (6.7) as

$$x_1^{(j)}(t)=\frac{A}{2}H_1^{(j:a)}(\omega_1)e^{j\omega_1 t}+\frac{B}{2}H_1^{(j:b)}(\omega_2)e^{j\omega_2 t}$$
$$+\text{ complex conjugates} \qquad (6.9a)$$

$$x_2^{(j)}(t)=\frac{A^2}{2}H_2^{(j:aa)}(\omega_1,-\omega_1)+\frac{B^2}{2}H_2^{(j:bb)}(\omega_2,-\omega_2)$$
$$+\frac{A^2}{4}H_2^{(j:aa)}(\omega_1,\omega_1)e^{j2\omega_1 t}+\frac{B^2}{4}H_2^{(j:bb)}(\omega_2,\omega_2)e^{j2\omega_2 t}$$
$$+\frac{AB}{2}H_2^{(j:ab)}(\omega_1,\omega_2)e^{j(\omega_1+\omega_2)t}+\frac{AB}{2}H_2^{(j:ab)}(\omega_1,-\omega_2)e^{j(\omega_1-\omega_2)t}$$
$$+\text{ complex conjugates} \qquad (6.9b)$$

$$x_3^{(j)}(t) = \frac{A^3}{8} H_3^{(j:aaa)}(\omega_1,\omega_1,\omega_1)e^{j3\omega_1 t} + \frac{3A^3}{8} H_3^{(j:aaa)}(\omega_1,\omega_1,-\omega_1)e^{j\omega_1 t}$$
$$+ \frac{B^3}{8} H_3^{(j:bbb)}(\omega_2,\omega_2,\omega_2)e^{j3\omega_2 t} + \frac{3B^3}{8} H_3^{(j:bbb)}(\omega_2,\omega_2,-\omega_2)e^{j\omega_2 t}$$
$$+ \frac{3AB^2}{4} H_3^{(j:abb)}(\omega_1,\omega_2,-\omega_2)e^{j\omega_1 t} + \frac{3A^2B}{4} H_3^{(j:aab)}(\omega_1,-\omega_1,\omega_2)e^{j\omega_2 t}$$
$$+ \frac{3A^2B}{8} H_3^{(j:aab)}(\omega_1,\omega_1,\omega_2)e^{j(2\omega_1+\omega_2)t} + \frac{3A^2B}{8} H_3^{(j:aab)}(\omega_1,\omega_1,-\omega_2)e^{j(2\omega_1-\omega_2)t}$$
$$+ \frac{3AB^2}{8} H_3^{(j:abb)}(\omega_1,\omega_2,\omega_2)e^{j(2\omega_2+\omega_1)t} + \frac{3AB^2}{8} H_3^{(j:abb)}(-\omega_1,\omega_2,\omega_2)e^{j(2\omega_2-\omega_1)t}$$
$$+ \text{complex conjugates} \qquad (6.9c)$$

The generic expression for the nth order response component can be developed as

$$x_n^{(j)}(t) = \frac{1}{2^n} \sum A^{p+q} B^{s+u} C_{p,q,s,u} H_n^{(j:a_{(p+q)}b_{(s+u)})p,q,s,u}(\omega) e^{j\omega_{p,q,s,u}t} \qquad (6.10)$$

where, $H_n^{(j:a_{(p+q)}b_{(s+u)})p,q,s,u}(\omega)$ denotes the nth order kernel transforms with $f_x(t)$ considered $(p+q)$ times and $f_y(t)$ considered $(s+u)$ times in the convolution integral, i.e.,

$$H_n^{(j:a_{(p+q)}b_{(s+u)})p,q,s,u}(\omega) = H_n^{(j:\underbrace{aaa...}_{p+q \text{ times}}\underbrace{bbb...}_{s+u \text{ times}})}(\underbrace{\omega_1,...,}_{p \text{ times}}\underbrace{-\omega_1,...,}_{q \text{ times}}\underbrace{\omega_2,...,}_{s \text{ times}}\underbrace{-\omega_2,...,}_{u \text{ times}})$$

and

$$\omega_{p,q,s,u} = (p-q)\omega_1 + (s-u)\omega_2$$

Total response $x^{(j)}(t)$, at jth coordinate of measurement, then becomes

$$x^{(j)}(t) = \sum_{n=1}^{\infty} \frac{1}{2^n} \sum A^{p+q} B^{s+u} C_{p,q,s,u} H_n^{(j:a_{(p+q)}b_{(s+u)})p,q,s,u}(\omega) e^{j\omega_{p,q,s,u}t} \qquad (6.11)$$

The response will consist of fundamental harmonics at ω_1, ω_2 along with higher order harmonics of the general form $(m_1\omega_1 + m_2\omega_2)$. Collecting the terms with $p-q=1$ and $s-u=0$ from the series (6.11) one obtains the response amplitude $X^{(j)}(\omega_1)$ as

$$X^{(j)}(\omega_1) = AH_1^{(j:a)}(\omega_1) + \frac{3A^3}{4} H_3^{(j:aaa)}(\omega_1,\omega_1,-\omega_1) + \frac{3AB^2}{2} H_3^{(j:abb)}(\omega_1,\omega_2,-\omega_2)$$
$$+ \frac{5A^5}{8} H_5^{(j:aaaaa)}(\omega_1,\omega_1,\omega_1,-\omega_1,-\omega_1) + \frac{15A^3B^2}{4} H_5^{(j:aaabb)}(\omega_1,\omega_1,-\omega_1,\omega_2,-\omega_2)$$
$$+ \frac{5AB^4}{16} H_5^{(j:abbbb)}(\omega_1,\omega_2,\omega_2,-\omega_2,-\omega_2) + \text{ higher order terms}$$

(6.12a)

Similarly, collecting the terms with $p-q=0$ and $s-u=1$, one obtains the response amplitude $X^{(j)}(\omega_2)$ as

$$X^{(j)}(\omega_2) = BH_1^{(j:b)}(\omega_2) + \frac{3B^3}{4} H_3^{(j:bbb)}(\omega_2,\omega_2,-\omega_2) + \frac{3A^2B}{2} H_3^{(j:aab)}(\omega_1,-\omega_1,\omega_2)$$
$$+ \frac{5B^5}{8} H_5^{(j:bbbbb)}(\omega_2,\omega_2,\omega_2,-\omega_2,-\omega_2) + \frac{15A^2B^3}{4} H_5^{(j:aabbb)}(\omega_1,-\omega_1,\omega_2,\omega_2,-\omega_2)$$
$$+ \frac{5A^4B}{16} H_5^{(j:aaaab)}(\omega_1,\omega_1,-\omega_1,-\omega_1,\omega_2) + \text{ higher order terms}$$

(6.12b)

Collecting terms with $p-q=m_1$ and $s-u=m_2$ from the series (6.11), one obtains the response amplitude for a general higher order combination tone as

$$X^{(j)}(m_1\omega_1 + m_2\omega_2) = \sum_{i=1}^{\infty} \frac{1}{2^{n+2i-3}} \sum_{\substack{p+s \\ =i-1}} A^{m_1+2p} B^{m_2+2s} \; C_{m_1+p,p,m_2+s,s}$$
$$* H_{n+2i-2}^{(j:a_{(m_1+2p)}b_{(m_2+2s)})\, m_1+p,p,m_2+s,s}(\omega)$$

where $n = |m_1| + |m_2|$ (6.13)

6.3 Kernel Synthesis for a Two-Degree-Of-Freedom System.

As in single-degree-of-freedom systems with polynomial nonlinearity, higher order kernels can be represented as synthesis of lower order ones, for systems with more than one degree of freedom. This is illustrated here for a two degree of freedom system with general form of polynomial nonlinearity up to the cubic term. The governing equation is written below

$$m_x\ddot{x}(t)+c_{xx}\dot{x}(t)+c_{xy}\dot{y}(t)+k_{xx}x(t)+k_{xy}y(t)+k_{2x}^{(xx)}x^2(t)+k_{2x}^{(xy)}x(t)y(t)$$
$$+k_{2x}^{(yy)}y^2(t)+k_{3x}^{(xxx)}x^3(t)+k_{3x}^{(xxy)}x^2(t)y(t)+k_{3x}^{(xyy)}x(t)y^2(t)+k_{3x}^{(yyy)}y^3(t)\ =\ f_x(t) \tag{6.14a}$$

$$m_y\ddot{y}(t)+c_{yx}\dot{x}(t)+c_{yy}\dot{y}(t)+k_{yx}x(t)+k_{yy}y(t)+k_{2y}^{(xx)}x^2(t)+k_{2y}^{(xy)}x(t)y(t)$$
$$+k_{2y}^{(yy)}y^2(t)+k_{3y}^{(xxx)}x^3(t)+k_{3y}^{(xxy)}x^2(t)y(t)+k_{3y}^{(xyy)}x(t)y^2(t)+k_{3y}^{(yyy)}y^3(t)\ =\ f_y(t) \tag{6.14b}$$

The parameters involved in the above equations are:

Linear Parameters:

$$[M]=\begin{bmatrix} m_x & 0 \\ 0 & m_y \end{bmatrix}, \qquad [C]=\begin{bmatrix} c_{xx} & c_{xy} \\ c_{yx} & c_{yy} \end{bmatrix} \quad \text{and} \quad [K]=\begin{bmatrix} k_{xx} & k_{xy} \\ k_{yx} & k_{yy} \end{bmatrix} \tag{6.15}$$

Nonlinear parameters of second order:

The set of second order nonlinear parameters can be arranged in a vector form as

$$\{K_2\}=\begin{Bmatrix} \{K_{2x}\} \\ \{K_{2y}\} \end{Bmatrix} \text{ with}$$

$$\{K_{2x}\}=\left\{k_{2x}^{(xx)},\ k_{2x}^{(yy)},\ k_{2x}^{(xy)}\right\}^T \quad \text{and} \quad \{K_{2y}\}=\left\{k_{2y}^{(xx)},\ k_{2y}^{(yy)},\ k_{2y}^{(xy)}\right\}^T \tag{6.16}$$

The first number in the subscript indicates the order of the nonlinear term and the second number indicates the response coordinate to which it corresponds. The superscript notations indicate the product combination of the response coordinates associated with the parameter.

Nonlinear parameters of third order:

The set of third order nonlinear parameters can similarly be arranged in a vector form as

$$\{K_3\}=\begin{Bmatrix} \{K_{3x}\} \\ \{K_{3y}\} \end{Bmatrix} \text{ with}$$

$$\{K_{3x}\}=\left\{k_{3x}^{(xxx)},\ k_{3x}^{(yyy)},\ k_{3x}^{(xxy)},\ k_{3x}^{(xyy)}\right\}^T \text{ and } \{K_{3y}\}=\left\{k_{3y}^{(xxx)},\ k_{3y}^{(yyy)},\ k_{3y}^{(xxy)},\ k_{3y}^{(xyy)}\right\}^T \tag{6.17}$$

with similar notations as in the case of second order nonlinear parameters, above.

6.3.1 First Order Kernel Transforms

For extraction of first order kernels, harmonic excitation of the form $f_x(t) = A\cos\omega_1 t$ and $f_y(t) = B\cos\omega_2 t$ is considered. The Volterra series response for this multi-point excitation, from equation (6.9), is

$$x(t) = \frac{A}{2}H_1^{(x:x)}(\omega_1)e^{j\omega_1 t} + \frac{B}{2}H_1^{(x:y)}(\omega_2)e^{j\omega_2 t} + \frac{A^2}{2}H_2^{(x:xx)}(\omega_1,-\omega_1) + \frac{B^2}{2}H_2^{(x:yy)}(\omega_2,-\omega_2)$$
$$+\frac{A^2}{4}H_2^{(x:xx)}(\omega_1,\omega_1)e^{j2\omega_1 t} + \frac{B^2}{4}H_2^{(x:yy)}(\omega_2,\omega_2)e^{j2\omega_2 t} + \frac{AB}{2}H_2^{(x:xy)}(\omega_1,\omega_2)e^{j(\omega_1+\omega_2)}$$
$$+\frac{AB}{2}H_2^{(x:xy)}(\omega_1,-\omega_2)e^{j(\omega_1-\omega_2)} + \frac{A^3}{8}H_3^{(x:xxx)}(\omega_1,\omega_1,\omega_1)e^{j3\omega_1 t}$$
$$+\frac{3A^3}{8}H_3^{(x:xxx)}(\omega_1,\omega_1,-\omega_1)e^{j\omega_1 t} + \frac{B^3}{8}H_3^{(x:yyy)}(\omega_2,\omega_2,\omega_2)e^{j3\omega_2 t}$$
$$+\frac{3B^3}{8}H_3^{(x:yyy)}(\omega_2,\omega_2,-\omega_2)e^{j\omega_2 t} + \frac{3A^2B}{4}H_3^{(x:xxy)}(\omega_1,-\omega_1,\omega_2)e^{j\omega_2 t}$$
$$+\frac{3A^2B}{8}H_3^{(x:xxy)}(\omega_1,\omega_1,\omega_2)e^{j(2\omega_1+\omega_2)t} + \frac{3A^2B}{8}H_3^{(x:xxy)}(\omega_1,\omega_1,-\omega_2)e^{j(2\omega_1-\omega_2)t}$$
$$+\frac{3AB^2}{4}H_3^{(x:xyy)}(\omega_1,\omega_2,-\omega_2)e^{j\omega_1 t} + \frac{3AB^2}{8}H_3^{(x:xyy)}(\omega_1,\omega_2,\omega_2)e^{j(2\omega_2+\omega_1)t}$$
$$+\frac{3AB^2}{8}H_3^{(x:xyy)}(-\omega_1,\omega_2,\omega_2)e^{j(2\omega_2-\omega_1)t} + \text{complex conjugate terms}$$
$$+ \text{higher order terms} \qquad (6.18a)$$

$$y(t) = \frac{A}{2}H_1^{(y:x)}(\omega_1)e^{j\omega_1 t} + \frac{B}{2}H_1^{(y:y)}(\omega_2)e^{j\omega_2 t} + \frac{A^2}{2}H_2^{(y:xx)}(\omega_1,-\omega_1) + \frac{B^2}{2}H_2^{(y:yy)}(\omega_2,-\omega_2)$$
$$+\frac{A^2}{4}H_2^{(y:xx)}(\omega_1,\omega_1)e^{j2\omega_1 t} + \frac{B^2}{4}H_2^{(y:yy)}(\omega_2,\omega_2)e^{j2\omega_2 t} + \frac{AB}{2}H_2^{(y:xy)}(\omega_1,\omega_2)e^{j(\omega_1+\omega_2)}$$
$$+\frac{AB}{2}H_2^{(y:xy)}(\omega_1,-\omega_2)e^{j(\omega_1-\omega_2)} + \frac{A^3}{8}H_3^{(y:xxx)}(\omega_1,\omega_1,\omega_1)e^{j3\omega_1 t}$$
$$+\frac{3A^3}{8}H_3^{(y:xxx)}(\omega_1,\omega_1,-\omega_1)e^{j\omega_1 t} + \frac{B^3}{8}H_3^{(y:yyy)}(\omega_2,\omega_2,\omega_2)e^{j3\omega_2 t}$$

$$+\frac{3B^3}{8}H_3^{(y:yyy)}(\omega_2,\omega_2,-\omega_2)e^{j\omega_2 t}+\frac{3A^2B}{4}H_3^{(y:xxy)}(\omega_1,-\omega_1,\omega_2)e^{j\omega_2 t}$$

$$+\frac{3A^2B}{8}H_3^{(y:xxy)}(\omega_1,\omega_1,\omega_2)e^{j(2\omega_1+\omega_2)t}+\frac{3A^2B}{8}H_3^{(y:xxy)}(\omega_1,\omega_1,-\omega_2)e^{j(2\omega_1-\omega_2)t}$$

$$+\frac{3AB^2}{4}H_3^{(y:xyy)}(\omega_1,\omega_2,-\omega_2)e^{j\omega_1 t}+\frac{3AB^2}{8}H_3^{(y:xyy)}(\omega_1,\omega_2,\omega_2)e^{j(2\omega_2+\omega_1)t}$$

$$+\frac{3AB^2}{8}H_3^{(y:xyy)}(-\omega_1,\omega_2,\omega_2)e^{j(2\omega_2-\omega_1)t}+\text{complex conjugate terms}$$

+ higher order terms (6.18b)

Substituting the response expressions (6.18a,b) in the governing equations of motion (6.14a,b) and equating the coefficients of $\frac{A}{2}e^{j\omega_1 t}$, one obtains

$$\begin{bmatrix}\left[-\omega_1^2 m_x+j\omega_1 c_{xx}+k_{xx}\right] & \left[j\omega_1 c_{xy}+k_{xy}\right]\\ \left[j\omega_1 c_{yx}+k_{yx}\right] & \left[-\omega_1^2 m_y+j\omega_1 c_{yy}+k_{yy}\right]\end{bmatrix}\begin{Bmatrix}H_1^{(x:x)}(\omega_1)\\ H_1^{(y:x)}(\omega_1)\end{Bmatrix}=\begin{Bmatrix}1\\0\end{Bmatrix} \tag{6.19}$$

Similarly, equating coefficients of $\frac{B}{2}e^{j\omega_2 t}$, one obtains

$$\begin{bmatrix}\left[-\omega_2^2 m_x+j\omega_2 c_{xx}+k_{xx}\right] & \left[j\omega_2 c_{xy}+k_{xy}\right]\\ \left[j\omega_2 c_{yx}+k_{yx}\right] & \left[-\omega_2^2 m_y+j\omega_2 c_{yy}+k_{yy}\right]\end{bmatrix}\begin{Bmatrix}H_1^{(x:y)}(\omega_2)\\ H_1^{(y:y)}(\omega_2)\end{Bmatrix}=\begin{Bmatrix}0\\1\end{Bmatrix} \tag{6.20}$$

Combining the equations (6.19 and 6.20) one obtains

$$\begin{bmatrix}\left[-\omega^2 m_x+j\omega c_{xx}+k_{xx}\right] & \left[j\omega c_{xy}+k_{xy}\right]\\ \left[j\omega c_{yx}+k_{yx}\right] & \left[-\omega^2 m_y+j\omega c_{yy}+k_{yy}\right]\end{bmatrix}\begin{bmatrix}H_1^{(x:x)}(\omega) & H_1^{(x:y)}(\omega)\\ H_1^{(y:x)}(\omega) & H_1^{(y:y)}(\omega)\end{bmatrix}=\begin{bmatrix}1 & 0\\0 & 1\end{bmatrix} \tag{6.21}$$

The above can be condensed further to

$$\left[-\omega^2[M]+j\omega[C]+[K]\right]\begin{bmatrix}H_1^{(x:x)}(\omega) & H_1^{(x:y)}(\omega)\\ H_1^{(y:x)}(\omega) & H_1^{(y:y)}(\omega)\end{bmatrix}=\begin{bmatrix}1 & 0\\0 & 1\end{bmatrix} \tag{6.22}$$

where $[M]$, $[C]$, $[K]$ are mass, damping and linear stiffness matrices as defined in equations 6.15.

The first order kernel transforms can now be readily expressed in terms of the linear parameters of the system as

$$\begin{bmatrix} H_1^{(x:x)}(\omega) & H_1^{(x:y)}(\omega) \\ H_1^{(y:x)}(\omega) & H_1^{(y:y)}(\omega) \end{bmatrix} = \left[-\omega^2[M]+j\omega[C]+[K]\right]^{-1} \tag{6.23}$$

6.3.2 Synthesis of Second Order Kernel Transforms

It can be seen from the response series (equation 6.18), that there are three types of second order kernel transforms, $H_2^{(j:xx)}(\omega_1,\omega_2)$, $H_2^{(j:xy)}(\omega_1,\omega_2)$ and $H_2^{(j:yy)}(\omega_1,\omega_2)$, $j=x,y$. While $H_2^{(j:xx)}(\omega_1,\omega_2)$ and $H_2^{(j:yy)}(\omega_1,\omega_2)$ are the direct kernel transforms, $H_2^{(j:xy)}(\omega_1,\omega_2)$ is the cross-kernel transform. Expressions for these second order kernel transforms can be obtained in terms of first order kernel transforms by equating the coefficients of $\frac{AB}{2}e^{j(\omega_1+\omega_2)t}$ in the governing equations of motion (6.14), after substitution of the response expressions (equation 6.18), in the following form as

$$\left[-(\omega_1+\omega_2)^2[M]+j(\omega_1+\omega_2)[C]+[K]\right]\begin{Bmatrix} H_2^{(x:xy)}(\omega_1,\omega_2) \\ H_2^{(y:xy)}(\omega_1,\omega_2) \end{Bmatrix} = \begin{Bmatrix} p_{xy} \\ q_{xy} \end{Bmatrix} \tag{6.24}$$

where

$$\begin{aligned} p_{xy} = &-k_{2x}^{(xx)}H_1^{(x:x)}(\omega_1)H_1^{(x:y)}(\omega_2)-k_{2x}^{(yy)}H_1^{(y:x)}(\omega_1)H_1^{(y:y)}(\omega_2) \\ &-\frac{k_{2x}^{(xy)}}{2}\left\{H_1^{(x:x)}(\omega_1)H_1^{(y:y)}(\omega_2)+H_1^{(x:y)}(\omega_2)H_1^{(y:x)}(\omega_1)\right\} \end{aligned} \tag{6.25a}$$

and

$$\begin{aligned} q_{xy} = &-k_{2y}^{(xx)}H_1^{(x:x)}(\omega_1)H_1^{(x:y)}(\omega_2)-k_{2y}^{(yy)}H_1^{(y:x)}(\omega_1)H_1^{(y:y)}(\omega_2) \\ &-\frac{k_{2y}^{(xy)}}{2}\left\{H_1^{(x:x)}(\omega_1)H_1^{(y:y)}(\omega_2)+H_1^{(x:y)}(\omega_2)H_1^{(y:x)}(\omega_1)\right\} \end{aligned} \tag{6.25b}$$

Using equation (6.23), second order kernel transform expressions (equation 6.24) can be re-written, as

$$\begin{Bmatrix} H_2^{(x:xy)}(\omega_1,\omega_2) \\ H_2^{(x:xy)}(\omega_1,\omega_2) \end{Bmatrix} = \left[-(\omega_1+\omega_2)^2[M]+j(\omega_1+\omega_2)[C]+[K]\right]^{-1} \begin{Bmatrix} p_{xy} \\ q_{xy} \end{Bmatrix}$$

$$= \begin{bmatrix} H_1^{(x:x)}(\omega_1+\omega_2) & H_1^{(x:y)}(\omega_1+\omega_2) \\ H_1^{(y:x)}(\omega_1+\omega_2) & H_1^{(y:y)}(\omega_1+\omega_2) \end{bmatrix} \begin{Bmatrix} p_{xy} \\ q_{xy} \end{Bmatrix} \tag{6.26}$$

Similarly with the excitation, $f_x(t) = ACos\omega_1 t + BCos\omega_2 t$ and $f_y(t) = 0$, and equating the coefficients of $\frac{AB}{2} e^{j(\omega_1+\omega_2)t}$ in equation (6.14), one obtains

$$\begin{Bmatrix} H_2^{(x:xx)}(\omega_1,\omega_2) \\ H_2^{(y:xx)}(\omega_1,\omega_2) \end{Bmatrix} = \begin{bmatrix} H_1^{(x:x)}(\omega_1+\omega_2) & H_1^{(x:y)}(\omega_1+\omega_2) \\ H_1^{(y:x)}(\omega_1+\omega_2) & H_1^{(y:y)}(\omega_1+\omega_2) \end{bmatrix} \begin{Bmatrix} p_{xx} \\ q_{xx} \end{Bmatrix} \tag{6.27}$$

where,

$$p_{xx} = -k_{2x}^{(xx)} H_1^{(x:x)}(\omega_1) H_1^{(x:x)}(\omega_2) - k_{2x}^{(yy)} H_1^{(y:x)}(\omega_1) H_1^{(y:x)}(\omega_2) - k_{2x}^{(xy)} H_1^{(x:x)}(\omega_1) H_1^{(y:x)}(\omega_2) \tag{6.28a}$$

and

$$q_{xx} = -k_{2y}^{(xx)} H_1^{(x:x)}(\omega_1) H_1^{(x:x)}(\omega_2) - k_{2y}^{(yy)} H_1^{(y:x)}(\omega_1) H_1^{(y:x)}(\omega_2) - k_{2y}^{(xy)} H_1^{(x:x)}(\omega_1) H_1^{(y:x)}(\omega_2) \tag{6.28b}$$

Proceeding similarly with $f_x(t) = 0$, $f_y(t) = ACos\omega_1 t + BCos\omega_2 t$ and then equating the coefficients of $\frac{AB}{2} e^{j(\omega_1+\omega_2)t}$, one obtains

$$\begin{Bmatrix} H_2^{(x:yy)}(\omega_1,\omega_2) \\ H_2^{(y:yy)}(\omega_1,\omega_2) \end{Bmatrix} = \begin{bmatrix} H_1^{(x:x)}(\omega_1+\omega_2) & H_1^{(x:y)}(\omega_1+\omega_2) \\ H_1^{(y:x)}(\omega_1+\omega_2) & H_1^{(y:y)}(\omega_1+\omega_2) \end{bmatrix} \begin{Bmatrix} p_{yy} \\ q_{yy} \end{Bmatrix} \tag{6.29}$$

where,

$$p_{yy} = -k_{2x}^{(xx)} H_1^{(x:y)}(\omega_1) H_1^{(x:y)}(\omega_2) - k_{2x}^{(yy)} H_1^{(y:y)}(\omega_1) H_1^{(y:y)}(\omega_2) - k_{2x}^{(xy)} H_1^{(x:y)}(\omega_1) H_1^{(y:y)}(\omega_2) \tag{6.30a}$$

$$q_{yy} = -k_{2y}^{(xx)} H_1^{(x:y)}(\omega_1) H_1^{(x:y)}(\omega_2) - k_{2y}^{(yy)} H_1^{(y:y)}(\omega_1) H_1^{(y:y)}(\omega_2) - k_{2y}^{(xy)} H_1^{(x:y)}(\omega_1) H_1^{(y:y)}(\omega_2) \quad (6.30b)$$

Using equations (6.26), (6.27) and (6.29), all the second order kernel transforms can be expressed in a generic form as

$$\begin{Bmatrix} H_2^{(x:\eta_1\eta_2)}(\omega_1,\omega_2) \\ H_2^{(y:\eta_1\eta_2)}(\omega_1,\omega_2) \end{Bmatrix} = \begin{bmatrix} H_1^{(x:x)}(\omega_1+\omega_2) & H_1^{(x:y)}(\omega_1+\omega_2) \\ H_1^{(y:x)}(\omega_1+\omega_2) & H_1^{(y:y)}(\omega_1+\omega_2) \end{bmatrix} \begin{Bmatrix} p_{\eta_1\eta_2} \\ q_{\eta_1\eta_2} \end{Bmatrix}, \qquad \eta_1,\eta_2 = x,y \quad (6.31)$$

with

$$p_{\eta_1\eta_2} = -k_{2x}^{(xx)} H_1^{(x:\eta_1)}(\omega_1) H_1^{(x:\eta_2)}(\omega_2) - k_{2x}^{(yy)} H_1^{(y:\eta_1)}(\omega_1) H_1^{(y:\eta_2)}(\omega_2) - \frac{k_{2x}^{(xy)}}{2}\left\{H_1^{(x:\eta_1)}(\omega_1) H_1^{(y:\eta_2)}(\omega_2) + H_1^{(x:\eta_2)}(\omega_1) H_1^{(y:\eta_1)}(\omega_2)\right\} \quad (6.32a)$$

and

$$q_{\eta_1\eta_2} = -k_{2y}^{(xx)} H_1^{(x:\eta_1)}(\omega_1) H_1^{(x:\eta_2)}(\omega_2) - k_{2y}^{(yy)} H_1^{(y:\eta_1)}(\omega_1) H_1^{(y:\eta_2)}(\omega_2) - \frac{k_{2y}^{(xy)}}{2}\left\{H_1^{(x:\eta_1)}(\omega_1) H_1^{(y:\eta_2)}(\omega_2) + H_1^{(x:\eta_2)}(\omega_1) H_1^{(y:\eta_1)}(\omega_2)\right\} \quad (6.32b)$$

Equation (6.31) can be re-written to express second order kernel transforms as function of the nonlinear parameter vector, $\{\{K_{2x}\} \quad \{K_{2y}\}\}^T$, as

$$\begin{Bmatrix} H_2^{(x:\eta_1\eta_2)}(\omega_1,\omega_2) \\ H_2^{(y:\eta_1\eta_2)}(\omega_1,\omega_2) \end{Bmatrix} = \begin{bmatrix} H_1^{(x:x)}(\omega_1+\omega_2) & H_1^{(x:y)}(\omega_1+\omega_2) \\ H_1^{(y:x)}(\omega_1+\omega_2) & H_1^{(y:y)}(\omega_1+\omega_2) \end{bmatrix} \begin{bmatrix} \{G\} & \{0\} \\ \{0\} & \{G\} \end{bmatrix} \begin{Bmatrix} \{K_{2x}\} \\ \{K_{2y}\} \end{Bmatrix} \quad (6.33)$$

where

$$\{G\} = \begin{Bmatrix} G_1^{(\eta_1\eta_2)} & G_2^{(\eta_1\eta_2)} & G_3^{(\eta_1\eta_2)} \end{Bmatrix} \quad (6.34)$$

with

$$G_1^{(\eta_1\eta_2)} = -H_1^{(x:\eta_1)}(\omega_1) H_1^{(x:\eta_2)}(\omega_2)$$

$$G_2^{(\eta_1\eta_2)} = -H_1^{(y:\eta_1)}(\omega_1) H_1^{(y:\eta_2)}(\omega_2)$$

$$G_3^{(\eta_1\eta_2)} = -0.5\{H_1^{(x:\eta_1)}(\omega_1)H_1^{(y:\eta_2)}(\omega_2) + H_1^{(x:\eta_2)}(\omega_1)H_1^{(y:\eta_1)}(\omega_2)$$

and $\{0\}$ is a null row vector of dimension 1×3

Equations (6.33) relate the general second order kernel transforms $H_2^{(x:\eta_1\eta_2)}(\omega_1,\omega_2)$ and $H_2^{(y:\eta_1\eta_2)}(\omega_1,\omega_2)$ to the second order nonlinear parameter vector $\{K_2\}$ through a coefficient matrix whose elements are functions of the first order kernel transforms alone.

6.3.3 Synthesis of Third Order Kernel Transforms

It can be seen from response series (6.18a,b) that there are four types of third order kernel transforms, $H_3^{(j:xxx)}(\omega_1,\omega_2,\omega_3)$, $H_3^{(j:yyy)}(\omega_1,\omega_2,\omega_3)$, $H_3^{(j:xxy)}(\omega_1,\omega_2,\omega_3)$ and $H_3^{(j:xyy)}(\omega_1,\omega_2,\omega_3)$. While the first two are direct kernel transforms, the remaining two are cross-kernel transforms. The procedure to synthesise these kernel transforms from first order kernel transforms, over the complete three-dimensional frequency space, is given below. Kernel transforms are individually synthesised through application of the specific set of forcing functions as listed below -

Kernel	Forcing Functions
$H_3^{(j:xxx)}(\omega_1,\omega_2,\omega_3)$	$f_x(t) = A\cos\omega_1 t + B\cos\omega_2 t + C\cos\omega_3 t, \quad f_y(t) = 0$
$H_3^{(j:yyy)}(\omega_1,\omega_2,\omega_3)$	$f_x(t) = 0, \quad f_y(t) = A\cos\omega_1 t + B\cos\omega_2 t + C\cos\omega_3 t$
$H_3^{(j:xxy)}(\omega_1,\omega_2,\omega_3)$	$f_x(t) = A\cos\omega_1 t + B\cos\omega_2 t, \; f_y(t) = C\cos\omega_3 t$
$H_3^{(j:xyy)}(\omega_1,\omega_2,\omega_3)$	$f_x(t) = A\cos\omega_1 t, \quad f_y(t) = B\cos\omega_2 t + C\cos\omega_3 t$

$j = x, y$ (6.35)

For synthesis of third order kernel transform $H_3^{(j:xxx)}(\omega_1,\omega_2,\omega_3)$, excitation as in the first case is applied and coefficients of $\frac{3ABC}{4}e^{j(\omega_1+\omega_2+\omega_3)t}$ are equated in the governing equation (6.14), after substitution of the corresponding response representation, to obtain the expressions for third order kernel transforms as

$$\begin{Bmatrix} H_3^{(x:xxx)}(\omega_1,\omega_2,\omega_3) \\ H_3^{(y:xxx)}(\omega_1,\omega_2,\omega_3) \end{Bmatrix} = \begin{bmatrix} H_1^{(x:x)}(\omega_1+\omega_2+\omega_3) & H_1^{(x:y)}(\omega_1+\omega_2+\omega_3) \\ H_1^{(y:x)}(\omega_1+\omega_2+\omega_3) & H_1^{(y:y)}(\omega_1+\omega_2+\omega_3) \end{bmatrix} \begin{Bmatrix} p_{xxx} \\ q_{xxx} \end{Bmatrix} \quad (6.36)$$

where

$$\begin{aligned} p_{xxx} = & -\frac{2k_{2x}^{(xx)}}{3}\begin{Bmatrix} H_1^{(x:x)}(\omega_1)H_2^{(x:xx)}(\omega_2,\omega_3)+H_1^{(x:x)}(\omega_2)H_2^{(x:xx)}(\omega_1,\omega_3) \\ +H_1^{(x:x)}(\omega_1)H_2^{(x:xx)}(\omega_2,\omega_3) \end{Bmatrix} \\ & -\frac{2k_{2x}^{(yy)}}{3}\begin{Bmatrix} H_1^{(y:x)}(\omega_1)H_2^{(y:xx)}(\omega_2,\omega_3)+H_1^{(y:x)}(\omega_2)H_2^{(y:xx)}(\omega_1,\omega_3) \\ +H_1^{(y:x)}(\omega_1)H_2^{(y:xx)}(\omega_2,\omega_3) \end{Bmatrix} \\ & -\frac{k_{2x}^{(xy)}}{3}\begin{Bmatrix} H_1^{(x:x)}(\omega_1)H_2^{(y:xx)}(\omega_2,\omega_3)+H_1^{(x:x)}(\omega_2)H_2^{(y:xx)}(\omega_1,\omega_3) \\ +H_1^{(x:x)}(\omega_1)H_2^{(y:xx)}(\omega_2,\omega_3)+H_1^{(y:x)}(\omega_1)H_2^{(x:xx)}(\omega_2,\omega_3) \\ H_1^{(y:x)}(\omega_2)H_2^{(x:xx)}(\omega_1,\omega_3)+H_1^{(y:x)}(\omega_1)H_2^{(x:xx)}(\omega_2,\omega_3) \end{Bmatrix} \\ & -k_{3x}^{(xxx)}H_1^{(x:x)}(\omega_1)H_1^{(x:x)}(\omega_2)H_1^{(x:x)}(\omega_3)-k_{3x}^{(yyy)}H_1^{(y:x)}(\omega_1)H_1^{(y:x)}(\omega_2)H_1^{(y:x)}(\omega_3) \\ & -k_{3x}^{(xxy)}\begin{Bmatrix} H_1^{(x:x)}(\omega_1)H_1^{(x:x)}(\omega_2)H_1^{(y:x)}(\omega_3)+H_1^{(x:x)}(\omega_1)H_1^{(y:x)}(\omega_2)H_1^{(x:x)}(\omega_3) \\ H_1^{(y:x)}(\omega_1)H_1^{(x:x)}(\omega_2)H_1^{(x:x)}(\omega_3) \end{Bmatrix} \\ & -k_{3x}^{(xyy)}\begin{Bmatrix} H_1^{(x:x)}(\omega_1)H_1^{(y:x)}(\omega_2)H_1^{(y:x)}(\omega_3)+H_1^{(y:x)}(\omega_1)H_1^{(y:x)}(\omega_2)H_1^{(x:x)}(\omega_3) \\ H_1^{(y:x)}(\omega_1)H_1^{(x:x)}(\omega_2)H_1^{(y:x)}(\omega_3) \end{Bmatrix} \end{aligned} \quad (6.37a)$$

and

$$\begin{aligned} q_{xxx} = & -\frac{2k_{2y}^{(xx)}}{3}\begin{Bmatrix} H_1^{(x:x)}(\omega_1)H_2^{(x:xx)}(\omega_2,\omega_3)+H_1^{(x:x)}(\omega_2)H_2^{(x:xx)}(\omega_1,\omega_3) \\ +H_1^{(x:x)}(\omega_1)H_2^{(x:xx)}(\omega_2,\omega_3) \end{Bmatrix} \\ & -\frac{2k_{2y}^{(yy)}}{3}\begin{Bmatrix} H_1^{(y:x)}(\omega_1)H_2^{(y:xx)}(\omega_2,\omega_3)+H_1^{(y:x)}(\omega_2)H_2^{(y:xx)}(\omega_1,\omega_3) \\ +H_1^{(y:x)}(\omega_1)H_2^{(y:xx)}(\omega_2,\omega_3) \end{Bmatrix} \\ & -\frac{k_{2y}^{(xy)}}{3}\begin{Bmatrix} H_1^{(x:x)}(\omega_1)H_2^{(y:xx)}(\omega_2,\omega_3)+H_1^{(x:x)}(\omega_2)H_2^{(y:xx)}(\omega_1,\omega_3) \\ +H_1^{(x:x)}(\omega_1)H_2^{(y:xx)}(\omega_2,\omega_3)+H_1^{(y:x)}(\omega_1)H_2^{(x:xx)}(\omega_2,\omega_3) \\ H_1^{(y:x)}(\omega_2)H_2^{(x:xx)}(\omega_1,\omega_3)+H_1^{(y:x)}(\omega_1)H_2^{(x:xx)}(\omega_2,\omega_3) \end{Bmatrix} \\ & -k_{3y}^{(xxx)}H_1^{(x:x)}(\omega_1)H_1^{(x:x)}(\omega_2)H_1^{(x:x)}(\omega_3)-k_{3y}^{(yyy)}H_1^{(y:x)}(\omega_1)H_1^{(y:x)}(\omega_2)H_1^{(y:x)}(\omega_3) \end{aligned}$$

$$-k_{3y}^{(xxy)}\begin{Bmatrix} H_1^{(x:x)}(\omega_1)H_1^{(x:x)}(\omega_2)H_1^{(y:x)}(\omega_3)+H_1^{(x:x)}(\omega_1)H_1^{(y:x)}(\omega_2)H_1^{(x:x)}(\omega_3) \\ H_1^{(y:x)}(\omega_1)H_1^{(x:x)}(\omega_2)H_1^{(x:x)}(\omega_3) \end{Bmatrix}$$

$$-k_{3y}^{(xyy)}\begin{Bmatrix} H_1^{(x:x)}(\omega_1)H_1^{(y:x)}(\omega_2)H_1^{(y:x)}(\omega_3)+H_1^{(y:x)}(\omega_1)H_1^{(y:x)}(\omega_2)H_1^{(x:x)}(\omega_3) \\ H_1^{(y:x)}(\omega_1)H_1^{(x:x)}(\omega_2)H_1^{(y:x)}(\omega_3) \end{Bmatrix} \quad (6.37b)$$

Following similar procedure, the remaining three third order kernel transforms are also synthesised.

Based on the above, the generic expression for the third order kernel transforms is developed as

$$\begin{Bmatrix} H_3^{(x:\eta_1\eta_2\eta_3)}(\omega_1,\omega_2,\omega_3) \\ H_3^{(y:\eta_1\eta_2\eta_3)}(\omega_1,\omega_2,\omega_3) \end{Bmatrix} = \begin{bmatrix} H_1^{(x:x)}(\omega_1+\omega_2+\omega_3) & H_1^{(x:y)}(\omega_1+\omega_2+\omega_3) \\ H_1^{(y:x)}(\omega_1+\omega_2+\omega_3) & H_1^{(y:y)}(\omega_1+\omega_2+\omega_3) \end{bmatrix} \begin{Bmatrix} p_{\eta_1\eta_2\eta_3} \\ q_{\eta_1\eta_2\eta_3} \end{Bmatrix},$$

$$\eta_i = x, y \; ; i = 1,2,3 \quad (6.38)$$

where,

$$p_{\eta_1\eta_2\eta_3} = -\frac{2k_{2x}^{(xx)}}{3}\sum_{\substack{i,j,k=1,2,3 \\ i\neq j\neq k}} H_1^{(x:\eta_i)}(\omega_i)H_2^{(x:\eta_j\eta_k)}(\omega_j,\omega_k)$$

$$-\frac{2k_{2x}^{(yy)}}{3}\sum_{\substack{i,j,k=1,2,3 \\ i\neq j\neq k}} H_1^{(y:\eta_i)}(\omega_i)H_2^{(y:\eta_j\eta_k)}(\omega_j,\omega_k)$$

$$-\frac{k_{2x}^{(xy)}}{3}\sum_{\substack{m,n=x,y \\ m\neq n}}\sum_{\substack{i,j,k=1,2,3 \\ i\neq j\neq k}} H_1^{(m:\eta_i)}(\omega_i)H_2^{(n:\eta_j\eta_k)}(\omega_j,\omega_k)$$

$$-k_{3x}^{(xxx)}H_1^{(x:\eta_1)}(\omega_1)H_1^{(x:\eta_2)}(\omega_2)H_1^{(x:\eta_3)}(\omega_3)$$

$$-k_{3x}^{(yyy)}H_1^{(y:\eta_1)}(\omega_1)H_1^{(y:\eta_2)}(\omega_2)H_1^{(y:\eta_3)}(\omega_3)$$

$$-k_{3x}^{(xxy)}\sum_{\substack{i,j,k=1,2,3 \\ i\neq j\neq k}} H_1^{(x:\eta_i)}(\omega_i)H_1^{(x:\eta_j)}(\omega_j)H_1^{(y:\eta_k)}(\omega_k) \quad (6.39a)$$

$$-k_{3x}^{(xyy)}\sum_{\substack{i,j,k=1,2,3 \\ i\neq j\neq k}} H_1^{(x:\eta_i)}(\omega_i)H_1^{(y:\eta_j)}(\omega_j)H_1^{(y:\eta_k)}(\omega_k)$$

$$q_{\eta_1\eta_2\eta_3} = -\frac{2k_{2y}^{(xx)}}{3} \sum_{\substack{i,j,k=1,2,3 \\ i\neq j\neq k}} H_1^{(x:\eta_i)}(\omega_i) H_2^{(x:\eta_j\eta_k)}(\omega_j,\omega_k)$$

$$-\frac{2k_{2y}^{(yy)}}{3} \sum_{\substack{i,j,k=1,2,3 \\ i\neq j\neq k}} H_1^{(y:\eta_i)}(\omega_i) H_2^{(y:\eta_j\eta_k)}(\omega_j,\omega_k)$$

$$-\frac{k_{2y}^{(yx)}}{3} \sum_{\substack{m,n=x,y \\ m\neq n}} \sum_{\substack{i,j,k=1,2,3 \\ i\neq j\neq k}} H_1^{(m:\eta_i)}(\omega_i) H_2^{(n:\eta_j\eta_k)}(\omega_j,\omega_k)$$

$$-k_{3y}^{(xxx)} H_1^{(x:\eta_1)}(\omega_1) H_1^{(x:\eta_2)}(\omega_2) H_1^{(x:\eta_3)}(\omega_3)$$

$$-k_{3y}^{(yyy)} H_1^{(y:\eta_1)}(\omega_1) H_1^{(y:\eta_2)}(\omega_2) H_1^{(y2:\eta_3)}(\omega_3)$$

$$-k_{3y}^{(xxy)} \sum_{\substack{i,j,k=1,2,3 \\ i\neq j\neq k}} H_1^{(x:\eta_i)}(\omega_i) H_1^{(x:\eta_j)}(\omega_j) H_1^{(y:\eta_k)}(\omega_k) \qquad (6.39b)$$

$$-k_{3y}^{(xyy)} \sum_{\substack{i,j,k=1,2,3 \\ i\neq j\neq k}} H_1^{(x:\eta_i)}(\omega_i) H_1^{(y:\eta_j)}(\omega_j) H_1^{(y:\eta_k)}(\omega_k)$$

Expressions explicitly relating third order kernel transforms to third order nonlinear parameters can be developed by denoting

$$\{T\} = \begin{Bmatrix} T_1^{(\eta_1\eta_2\eta_3)} & T_2^{(\eta_1\eta_2\eta_3)} & T_3^{(\eta_1\eta_2\eta_3)} \end{Bmatrix} \qquad (6.40)$$

with

$$T_1^{(\eta_1\eta_2\eta_3)} = -\frac{2}{3} \sum_{\substack{i,j,k=1 \\ i\neq j\neq k}} H_1^{(x:\eta_i)}(\omega_i) H_2^{(x:\eta_j\eta_k)}(\omega_j,\omega_k)$$

$$T_2^{(\eta_1\eta_2\eta_3)} = -\frac{2}{3} \sum_{\substack{i,j,k=1 \\ i\neq j}} H_1^{(y:\eta_i)}(\omega_i) H_2^{(y:\eta_j\eta_k)}(\omega_j,\omega_k)$$

$$T_3^{(\eta_1\eta_2\eta_3)} = -\frac{1}{3} \sum_{\substack{m,n=x,y \\ m\neq n}} \sum_{\substack{i,j,k=1 \\ i\neq j}} H_1^{(m:\eta_i)}(\omega_i) H_2^{(n:\eta_j\eta_k)}(\omega_j,\omega_k)$$

and

$$\{S\} = \begin{Bmatrix} S_1^{(\eta_1\eta_2\eta_3)} & S_2^{(\eta_1\eta_2\eta_3)} & S_3^{(\eta_1\eta_2\eta_3)} & S_4^{(\eta_1\eta_2\eta_3)} \end{Bmatrix} \qquad (6.41)$$

with

$$S_1^{(\eta_1\eta_2\eta_3)} = -H_1^{(x:\eta_1)}(\omega_1)H_1^{(x:\eta_2)}(\omega_2)H_1^{(x:\eta_3)}(\omega_3)$$

$$S_2^{(\eta_1\eta_2\eta_3)} = -H_1^{(y:\eta_1)}(\omega_1)H_1^{(y:\eta_2)}(\omega_2)H_1^{(y:\eta_3)}(\omega_3)$$

$$S_3^{(\eta_1\eta_2\eta_3)} = -\sum_{\substack{i,j,k=1,2,3 \\ i\neq j\neq k}} H_1^{(x:\eta_1)}(\omega_1)H_1^{(x:\eta_2)}(\omega_2)H_1^{(y:\eta_3)}(\omega_3)$$

$$S_4^{(\eta_1\eta_2\eta_3)} = -\sum_{\substack{i,j,k=1,2,3 \\ i\neq j\neq k}} H_1^{(x:\eta_1)}(\omega_1)H_1^{(y:\eta_2)}(\omega_2)H_1^{(y:\eta_3)}(\omega_3)$$

to modify equation (6.38) as

$$\begin{Bmatrix} H_3^{(x:\eta_i\eta_j\eta_k)}(\omega_1,\omega_2,\omega_3) \\ H_3^{(y:\eta_i\eta_j\eta_k)}(\omega_1,\omega_2,\omega_3) \end{Bmatrix} - \begin{bmatrix} H_1^{(x:x)}(\omega_1+\omega_2+\omega_3) & H_1^{(x:y)}(\omega_1+\omega_2+\omega_3) \\ H_1^{(y:x)}(\omega_1+\omega_2+\omega_3) & H_1^{(y:y)}(\omega_1+\omega_2+\omega_3) \end{bmatrix} \begin{bmatrix} \{T\} & 0 \\ 0 & \{T\} \end{bmatrix} \begin{Bmatrix} K_{2x} \\ K_{2y} \end{Bmatrix}$$

$$= \begin{bmatrix} H_1^{(x:x)}(\omega_1+\omega_2+\omega_3) & H_1^{(x:y)}(\omega_1+\omega_2+\omega_3) \\ H_1^{(y:x)}(\omega_1+\omega_2+\omega_3) & H_1^{(y:y)}(\omega_1+\omega_2+\omega_3) \end{bmatrix} \begin{bmatrix} \{S\} & 0 \\ 0 & \{S\} \end{bmatrix} \begin{Bmatrix} K_{3x} \\ K_{3y} \end{Bmatrix} \tag{6.42}$$

6.4 Parameter Estimation by Recursive Iteration.

Parameter estimation procedure employs the relationships given by equations (6.33) and (6.42), for determination of the second and third order nonlinear parameters respectively. First and higher order kernel transforms are obtained from measurements of response harmonics. The nonlinear parameters are estimated by regression of these transforms through relationships (6.33) and (6.42). The kernel transforms are determined in an iterative manner, to include maximum possible converging terms from the Volterra series, to recursively refine the nonlinear estimates.

The Volterra series expression for general response harmonic amplitude given in equation (6.13), can be rewritten for x and y-coordinates as

$$X(m_1\omega_1 + m_2\omega_2) = \sum_{i=1}^{\infty} {}^{x}\sigma_i(m_1\omega_1 + m_2\omega_2) \tag{6.43}$$

and

$$Y(m_1\omega_1 + m_2\omega_2) = \sum_{i=1}^{\infty} {}^{y}\sigma_i(m_1\omega_1 + m_2\omega_2) \tag{6.44}$$

with

$${}^{x}\sigma_i(m_1\omega_1 + m_2\omega_2) = \frac{1}{2^{n+2i-3}} \sum_{\substack{p+s \\ =i-1}} A^{m_1+2p} B^{m_2+2s} C_{m_1+p,p,m_2+s,s} H_{n+2i-2}^{(x:x_{(2p+m_1)}y_{(2s+m_2)})\, m_1+p,p,m_2+s,s}(\omega) \tag{6.45}$$

and

$${}^{y}\sigma_i(m_1\omega_1 + m_2\omega_2) = \frac{1}{2^{n+2i-3}} \sum_{\substack{p+s \\ =i-1}} A^{m_1+2p} B^{m_2+2s} C_{m_1+p,p,m_2+s,s} H_{n+2i-2}^{(y:x_{(2p+m_1)}y_{(2s+m_2)})\, m_1+p,p,m_2+s,s}(\omega)$$

where $n = |m_1| + |m_2|$ (6.46)

6.4.1 Preliminary Estimates of Linear parameters

Response harmonic amplitudes $X(\omega_1), X(\omega_2), Y(\omega_1)$ and $Y(\omega_2)$ can be filtered, for a typical two input single-tone excitation $f_x(t) = A\cos\omega_1 t$ and $f_y(t) = B\cos\omega_2 t$, from measurements of response $x(t)$, $y(t)$. Truncating the infinite series expressions in (6.43,6.44) up to *k*-terms, one obtains

$$H_1^{(x:x)}(\omega_1) \approx \frac{1}{A}\left[X(\omega_1) - \sum_{i=2}^{k} {}^{x}\sigma_i(\omega_1)\right] \tag{6.47a}$$

$$H_1^{(x:y)}(\omega_2) \approx \frac{1}{B}\left[X(\omega_2) - \sum_{i=2}^{k} {}^{x}\sigma_i(\omega_2)\right] \tag{6.47b}$$

$$H_1^{(y:x)}(\omega_1) \approx \frac{1}{A}\left[Y(\omega_1) - \sum_{i=2}^{k} {}^{y}\sigma_i(\omega_1)\right] \tag{6.47c}$$

$$H_1^{(y:y)}(\omega_2) \approx \frac{1}{B}\left[Y(\omega_2) - \sum_{i=2}^{k} {}^{y}\sigma_i(\omega_2)\right] \tag{6.47d}$$

A preliminary estimation of the first order kernel transforms $H_1^{(x:x)}(\omega_1)$, $H_1^{(x:y)}(\omega_2)$, $H_1^{(y:x)}(\omega_1)$ and $H_1^{(y:y)}(\omega_2)$ is made by ignoring the contribution from the higher order series terms. Similarly applying excitation $f_x(t) = A\cos\omega_2 t$ and $f_y(t) = B\cos\omega_1 t$, kernel transforms $H_1^{(x:x)}(\omega_2)$, $H_1^{(x:y)}(\omega_1)$, $H_1^{(y:x)}(\omega_2)$ and $H_1^{(y:y)}(\omega_1)$ can be obtained.

Using these values of first order kernel transforms, for a set of excitation frequencies ω_i, preliminary estimates of the linear parameter matrices $[M]$, $[C]$ and $[K]$ are obtained through regression of equation (6.23).

6.4.2 Preliminary Estimates of Second Order Nonlinear Parameters

Equation (6.33) provides the synthesis relationship of second order kernel transforms in terms of the nonlinear parameter vector $\{K_2\}$. Also, the relationship is in generic form and is valid for any combination of $\eta_1 = x, y$; $\eta_2 = x, y$. Noting that the vector $\{K_2\}$ consists of six unknown parameters, the relationship can be employed for estimation of these parameters if values of six second order kernel transforms are available. This can be obtained through measurement of second order response harmonic amplitudes $X(2\omega_1)$, $X(2\omega_2)$, $X(\omega_1+\omega_2)$, $Y(2\omega_1)$, $Y(2\omega_2)$, and $Y(\omega_1+\omega_2)$. Truncating the infinite series expressions in (6.43, 6.44) up to k terms, the corresponding second order kernel transforms can be written in the form

$$H_2^{(x:xx)}(\omega_1,\omega_1) \approx \frac{2}{A^2}\left[X(2\omega_1) - \sum_{i=2}^{k} {}^{x}\sigma_i(2\omega_1)\right] \tag{6.48a}$$

$$H_2^{(x:yy)}(\omega_2,\omega_2) \approx \frac{2}{B^2}\left[X(2\omega_2) - \sum_{i=2}^{k} {}^{x}\sigma_i(2\omega_2)\right] \tag{6.48b}$$

$$H_2^{(y:xx)}(\omega_1,\omega_1) \approx \frac{2}{A^2}\left[Y(2\omega_1) - \sum_{i=2}^{k} {}^{y}\sigma_i(2\omega_1)\right] \tag{6.48c}$$

$$H_2^{(y:yy)}(\omega_2,\omega_2) \approx \frac{2}{B^2}\left[Y(2\omega_2) - \sum_{i=2}^{k} {}^{y}\sigma_i(2\omega_2)\right] \tag{6.48d}$$

$$H_2^{(x:xy)}(\omega_1,\omega_2) \approx \frac{1}{AB}\left[X(\omega_1+\omega_2) - \sum_{i=2}^{k} {}^{x}\sigma_i(\omega_1+\omega_2)\right] \tag{6.48e}$$

$$H_2^{(y:xy)}(\omega_1,\omega_2) \approx \frac{1}{AB}\left[Y(\omega_1+\omega_2) - \sum_{i=2}^{k} {}^{y}\sigma_i(\omega_1+\omega_2)\right] \tag{6.48f}$$

In the above, second order response harmonic amplitudes $X(2\omega_1)$ $X(2\omega_2)$, $X(\omega_1+\omega_2)$, $Y(2\omega_1)$, $Y(2\omega_2)$, and $Y(\omega_1+\omega_2)$ are filtered from the

measured responses for the excitation $f_x(t) = A\cos\omega_1 t$ and $f_y(t) = B\cos\omega_2 t$. Neglecting the contributions from the higher order terms in the equations (6.48 a-e) above, preliminary estimates of the second order kernel transforms are obtained. These kernel transforms can be related to the set of six nonlinear parameters, using equation (6.33), as

$$\begin{Bmatrix} H_2^{(x:xx)}(\omega_1,\omega_1) \\ H_2^{(y:xx)}(\omega_1,\omega_1) \\ \hline H_2^{(x:yy)}(\omega_2,\omega_2) \\ H_2^{(y:yy)}(\omega_2,\omega_2) \\ \hline H_2^{(x:xy)}(\omega_1,\omega_2) \\ H_2^{(y:xy)}(\omega_1,\omega_2) \end{Bmatrix} = \left[\begin{array}{c|c} [P^{(xx)}] & [Q^{(xx)}] \\ \hline [P^{(yy)}] & [Q^{(yy)}] \\ \hline [P^{(xy)}] & [Q^{(xy)}] \end{array}\right] \left\{\begin{array}{c} k_{2x}^{(xx)} \\ k_{2x}^{(yy)} \\ k_{2x}^{(xy)} \\ \hline k_{2y}^{(xx)} \\ k_{2y}^{(yy)} \\ k_{2y}^{(xy)} \end{array}\right\} \tag{6.49}$$

where

$$[P^{(\eta_1\eta_2)}] = \begin{bmatrix} H_1^{(x:x)}(m\omega_1+n\omega_2) & H_1^{(x:y)}(m\omega_1+n\omega_2) \\ H_1^{(y:x)}(m\omega_1+n\omega_2) & H_1^{(y:y)}(m\omega_1+n\omega_2) \end{bmatrix} \begin{bmatrix} G_1^{(\eta_1\eta_2)} & G_2^{(\eta_1\eta_2)} & G_3^{(\eta_1\eta_2)} \\ 0 & 0 & 0 \end{bmatrix} \tag{6.50a}$$

and

$$[Q^{(\eta_1\eta_2)}] = \begin{bmatrix} H_1^{(x:x)}(m\omega_1+n\omega_2) & H_1^{(x:y)}(m\omega_1+n\omega_2) \\ H_1^{(y:x)}(m\omega_1+n\omega_2) & H_1^{(y:y)}(m\omega_1+n\omega_2) \end{bmatrix} \begin{bmatrix} 0 & 0 & 0 \\ G_1^{(\eta_1\eta_2)} & G_2^{(\eta_1\eta_2)} & G_3^{(\eta_1\eta_2)} \end{bmatrix} \tag{6.50b}$$

with notations $G_1^{(\eta_1\eta_2)}$, $G_2^{(\eta_1\eta_2)}$, $G_3^{(\eta_1\eta_2)}$ as explained in equation (6.34). The combination tone $m\omega_1 + n\omega_2$ represents the six second order harmonics selected for response amplitude measurement.

Regression of equation (6.49) with the set of measured second order kernel transforms, gives the preliminary estimates of the six nonlinear parameters in the vector $\{K_2\}$. The measurements of second order kernel transforms can also be obtained for a number of

frequency sets $(\omega_1,\omega_2)_i$, and the resultant over-determined system of equations can be solved by taking generalized inverse of the coefficient matrix formed from equation (6.49).

6.4.3 Preliminary Estimates of Third Order Nonlinear Parameters

Equation (6.42) can be employed for estimation of the third order nonlinear parameter vector, $\{K_3\}$, containing eight unknown parameters, with measurements of eight response harmonic amplitudes $X(3\omega_1), X(3\omega_2)$, $Y(3\omega_1)$, $Y(3\omega_2)$, $X(2\omega_1+\omega_2)$, $X(2\omega_2+\omega_1)$, $Y(2\omega_1+\omega_2)$ and $Y(2\omega_2+\omega_1)$. For measurement of the corresponding third order kernel transforms, the following k term truncations of series expressions in (6.43, 6.44) are employed.

$$H_3^{(x:xxx)}(\omega_1,\omega_1,\omega_1) \approx \frac{4}{A^3}\left[X(3\omega_1) - \sum_{i=2}^{k} {}^{x}\sigma_i(3\omega_1)\right] \tag{6.51a}$$

$$H_3^{(x:yyy)}(\omega_2,\omega_2,\omega_2) \approx \frac{4}{B^3}\left[X(3\omega_2) - \sum_{i=2}^{k} {}^{x}\sigma_i(3\omega_2)\right] \tag{6.51b}$$

$$H_3^{(x:xxy)}(\omega_1,\omega_1,\omega_2) \approx \frac{4}{3A^2B}\left[X(2\omega_1+\omega_2) - \sum_{i=2}^{k} {}^{x}\sigma_i(2\omega_1+\omega_2)\right] \tag{6.51c}$$

$$H_3^{(x:xyy)}(\omega_1,\omega_2,\omega_2) \approx \frac{4}{3AB^2}\left[X(2\omega_2+\omega_1) - \sum_{i=2}^{k} {}^{x}\sigma_i(2\omega_2+\omega_1)\right] \tag{6.51d}$$

$$H_3^{(y:xxx)}(\omega_1,\omega_1,\omega_1) \approx \frac{4}{A^3}\left[Y(3\omega_1) - \sum_{i=2}^{k} {}^{y}\sigma_i(3\omega_1)\right] \tag{6.51e}$$

$$H_3^{(y:yyy)}(\omega_2,\omega_2,\omega_2) \approx \frac{4}{B^3}\left[Y(3\omega_2) - \sum_{i=2}^{k} {}^{y}\sigma_i(3\omega_2)\right] \tag{6.51f}$$

$$H_3^{(y:xxy)}(\omega_1,\omega_1,\omega_2) \approx \frac{4}{3A^2B}\left[Y(2\omega_1+\omega_2) - \sum_{i=2}^{k} {}^{y}\sigma_i(2\omega_1+\omega_2)\right] \tag{6.51g}$$

$$H_3^{(y:xyy)}(\omega_1,\omega_2,\omega_2) \approx \frac{4}{3AB^2}\left[Y(2\omega_2+\omega_1) - \sum_{i=2}^{k} {}^{y}\sigma_i(2\omega_2+\omega_1)\right] \tag{6.51h}$$

Third order response harmonic amplitudes $X(3\omega_1)$, $X(3\omega_2)$, $Y(3\omega_1)$, $Y(3\omega_2)$, $X(2\omega_1+\omega_2)$, $X(2\omega_2+\omega_1)$, $Y(2\omega_1+\omega_2)$ and $Y(2\omega_2+\omega_1)$ are filtered from the measured responses. Neglecting contributions from the higher order terms in the equations (6.51 a-h) above, preliminary estimates of the third order kernel transforms are obtained. These kernel transforms can be related to the set of eight nonlinear parameters, using equation (6.42), as

$$\begin{Bmatrix} H_3^{(x:xxx)}(\omega_1,\omega_1,\omega_1) \\ H_3^{(y:xxx)}(\omega_1,\omega_1,\omega_1) \\ \hline H_3^{(x:yyy)}(\omega_2,\omega_2,\omega_2) \\ H_3^{(y:yyy)}(\omega_2,\omega_2,\omega_2) \\ \hline H_3^{(x:xxy)}(\omega_1,\omega_1,\omega_2) \\ H_3^{(y:xxy)}(\omega_1,\omega_1,\omega_2) \\ \hline H_3^{(x:xyy)}(\omega_1,\omega_2,\omega_2) \\ H_3^{(y:xyy)}(\omega_1,\omega_2,\omega_2) \end{Bmatrix} - \begin{bmatrix} [P^{(xxx)}] & [Q^{(xxx)}] \\ \hline [P^{(yyy)}] & [Q^{(yyy)}] \\ \hline [P^{(xxy)}] & [Q^{(xxy)}] \\ \hline [P^{(xyy)}] & [Q^{(xyy)}] \end{bmatrix} \begin{Bmatrix} k_{2x}^{(xx)} \\ k_{2x}^{(yy)} \\ k_{2x}^{(xy)} \\ \hline k_{2y}^{(xx)} \\ k_{2y}^{(yy)} \\ k_{2y}^{(xy)} \end{Bmatrix} = \begin{bmatrix} [U^{(xxx)}] & [V^{(xxx)}] \\ \hline [U^{(yyy)}] & [V^{(yyy)}] \\ \hline [U^{(xxy)}] & [V^{(xxy)}] \\ \hline [U^{(xyy)}] & [V^{(xyy)}] \end{bmatrix} \begin{Bmatrix} k_{3x}^{(xxx)} \\ k_{3x}^{(yyy)} \\ k_{3x}^{(xxy)} \\ k_{3x}^{(xyy)} \\ \hline k_{3y}^{(xxx)} \\ k_{3y}^{(yyy)} \\ k_{3y}^{(xxy)} \\ k_{3y}^{(xyy)} \end{Bmatrix} \tag{6.52}$$

where

$$\left[P^{(\eta_1\eta_2\eta_3)}\right] = \begin{bmatrix} H_1^{(x:x)}(m\omega_1+n\omega_2) & H_1^{(x:y)}(m\omega_1+n\omega_2) \\ H_1^{(y:x)}(m\omega_1+n\omega_2) & H_1^{(y:y)}(m\omega_1+n\omega_2) \end{bmatrix} \begin{bmatrix} T_1^{(\eta_1\eta_2\eta_3)} & T_2^{(\eta_1\eta_2\eta_3)} & T_3^{(\eta_1\eta_2\eta_3)} \\ 0 & 0 & 0 \end{bmatrix} \tag{6.53a}$$

$$\left[Q^{(\eta_1\eta_2\eta_3)}\right] = \begin{bmatrix} H_1^{(x:x)}(m\omega_1+n\omega_2) & H_1^{(x:y)}(m\omega_1+n\omega_2) \\ H_1^{(y:x)}(m\omega_1+n\omega_2) & H_1^{(y:y)}(m\omega_1+n\omega_2) \end{bmatrix} \begin{bmatrix} 0 & 0 & 0 \\ T_1^{(\eta_1\eta_2\eta_3)} & T_2^{(\eta_1\eta_2\eta_3)} & T_3^{(\eta_1\eta_2\eta_3)} \end{bmatrix} \tag{6.53b}$$

and

$$\left[U^{(\eta_1\eta_2\eta_3)}\right]=\begin{bmatrix} H_1^{(x:x)}(m\omega_1+n\omega_2) & H_1^{(x:y)}(m\omega_1+n\omega_2) \\ H_1^{(y:x)}(m\omega_1+n\omega_2) & H_1^{(y:y)}(m\omega_1+n\omega_2) \end{bmatrix}\begin{bmatrix} S_1^{(\eta_1\eta_2\eta_3)} & S_2^{(\eta_1\eta_2\eta_3)} & S_3^{(\eta_1\eta_2\eta_3)} & S_4^{(\eta_1\eta_2\eta_3)} \\ 0 & 0 & 0 & 0 \end{bmatrix}$$

(6.53c)

$$\left[V^{(\eta_1\eta_2\eta_3)}\right]=\begin{bmatrix} H_1^{(x:x)}(m\omega_1+n\omega_2) & H_1^{(x:y)}(m\omega_1+n\omega_2) \\ H_1^{(y:x)}(m\omega_1+n\omega_2) & H_1^{(y:y)}(m\omega_1+n\omega_2) \end{bmatrix}\begin{bmatrix} 0 & 0 & 0 & 0 \\ S_1^{(\eta_1\eta_2\eta_3)} & S_2^{(\eta_1\eta_2\eta_3)} & S_3^{(\eta_1\eta_2\eta_3)} & S_4^{(\eta_1\eta_2\eta_3)} \end{bmatrix}$$

(6.53d)

Notations $T_i^{(\eta_1\eta_2\eta_3)}$ and $S_i^{(\eta_1\eta_2\eta_3)}$ are as explained in equations (6.40) and (6.41). The combination tone $m\omega_1+n\omega_2$ represents the eight third order harmonics selected for response amplitude measurement.

Regression of equation (6.52) with the set of measured third order kernel transforms, gives the preliminary estimates of the eight nonlinear parameters in the vector $\{K_3\}$. The measurements of third order kernel transforms can be obtained for a number of frequency sets $(\omega_1,\omega_2)_i$, and the resultant over-determined system of equations can be solved as discussed before.

6.4.4 Iterative Refinement

The preliminary estimates of the nonlinear parameters $\{K_2\}$ and $\{K_3\}$ are now employed to compute the previously ignored higher order terms, ${}^x\sigma_i(m_1\omega_1+m_2\omega_2)$, ${}^y\sigma_i(m_1\omega_1+m_2\omega_2)$, in the equations (6.47), (6.48) and (6.51), to get refined estimates of first, second and third order kernel transforms, respectively. The fresh estimates of the kernel transforms are used to regress the values of the second and third order nonlinear parameters from equations, (6.49) and (6.52), respectively. The iterative process is continued to obtain converged values of these parameters. The number k of the higher order terms, to be included in the refinement would be dependent on the convergence limit for the applied excitation amplitudes and frequencies. The convergence limit can be applied through ratio test, while computing the successive higher order terms.

6.5 Convergence Study and Error Analysis

A simplified model with only cubic nonlinearity is studied for convergence of the Volterra series. The equations of motion (6.14), then reduce to

$$m_x\ddot{x}(t)+c_{xx}\dot{x}(t)+k_{xx}x(t)+k_{xy}y(t)+k_{3x}^{(xxx)}x^3(t)+k_{3x}^{(yyy)}y^3(t) = f_x(t) \qquad (6.54a)$$

$$m_y\ddot{y}(t)+c_{yy}\dot{y}(t)+k_{yx}x(t)+k_{yy}y(t)+k_{3y}^{(xxx)}x^3(t)+k_{3y}^{(yyy)}y^3(t) = f_y(t) \qquad (6.54b)$$

Such a system can typically represent a rigid rotor supported in flexible bearings (Khan and Vyas, 1999), shown in Figure 6.1. k_{xx}, k_{yy} are the direct linear stiffness coefficients of the bearing in the vertical and horizontal directions, respectively. Terms k_{xy}, k_{yx} represent the cross-coupling effects in linear stiffness. $k_{3x}^{(xxx)}, k_{3y}^{(yyy)}$ are the direct nonlinear stiffness coefficients, while $k_{3y}^{(xxx)}, k_{3x}^{(yyy)}$ represent the nonlinear cross-coupling terms. The bearing damping is modeled by direct linear terms only.

Convergence study is carried out in terms of non-dimensional parameters. Defining,

$$\tau = \sqrt{k_{xx}/m_x}\,t \qquad {}^x\eta(\tau) = x/X_{st}, \qquad {}^y\eta(\tau) = y/X_{st} \qquad X_{st} = f_{\max}/k_{xx}$$

$$\bar{f}_i(\tau) = f_i(\tau)/f_{\max} \qquad i = x,y$$

$$\varsigma_{ii} = \frac{c_{ii}}{2\sqrt{k_{xx}m_x}}, \qquad \lambda_{ij}^L = \frac{k_{ij}}{k_{xx}}, \qquad , \quad i = x,y \text{ and } j = x,y \qquad \mu = m_y/m_x$$

$$\lambda_{xx}^N = \frac{k_{3x}^{(xxx)}f_{\max}^2}{k_{xx}^3}, \qquad \lambda_{yy}^N = \frac{k_{3y}^{(yyy)}f_{\max}^2}{k_{xx}^3}, \qquad \lambda_{xy}^N = \frac{k_{3x}^{(yyy)}f_{\max}^2}{k_{xx}^3}, \qquad \lambda_{yx}^N = \frac{k_{3y}^{(xxx)}f_{\max}^2}{k_{xx}^3}$$

the equations of motion (6.54) is converted in non-dimensional form as

$$\begin{aligned} &{}^x\eta''(\tau)+2\varsigma_{xx}{}^x\eta'(\tau)+{}^x\eta(\tau)+\lambda_{xy}^L{}^y\eta(\tau)+\lambda_{xx}^N{}^x\eta^3(\tau)+\lambda_{xy}^N{}^y\eta^3(\tau) = \bar{f}_x(\tau) \\ &\mu\,{}^y\eta''(\tau)+2\varsigma_{yy}{}^y\eta'(\tau)+\lambda_{yy}^L{}^y\eta(\tau)+\lambda_{yx}^L{}^x\eta(\tau)+\lambda_{yy}^N{}^y\eta^3(\tau)+\lambda_{yx}^N{}^x\eta^3(\tau) = \bar{f}_y(\tau) \end{aligned} \qquad (6.55)$$

For a single-tone non-dimensional harmonic excitation

$$\bar{f}_x(\tau) = e^{jr\tau}/2+e^{-jr\tau}/2; \qquad \bar{f}_y(\tau) = 0 \qquad \text{with} \qquad r = \omega/\sqrt{k_{xx}/m_x}$$

the response representation (6.11) reduces to

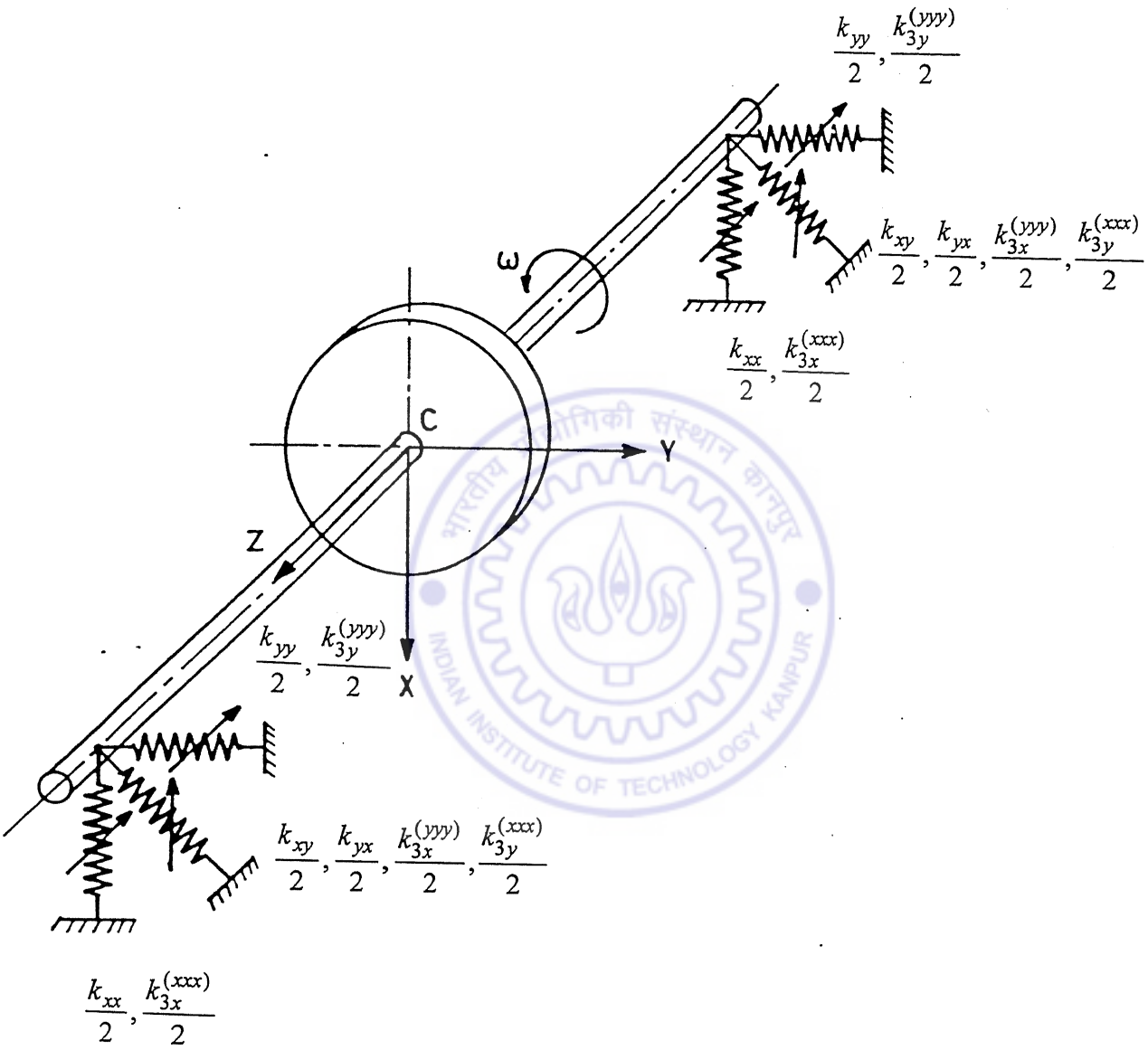

Figure 6.1 Rigid rotor in bearings with cross coupling

$$^{\kappa}\eta(\tau) = \sum_{n=1}^{\infty}\left(\frac{1}{2}\right)^{n} \sum_{p+q=n} {}^{n}C_{q}\, H_{n}^{(\kappa:x)p,q}(r)\, e^{jr_{p,q}\tau} \qquad \kappa = x, y \tag{6.56}$$

Applying method of harmonic probing, the kernel synthesis formulation, for the system given by equations (6.54), for first order and higher order kernel transforms are obtained as

$$H_1^{(x:x)}(r) = \frac{\left[-\mu r^2 + \lambda_{yy}^L + j2\varsigma_{yy}r\right]}{\left[-r^2 + 1 + j2\varsigma_{xx}r\right]\left[-\mu r^2 + \lambda_{yy}^L + j2\varsigma_{yy}r\right] - \lambda_{xy}^L\lambda_{yx}^L} \tag{6.57a}$$

$$H_1^{(y:x)}(r) = \frac{-\lambda_{yx}^L}{\left[-r^2 + 1 + j2\varsigma_{xx}r\right]\left[-\mu r^2 + \lambda_{yy}^L + j2\varsigma_{yy}r\right] - \lambda_{xy}^L\lambda_{yx}^L} \tag{6.57b}$$

and

$$H_n^{(x:xx..)p,q}(r) = \frac{-B_1\left[-\mu r_{p,q}^2 + \lambda_{yy}^L + j2\varsigma_{yy}r_{p,q}\right] + B_2\lambda_{xy}^L}{{}^{n}C_q\left\{\left[-r_{p,q}^2 + 1 + j2\varsigma_{xx}r_{p,q}\right]\left[-\mu r_{p,q}^2 + \lambda_{yy}^L + j2\varsigma_{yy}r_{p,q}\right] - \lambda_{xy}^L\lambda_{yx}^L\right\}} \tag{6.58a}$$

$$H_n^{(y:xx...)p,q}(r) = \frac{-B_2\left[-r_{p,q}^2 + 1 + j2\varsigma_{xx}r_{p,q}\right] + B_1\lambda_{yx}^L}{{}^{n}C_q\left\{\left[-r_{p,q}^2 + 1 + j2\varsigma_{xx}r_{p,q}\right]\left[-\mu r_{p,q}^2 + \lambda_{yy}^L + j2\varsigma_{yy}r_{p,q}\right] - \lambda_{xy}^L\lambda_{yx}^L\right\}} \tag{6.58b}$$

where

$$B_1 = \lambda_{xx}^N \sum_{\substack{p_i+q_i=n_i \\ n_1+n_2+n_3=n}} \left[{}^{n_1}C_{q_1}\, H_{n_1}^{(x:xx..)p_1,q_1}(r)\right]\left[{}^{n_2}C_{q_2}\, H_{n_2}^{(x:xx..)p_2,q_2}(r)\right]\left[{}^{n_3}C_{q_3}\, H_{n_3}^{(x:xx...)p_3,q_3}(r)\right]$$
$$+ \lambda_{xy}^N \sum_{\substack{p_i+q_i=n_i \\ n_1+n_2+n_3=n}} \left[{}^{n_1}C_{q_1}\, H_{n_1}^{(y:xx..)p_1,q_1}(r)\right]\left[{}^{n_2}C_{q_2}\, H_{n2}^{(y:xx...)p_2,q_2}(r)\right]\left[{}^{n_3}C_{q_3}\, H_{n_3}^{(y:xx...)p_3,q_3}(r)\right]$$

and

$$B_2 = \lambda_{yx}^N \sum_{\substack{p_i+q_i=n_i \\ n_1+n_2+n_3=n}} \left[{}^{n_1}C_{q_1}\, H_{n_1}^{(x:xx...)p_1,q_1}(r)\right]\left[{}^{n_2}C_{q_2} H_{n_2}^{(x:xx...)p_2,q_2}(r)\right]\left[{}^{n_3}C_{q_3}\, H_{n_3}^{(x:xx...)p_3,q_3}(r)\right]$$
$$+ \lambda_{yy}^N \sum_{\substack{p_i+q_i=n_i \\ n_1+n_2+n_3=n}} \left[{}^{n_1}C_{q_1}\, H_{n_1}^{(y:xx...)p_1,q_1}(r)\right]\left[{}^{n_2}C_{q_2}\, H_{n_2}^{(y:xx...)p_2,q_2}(r)\right]\left[{}^{n_3}C_{q_3}\, H_{n_3}^{(y:xx...)p_3,q_3}(r)\right.$$

Following equations (6.43-6.46), the *n*th order response harmonic amplitude in non-dimensional form, ${}^{\kappa}Z(nr)$, is obtained as

$$ {}^{\kappa}Z(nr) = 2\sum_{i=1}^{\infty}\left(\frac{1}{2}\right)^{n} {}_{n+2i-2}C_{i-1}\ {}^{\kappa}H_{n+2i-2}^{n+i-1,i-1}(r), \qquad \kappa = x \text{ or } y \tag{6.59} $$

A *k*-term approximation of the response series would be given by

$$ {}_{k}^{\kappa}Z(nr) = \sum_{i=1}^{k} {}^{\kappa}\sigma_i(nr) \tag{6.60} $$

where,

$$ {}^{\kappa}\sigma_i(nr) = 2\left(\frac{1}{2}\right)^{n} {}_{n+2i-2}C_{i-1}\ {}^{\kappa}H_{n+2i-2}^{(n+i-1,i-1}(r) \tag{6.61} $$

The error between above approximation and the exact value of the harmonic is

$$ {}^{\kappa}e_k(nr) = \left|[{}^{\kappa}Z(nr) - {}_{k}^{\kappa}Z(nr)]/{}^{\kappa}Z(nr)\right| \tag{6.62} $$

The approximated response harmonic ${}_{k}^{\kappa}Z(nr)$ can be synthesized after determining the higher order kernel transforms ${}^{\kappa}H_{n+2i-2}^{n+i-1,i-1}(r)$, using equations (6.57,6.58). The exact response harmonics are obtained by fourth order Runge-Kutta numerical solution of equations (6.54). Similar to the convergence exercise carried out for single-degree-of-freedom systems in section 5.2.1, the limit of convergence of the response harmonic ${}^{\kappa}Z(nr)$ can be represented by a set of critical values of the non-dimensional parameters ${}_{k}^{n}\left(\lambda_{xx}^{N}, \lambda_{yy}^{N}, \lambda_{xy}^{N}, \lambda_{yx}^{N}\right)_{crit}^{\kappa}$. These four non-dimensional non-linear parameters along with the number of terms, *k*, constitute a 5-dimensional parametric space which is divided into two regions of convergence and divergence by the hyper surface represented by ${}_{k}^{n}\left(\lambda_{xx}^{N}, \lambda_{yy}^{N}, \lambda_{xy}^{N}, \lambda_{yx}^{N}\right)_{crit}^{\kappa}$. For ease of computation, cross nonlinear stiffnesses, λ_{xy}^{N} and λ_{yx}^{N}, are taken as zero in the present computer simulation. The parametric space, then reduces to 3-dimensional space comprising of $\lambda_{xx}^{N}, \lambda_{yy}^{N}$ and *k*.

The following values of linear parameters are considered for computer simulation of equations (6.54)

$\mu = 1.0 \qquad \lambda^L_{xx} = \lambda^L_{yy} = 1.0$

$\lambda^L_{xy} = \lambda^L_{xy} = 0.1$ and 0.5

$\varsigma_{xx} = \varsigma_{yy} = 0.01$

Defining a scaling parameter $\beta = \lambda^N_{yy} / \lambda^N_{xx}$, the convergence is analysed numerically as a function of λ^N_{xx}, β and the number of terms, k, in the response harmonic series.

For a specific value of β, the limiting value of λ^N_{xx} for which a k-term series for nth order harmonic is convergent is termed as the critical non-dimensional parameter ${}^n_k\lambda^{(\kappa)}_{crit}$. The variation of this parameter with the excitation frequency r, for a typical value of k = 3, is shown for both x and y direction response in Figures 6.2a,b. The plots are shown for three different values of the scaling parameter $\beta = 0.1, 1.0, 10.0$. These plots pertain to a case of linear coupling numerically taken as $\lambda^L_{xy} = \lambda^L_{yx} = 0.5$. It can be observed that the critical values ${}^n_k\lambda^{(\kappa)}_{crit}$ are small at the system natural frequencies (which, for $\lambda^L_{xy} = \lambda^L_{yx} = 0.5$, are r = 0.7 and r = 1.224.) and their 1/3 subharmonics at r = 0.233 and r = 0.408. It is maximum in the vicinity of the anti-resonance frequency at r = 1.0. Similar characteristics are observed, for a case with weaker linear coupling ($\lambda^L_{xy} = \lambda^L_{yx} = 0.1$), in Figures 6.3a,b. However, the coupling being weak, the effect of scaling parameter β is also weaker than in the previous case, of Figures 6.2a,b.

The critical values ${}^n_k\lambda^{(\kappa)}_{crit}$ discussed above are obtained through the ratio test similar to that of single-degree-of-freedom system (section 5.2.2). A comparison of these critical values with those obtained through iterative simulation is shown in Figures 6.4a-c for various values of scaling parameter β. The figure shows the zone of convergence and zone of divergence in terms of critical value of the non-dimensional parameters.

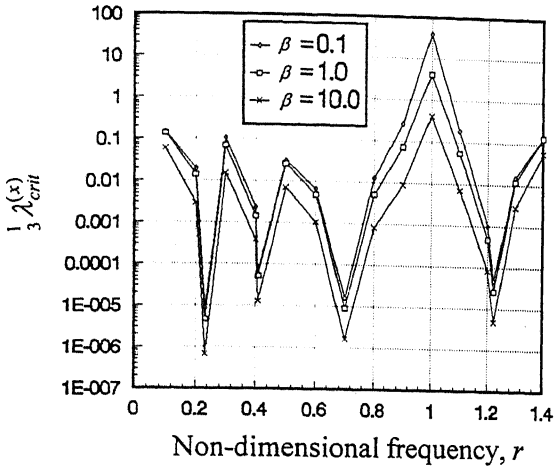

a) x-response

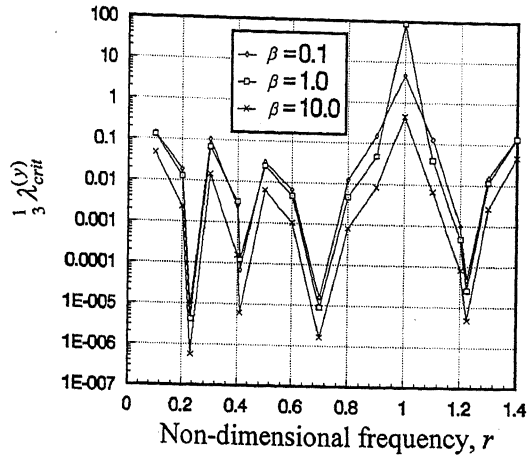

b) y-response

Figure 6.2 Variation of critical non-dimensional parameter, $\frac{1}{3}\lambda_{crit}$, with non-dimensional frequency, r, for two-degree-of-freedom system. $[\lambda_{xy}^{L} = \lambda_{yx}^{L} = 0.5]$

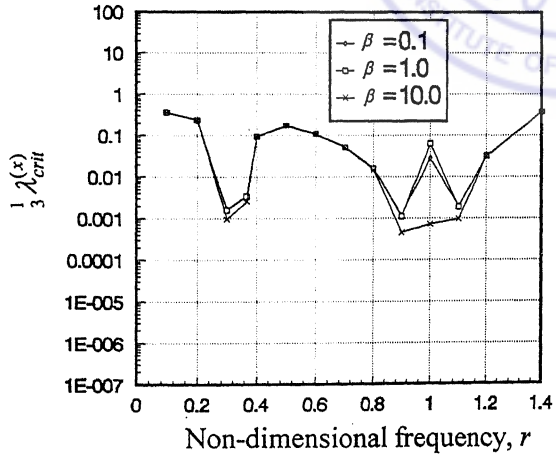

a) x-response

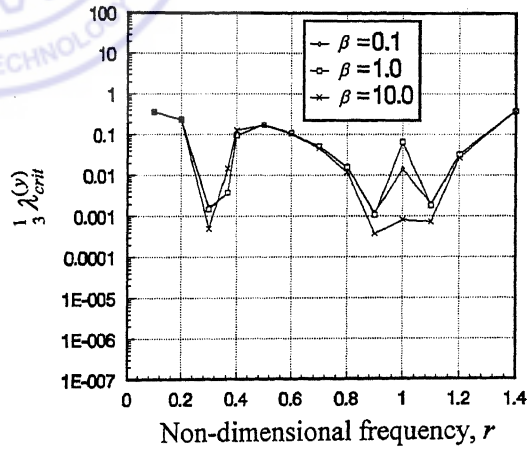

b) y-response

Figure 6.3 Variation of critical non-dimensional parameter, $\frac{1}{3}\lambda_{crit}$, with non-dimensional frequency, r, for two-degree-of-freedom system.

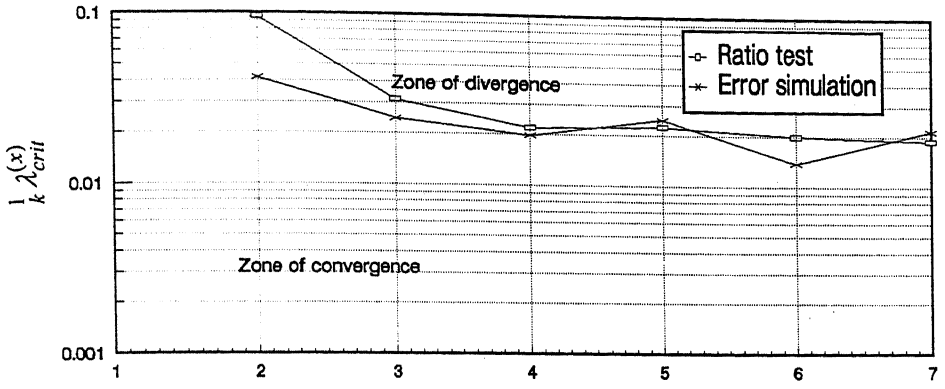

a) $\beta = 0.1$

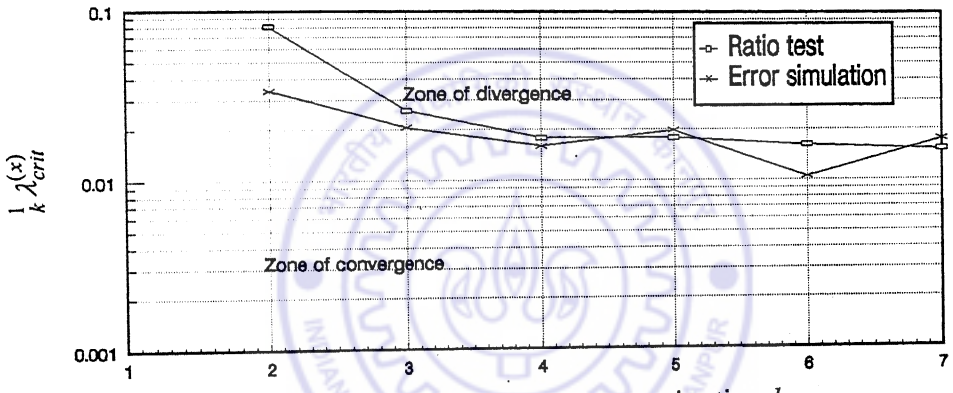

b) $\beta = 1.0$

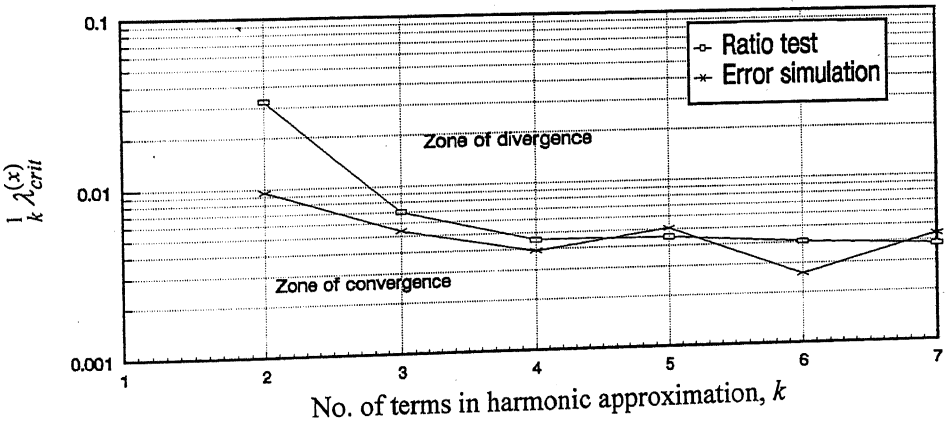

c) $\beta = 10.0$

Figure 6.4 Convergence-divergence zone of two-degree-of-freedom system

[x-response, $r = 0.5$, $\lambda_{xy}^{L} = \lambda_{yx}^{L} = 0.5$]

6.6 Selection of Excitation Level for First Harmonic Measurement

The convergence analysis presented above provides the basis for selection of the limiting number of series terms in the response harmonic approximation (6.60). Figures 6.5(a), (b) show the variation of approximation error for constant excitation amplitudes, for various number of series terms, over the frequency range, for $\lambda_{xy}^{L} = \lambda_{yx}^{L} = 0.5$. It can be seen from these figures that approximation errors are very high near the natural frequencies ($r = \omega / \sqrt{k_{xx} / m_x} = 0.71$ and 1.224) and at their sub-harmonics. This shows that the excitation levels should be reduced near natural frequencies of the system so as to keep the error in acceptable limits. Since, it is not possible to determine the excitation levels for uniform error, in absence of *a-priori* information about the unknown parameters, excitation level, alternatively, is selected by constant response amplitude criterion. Figure 6.6(a) shows a variation in the excitation force, in terms of non-dimensional parameter, λ_3, controlled for constant harmonic amplitude, $X(\omega)$. Approximation errors in the response harmonics, $X(\omega)$ and $Y(\omega)$ are plotted in Figures 6.6(b), (c) respectively. Errors are relatively high near the natural frequencies but they are much less compared to constant excitation level case (Figure 6.5).

6.7 Signal Strength and Measurability of Third Response Harmonic

Estimation of nonlinear parameters is done through the measurement of higher order harmonic amplitudes. However, these harmonic amplitudes are generally small in comparison to the fundamental harmonic amplitude. Non-dimensional response amplitude of general third order harmonics $X(\omega_1 + \omega_2 + \omega_3)$ and $Y(\omega_1 + \omega_2 + \omega_3)$ are plotted in Figures 6.7(a) and 6.8(a) respectively for ω_1 and ω_2 varying over a wide range with ω_3 kept constant at $0.1\sqrt{k_{xx} / m_x}$ (for case $\lambda_{xy}^{L} = \lambda_{yx}^{L} = 0.5$). These plots have been obtained through numerical simulation using, fourth order Runge-Kutta algorithm, with three-tone excitation of the nonlinear system under consideration. This numerical solution can be termed as *exact* response. Figures 6.9(a) and 6.10(a) show similar graphs

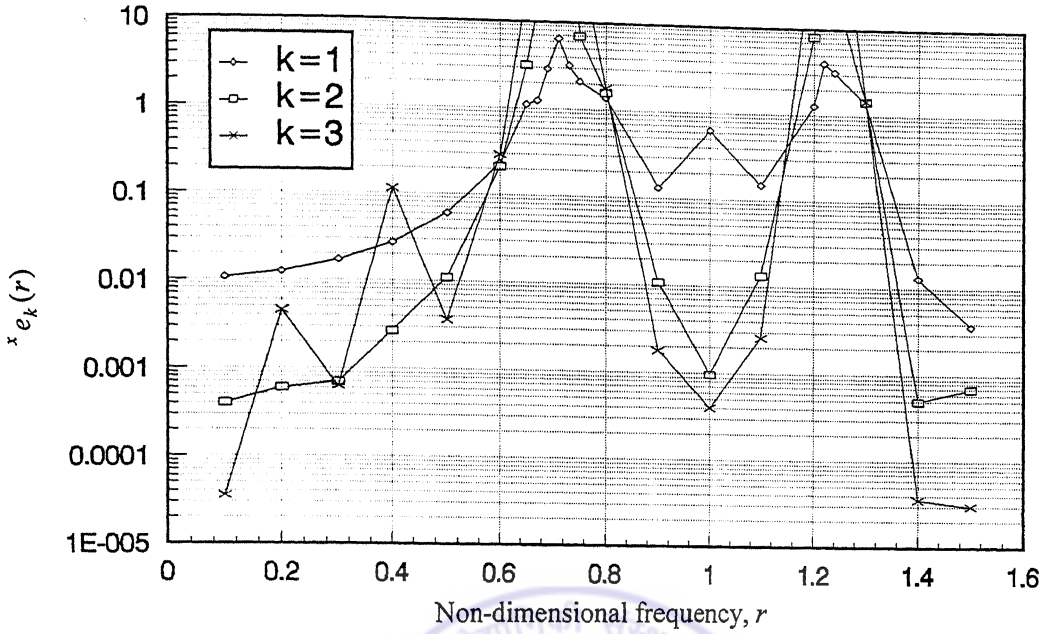

a) Error in $X(\omega)$

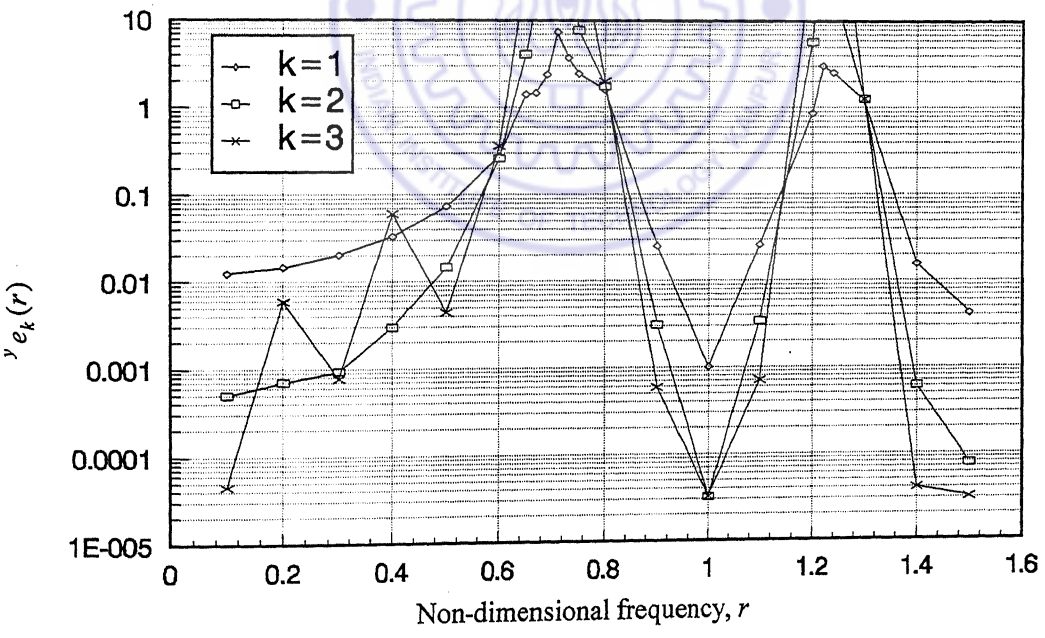

b) Error in $Y(\omega)$

Figure 6.5 Variation of series approximation error in response harmonics $X(\omega)$ and $Y(\omega)$. $[\lambda_{xy}^{N} = \lambda_{yx}^{N} = 0.005]$

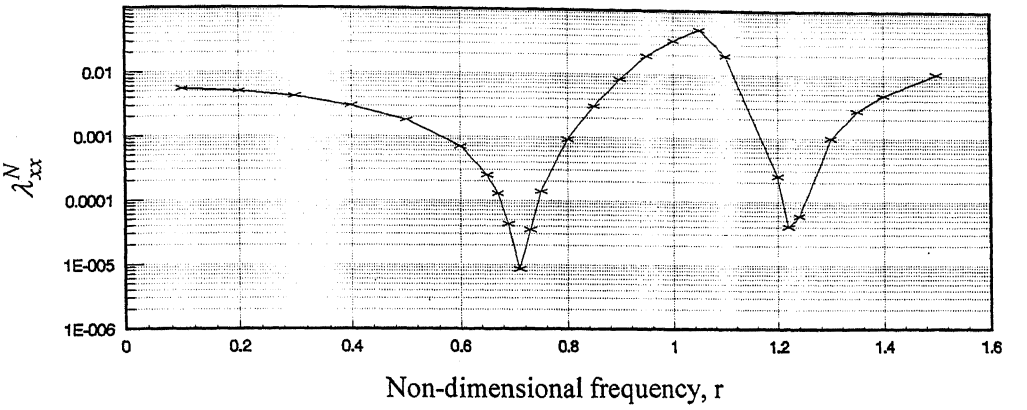

a) Variation in excitation level

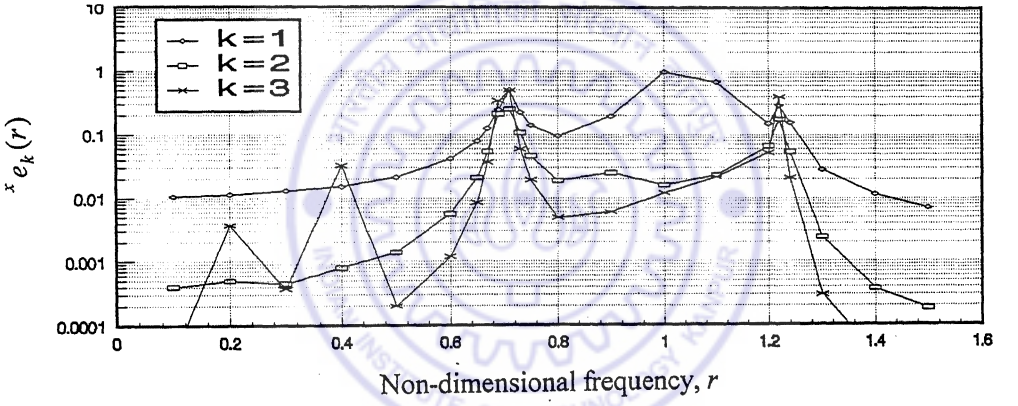

b) Error in $X(\omega)$

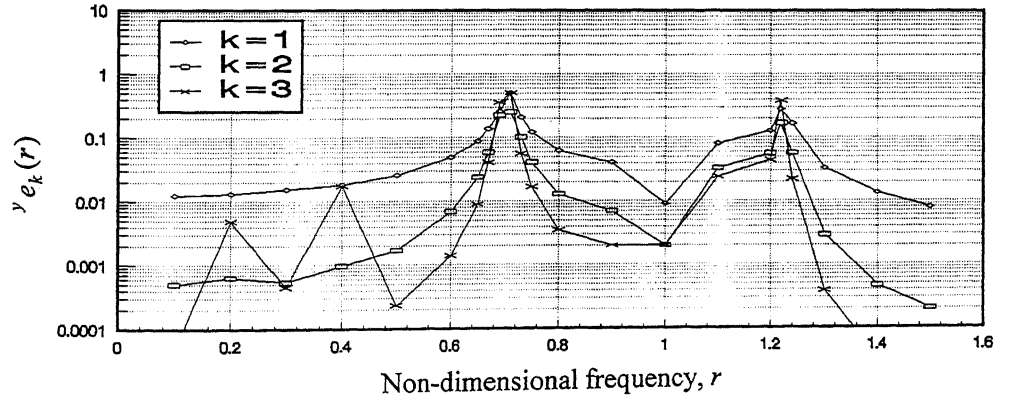

c) Error in $Y(\omega)$

Figure 6.6 Variation in series approximation error with excitation level selected for constant response harmonic amplitude

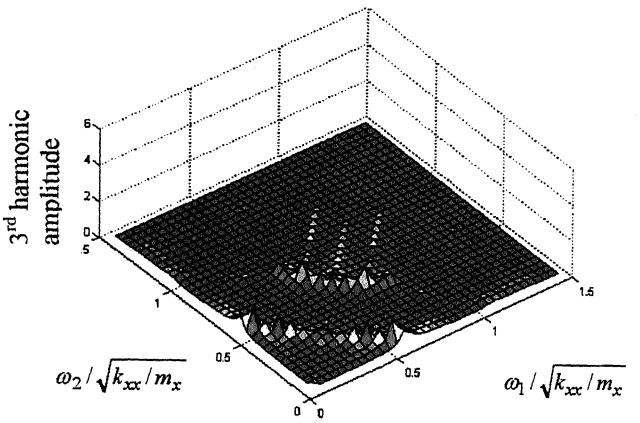

a) Third harmonic $X(\omega_1 + \omega_2 + \omega_3)$

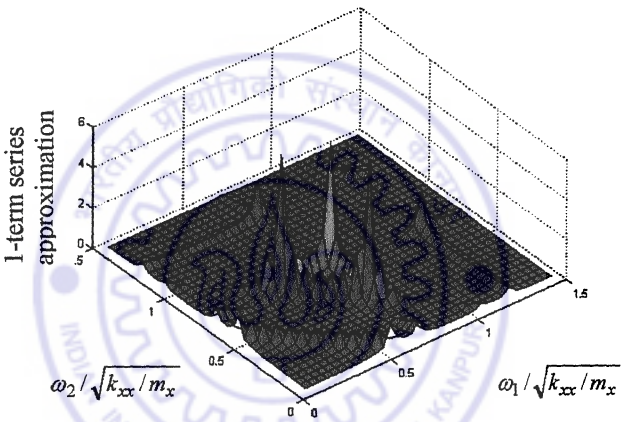

b) Single-term series approximation

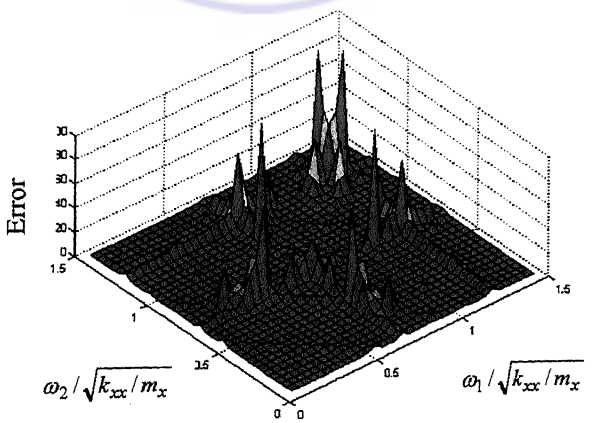

c) Error of approximation

Figure 6.7 Third harmonic amplitude, $X(\omega_1 + \omega_2 + \omega_3)$ and the error in single-term series approximation. $[\omega_3 = 0.1 \times \sqrt{k_{xx}/m_x}]$

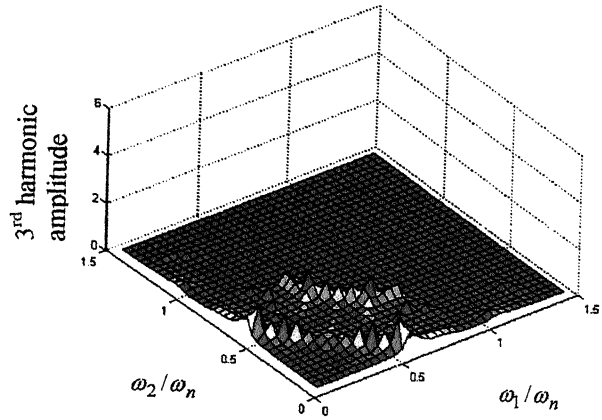

a) Third harmonic amplitude

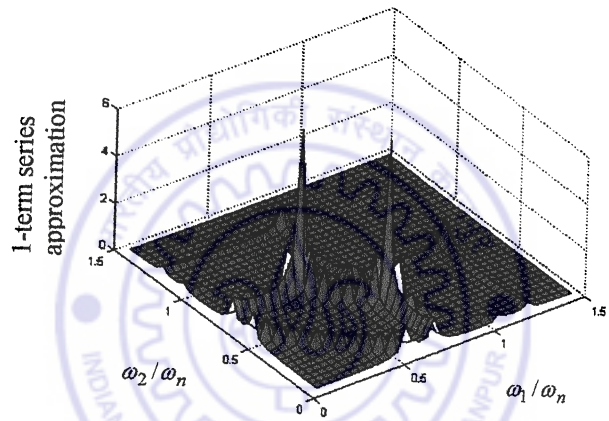

b) Single-term series approximation

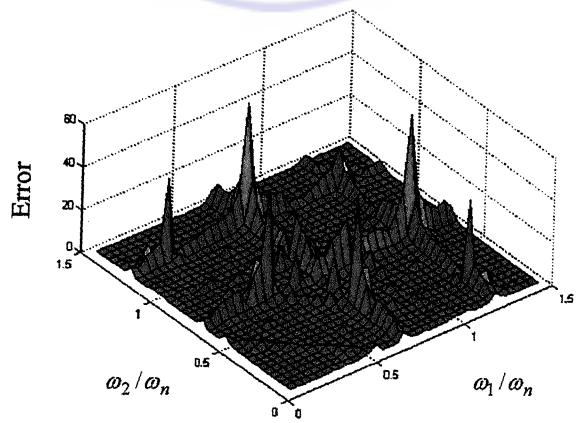

c) Error of approximation

Figure 6.8 Third harmonic amplitude, $Y(\omega_1+\omega_2+\omega_3)$ and the error in single-term series approximation. $[\omega_3 = 0.1\times\sqrt{k_{xx}/m_x}]$

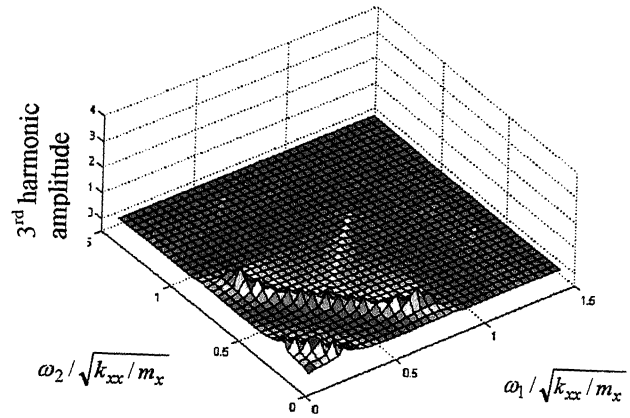

a) Third harmonic $X(\omega_1+\omega_2+\omega_3)$

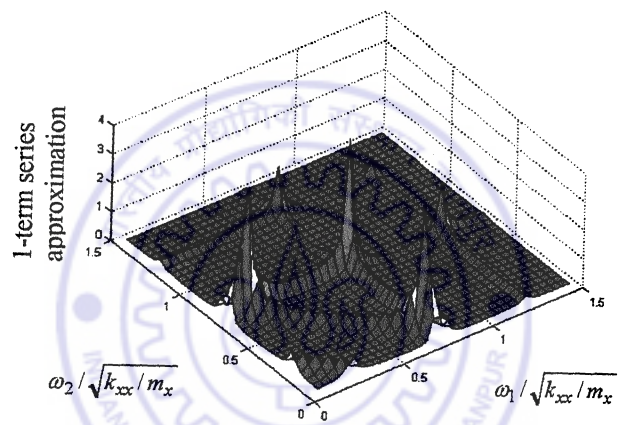

b) Single-term series approximation

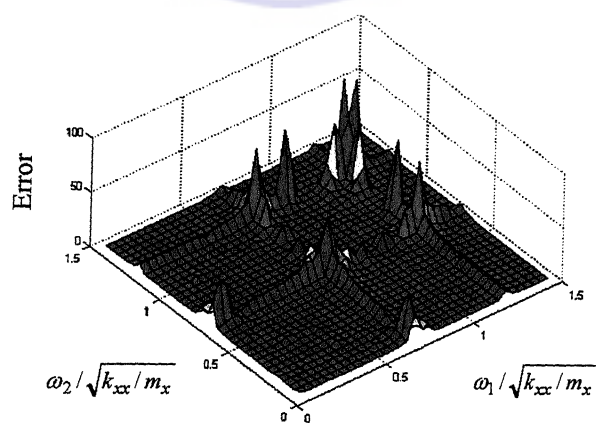

c) Error of approximation

Figure 6.9 Third harmonic amplitude, $X(\omega_1+\omega_2+\omega_3)$ and the error in single-term series approximation. $[\omega_3 = 0.4\times\sqrt{k_{xx}/m_x}]$

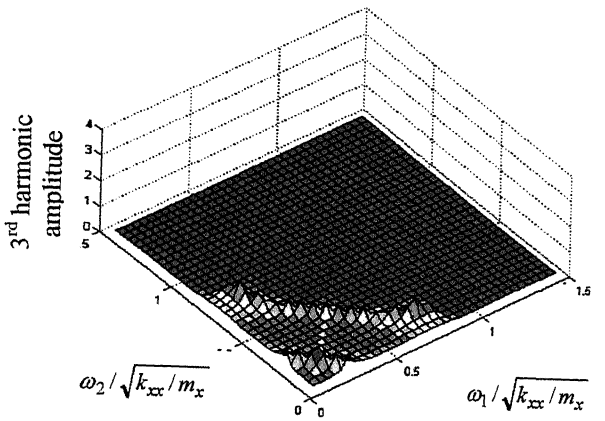

a) Third harmonic $Y(\omega_1+\omega_2+\omega_3)$

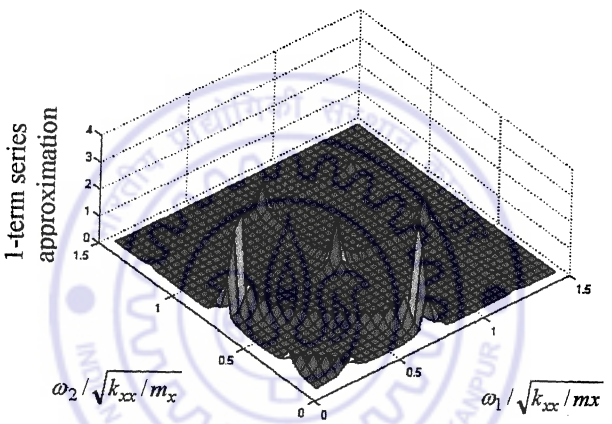

b) Single-term series approximation

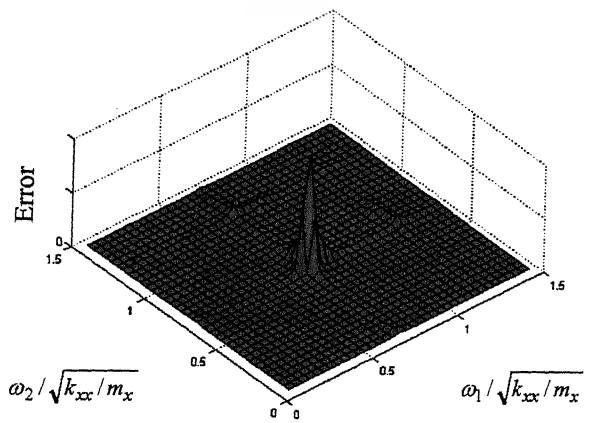

c) Error of approximation

Figure 6.10 Third harmonic amplitude, $Y(\omega_1+\omega_2+\omega_3)$ and the error in single-term series approximation. $[\omega_3 = 0.4\times\sqrt{k_{xx}/m_x}]$

for ω_3 kept constant at $0.4\sqrt{k_{xx}/m_x}$. From these figures it can be seen that the third harmonic amplitudes are significant or measurable only along the frequency combinations $\omega_1+\omega_2+\omega_3=\omega_{n_1}$ and $\omega_1+\omega_2+\omega_3=\omega_{n_2}$. It may be noted here that in this case, for $\lambda^L_{xy}=\lambda^L_{yx}=0.5$, $\omega_{n_1}=0.71\sqrt{k_{xx}/m_x}$ and $\omega_{n_2}=1.224\sqrt{k_{xx}/m_x}$.

Figures 6.7(b), 6.8(b), 6.9(b) and 6.10(b) show the Volterra series single-term approximation of the third harmonic amplitude series for respective cases. Errors between these approximations and the *exact* solutions of Figures 6.7(a), 6.8(a), 6.9(a) and 6.10(a) are plotted in Figures 6.7(c), 6.8(c), 6.9(c) and 6.10(c). The error is seen to be low along the frequency combination $\omega_1+\omega_2+\omega_3=\omega_{n_1}$ or ω_{n_2}.

These observations indicate that the third order response harmonics should be measured along the frequency combination line $\omega_1+\omega_2+\omega_3=\omega_{n_1}$ or ω_{n_2}. Similar to single-degree-of-freedom systems, a measurability index is defined here as the ratio of higher harmonic amplitudes to first harmonic amplitude. Figures 6.11(a),(b) show the variation in measurability over the frequency range for harmonics $X(3\omega)$ and $Y(3\omega)$, respectively. Measurability is maximum at $\omega_{n_1}/3=0.237\sqrt{k_{xx}/m_x}$. Figure 6.12(a) shows that a peak measurability of 10% can be achieved with excitation level corresponding to $\lambda^N_{xx}=\lambda^N_{yy}=0.0048$. Similarly for a peak measurability of 5% an excitation level corresponding to $\lambda^N_{xx}=\lambda^N_{yy}=0.0021$, is required. The corresponding errors in the approximation of third harmonic amplitude series are plotted in Figures 6.12 (b), (c) respectively. For 10% measurability the peak error is 30%, whereas for 5% measurability it is about 9%. These figures also show the errors as function of the number of terms included in the Volterra series approximation. Error decreases sharply slightly away from the one-third natural frequency value and it is therefore suggested to select a set of excitation frequencies in this vicinity.

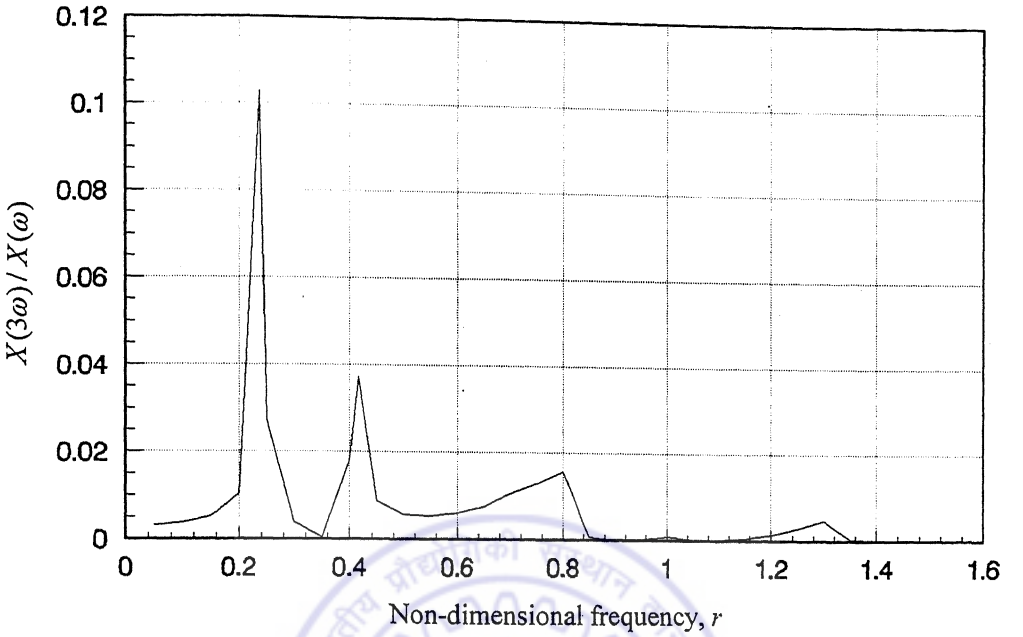

a) Response harmonic $X(3\omega)$

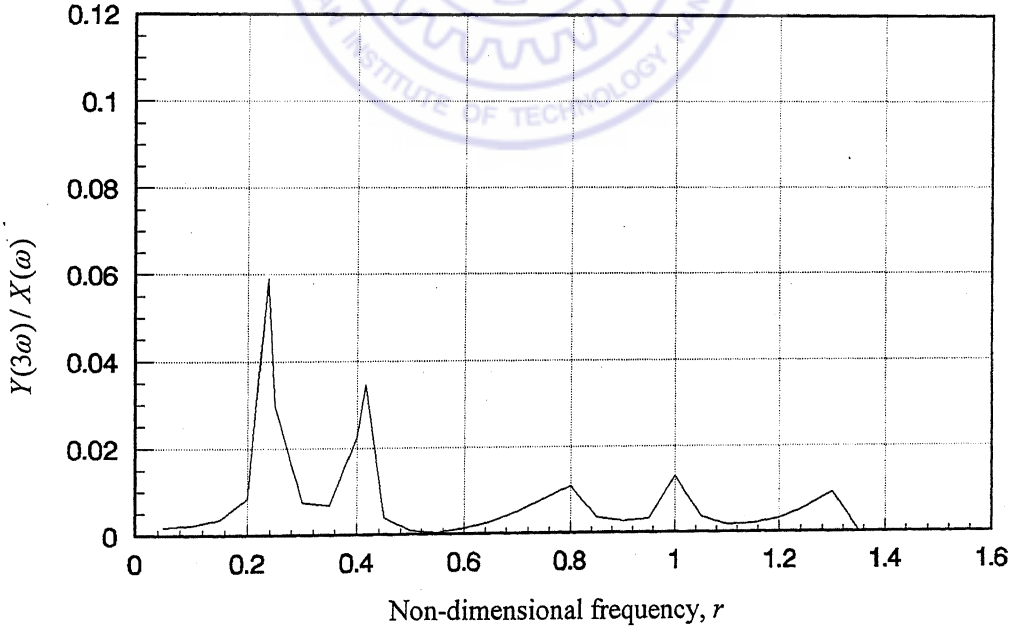

b) Response harmonic $Y(3\omega)$

Figure 6.11 Measurability of third response harmonics over the frequency range, with excitation level corresponding to $\lambda_{xx}^{N} = \lambda_{yy}^{N} = 0.005$

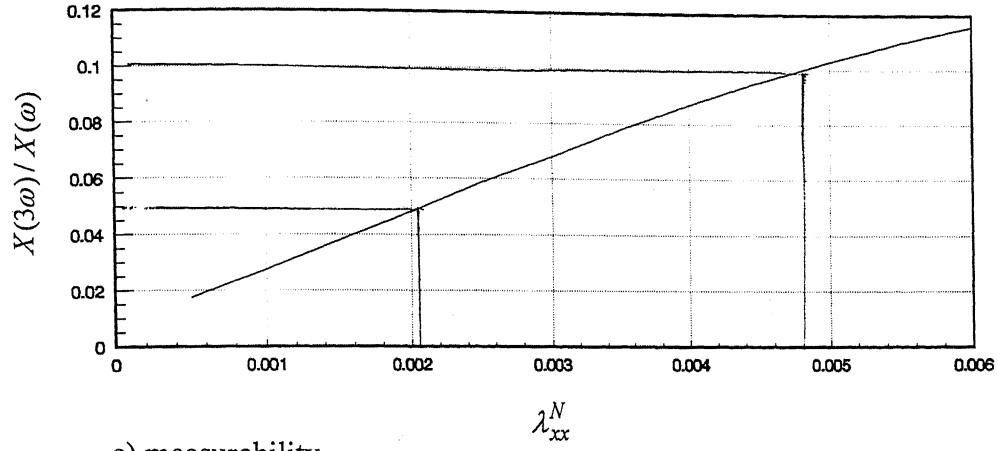

a) measurability

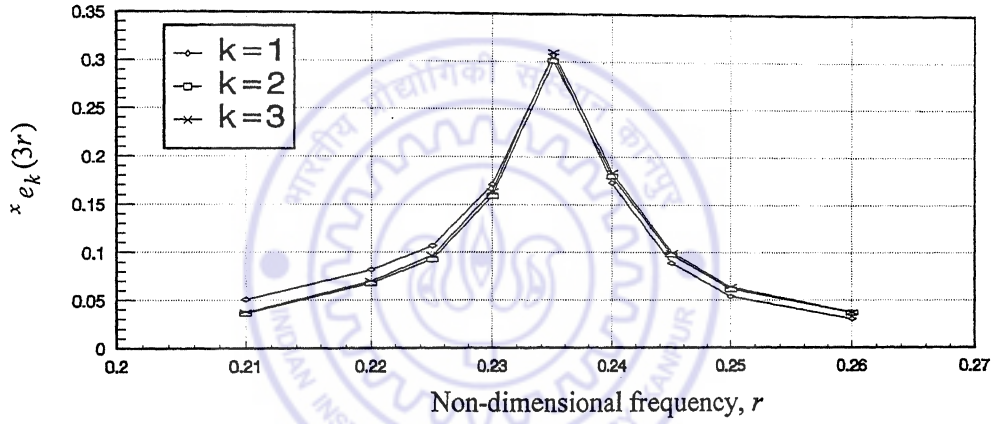

b) Error with 10% peak measurability

$\lambda_{xx}^N = \lambda_{yy}^N = 0.0048$

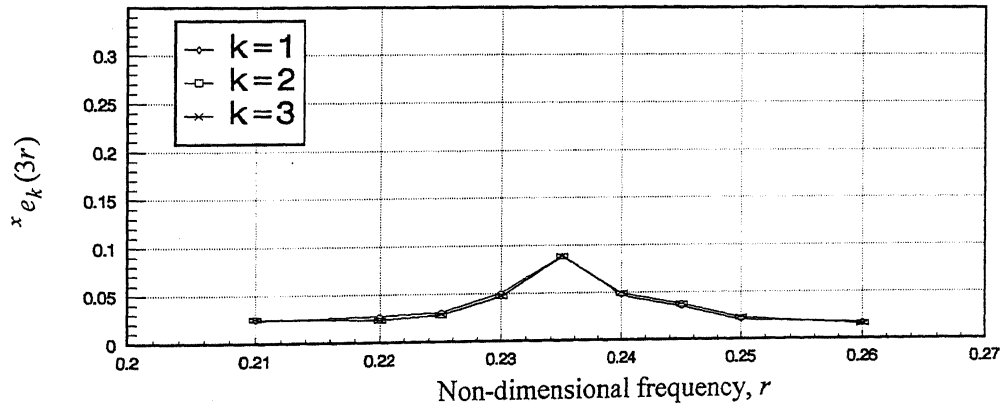

c) Error with 5% peak measurability

$\lambda_{xx}^N = \lambda_{yy}^N = 0.0021$

Figure 6.12 Peak measurability and series approximation error in $X(3\omega)$ around $\omega_{n_1}/3 = 0.237\sqrt{k_{xx}/m_x}$.

6.8 Illustration

Parameter estimation is illustrated for the following values of linear and nonlinear parameters in equation (6.54 a, b)

Linear parameters

$m_x = m_y = 1.0\,\text{kg}$

$k_{xx} = k_{yy} = 1.0\times10^7\ \text{N/m}$

$\zeta_{xx} = \zeta_{yy} = 0.01$

$k_{xy} = k_{yx} = 0.5\times10^7\ \text{N/m}$

Nonlinear parameters

- Case 1:
  $k_{3x}^{(xxx)} = k_{3y}^{(yyy)} = 1.0\times10^{19}\ \text{N/m}$
- Case 2:
  $k_{3x}^{(xxx)} = 1.0\times10^{19}\ \text{N/m}$ and $k_{3y}^{(yyy)} = 1.0\times10^{18}\ \text{N/m}$ $\quad (\beta = k_{3y}^{(yyy)} / k_{3x}^{(xxx)} = 0.1)$

Responses $x(t)$ and $y(t)$ are obtained from integration of equations of motion (6.54a,b) by Runge-Kutta algorithm and response is processed in accordance with the suggested procedure to estimate values of the linear and nonlinear parameters. For computational ease the cross-coupled nonlinear parameters $k_{3x}^{(yyy)}$ and $k_{3y}^{(xxx)}$ are taken as zero. Case 1 represents identical nonlinear stiffness coefficients in both x and y directions, whereas Case 2 represents asymmetrical nonlinearity in x and y directions. Single-point excitation – one at a time - at a time, first in the x-direction and then in y-direction, is employed.

Case 1:

The natural frequencies of the two-degree-freedom system under consideration are found to be $0.7\sqrt{k_{xx}/m_x}$ and $1.224\sqrt{k_{xx}/m_x}$. Frequency range, from $\omega = 0.1\sqrt{k_{xx}/m_x}$ to $\omega = 1.5\sqrt{k_{xx}/m_x}$, is selected for excitation to include both the natural frequencies. The amplitude of the harmonic excitation is varied over the frequency range so as to get a nearly constant response amplitude, throughout the frequency range (a constant

amplitude, $X(\omega) = 1.0 \times 10^{-7}$ m, is selected in the present case). The required variation in excitation amplitude is plotted in Figure 6.13(a), while the corresponding response levels $X(\omega)$ and $Y(\omega)$ are plotted in Figures 6.13 (b), (c). The preliminary estimates of the first order kernel transforms are obtained using equation (6.47). Excitation force is applied in the x-direction and kernel transforms $H_1^{(x:x)}(\omega)$ and $H_1^{(y:x)}(\omega)$ are estimated. Excitation force is applied next, in the y - direction, and kernel transforms $H_1^{(x:y)}(\omega)$ and $H_1^{(y:y)}(\omega)$ are estimated. Figures 6.14(a)-(d) show the estimated first order kernel transforms, $H_1^{(x:x)}(\omega), H_1^{(y:x)}(\omega), H_1^{(x:y)}(\omega)$ and $H_1^{(y:y)}(\omega)$. Due to symmetry in the numerical values of the parameters in this case, direct kernel transforms $H_1^{(x:x)}(\omega), H_1^{(y:y)}(\omega)$ are identical to each other. Similarly cross-kernel transforms $H_1^{(y:x)}(\omega), H_1^{(x:y)}(\omega)$ are mutually identical. Standard curve fitting procedure is applied to these kernels, in accordance with equation (3.18a) to obtain the following preliminary estimates of the linear parameters.

$k_{xx} = k_{yy} = 1.0042 \times 10^7$ N/m $\qquad$ $k_{xy} = k_{yx} = 0.4960 \times 10^7$ N/m

$m_x = m_y = 0.9549$ kg $\qquad$ $\zeta_{xx} = \zeta_{yy} = 0.00883$

For 5% peak measurability of the third order harmonics, the excitation level is found to be 0.4582 N. Third order response harmonic amplitudes $X(3\omega)$ and $Y(3\omega)$ are obtained from the responses with excitation level set at above value for a set of four excitation frequencies, $\omega / \sqrt{k_{xx} / m_x} = 0.21, 0.22, 0.25$ and 0.26. These excitation frequencies are selected close to the one-third natural frequency value, $\omega_{n_1} / 3 = 0.237\sqrt{k_{xx} / m_x}$. The response spectra of overall responses $x(t)$ and $y(t)$ for these excitation frequencies are shown in Figures 6.15 and 6.16 respectively. Employing equation (6.51) and using the third order harmonic amplitudes, preliminary estimates of the nonlinear parameters is obtained as

$k_{3x}^{(xxx)} = k_{3y}^{(yyy)} = 0.8450 \times 10^{19}$ N/m

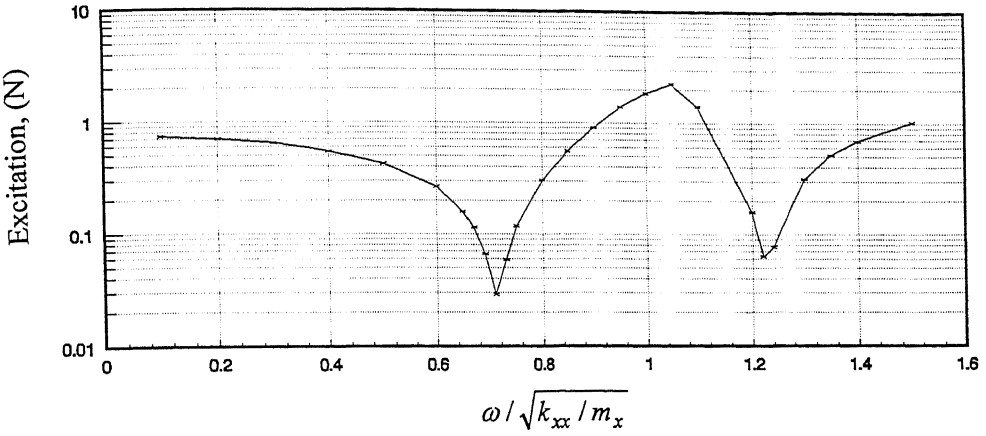

a) Variation in excitation level

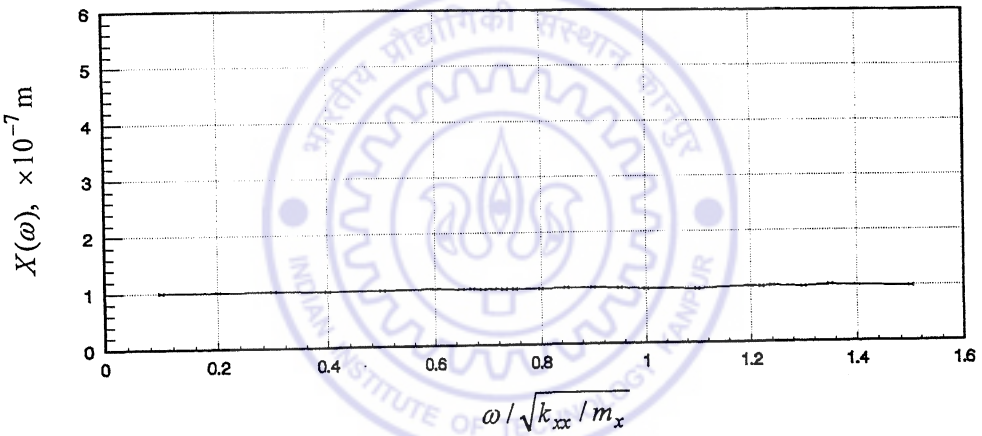

b) Harmonic amplitude, $X(\omega)$

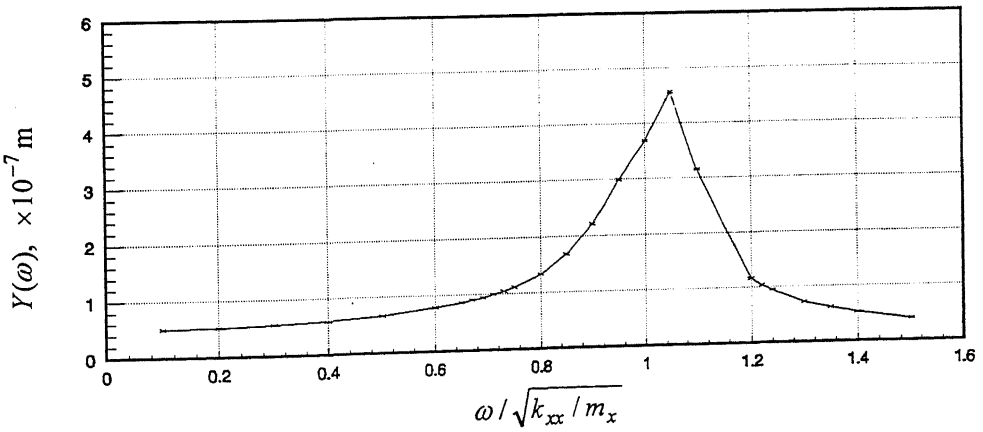

c) Harmonic amplitude, $Y(\omega)$

Figure 6.13 Variation in excitation level for constant harmonic amplitude, $X(\omega)$, and corresponding response harmonic amplitudes.

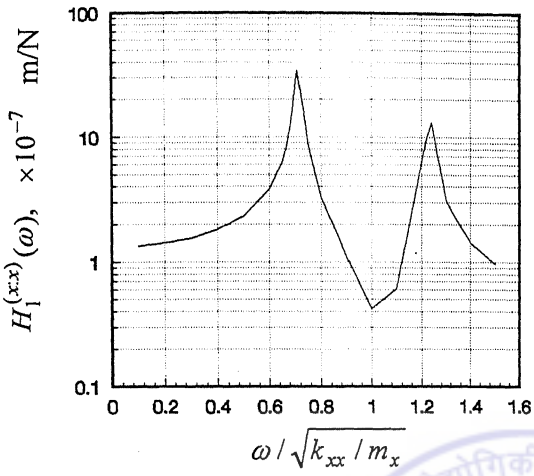

a) Kernel transform, $H_1^{(x:x)}(\omega)$

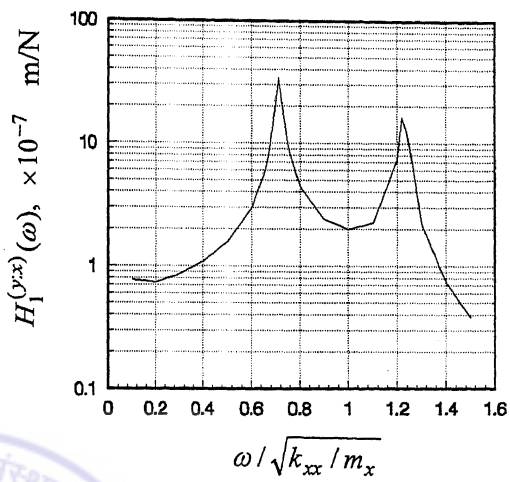

b) Kernel transform, $H_1^{(y:x)}(\omega)$

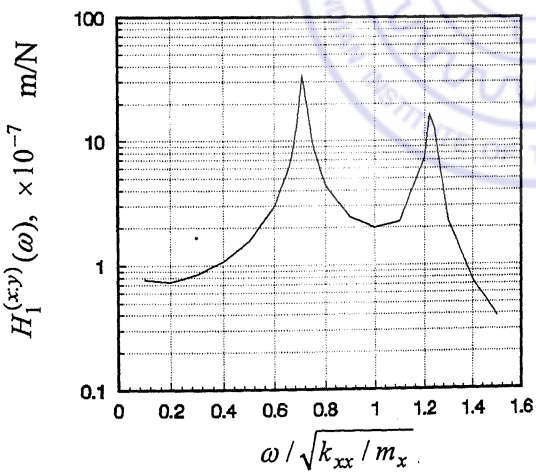

c) Kernel transform, $H_1^{(x:y)}(\omega)$

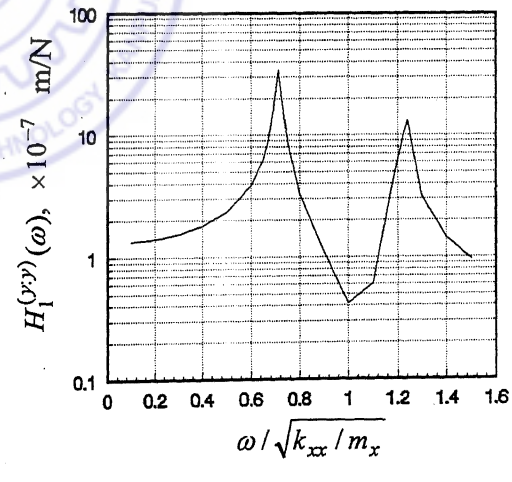

d) Kernel transform, $H_1^{(y:y)}(\omega)$

Figure 6.14 Preliminary estimates of first order kernel transforms. [Case:1]

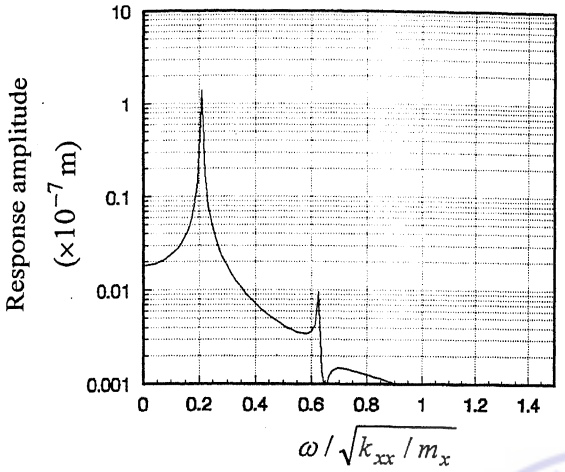

a) $\omega = 0.21\sqrt{k_{xx} / m_x}$

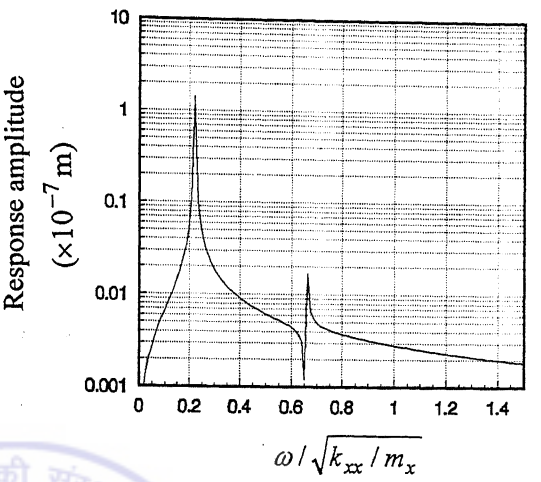

b) $\omega = 0.22\sqrt{k_{xx} / m_x}$

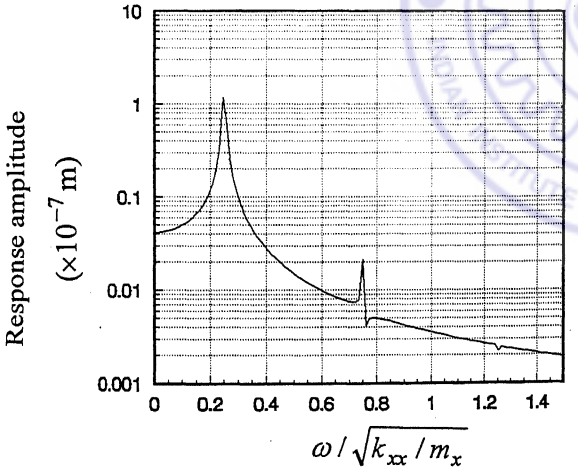

c) $\omega = 0.25\sqrt{k_{xx} / m_x}$

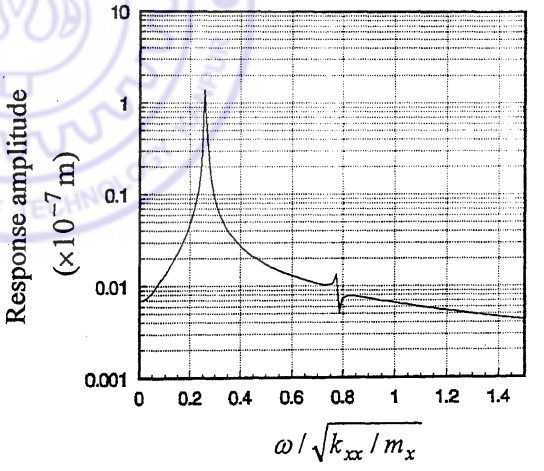

d) $\omega = 0.26\sqrt{k_{xx} / m_x}$

Figure 6.15 Response spectrum of x-response. [Case:1, 5% measurability]

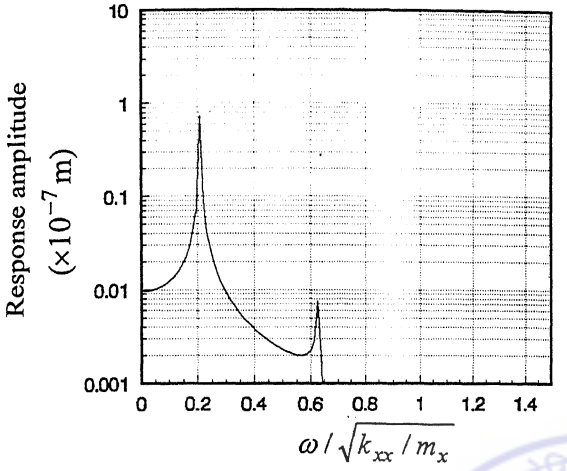

a) $\omega = 0.21\sqrt{k_{xx} / m_x}$

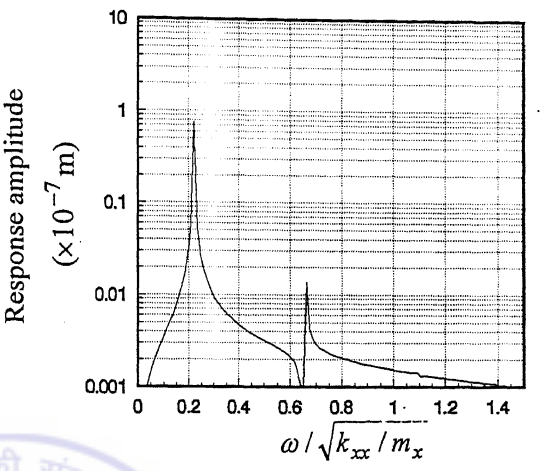

b) $\omega = 0.22\sqrt{k_{xx} / m_x}$

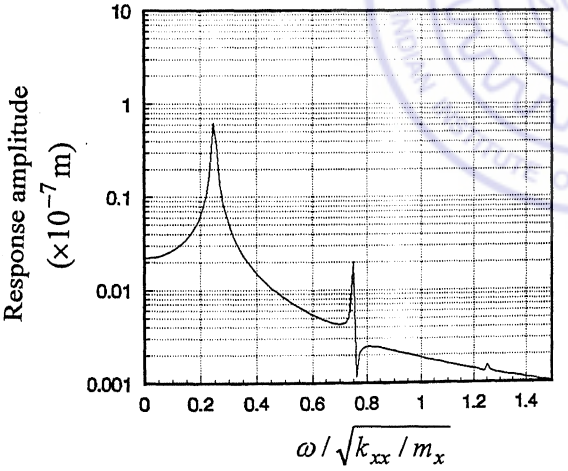

c) $\omega = 0.25\sqrt{k_{xx} / m_x}$

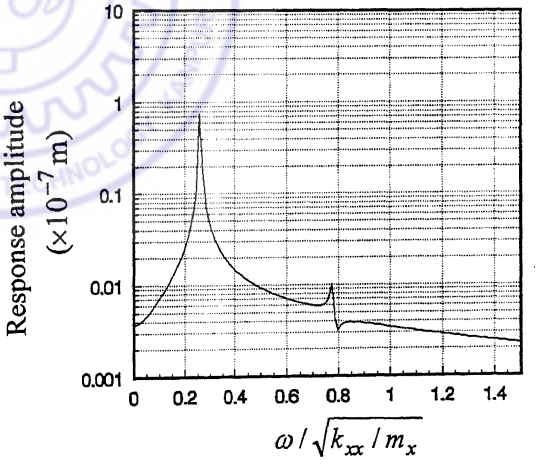

d) $\omega = 0.26\sqrt{k_{xx} / m_x}$

Figure 6.16 Response spectrum of y-response. [Case:1, 5% measurability]

The recursive iteration algorithm, for refinement of the estimates, includes appropriate number of higher order series terms in the equations (6.47,6.51), to give a convergent Volterra series solution. Iterations are continued till the estimated nonlinear parameters converge within a variation range of 0.1%. Figure 6.17(a) shows the convergence of iterative estimates of the nonlinear parameter, $k_{3x}^{(xxx)}$ with successive iterations (it is same for the other nonlinear parameter, $k_{3y}^{(yyy)}$). Corresponding error of estimation is plotted in Figure 6.17(b). A significant improvement in estimates is obtained through iteration giving error reduction from 15% to 0.29%. Figure 6.18 shows the final estimates of the kernel transforms. The final estimates of nonlinear parameters are

$$k_{3x}^{(xxx)} = k_{3y}^{(yyy)} = 0.9971 \times 10^{19} \text{ N/m}$$

Final estimates of linear parameters are

$$k_{xx} = k_{yy} = 0.9998 \times 10^{7} \text{ N/m} \qquad k_{xy} = k_{yx} = 0.5088 \times 10^{7} \text{ N/m}$$

$$m_x = m_y = 0.9994 \text{ kg} \qquad \zeta_{xx} = \zeta_{yy} = 0.01005$$

A significant feature of the recursive iteration procedure is the major improvement obtained in the damping estimates. The preliminary estimate was $\zeta_{xx} = \zeta_{yy} = 0.00883$, with an error of 11.7%. The final estimate is $\zeta_{xx} = \zeta_{yy} = 0.01005$, where the error has reduced to 0.05%

Similar exercise is carried out for 10% peak measurability, which is obtained at an excitation amplitude of 0.693 N. Figures (6.19) and (6.20) show the response spectra in x and y directions for the set of excitation frequencies $\omega / \sqrt{k_{xx} / m_x} = 0.21, 0.22, 0.25$ and 0.26. The convergence pattern for the estimates of nonlinear parameters and the corresponding error are shown in Figure 6.21 (a), (b). Final estimate of first order kernel transforms are shown in Figure 6.22. The estimated values are

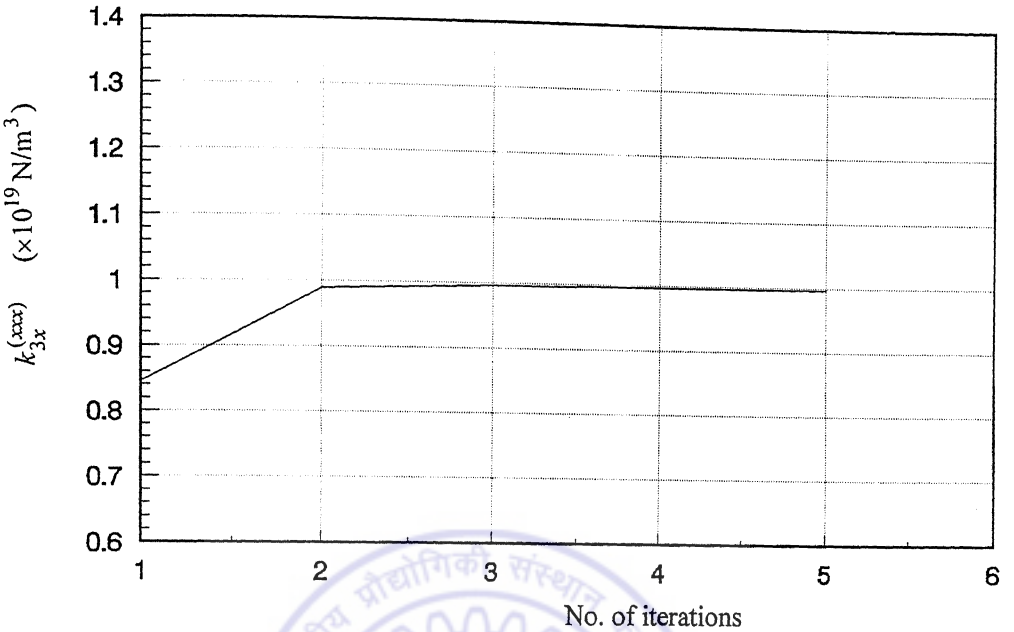

Figure 6.17(a) Iterative estimates of nonlinear parameters. [Case:1, 5%measurability]

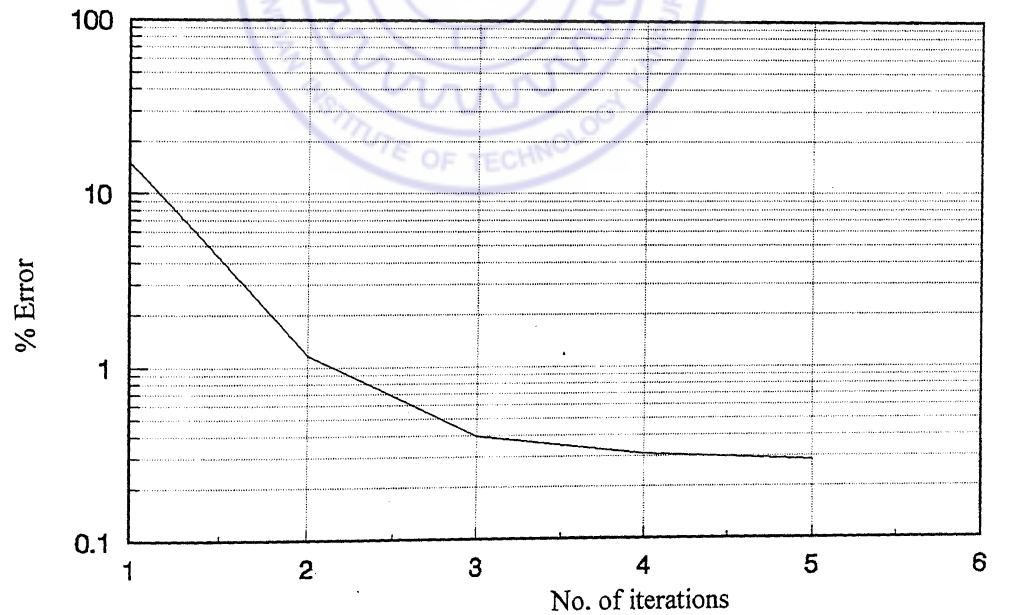

Figure 6.17(b) Convergence of estimation error with iterations. [Case:1, 5%measurability]

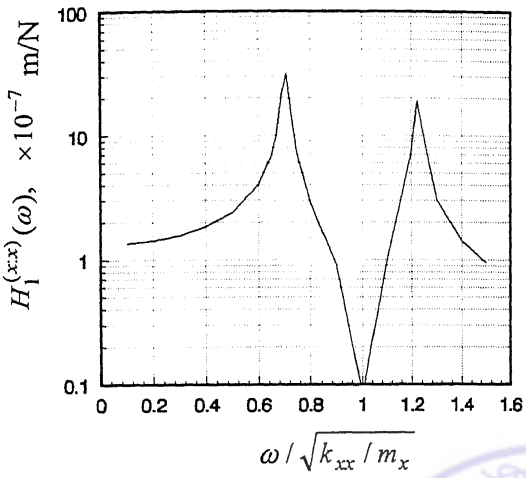

a) Kernel transform, $H_1^{(x:x)}(\omega)$

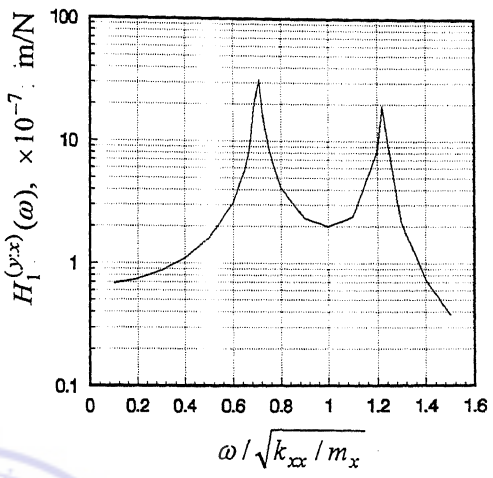

b) Kernel transform, $H_1^{(y:x)}(\omega)$

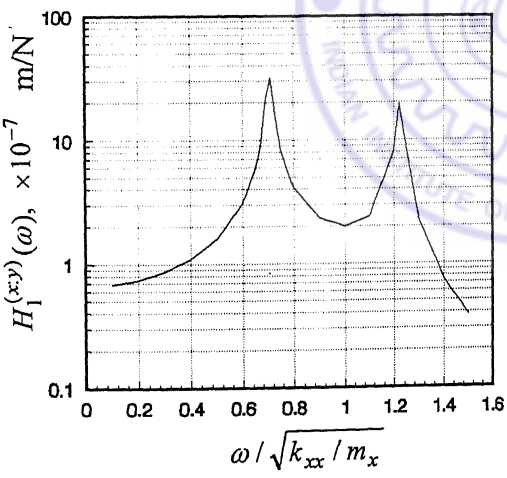

c) Kernel transform, $H_1^{(x:y)}(\omega)$

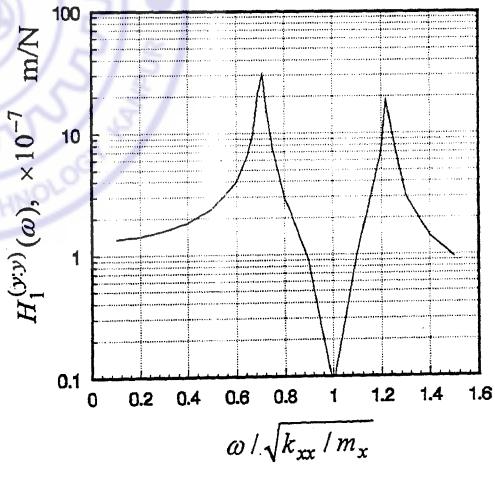

d) Kernel transform, $H_1^{(y:y)}(\omega)$

Figure 6.18 Final estimates of first order kernel transforms. [Case:1, 5%measurability]

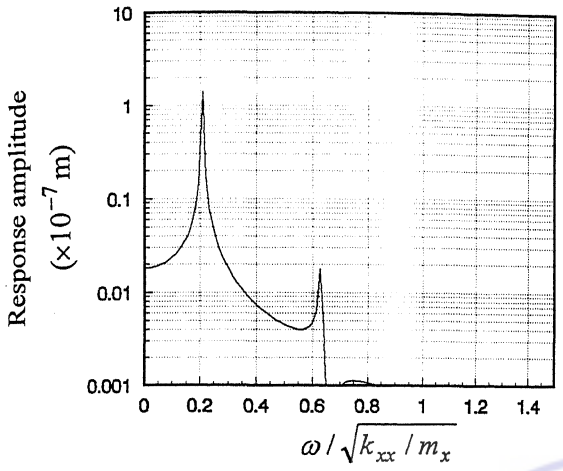

a) $\omega = 0.21\sqrt{k_{xx}/m_x}$

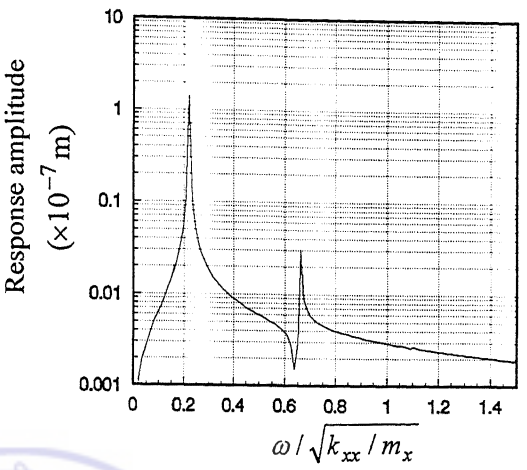

b) $\omega = 0.22\sqrt{k_{xx}/m_x}$

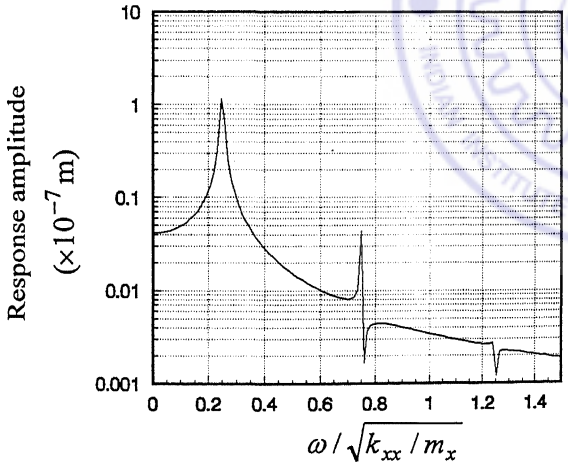

c) $\omega = 0.25\sqrt{k_{xx}/m_x}$

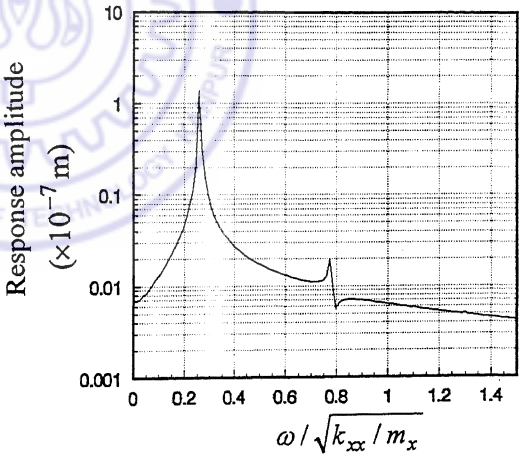

d) $\omega = 0.26\sqrt{k_{xx}/m_x}$

Figure 6.19 Response spectrum of x-response. [Case:1, 10% measurability]

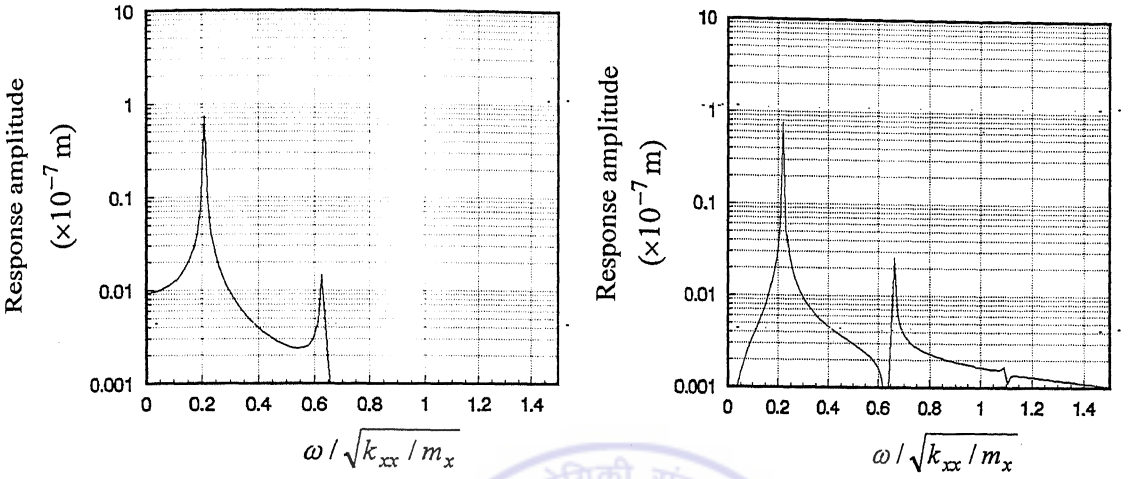

a) $\omega = 0.21\sqrt{k_{xx}/m_x}$

b) $\omega = 0.22\sqrt{k_{xx}/m_x}$

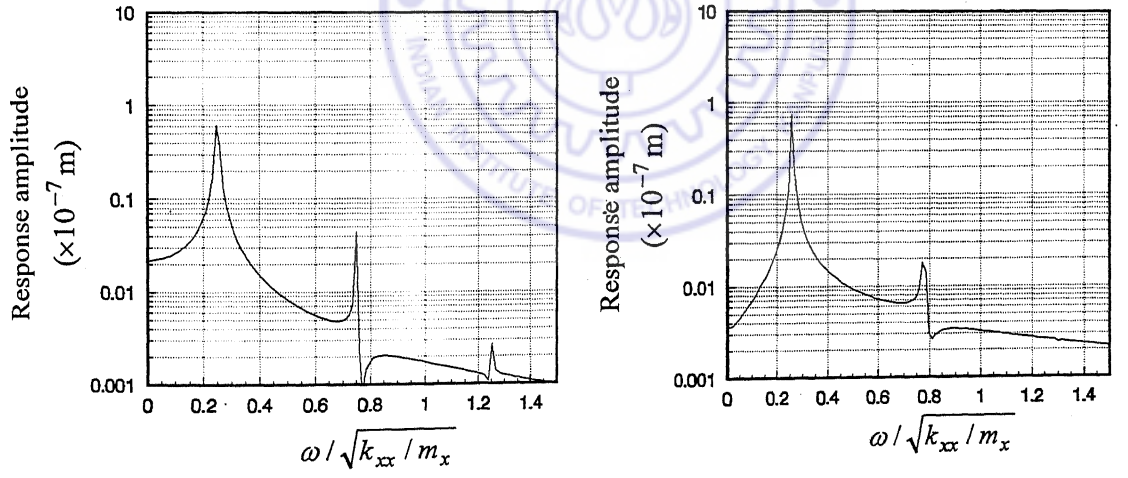

c) $\omega = 0.25\sqrt{k_{xx}/m_x}$

d) $\omega = 0.26\sqrt{k_{xx}/m_x}$

Figure 6.20 Response spectrum of y-response. [Case:1, 10% measurability]

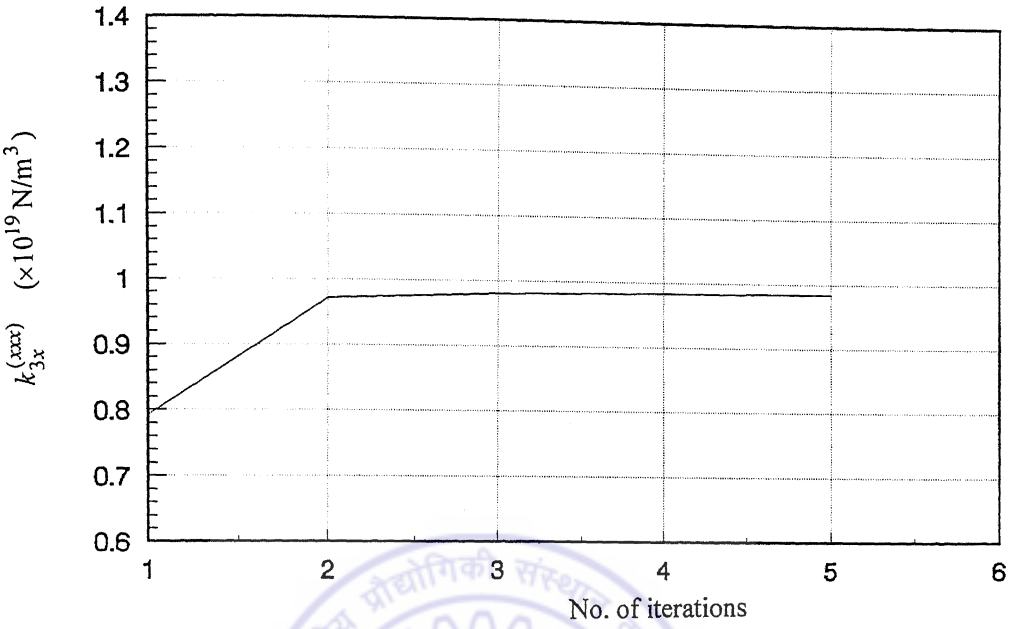

Figure 6.21(a) Iterative estimates of nonlinear parameters. [Case:1, 10%measurability]

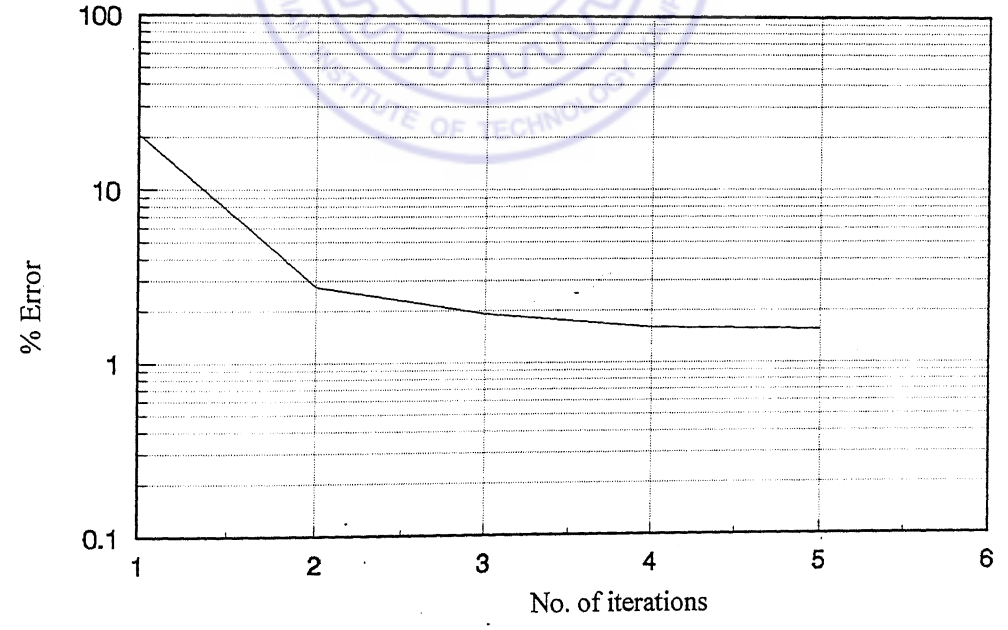

Figure 6.21(b) Convergence of estimation error with iterations. [Case:1, 10%measurability]

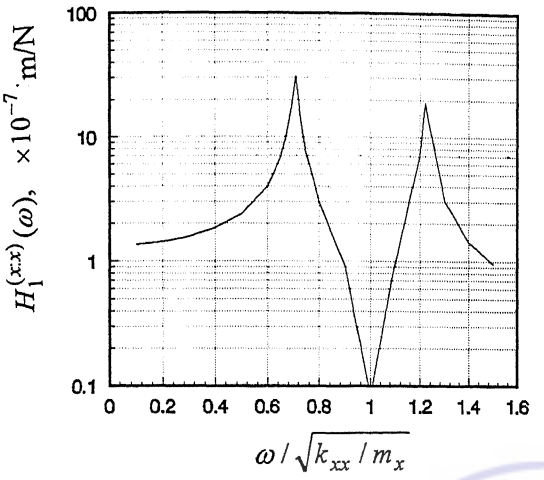

a) Kernel transform, $H_1^{(x:x)}(\omega)$

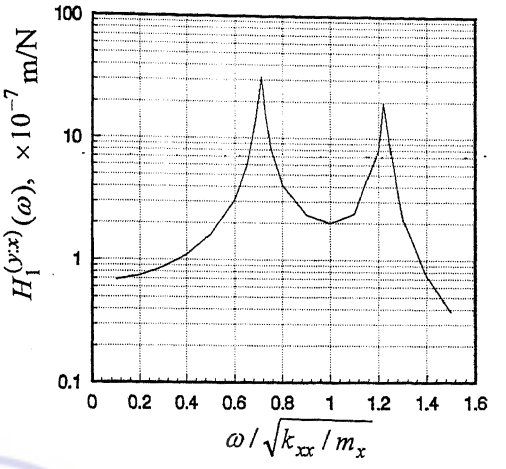

b) Kernel transform, $H_1^{(y:x)}(\omega)$

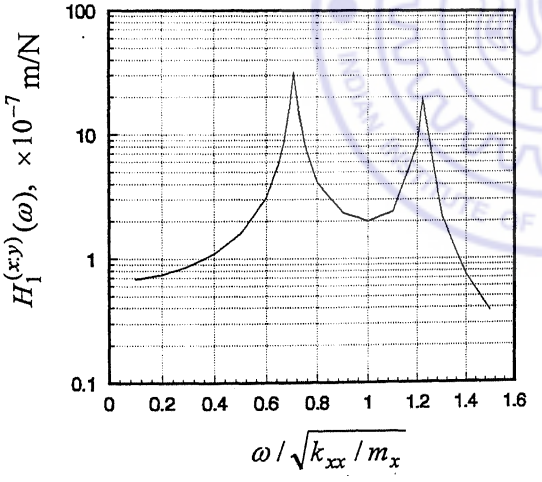

c) Kernel transform, $H_1^{(x:y)}(\omega)$

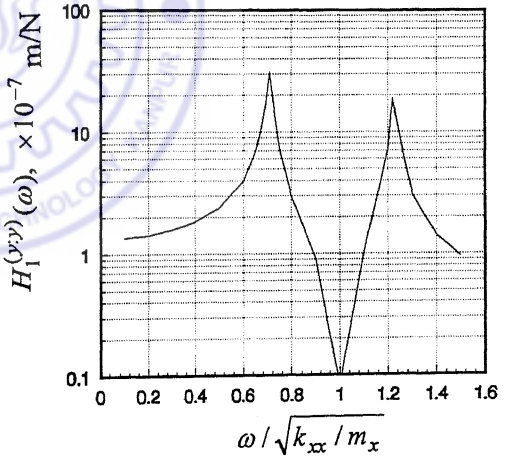

d) Kernel transform, $H_1^{(y:y)}(\omega)$

Figure 6.22 Final estimates of first order kernel transforms. [Case:1, 10% measurability]

$k_{3x}^{(xxx)} = k_{3y}^{(yyy)} = 0.9858 \times 10^{19}$ N/m

$k_{xx} = k_{yy} = 1.0010 \times 10^{7}$ N/m $\qquad$ $k_{xy} = k_{yx} = 0.5089 \times 10^{7}$ N/m

$m_x = m_y = 0.9996$ kg $\qquad$ $\zeta_{xx} = \zeta_{yy} = 0.01002$

A comparison of the above results with those obtained for the earlier case of 5% measurability reveals no significant change in the linear estimates. However, the demand for higher measurability results in higher error in estimates of nonlinear parameters (1.42% in the case of 10% measurability; 0.29% in case of 5% measurability; Figures 6.23a, b).

Case 2:

In this case nonlinear stiffness along y-direction is taken 0.1 times that along x-direction. This represents an asymmetric stiffness model. The simulation is carried out with same set of excitation levels as in Case 1, corresponding to 10% peak measurability. The estimated first order kernel transforms are shown in Figures 6.24. Final estimates of linear parameters are

$m_x = 0.9900$ kg $\qquad$ $m_y = 1.0254$ kg

$k_{xx} = 0.9828 \times 10^{7}$ N/m $\qquad$ $k_{xy} = 0.4997 \times 10^{7}$ N/m

$k_{yy} = 1.0277 \times 10^{7}$ N/m $\qquad$ $k_{yx} = 0.4998 \times 10^{7}$ N/m

$\zeta_{xx} = 0.00993$ $\qquad$ $\zeta_{yy} = 0.009927$

The convergence pattern of estimates of the nonlinear parameters during recursive iteration, along with the associated error, is shown in Figures 6.25(a), (b). Final estimates of nonlinear parameters are

$k_{3x}^{(xxx)} = 0.9948 \times 10^{19}$ N/m^3 $\qquad$ $k_{3y}^{(yyy)} = 1.0055 \times 10^{18}$ N/m^3

Final estimation errors are 0.52% and 0.58% respectively for the nonlinear parameters. It is found that in this case faster convergence is achieved than in Case 1.

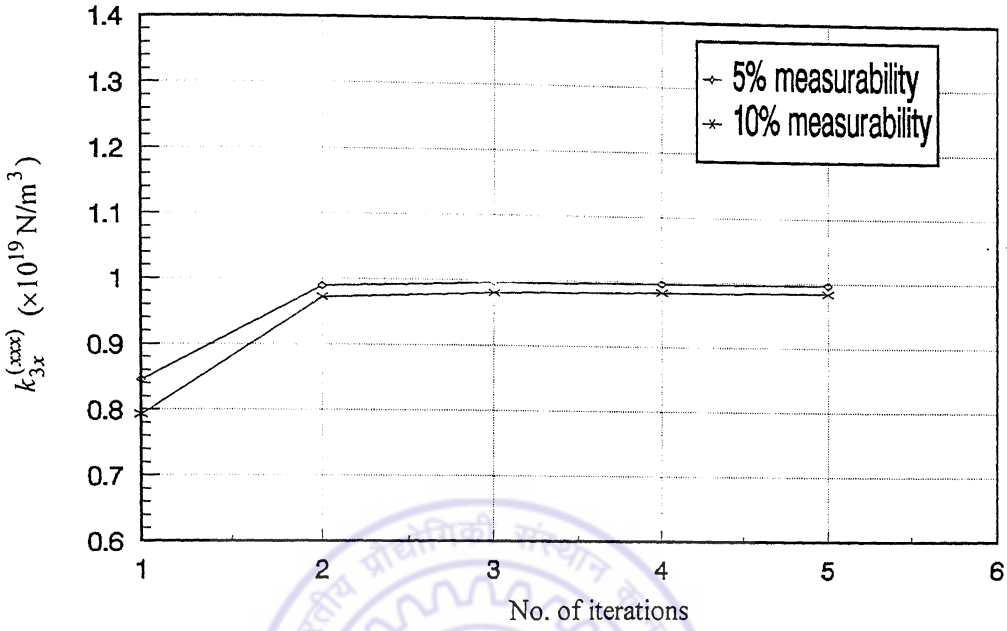

Figure 6.23(a) Comparison in estimation of nonlinear parameters, between 5% measurability and 10% measurability cases. [Case:1]

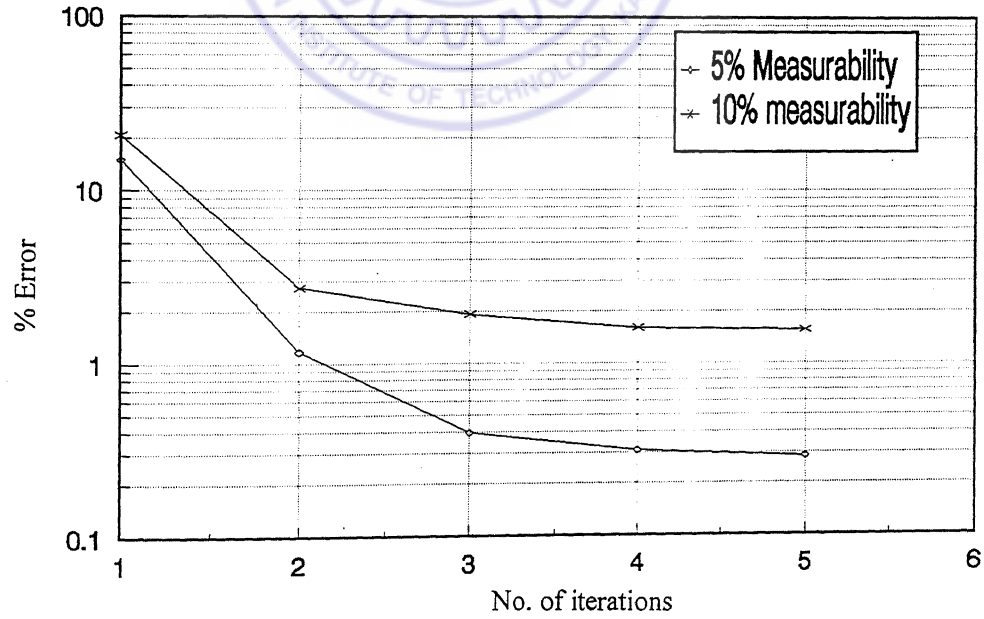

Figure 6.23(b) Comparison of estimation error between 5% measurability and 10% measurability Cases. [Case:1]

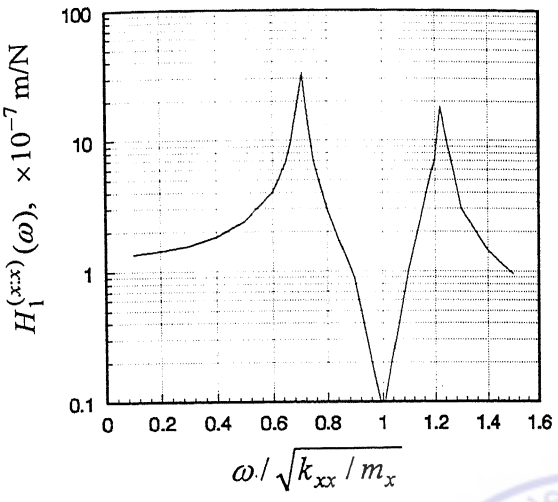

a) Kernel transform $H_1^{(x:x)}(\omega)$

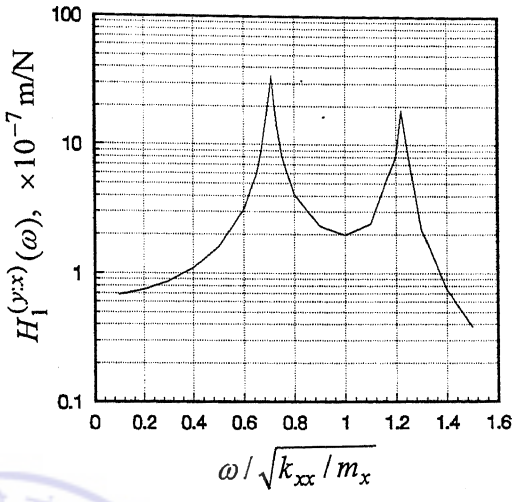

b) Kernel transform $H_1^{(y:x)}(\omega)$

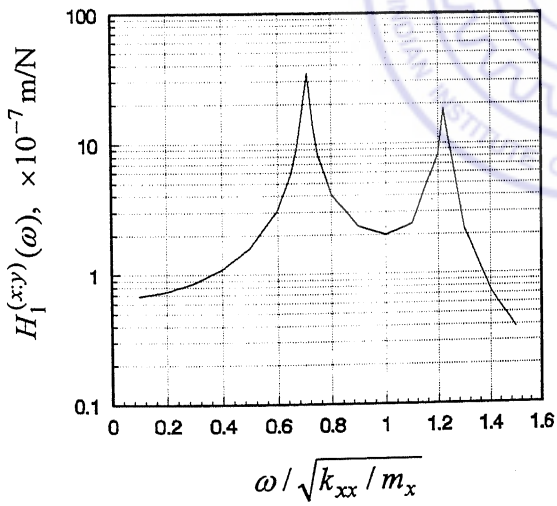

c) Kernel transform $H_1^{(x:y)}(\omega)$

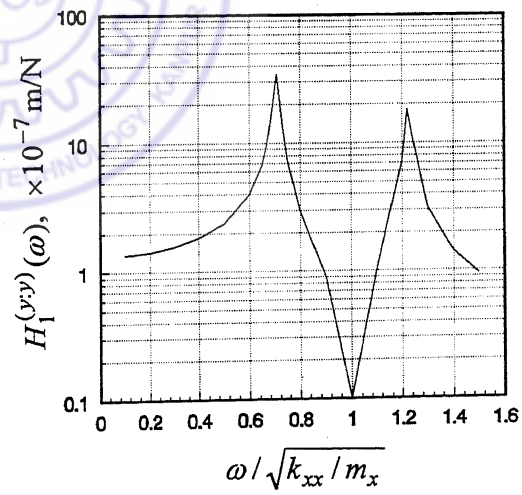

d) Kernel transform $H_1^{(y:y)}(\omega)$

Figure 6.24 Final estimates of first order kernel transforms. [Case:2, 10%measurability]

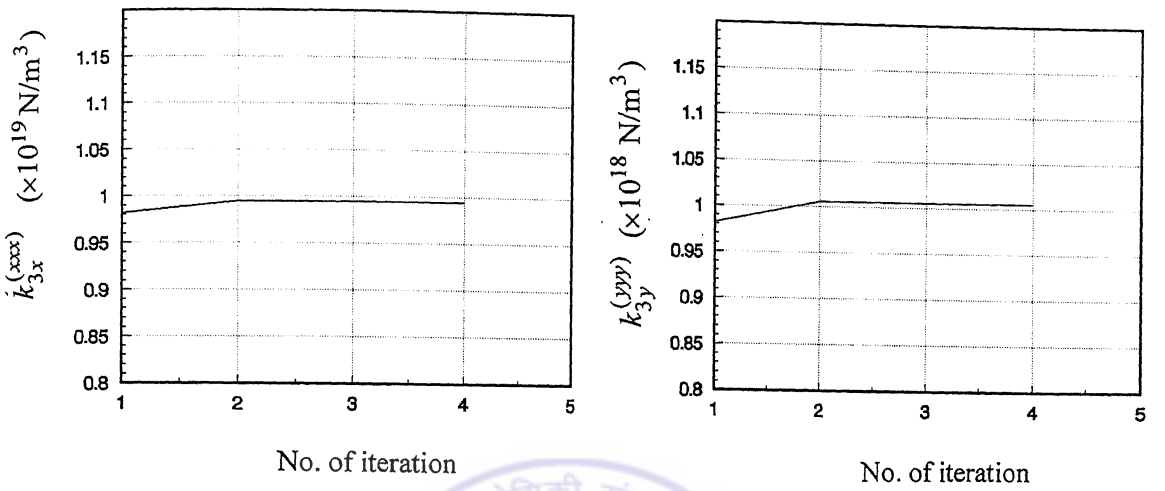

Figure 6.25(a) Iterative estimates of nonlinear parameters. [Case:2, 10%measurability]

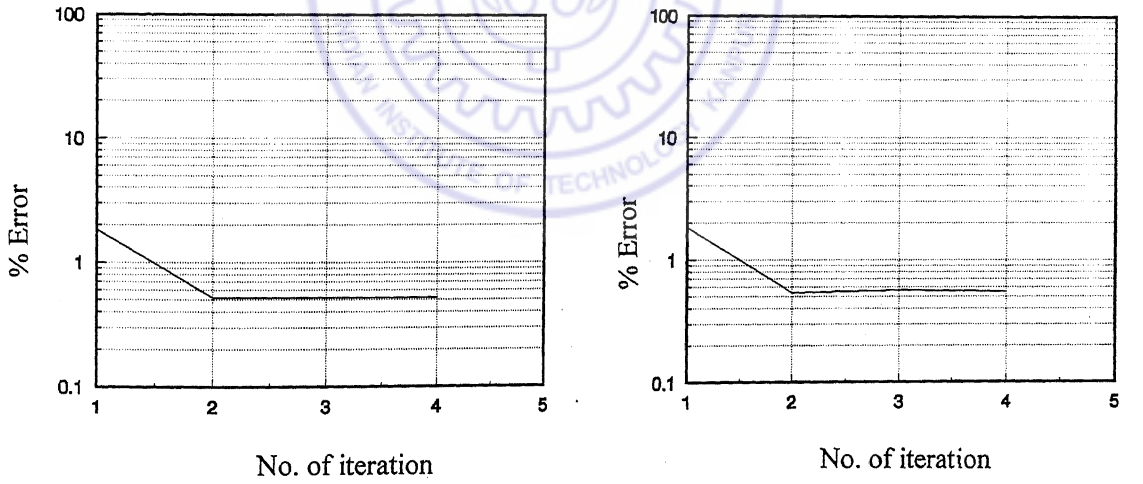

Figure 6.25(b) Convergence of estimation error with iterations. [Case:2,10%measurability]

6.9 Remarks

The iterative method of parameter estimation has been extended for multi-degree-of-freedom systems and illustrated with numerical simulations. Cross-kernels have been defined and generic expressions for their synthesis have been developed. Matrix form formulations for estimation of linear and nonlinear parameter vectors from the higher order kernel matrices have been developed. Numerical simulations indicate that the procedure can yield accurate estimates of linear parameters including damping. Nonlinear parameters are also estimated with good accuracy and the error is linked to the measurability condition of higher order response harmonics.

CHAPTER 7

EXPERIMENTAL INVESTIGATIONS

Experimental studies have been carried out on a simple rotor-bearing test rig in the laboratory for investigating the applicability and validation of the parameter estimation procedures. The test rig consists of a rotor shaft supported in ball bearings. For such bearings, cross-coupling stiffness parameters are negligible in comparison to the direct stiffness coefficients and accordingly the rotor-bearing system can be modeled as a single-degree-of-freedom system. Harmonic excitation is provided by a function generator, through power amplifier at one of the bearing caps. Measurements for excitation force and resultant vibration response are taken simultaneously at the point of force application itself, i.e., at the bearing cap. Measured signals are taken to a spectrum analyzer and time domain data are transferred to computer and processed in accordance with the procedure described in Chapter 5, for linear and nonlinear parameter estimation.

7.1 Experimental Setup

The laboratory rotor-bearing set up consists of a disc centrally mounted on a shaft supported in two ball bearings (Figure 7.1a). The shaft can be driven, if required, through a flexible coupling by a motor. The disc has a mass of 1.23 kg. The shaft has a length of 0.55 m and a diameter equal to 10 mm. Bearings are housed in pedestals comprising of an upper cap and a lower case. The bearings are SKF make with following specifications-

Ball bearing type	SKF 6200	Ball diameter	6 mm
Inner diameter	10 mm	Pitch diameter	20 mm
Outer diameter	30 mm	Ball race radius	3.09 mm
Number of balls	6	Allowable pre-load	0-2 μm

Overall rotor mass is 1.57 kg which gives per bearing rotor mass as 0.785 kg. The electro-dynamic exciter is vertically mounted between the driving end bearing cap and a

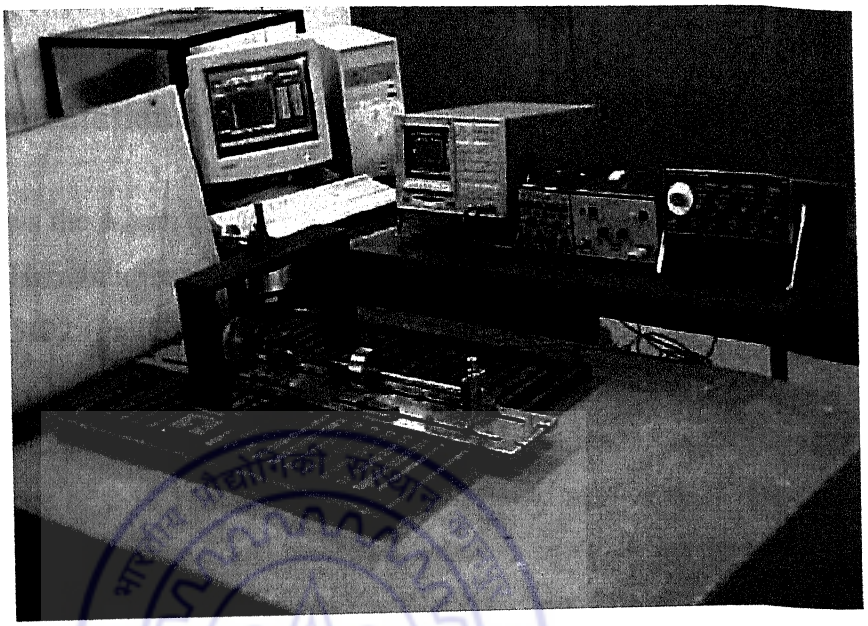

Figure 7.1(a) Experimental set up along with instrumentation.

Figure 7.1(b) Exciter mounting arrangement and impedance head.

rigid frame (Figure 7.1b). The excitation is given in vertical direction and response of bearing housing vibration is also measured in vertical direction.

7.2 Instrumentation

Figure 7.2 shows the schematic diagram of the experimental set up with instrumentation arrangements. Harmonic excitations at desired frequencies are generated in a Function Generator PM 5132 (Phillips make, 0.1-2MHz) and amplified in a Power Amplifier. The Power Amplifier is Brüel and Kjaer make, Type 2706 with a frequency range of 10 Hz to 20 kHz. The electro-dynamic shaker is also of Brüel and Kjaer make, Type 4810 with a frequency range of 0-18 kHz and a peak-to-peak force rating of 10 N. The excitation force and vibration response are measured, simultaneously by an impedance head, attached between the shaker and bearing cap. The impedance head is of Brüel and Kjaer make, Type 8001 with accelerometer sensitivity of 3 pC/ms^{-2} and force transducer has a sensitivity of 370 pC/N. The frequency range of the impedance head is 0-10000 Hz. The outputs from the impedance head are charge signals and are converted to voltage signals and conditioned through a pair of B&K charge amplifiers, Type 2635. The measured force and vibration data are acquired in a spectrum analyzer (ONO SOKKI make, CF-350Z) and transferred to a Pentium III PC. Preliminary measurements like adjustment of the excitation level for a uniform response amplitude and determination of excitation level for a given peak measurability condition are carried out through use of the spectrum analyzer. Parameter estimation is carried through specifically written algorithms in Fortran.

7.3 Measurements and Case studies

A schematic diagram of the rotor with nonlinear bearing stiffness modeling is shown in Figure 7.3. Rotor is considered rigid and cross-coupling stiffness coefficients of the bearings are neglected. For vibration along vertical direction only, the rotor-bearing system can be idealised by a single-degree-of-freedom model as

$$m\ddot{x}(t) + c\dot{x}(t) + g[x(t)] = A\cos\omega t \tag{7.1}$$

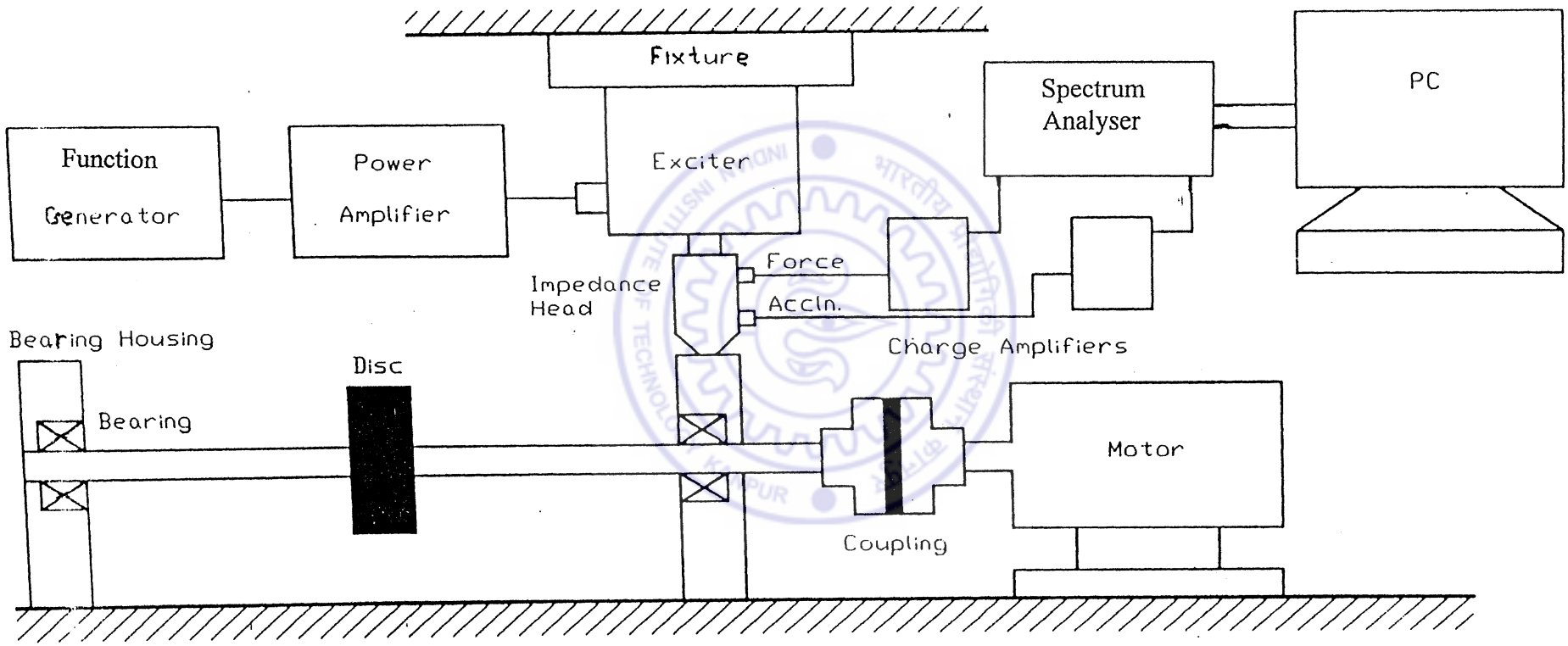

Figure 7.2 Schematic diagram of rotor-bearing test rig and instrumentation

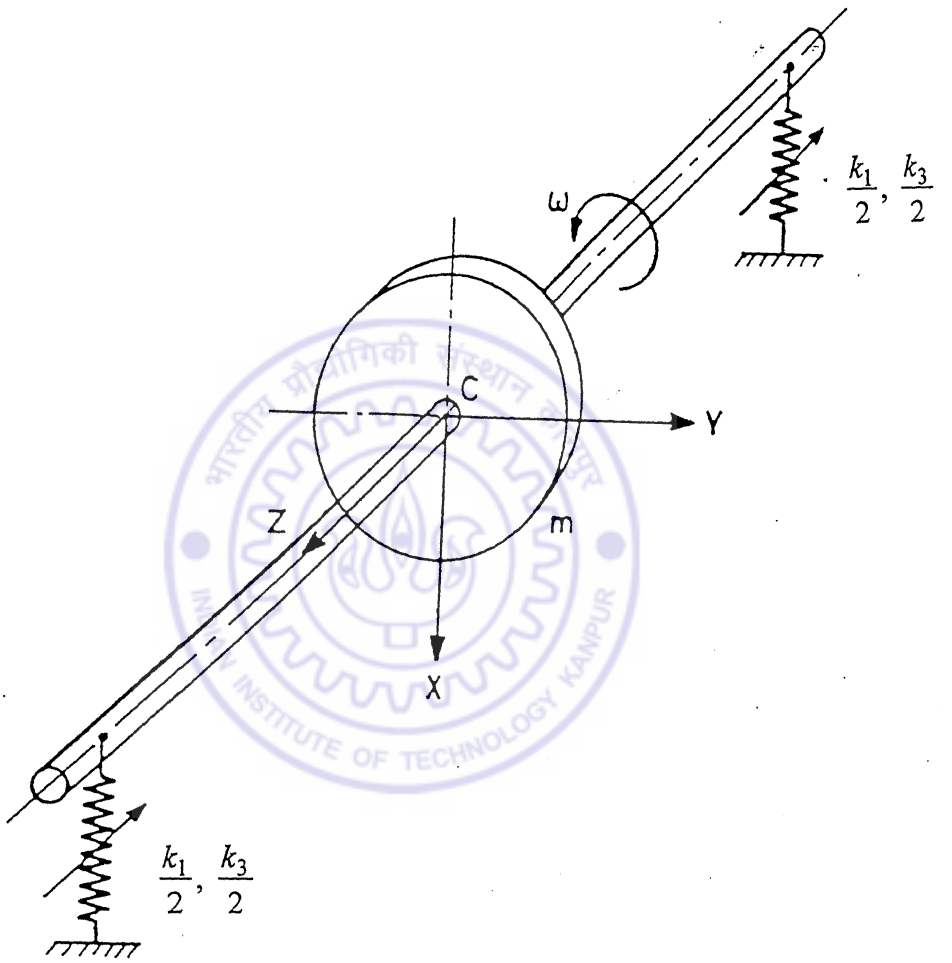

Figure 7.3 Rigid rotor in bearings without cross-coupling

An initial measurement of the natural frequency of the system is obtained through a rap test, using an impact hammer. The rap test response spectrum (Figure 7.4) shows that the natural frequency is in the vicinity of 1010 Hz. A preliminary experimental investigation is carried out first to find out the stiffness nonlinearity structure, $g[x(t)]$, of the system through ordered component separation method presented in Chapter 4.

7.3.1 Investigation of Stiffness Nonlinearity Structure

The system is harmonically excited at frequency, 1000 Hz. Frequency spectra of the applied force and response are shown in Figures 7.5 (a) and (b), respectively. Only odd harmonics are found to be present in the response spectrum, which indicate that the stiffness nonlinearity is of symmetric form. To further determine whether the stiffness nonlinearity is in polynomial form or not, response measurements were taken for three excitation levels (4N, 3N and 2N at excitation frequency equal to 330 Hz) and response components $x_1(t)$, $x_2(t)$, $x_3(t)$ are separated from the overall response $x(t)$ by order component separation method, explained in Section 4.1. Frequency domain transformation of $x_1(t)$, $x_2(t)$, $x_3(t)$ gives $X_1(\omega), X_2(\omega)$ and $X_3(\omega)$ which are probed to detect the presence of various harmonics of the excitation frequency. Figures 7.6(a), (b), (c) show the force time histories at various excitation levels and corresponding response time histories are shown in Figures 7.7(a), (b), (c). The frequency spectra of the response components (Figure 7.8) do not exhibit ordered harmonic characteristics, as discussed in Section 4.2 for characterisation of the nonlinearity as polynomial type. The Fourier transform, $X_1(\omega)$ of the first response component $x_1(t)$, in Figure 7.8(a), is seen to contain third harmonic at 990 Hz, in addition the fundamental harmonic at 330 Hz, corresponding to the frequency of excitation. This is in violation of the characteristics for polynomial class of nonlinearities, for which the first response component is expected to contain only the fundamental harmonic, refer Figure 4.1 (b). The second response component of the rotor bearing-system, can be seen to contain both first and third harmonics (Figure 7.8 b), which also is in violation of the characteristics for the polynomial class of nonlinearities. The rotor-bearing system, therefore, belongs to a class of nonlinear systems having a non-polynomial type of nonlinearity. However, the

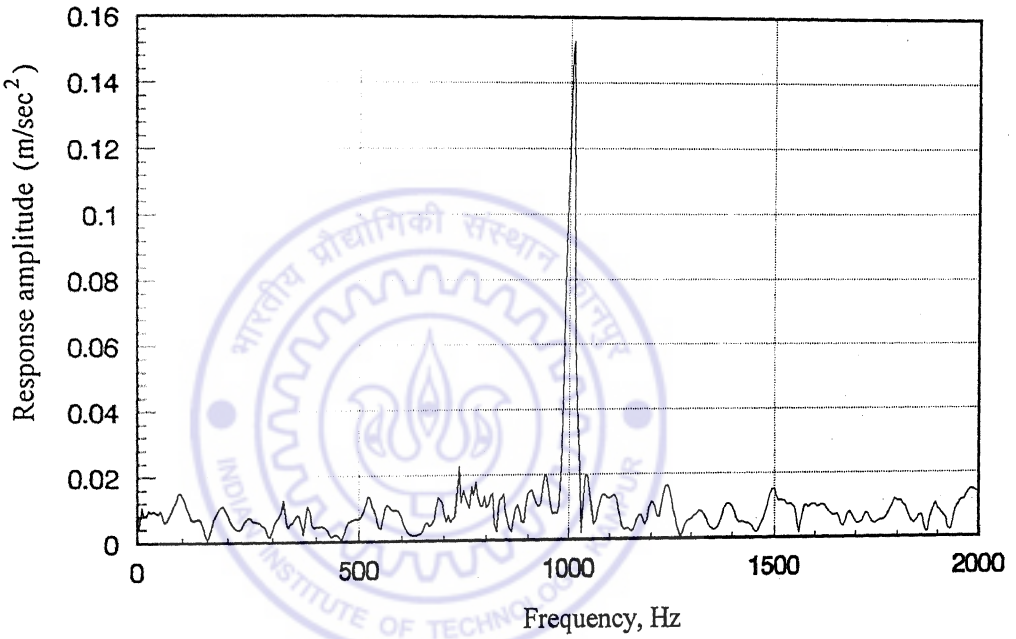

Figure 7.4 Response acceleration spectrum from rap test

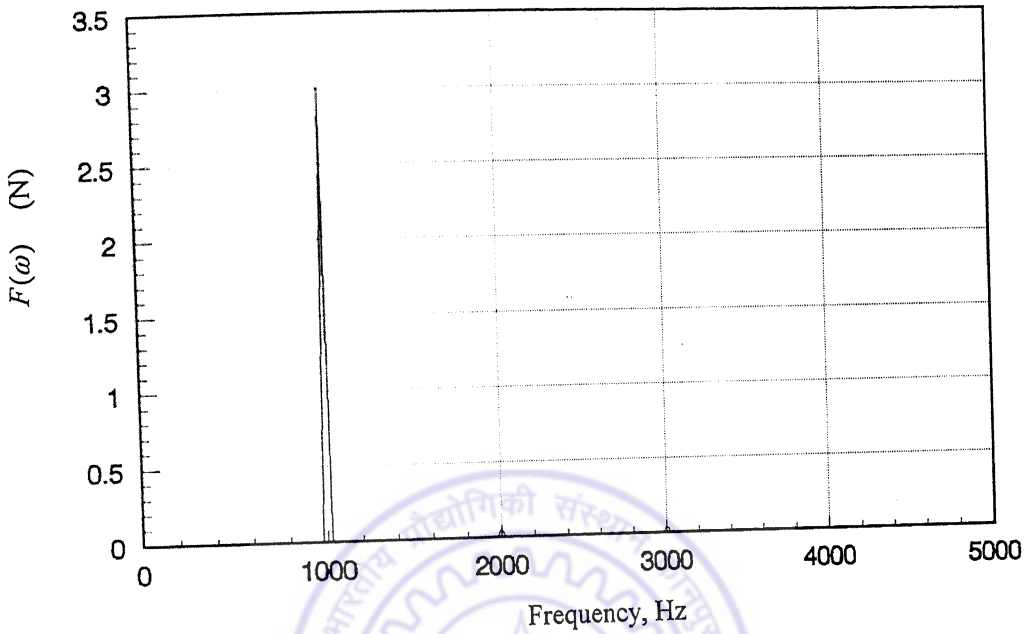

a) Excitation spectrum

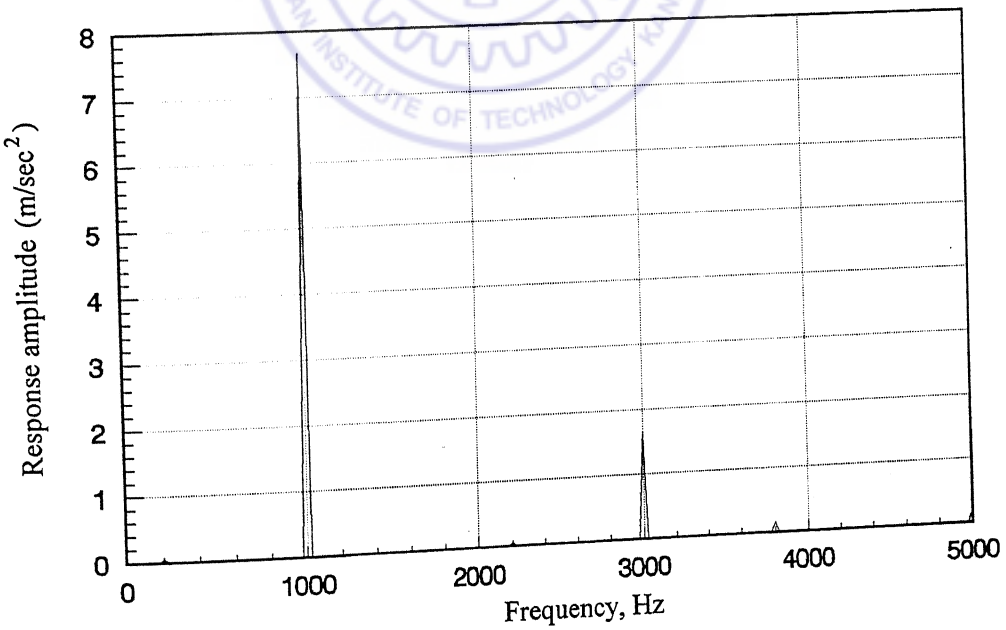

b) Acceleration response spectrum

Figure 7.5 Typical spectra of excitation force and response acceleration for $\omega = 1000$Hz.

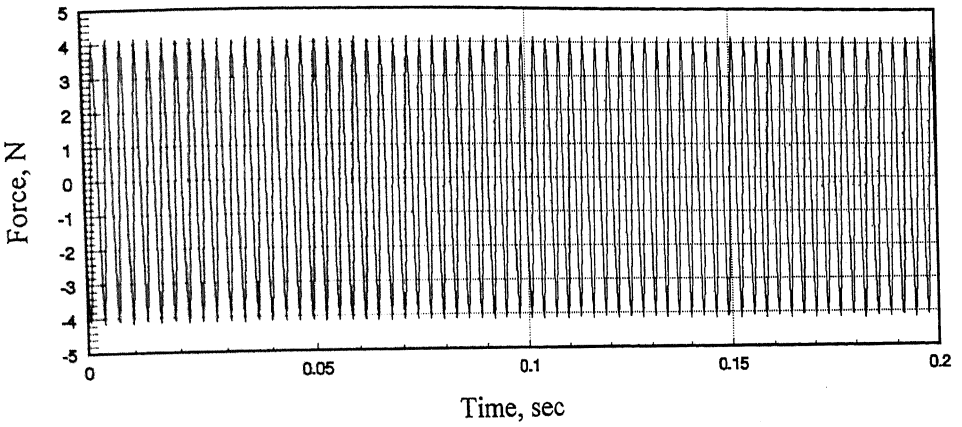

a) Force amplitude, 4N

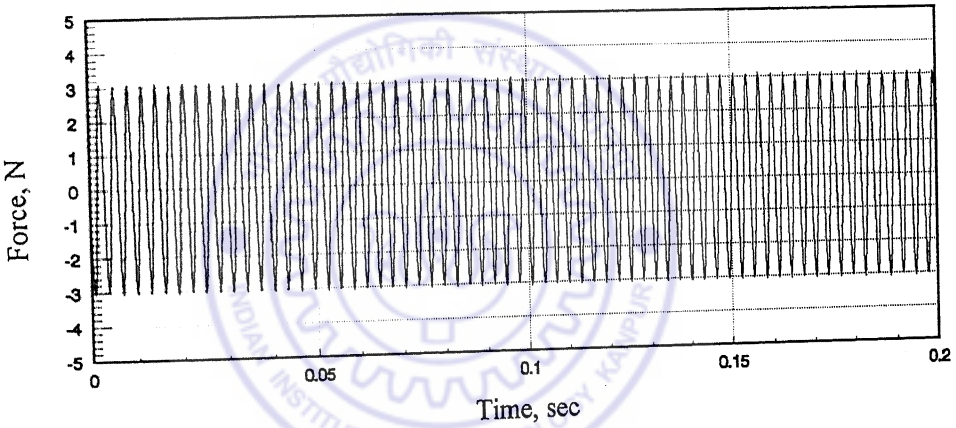

b) Force amplitude, 3N

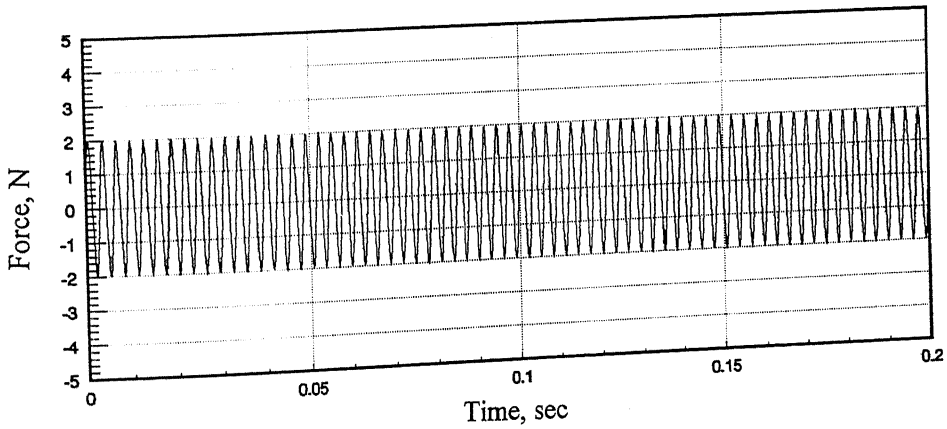

c) Force amplitude, 2N

Figure 7.6 Excitations for response component separation. [$\omega = 330$ Hz]

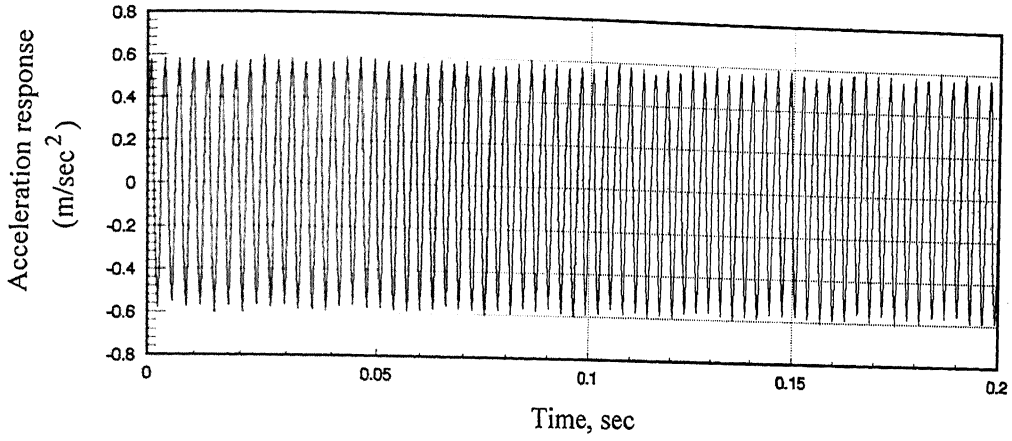

a) For force amplitude, 4N

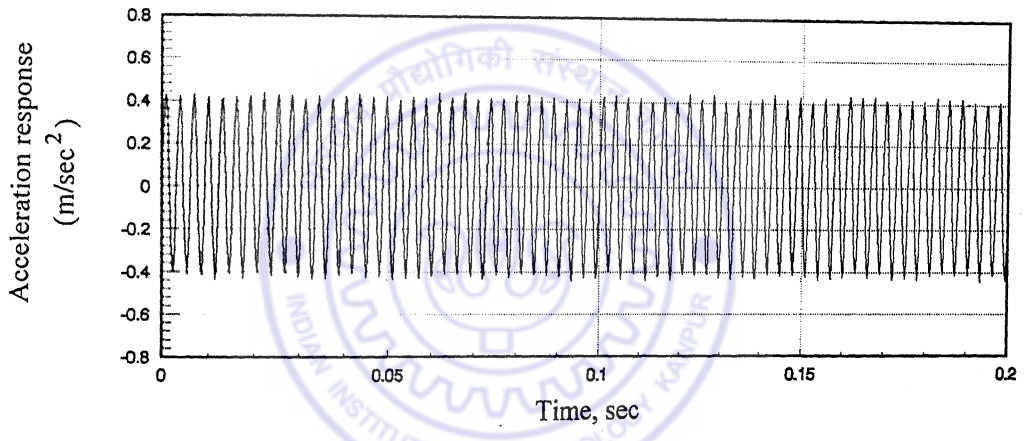

b) For force amplitude, 3N

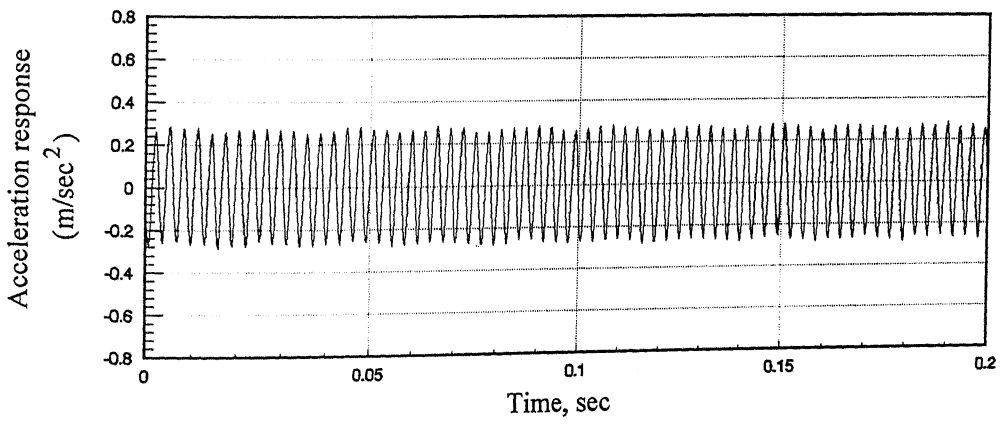

c) For force amplitude, 2N

Figure 7.7 Response time history for different excitation levels. [$\omega = 330$ Hz]

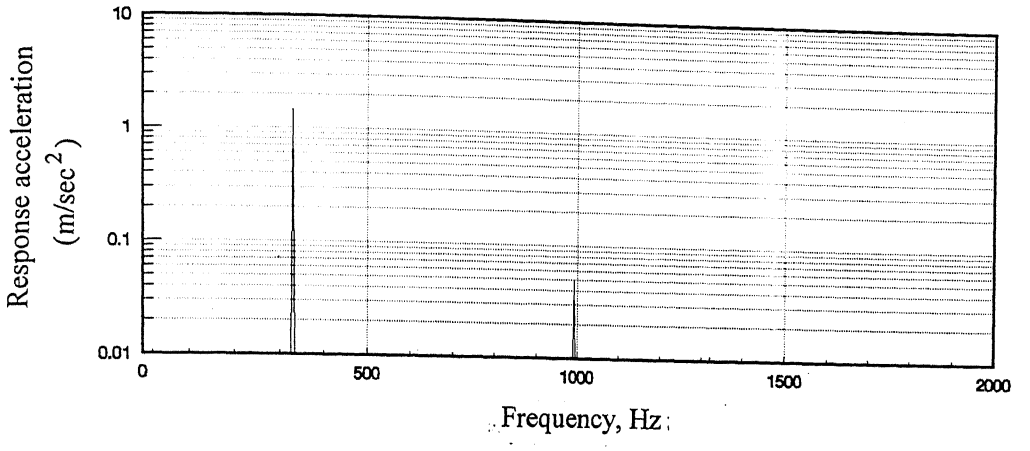

a) Response component, $\ddot{x}_1(t)$

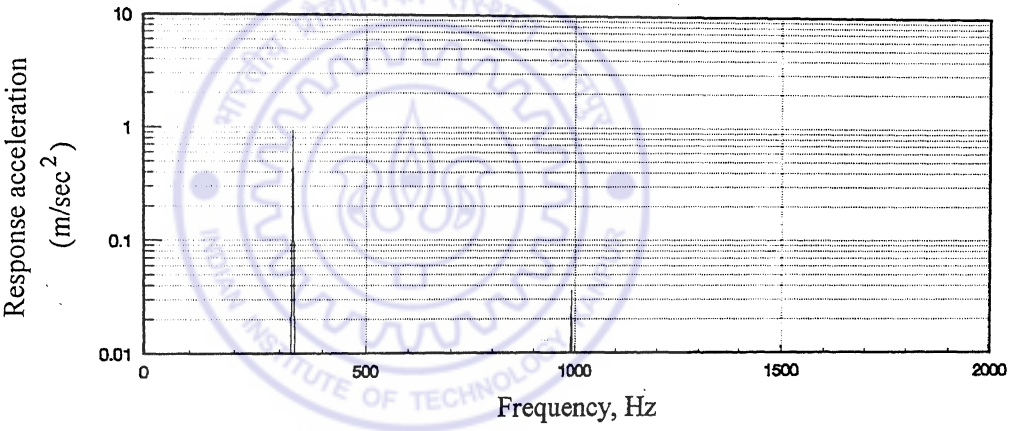

b) Response component, $\ddot{x}_2(t)$

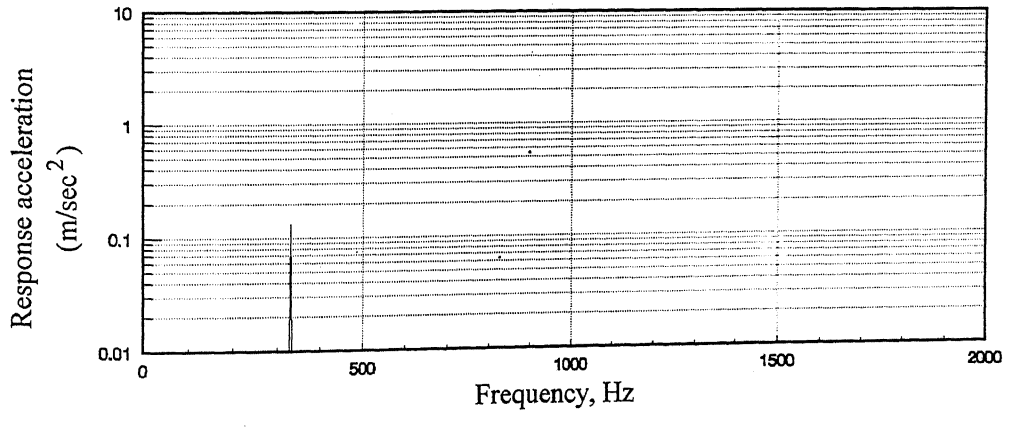

c) Response component, $\ddot{x}_3(t)$

Figure 7.8 Response component spectra for $\omega = 330$ Hz

absence of even order harmonics in the response spectra indicates that the nonlinearity is symmetric.

Theoretical formulations based on Hertzian contact theory, (Harris, 1984) also indicate that the nonlinear stiffness associated with rolling elements follows a fractional power relationship and not a polynomial form. The procedures developed, during the present study and discussed in Chapter 4, while being able to distinguish between polynomial and non-polynomial class of nonlinearities, are not capable of making further distinction within the non-polynomial class (i.e. classification into say, bi-linear or Van-der-pol or clearance type of nonlinearity). However, a continuous non-polynomial force-displacement relationship can be approximated by a polynomial within a given displacement range. Since the non-linearity is found to be symmetric in this case, the approximating polynomial will have odd power terms only. Ragulski (1974) has observed that for a small deformation $|x| \leq g$, where g is the pre-load in the bearing, the stiffness function is given by the form

$k(x) = a - bx^2$,

indicating that the load deflection curve posses negative cubic nonlinearity. Therefore, a cubic polynomial form of nonlinearity given by

$$g[x(t) \approx k_1 x(t) + k_3 x^3(t) \tag{7.2}$$

is considered in the present experimental model as an approximation to the bearing stiffness function and the experimentation is carried out to estimate the linear and nonlinear stiffness parameters, k_1 and k_3 of the rotor-bearing system.

7.3.2 Determination of Linear and Nonlinear Parameters

Experiments are focused on estimation of the nonlinear stiffness coefficient, k_3. Linear parameters are estimated in the form of damping factor, ζ, and natural frequency, ω_n. Linear stiffness coefficient, k_1, is obtained from the estimate of natural frequency, using the known value of rotor mass per bearing. For estimation of first kernel transforms, $H_1(\omega)$, the excitation frequency range 925-1035 Hz is selected. Keeping in view, the

single-degree-of-freedom treatment of the rotor-bearing set-up, a wider excitation frequency range is avoided in order to stay clear of some other structural modes which may influence measured vibration data. Figure 7.9 (a), (b) shows the time history and frequency spectrum of the excitation force for a typical excitation frequency of 925 Hz. Time history of the corresponding displacement response and its frequency spectrum are shown in Figures 7.10(a), (b). The displacement response amplitude at 925 Hz is of the order of 1.0×10^{-8} m. The response also shows presence of background noise, which is an order less in magnitude compared to displacement signal. Noise spectra are also separately measured after switching off the exciter. This is shown in Figures 7.11(a), (b).

As discussed in Chapter 5, excitation level is varied over the frequency set to obtain response amplitude at a constant level, which in this case was selected as 1.0×10^{-8} m. The variation of excitation level is plotted in Figure 7.12(a) and corresponding response harmonic amplitude, $X(\omega)$, is shown in Figure 7.12(b). Preliminary estimate of the first order kernel transform, $H_1(\omega)$, is obtained in Figure 7.12 (c), by dividing response $X(\omega)$ of Figure 7.12 (b) by the applied force of Figure 7.12 (a). Using standard curve fitting procedure (Ewins, 1984), linear parameters ω_n and ς are estimated. The best fit curve along with the estimated kernel transform data are shown in Figure 7.12(c). The estimated linear parameters are

$\omega_n = 1012.2$ Hz, $\varsigma = 0.01156$.

Estimation of nonlinear stiffness parameter k_3 is done through measurement of third response harmonic amplitude $X(3\omega)$. The displacement amplitude of the third response harmonic is low and therefore measurements were made for acceleration amplitudes. Figure 7.13(a), shows the acceleration amplitudes of the first and third order harmonics, for an excitation frequency of 330 Hz. The ratio between the amplitudes at third harmonic and first harmonic is computed. This gives the measurability index, which forms the basis of selecting the excitation level and frequency range for measurement of third response harmonic amplitude $X(3\omega)$. Figure 7.13(b) shows measurability indices for three different excitation amplitudes of 2N, 3N and 4N over a frequency range of 305 Hz-355 Hz. Corresponding peak measurability indices can be seen to be approximately of

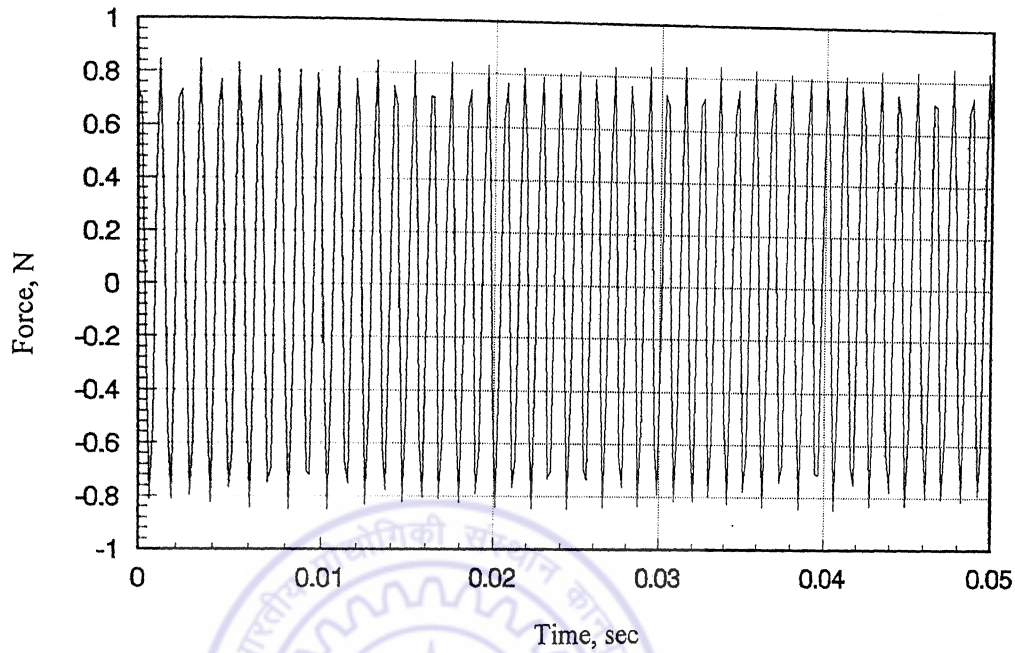

a) Time history

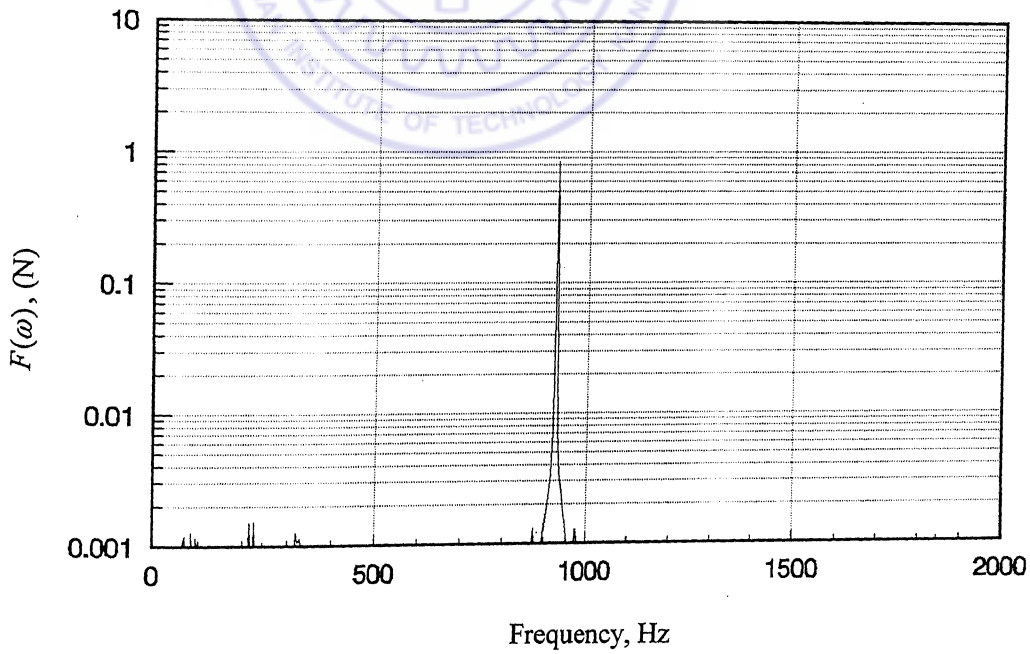

b) Spectrum

Figure 7.9 Typical excitation time history and its spectrum for $\omega = 925$ Hz

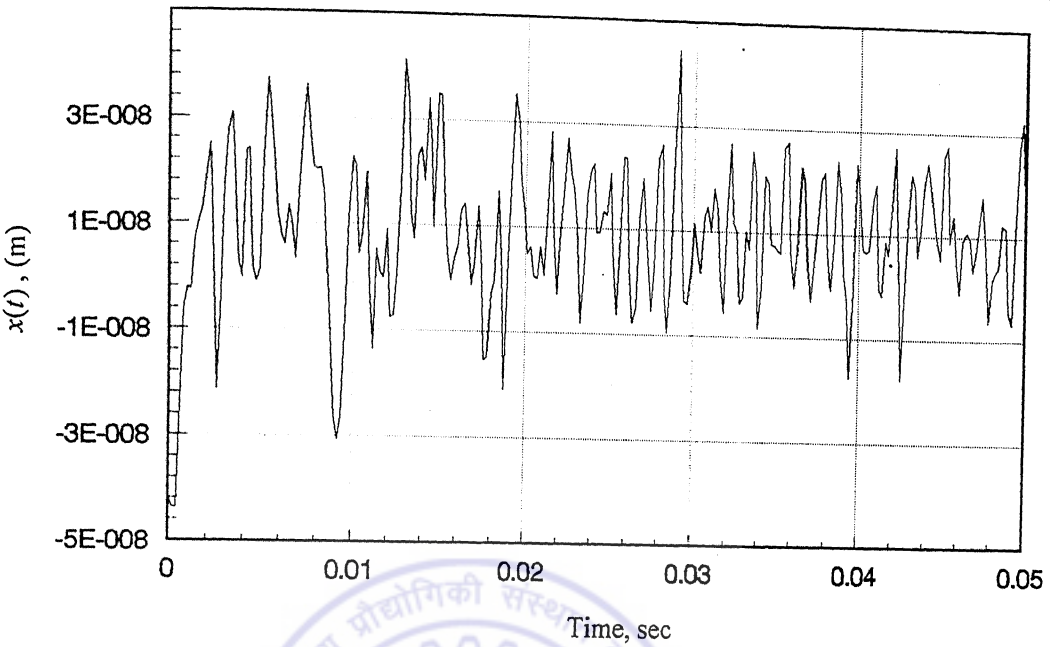

a) Displacement , $x(t)$

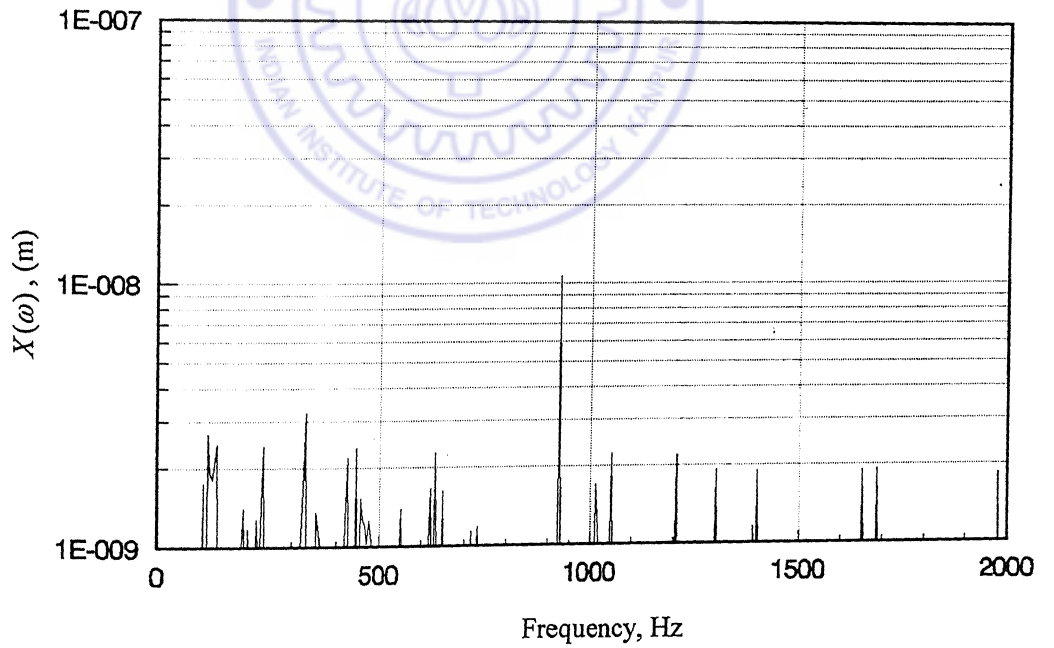

b) Response spectrum

Figure 7.10 Typical response time history and its spectrum for $\omega = 925$ Hz

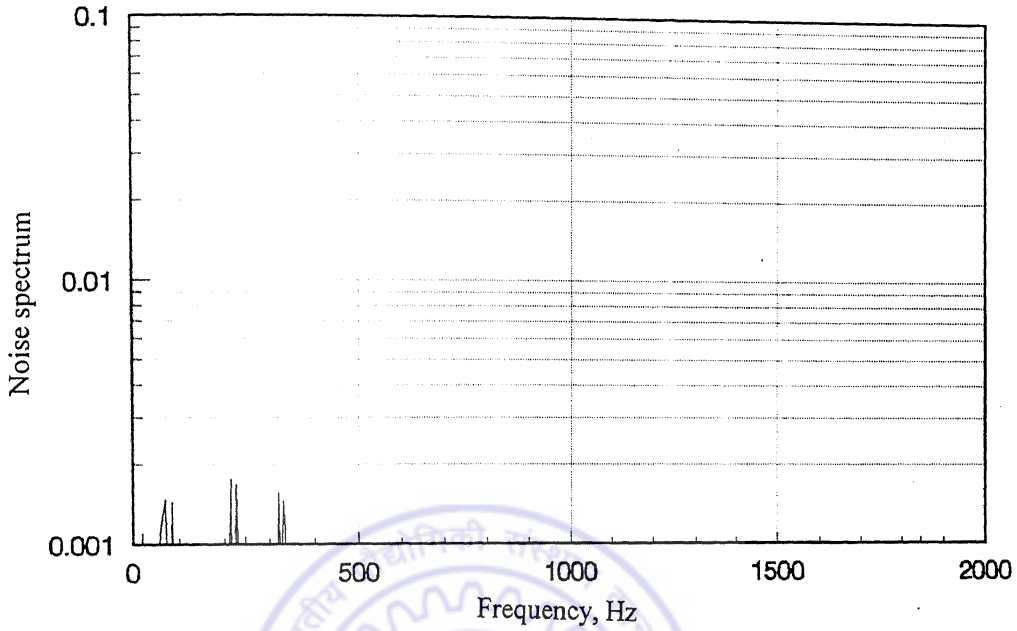

a) Excitation signal

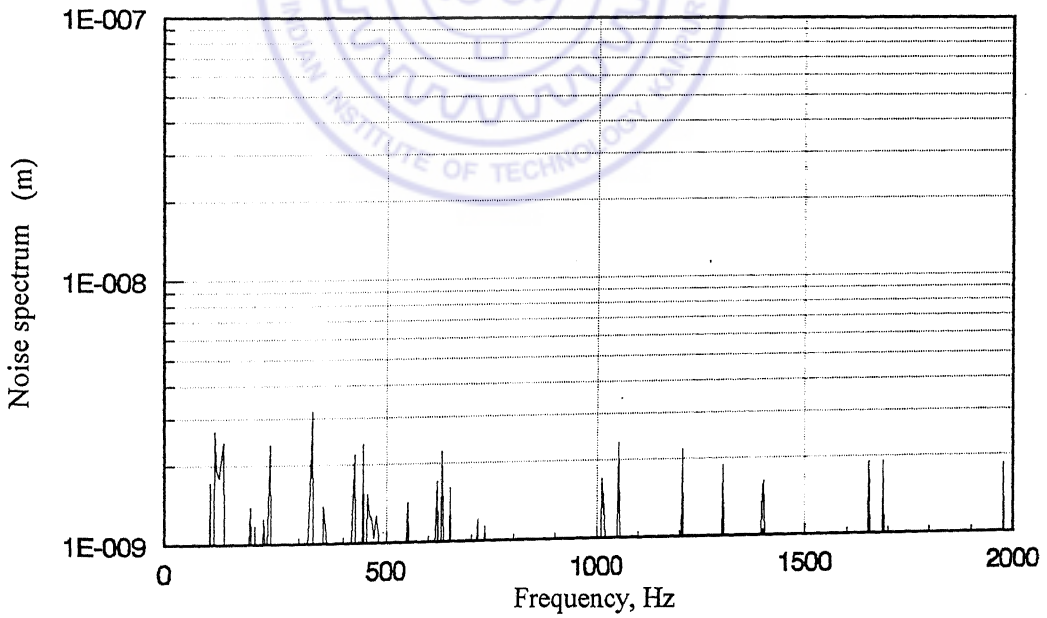

b) Response signal

Figure 7.11 Background noise spectra in excitation signal and in response signal

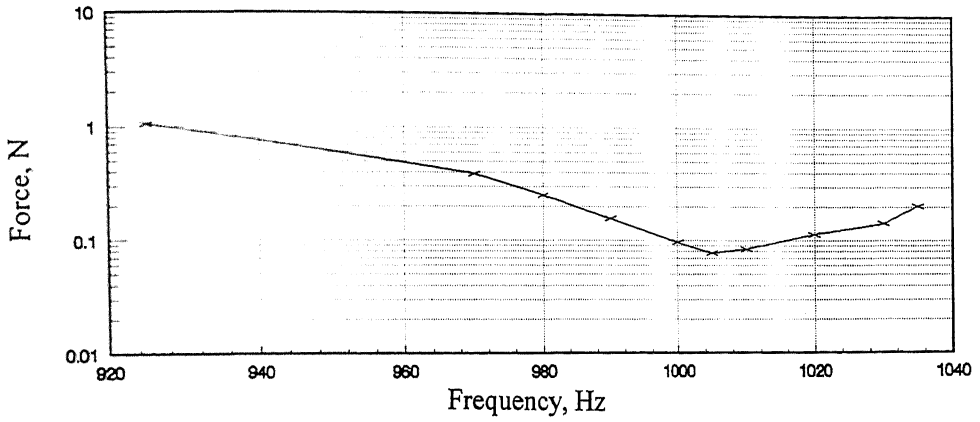

a) Variation in excitation level

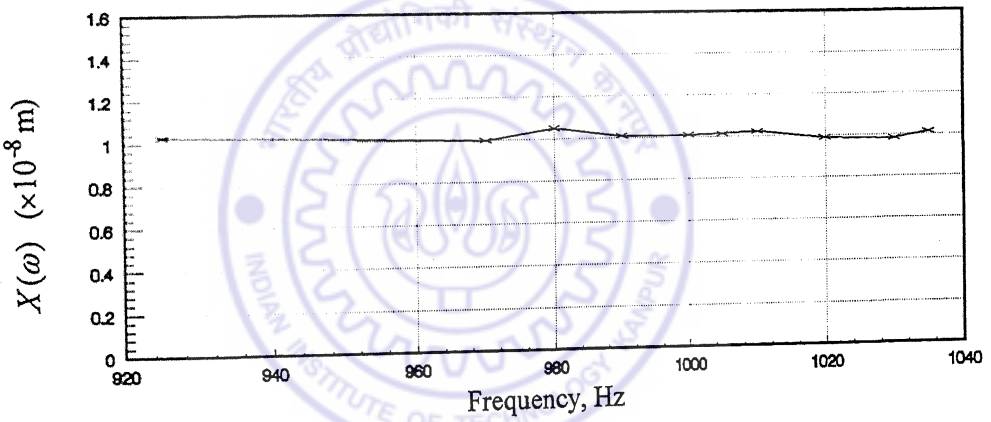

b) Response harmonic, $X(\omega)$

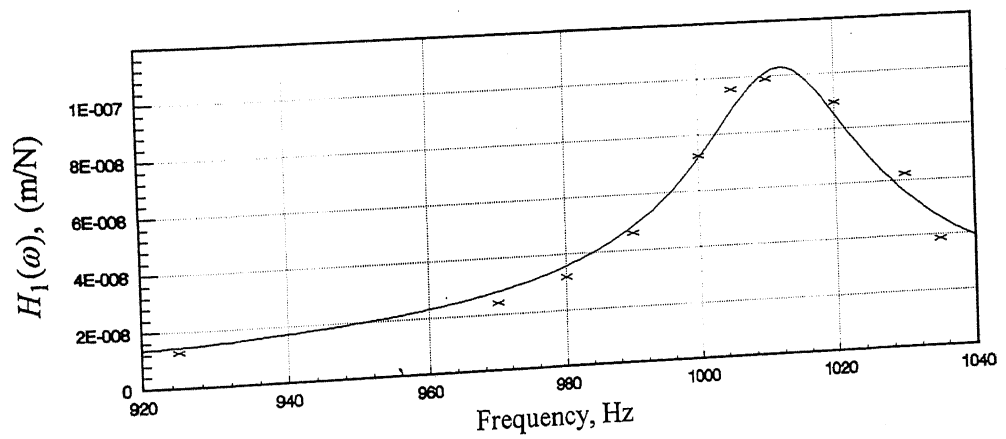

c) Estimate of $H_1(\omega)$

Figure 7.12 Excitation level variation, response amplitude, $X(\omega)$, and preliminary estimation of first order kernel transform, $H_1(\omega)$.

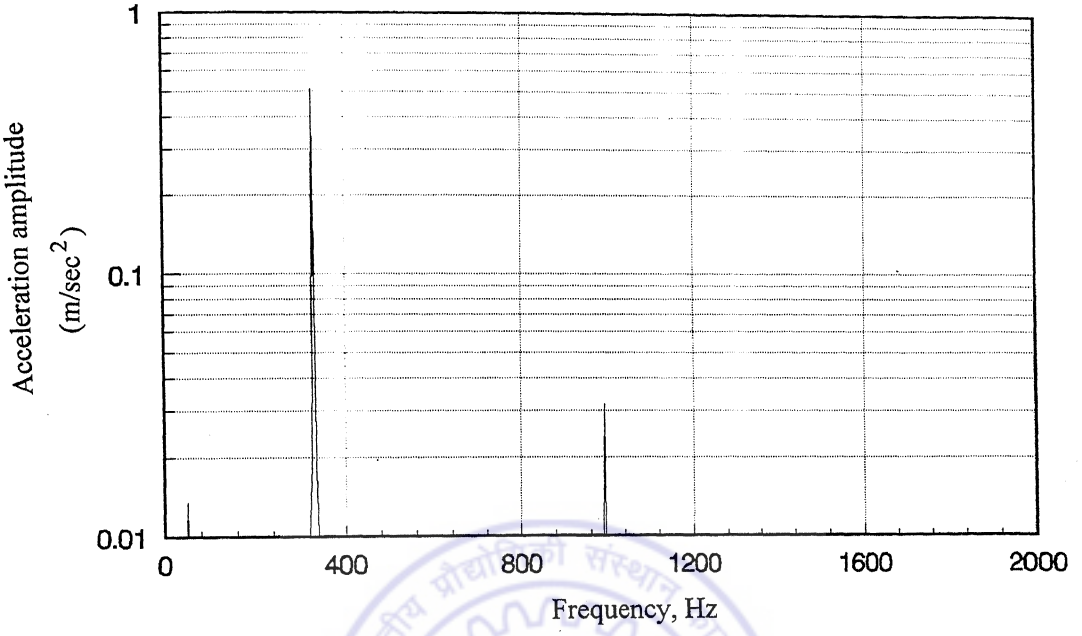

Figure 7.13a Typical response spectrum with excitation at $\omega = 330$ Hz

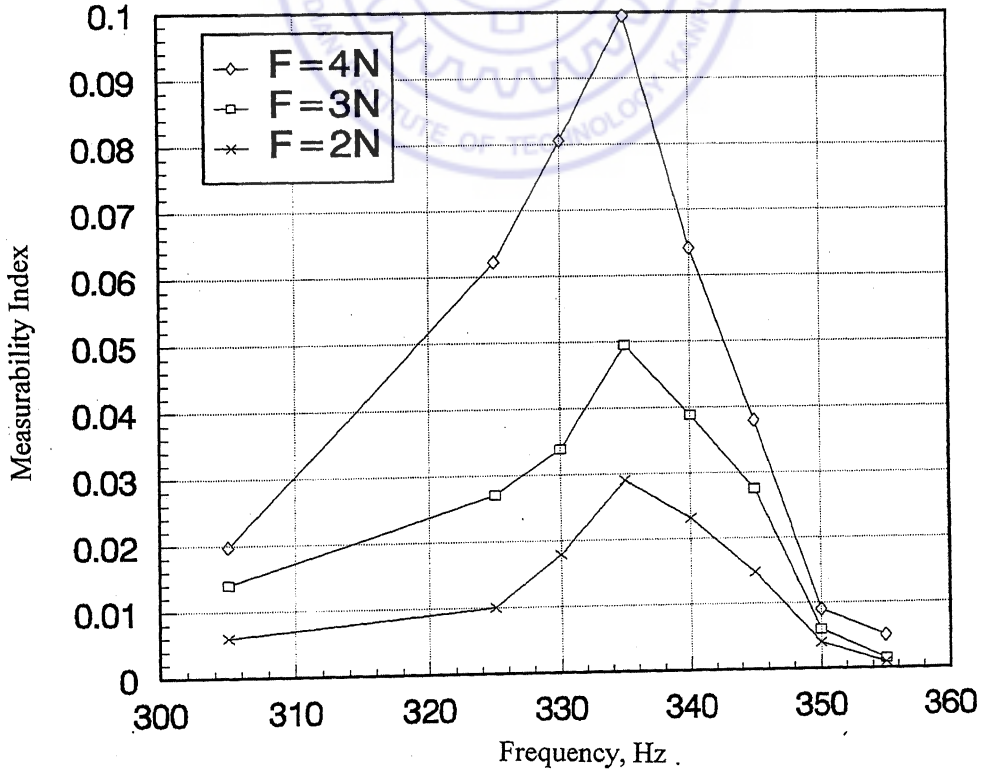

Figure 7.13b Measurability of third response harmonic at excitation levels 4N, 3N and 2N

the order of 3%, 5% and 10%. Excitation frequencies are selected at 330 Hz, 335 Hz, 340 Hz and 345 Hz, as measurability is higher in this range. Third response harmonic amplitude $X(3\omega)$ is then measured at these selected frequencies for three different excitation levels and the nonlinear parameter is estimated.

Case I (Excitation Amplitude 4.0 N)

The measured acceleration spectra at the four selected frequencies are shown in Figures 7.14(a-d). First a preliminary estimation of the nonlinear parameter k_3 is made and then method of recursive iteration is employed. The iteration procedure is repeated till estimated value of the nonlinear parameter converges within a limit, which in this case is specified as 0.1%. Figure 7.15(a) shows the estimated values of nonlinear parameter k_3 over the stages of successive iteration. Final estimate of k_3 is found to be 1.75×10^{19} N/m^3. Assuming that both the bearings are identical and act in parallel, the nonlinear stiffness of each bearing then becomes 0.875×10^{19} N/m^3. Figure 7.15(b) show the final estimate of the first order kernel transform along with its preliminary estimate. It is seen that the successive iterations have modified the FRF values significantly near and around the natural frequency. Final estimates of linear parameters are

$\omega_n = 1011.47$ Hz, $\quad \varsigma = 0.01078$.

The linear stiffness parameter of the bearing system is computed to be 1.585×10^7 N/m.

Case II (Excitation Amplitude 3.0 N)

Figures 7.16(a-d) show the measured acceleration spectra at the four selected frequencies. The converged value of k_3 is found to be 2.857×10^{19} N/m^3 (Figure 7.17(a)). This gives the value of nonlinear stiffness of each bearing as 1.4285×10^{19} N/m^3. Figure 7.17(b) show the preliminary and final estimates of the first order kernel transform. Final estimates of linear parameters are

$\omega_n = 1012.47$ Hz, $\quad \varsigma = 0.01015$.

The linear stiffness parameter of the bearing was computed as 1.535×10^7 N/m.

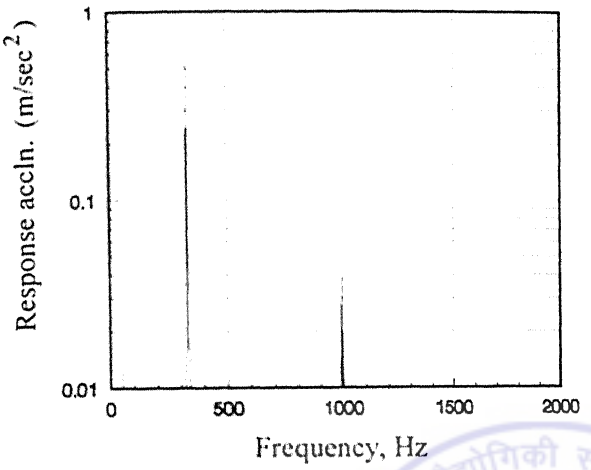

a) ω = 330 Hz

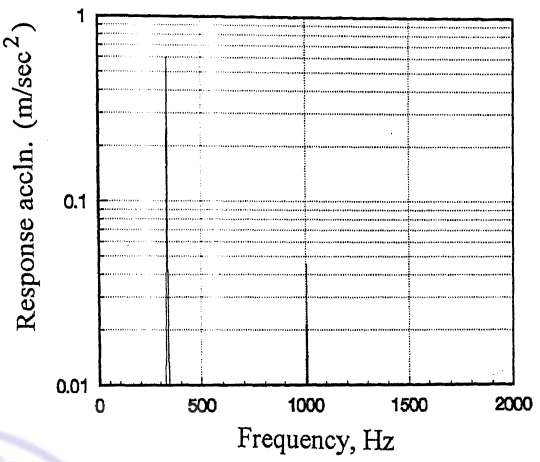

b) ω = 335 Hz

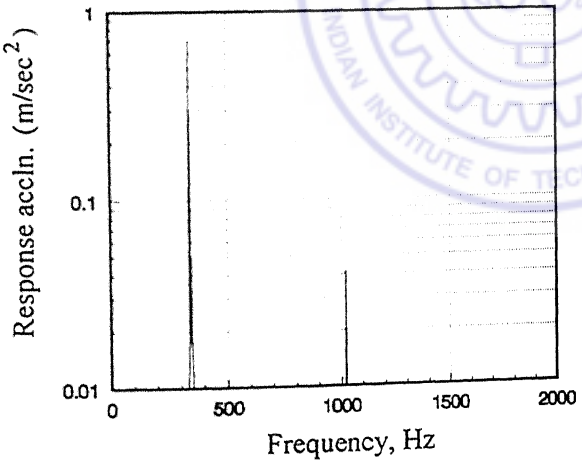

c) ω = 340 Hz

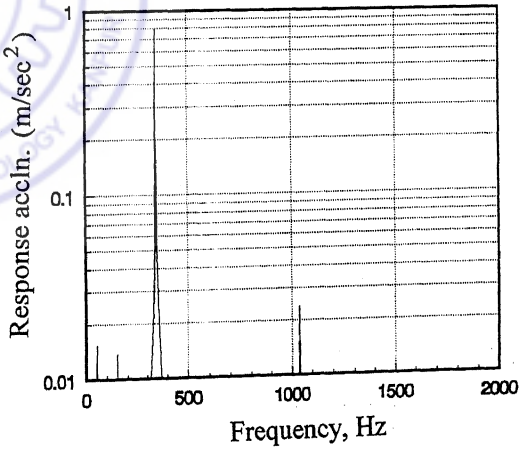

d) ω = 345 Hz

Figure 7.14 Acceleration response spectra for Case 1: Excitation amplitude = 4N

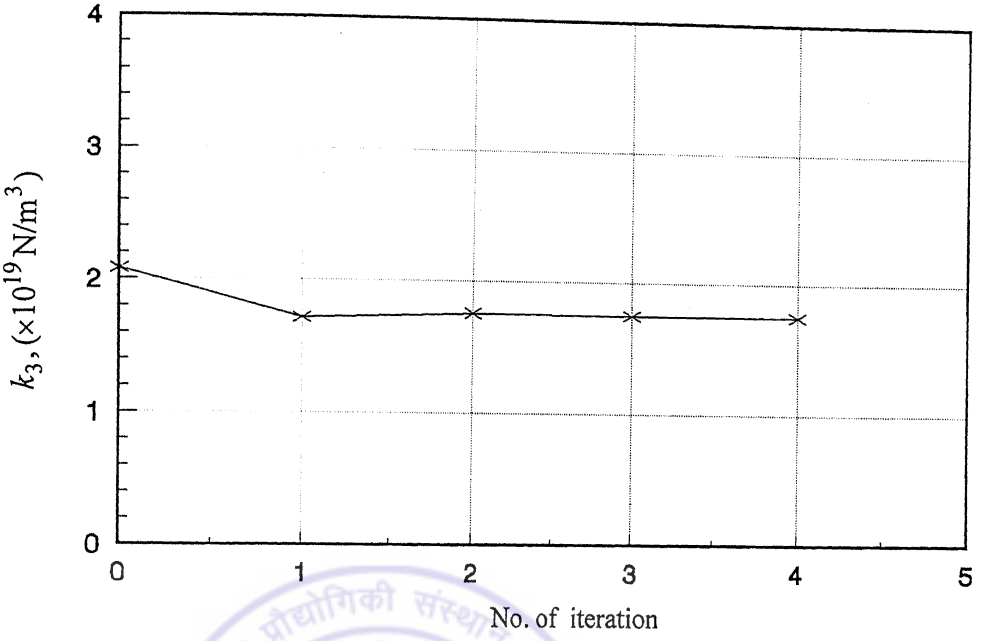

Figure 7.15(a) Iterative estimates of k_3, (Case I: Excitation amplitude = 4N)

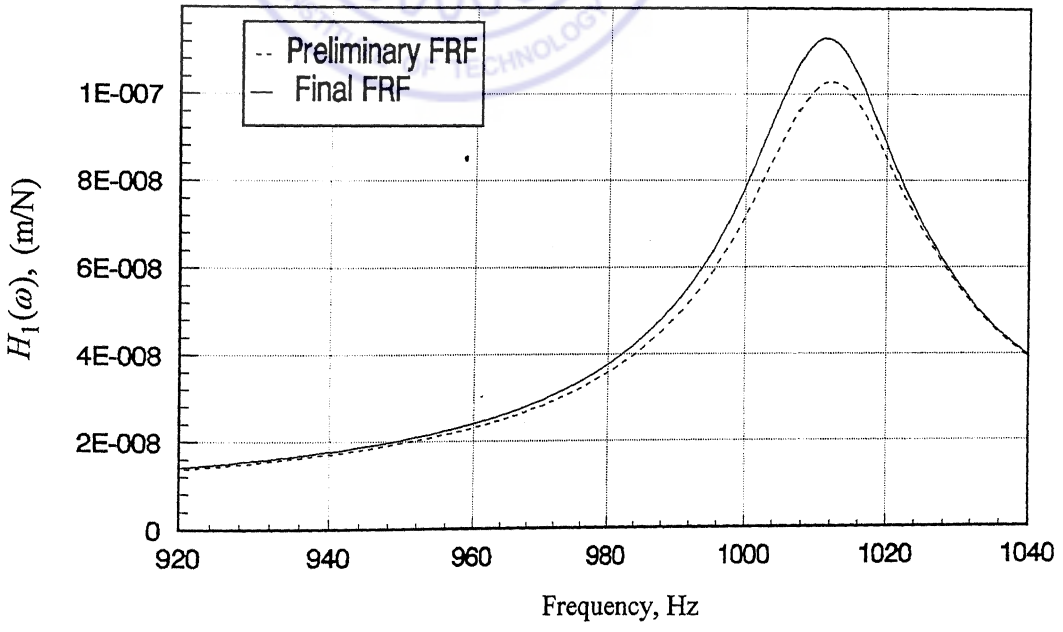

Figure 7.15(b) Final estimate of first order kernel transform, $H_1(\omega)$

(Case I: Excitation amplitude = 4N)

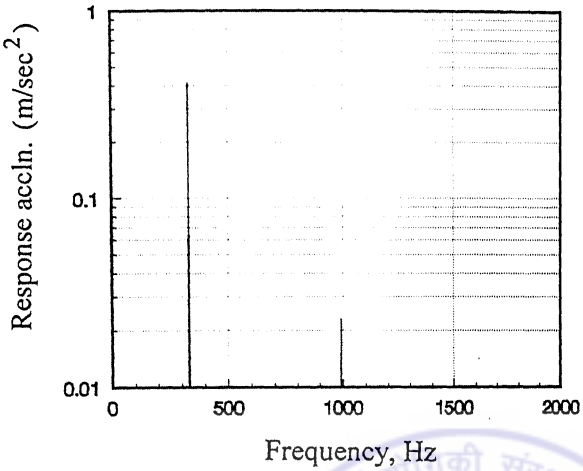

a) $\omega = 330$ Hz

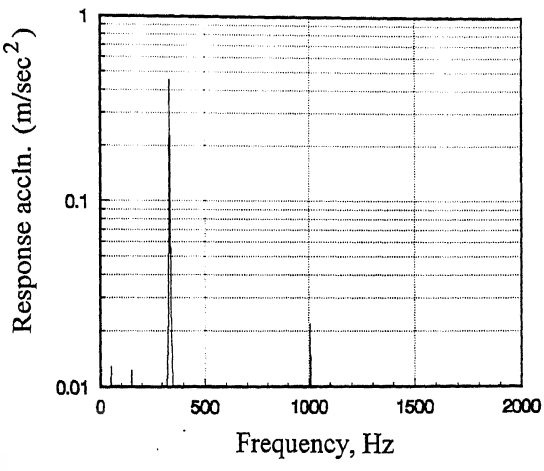

b) $\omega = 335$ Hz

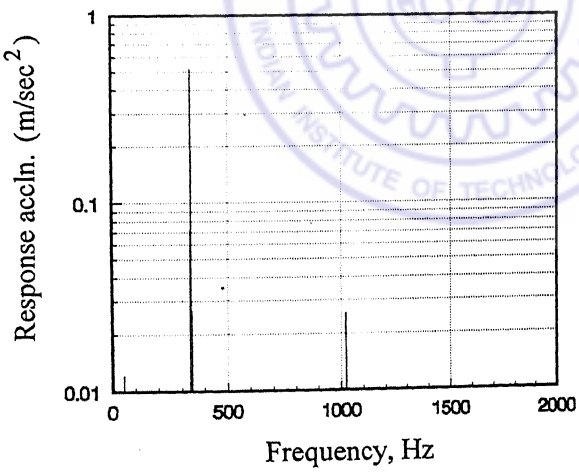

c) $\omega = 340$ Hz

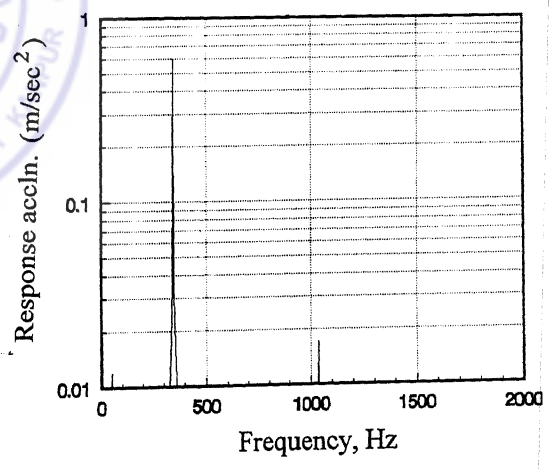

d) $\omega = 345$ Hz

Fig. 7.16 Acceleration response spectra for Case 2: Excitation amplitude = 3N

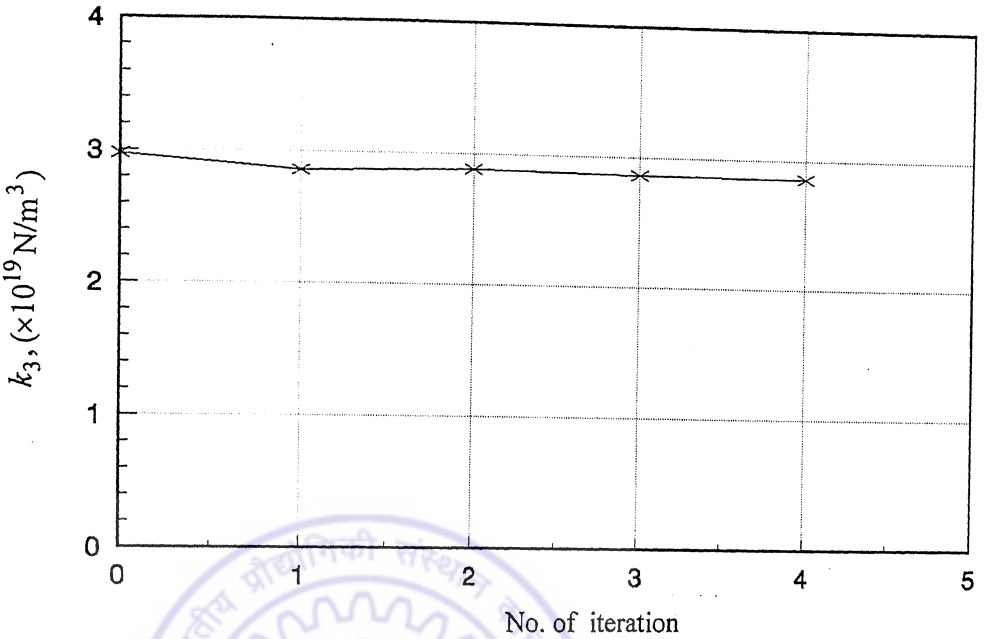

Figure 7.17(a) Iterative estimate of k_3, (Case II: Excitation amplitude = 3N)

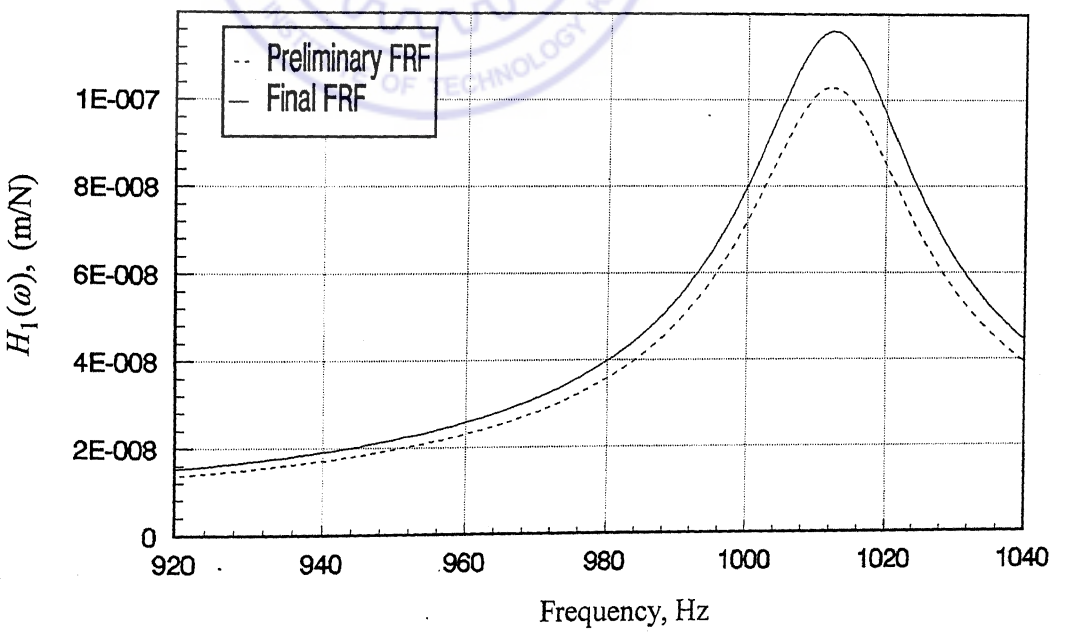

Figure 7.17(b) Final estimate of first order kernel transform, $H_1(\omega)$

(Case II: Excitation amplitude = 3N)

Case III (Excitation Amplitude 2.0 N)

Figures 7.18(a-d) show the measured acceleration spectra at the four selected frequencies. Convergence of estimated value of k_3 through successive iteration is shown in Figure 7.19(a). Final estimate of k_3 is found to be 3.48×10^{19} N/m^3, which gives the value of nonlinear stiffness of each bearing as 1.740×10^{19} N/m^3. Figure 7.19(b) shows the preliminary and final estimates of the first order kernel transform. Final estimates of linear parameters are

$\omega_n = 1011.90$ Hz, $\quad \varsigma = 0.01002$.

The linear stiffness parameter of the bearing was found to be 1.586×10^7 N/m.

For all three cases discussed above, while the values of the estimated linear parameters is practically the same, the estimate of the nonlinear parameter k_3, varies with the excitation amplitude. This, as expected, is due to the fact that the system nonlinearity does not belong to the polynomial class, and its polynomial approximation would be amplitude dependent.

7.3.3 Detection of Sign of Nonlinear Parameter k_3

The procedure for detection of the sign of nonlinear parameter k_3, has been described earlier in Section 5.4. It is done by looking for a change in the sign of real part of the complex response harmonic amplitude, $X(3\omega)$, as excitation frequency is varied through one-third of natural frequency. Figure 7.20 shows the sign variation of real part of $X(3\omega)$, over the excitation frequency range 330-345 Hz for excitation levels 4N, 3N and 2N. The sign of real part of $X(3\omega)$ is seen to change from positive values to negative values during frequency transition through one-third natural frequency. This, following the arguments presented in Section 5.4, indicates that the nonlinearity is negative in sign and the bearing has a softening spring.

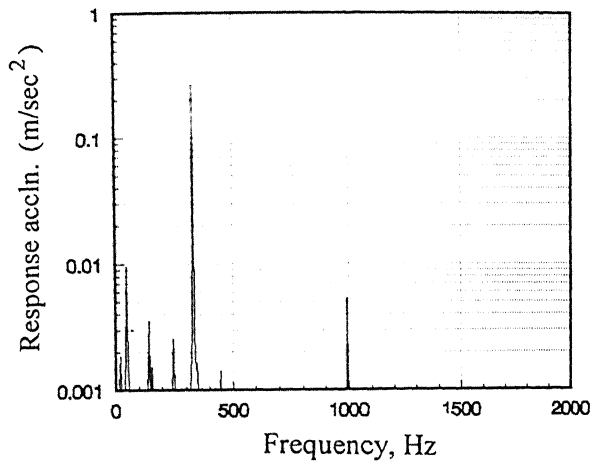

a) $\omega = 330$ Hz

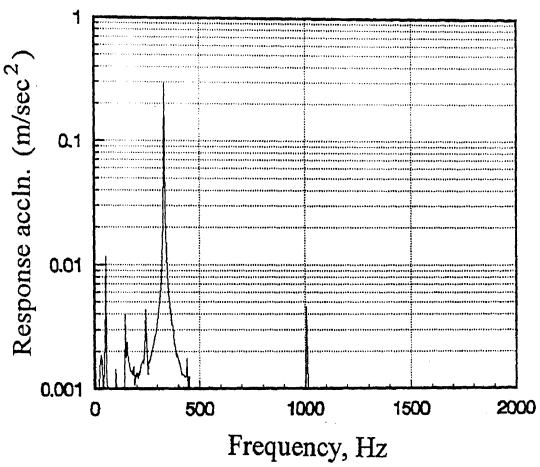

b) $\omega = 335$ Hz

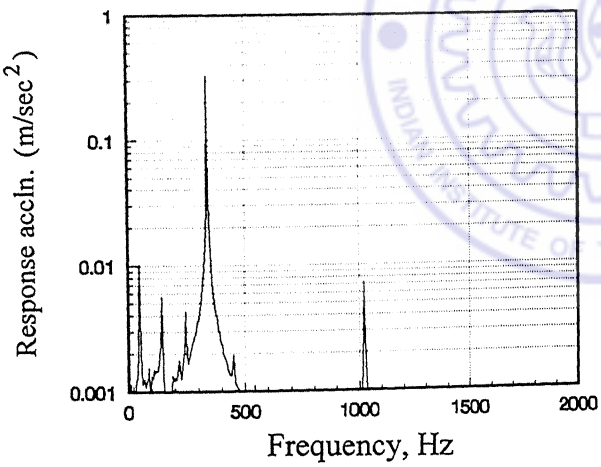

c) $\omega = 340$ Hz

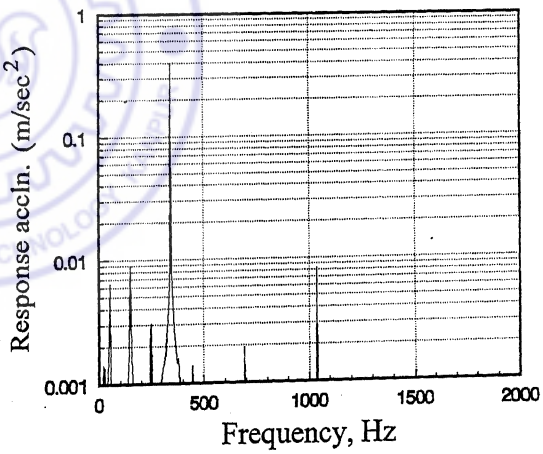

d) $\omega = 345$ Hz

Fig. 7.18 Acceleration response spectra for Case 3: Excitation amplitude = 2N.

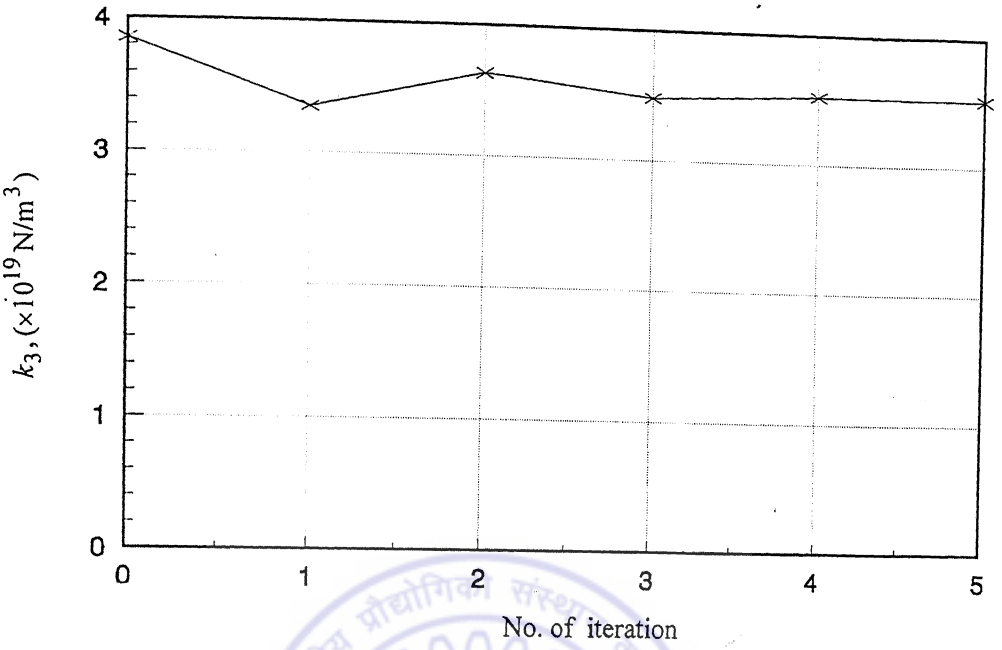

Figure 7.19(a) Iterative estimate of k_3, (Case III: Excitation amplitude = 2N)

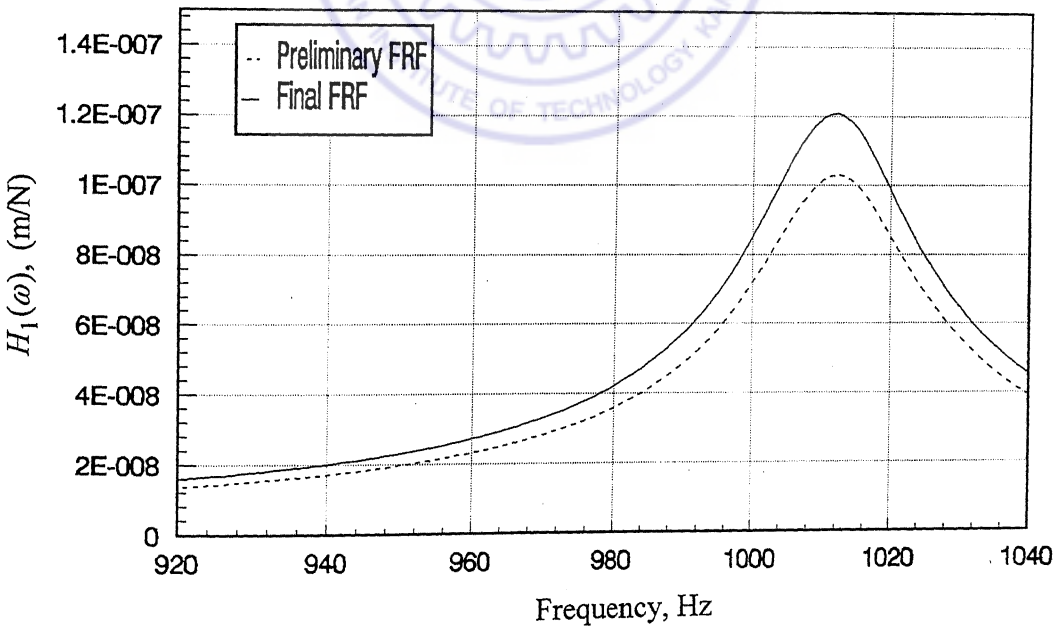

Figure 7.19(b) Final estimate of first order kernel transform, $H_1(\omega)$

(Case III: Excitation amplitude = 2N)

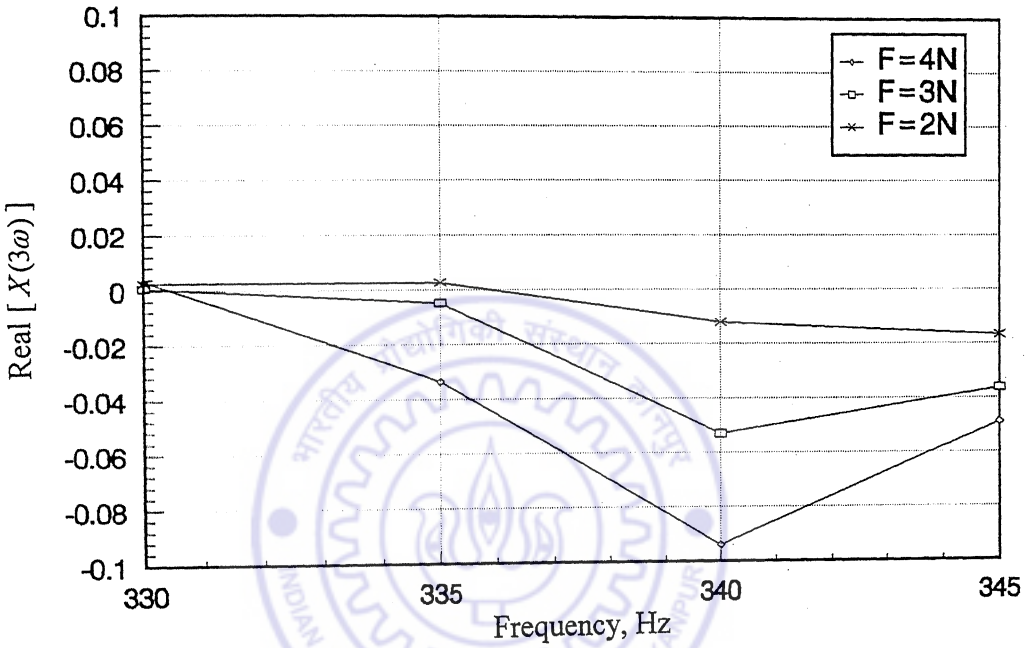

Figure 7.20 Variation in sign of real part of $X(3\omega)$ around $\omega_n/3$.

7.4 Validation

For validation of the experimentally estimated nonlinear stiffness parameter, analytical formulations of Harris (1984) and Ragulski et al (1974) are employed. These formulations are based on Hertz's theory of elastic contacts and treat the bearings in isolation of the shaft.

Figure 7.21 shows a typical isolated ball bearing configuration, in which external forces act along x-axis. η_i is the angle between load axis (i.e., x-axis) and the radial direction of a typical ith ball element. For a displacement (x,y) of the moving ring along the respective axes, total elastic force acting in radial direction at the point of contact of ith ball is given by

$$F_i = k_n (g + x\cos\eta_i + y\sin\eta_i)^{3/2} \tag{7.3}$$

and its projections along x and y axes respectively are

$$F_{xi} = k_n (g + x\cos\eta_i + y\sin\eta_i)^{3/2}\cos\eta_i \tag{7.4}$$

$$F_{yi} = k_n (g + x\cos\eta_i + y\sin\eta_i)^{3/2}\sin\eta_i \tag{7.5}$$

where g is the radial pre-load between the ball and the races, k_n is a coefficient of proportionality depending on the geometric and material properties of the bearing. The value of k_n, for the test bearing is estimated as 2.82×10^5 N/mm$^{1.5}$ (Harris,1984).

Total restoring force of the bearing is equal to sum of elastic forces of all the elements,

$$\text{i.e.,} \quad F = \sum_{i=1}^{n} F_{xi} \tag{7.6}$$

where n is the number of rolling elements in the bearing.

Using the condition of zero elastic force along y-axis (since no external force acts along this axis) and following equation (7.5), deformation y is obtained as

$$y = \frac{\sum_{i=1}^{n}[g + x\cos\eta_i]^{3/2}\sin\eta_i}{\sum_{i=1}^{n}[g + x\cos\eta_i]^{1/2}\sin^2\eta_i} \tag{7.7}$$

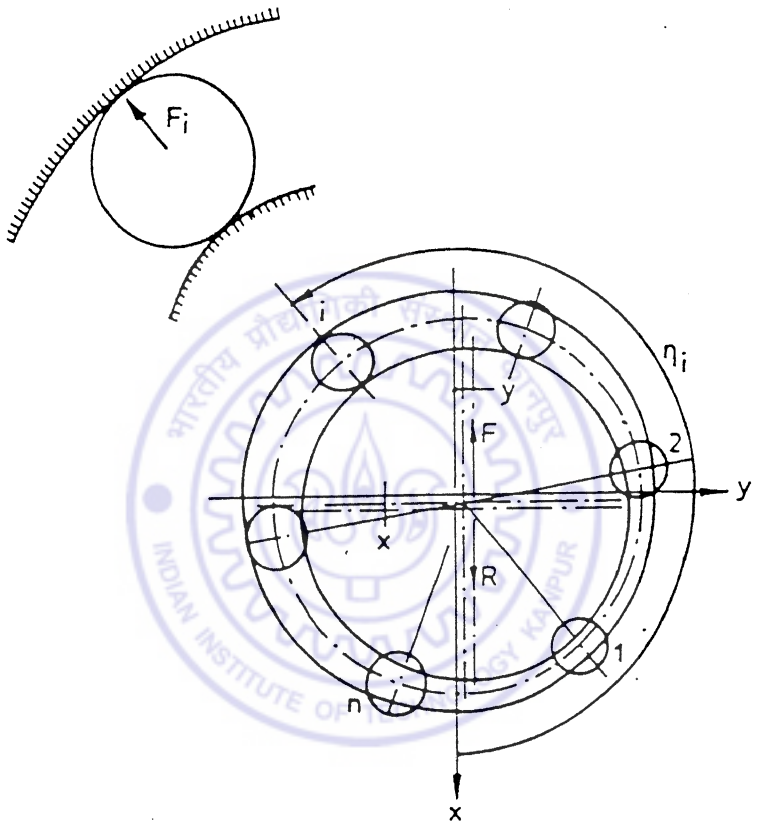

Fig. 7.21 Schematic diagram of a loaded ball bearing

Equations (7.4) and (7.7) are used in equation (7.6) and the bearing stiffness is determined as a function of deformation x as

$$k(x) = \partial F / \partial x \tag{7.8}$$

Substituting equation (7.6) in equation (7.8), taking into account equation (7.7) the bearing stiffness is expressed as a function of deformation as

$$k(x) = K_n \sum_{i=1}^{n} [g + x\cos\eta_i - (A/Bn)\sin\eta_i]^{1/2} [\cos\eta_i - \{CBn - AD(n-1)\}/(Bn)^2 \sin\eta_i] \cos\eta_i \tag{7.9}$$

where

$$A = \sum_{i=1}^{n} [g + x\cos\eta_i]^{3/2} \sin\eta_i \; ; \qquad B = \sum_{i=1}^{n} [g + x\cos\eta_i]^{3/2} \sin^2\eta_i$$

$$C = \sum_{i=1}^{n} [g + x\cos\eta_i]^{3/2} \sin\eta_i \cos\eta_i \qquad D = \sum_{i=1}^{n} [g + x\cos\eta_i]^{3/2} \sin^2\eta_i \cos\eta_i \tag{7.10}$$

It can be seen that the bearing stiffness is critically dependent on the pre-load g. Table 7.1 summerises the theoretical bearing stiffness parameters for different pre-load along with experimentally obtained stiffness parameters. The stiffness variations are graphically shown in Figure 7.22. The figure also shows experimental results of earlier researchers, Tiwari (1996) and Khan (1999), on the same experimental set up.

Table 7.1 Estimated and theoretical (Ragulski et al. 1974; Harris, 1984) bearing stiffness parameters.

Theoretical Stiffness (N/m)		Estimated Stiffness (N/m)
Pre-load (μm)	$k(x)$ from equation (7.8)	($k_1 - 3k_3x^2$)
0.2	$1.20\times10^7 - 4.01\times10^{19}x^2$	Case i): $1.585\times10^7 - 2.625\times10^{19}x^2$
0.3	$1.47\times10^7 - 2.18\times10^{19}x^2$	Case ii): $1.535\times10^7 - 4.285\times10^{19}x^2$
0.4	$1.69\times10^7 - 1.42\times10^{19}x^2$	Case iii): $1.586\times10^7 - 5.240\times10^{19}x^2$
0.5	$1.89\times10^7 - 1.02\times10^{19}x^2$	
0.6	$2.08\times10^7 - 0.61\times10^{19}x^2$	

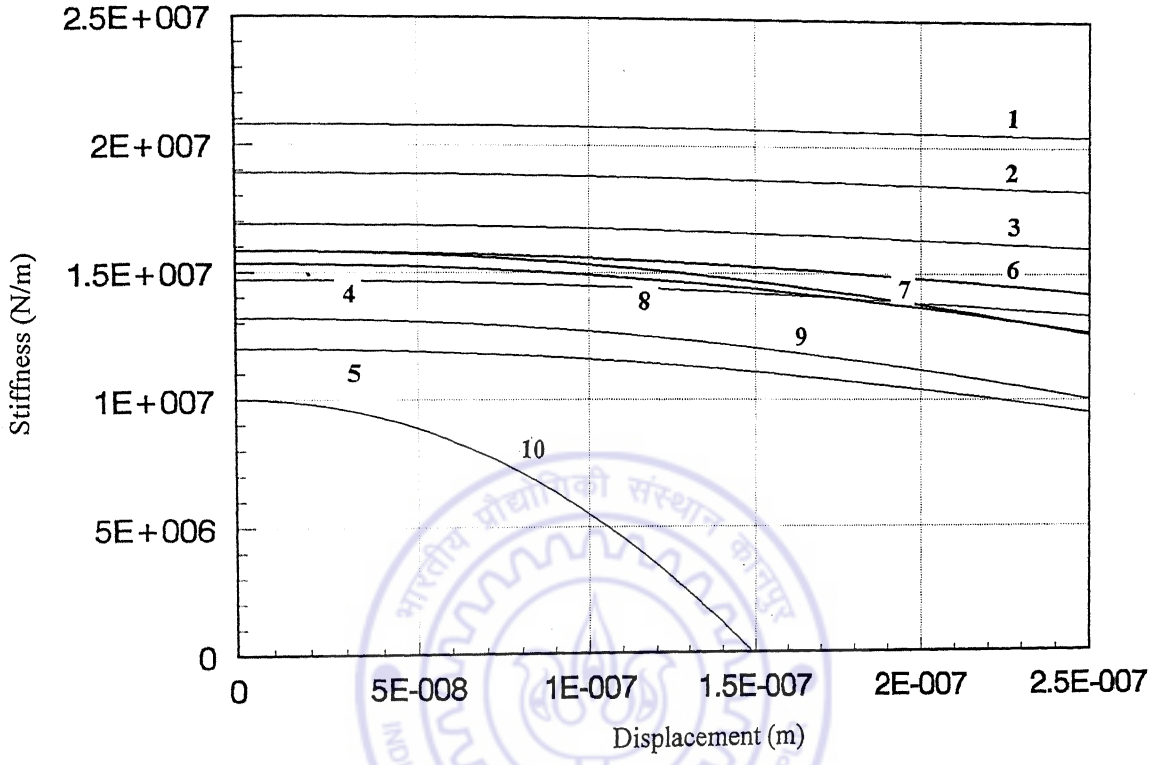

Fig. 7.22 Comparison of estimates of stiffness parameters

1-5: Theoretical values with pre-load 0.2, 0.3, 0.4, 0.5 and 0.6 μm respectively. [Harris(1984) and Ragulski et al. (1974)]

6,7,8: Present experimental estimates for cases I, II and III respectively.

9: Experimental estimate of Tiwari (1996).

10: Experimental estimate of Khan (1999)

7.5 Remarks

The stiffness parameter estimates from the experiment show reasonably good agreement with those from available analytical formulations for isolated ball bearings. The analytical formulation is dependent on the amount of preload and making numerical comparisons with experimentally estimated value is difficult. While, the manufacturer, at times may provide the preload range, the exact value of preloading of the bearing balls in the shaft-casing assembly, especially during operations which have involved wear and tear, would be difficult to determine. However the two sets of estimates are close. The nonlinearity in the rotor-bearing system was found to be of non-polynomial type. Parameter estimation has been based on its polynomial approximation for specific excitation amplitudes.

CHAPTER 8

CONCLUSION

The present study deals with the inverse problem of parameter estimation in nonlinear systems. Volterra theory for nonlinear analysis has been employed as a platform for development of identification and estimation procedures.

Procedures for identification of the type of nonlinearity are developed through analysis of structure of the system response as represented by Volterra Series. First and higher order components of the Volterra series response are analysed in the frequency domain. Characterstics of the harmonic contents of these components are employed in classification of system nonlinearity between polynomial and non-polynomial forms. Procedure to distinguish between symmetric and asymmetric forms is also presented. Techniques to estimate the series structure in case of polynomial nonlinearities are developed.

Issues relating to convergence of Volterra series have been investigated in detail. Series term expressions for individual harmonics in the response are developed and their convergence is discussed as a function of the excitation amplitude and frequency, system parameters and the number of terms to be employed in their approximation. The data generated can be usefully employed for design of experiments. A simple convergence criterion based on a ratio test is additionally suggested, which can be applied for wide frequency range and for any arbitrary number of series terms.

The estimation procedures employ measurements of various harmonics in the system response. Volterra kernel transforms are extracted from these harmonics. The first and higher order kernel transforms are related through unknown nonlinear parameters, for systems possessing polynomial form of nonlinearities. These relationships are analysed and employed along with the extracted values of the kernels to obtain estimates of nonlinear parameters through recursive iteration. The issue of measurability of higher harmonics for practical application has been analysed. A measurability index has been

defined and implicit errors and convergence aspects are quantitatively discussed. Procedures are illustrated through numerical simulation. The accuracy of estimates, including that of damping has been highlighted. Robustness of the algorithms, in presence of measurement noise, has been explored.

Procedures for parameter estimation for multi-degree-of-freedom systems are developed. Multi-input harmonic probing has been employed. Generic expressions for Volterra series representation of the response have been worked out. Convergence and error analysis has been carried out for the series and the estimation procedure is presented along with discussion on associated measurability issues. The procedures are demonstrated through case studies.

Experimental investigations have been carried out on a laboratory test rig of rotor-bearing system. Nonlinear bearing stiffness has been estimated by processing the vibration signals picked up from the bearing caps. Results are validated against those obtained from earlier investigations and theoretical approximations. Experiments were restricted to an available set-up, where the rotor was supported in ball bearings. Experimental work can be carried out in future on rotors supported in fluid-film bearings, in order to further investigate the utility of the procedures developed during the course of this study.

A limitation of the proposed methods is that they are applicable to polynomial forms of nonlinearity only. However, most non-polynomial forms can be suitably approximated by a polynomial form, within a specific range of response, and the procedures developed during the present study can be applied to them.

Estimation algorithms have been developed for nonlinear stiffness forces only. They can be readily extended and developed for the systems with nonlinear damping.

The theoretical platform provided by Volterra Series needs to be explored further for kernel characterization of systems with non-polynomial form of nonlinearities. Time domain input-output mapping may be more suitable for such investigations. This is an extensive area and is largely unexplored at present.

REFERENCES

Al-Hadid, M. A. and Wright, J. R., 1989, "*A Development of the Force State Mapping Technique for Nonlinear Systems and the Extension of the Location of Nonlinear Elements and Signal Processing*", Journal of Mechanical Systems and Signal Processing, **3**(3), pp. 269-290.

Ariaratnam, S. T., 1960, "*Random Vibration of Nonlinear Suspensions*", Journal of Mechanical Engineering Science, **2**(3),pp. 195-201.

Astrom, K. J. and Eykhoff, P., 1971, "*System Identification-A Survey*", Automatica, **7**, pp. 123-162.

Atkins, P. A., Wright, J. R. and Worden., K., 2000, "*An Extension Of Force Appropriation To The Identification Of Nonlinear Multi-Degree-Of-Freedom Systems*", Journal of Sound and Vibration, Vol. **237**(1), pp. 23-43.

Barret, J. F., 1963, "*The Use of Functionals in the Analysis of Nonlinear Physical Systems*", J. Electronic Control, **15**, pp. 567-615.

Baumgartner, S. L. and Rugh, W. J., 1975, "*Complete Identification of a Class of Nonlinear Systems from Steady-State Frequency Response*", IEEE Transactions on Circuits and Systems, **CAS-22**(9), pp. 753-759.

Bedrosian, E., and Rice, S.O., 1971, "*The Output Properties of Volterra Systems (Nonlinear System with Memory) Driven by Harmonic and Gaussian Inputs*", Proceedings of the IEEE, **59**(12), pp. 1688-1707.

Bendat, J. S., 1990, "*Nonlinear System Analysis and Identification from Random Data*", New York: John Wiley.

Bendat, J. S., and Piersol, A. G., 1982, "*Spectral Analysis of Nonlinear Systems Involving Square-Law Operations*", Journal of Sound and Vibrations, **81**(2), pp.199-213.

Bendat, J. S., and Piersol, A. G., 1986, "*Random Data Analysis and Measurement Procedures*", New York: Wiley-Interscience.

Bendat, J. S. and Piersol, A. G., 1986a, "*Decomposition of Wave Forces into Linear and Nonlinear Components*", Journal of Sound and Vibration, **106**(3), pp. 391-408.

Bendat, J. S., Palo, P. A. and Coppolino, R. N., 1992, "*A General Identification Technique for Nonlinear Differential Equations of Motion*", Probabilistic Engineering Mechanics, **7**, pp. 43-61.

Benhasi, Y., Penny, J. E. and Friswell, M. I., 1995, "*Identification of Damping Parameters of Vibrating Systems with Cubic Stiffness Nonlinearity*", Proceedings of 13th International Modal Analysis Conference pp. 623-629.

Billings, S. A., 1980, "*Identification of Nonlinear Systems-A Survey*", Proceedings of IEE, **127**(6), pp. 272-285.

Billings, S. A. and Fakhouri, S. Y., 1980, "*Identification of Nonlinear Systems usign Correlation Analysis and Pseudorandom Inputs*", International Journal of System Science, **11**(3), pp. 261-279.

Broersen, P. M. T., 1974, "*Estimation of Parameters of Nonlinear Dynamical Systems*", International Journal of Nonlinear Mechanics, **9**, pp. 355-361.

Boyd, S., Tang, Y. S. and Chua, L.O., 1983, "*Measuring Volterra Kernels*", IEEE Transactions on Circuits and Systems, **CAS-30**(8), pp. 571-577.

Brillinger, D. R., 1970, "*The Identification of Polynomial Systems by means of Higher Order Spectra*", Journal of Sound and Vibration, **12**(3), pp. 301-313.

Bussang, J. J., Ehrman, L. and Graham, J. W., 1974, "*Analysis of Nonlinear Systems with Multiple Inputs*", Proceedings of the IEEE, **62**(8), pp. 1088-1119.

Caughy, T. K., 1963, "*Derivation and Appplication of Fokker-Planck Equation to Discrete Non-Linear Dynamic Systems Subjected to White Random Excitation*", Journal of Acoustical Society of America, **35**(11), pp. 1683-1692.

Caughy, T. K. and Ma, F., 1983, "*The Exact Steady-State Solution of a Class of Nonlinear Stochastic Systems*", International Journal of Nonlinear Mechanics, **17**, pp. 137-142.

Choi, D., Miksad, R. W. and Powers, E. W., 1985, "*Application of Digital Cross-Bispectral Analysis Techniques to Model the Nonlinear Response of a Moored Vessel System in Random Seas*", Journal of Sound and Vibration, **99**(3), pp. 309-326.

Chrinstensen, S., 1968, "*On the Convergence of Volterra Series*", IEEE Transactions on Automatic Control, **13**, pp. 736-737.

Chua, L. O. and Liao, Y., 1989, "*Measuring Volterra kernels (II)*", Int. J. of Circuit Theory and Applications, **17**, pp.151-190.

Chua, L. O. and Liao, Y., 1991, *"Measuring Volterra kernels III: How to estimate the highest significant order"*, Int. J. of Circuit Theory and Applications, **19**, pp. 189-209.

Chua, L. O., and Ng., C. Y., 1979, "*Frequency Domain Analysis of Nonlinear Systems:General Theory*", IEE Journal on Electronic Circuits and Systems, **3**(4), pp. 165-185.

Chua, L. O., and Ng., C. Y., 1979a, "*Frequency Domain Analysis of Nonlinear Systems:Formulation of Transfer Functions*", IEE Journal on Electronic Circuits and Systems, **3**(6), pp. 257-267.

Chua, L. O. and Ushida, A., 1981, "*Algorithms for Computing Almost Periodic Steady-State Response of Nonlinear Systems to Multiple Input Frequencies*", IEEE Transactions on Circuits and Systems, **CAS-28**(10), pp. 953-971.

Chua, L. O. and Tang, Y. S., 1982, "*Nonlinear Oscillation Via Volterra Series*", IEEE Transactions on Circuits and Systems, **CAS-29**(3), pp. 150-168.

Czarniak, A. and Kudrewicz, J., 1984, *"The Convergence of Volterra Series for Nonlinear Networks*", IEEE Transactions on Circuits and Systems, **CAS-31**, pp. 751-752.

Distefano, N. and Rath, A., 1975, "*System Identification in Nonlinear Structural Seismic Dynamics*", Computer Method in Applied Mechanics and Engineering, **5**, pp. 353-372.

Dimentberg, M. F. and Sokolov, A. A., 1991, "*Identification of Restoring Force Nonlinearity from a System's Response to a White Noise Excitation*", International Journal of Nonlinear Mechanics, **26**(6), pp. 851-855.

Ewen, E. J. and Weiner, D. D., 1980, "*Identification of Weakly Nonlinear Systems Using Input and Output Measurements*", IEEE Transactions on Circuits and Systems, **CAS-27**(12), pp. 1255-1261.

Ewins, D. J., 1984, "*Modal Testing: Theory and Practice*", England: Research Studies Press.

Fakhouri, S. Y., 1980, "*Identification of a Class of Nonlinear Systems with Gaussian Non-White Inputs*", International Journal of System Science, **11**(5), pp. 541-555.

Fakhouri, S. Y., Billings, S. A. and Wormald, C. N., 1981, "*Analysis of Estimation Errors in the Identification of Nonlinear Systems*", Int. J. System Sci., Vol **12**(2), pp. 205-225.

Flake. R. H., 1963, "*Volterra Series Representation of Nonlinear Systems*", IEEE Transaction on App. Ind., **81**, pp. 810-815.

Fokker, A. P., 1914, "*Die mittlere energie rotierender electricher dipole im stahlungsfeld*", Aannals Physics, **43**, pp. 810-815.

French, A.S. and Butz E. G., 1973, "*Measuring the Wiener Kernels of a Nonlinear System using the Fast Fourier Transform Algorithm*", International Journal of Control, **17**(3), pp. 529-539.

French, A.S. and Butz E. G., 1974, "*The use of Walsh Functions in the Wiener Analysis of Nonlinear Systems*", IEEE Transaction on Computers, **C-23**(3), pp. 225-232.

Fretchet, M., 1910, "*Sur Les Fonctionnels Continues*", Annls. Scient. Ec. Norm. Sup., **27**, pp. 193-219.

Fritzen, S. J., 1986, "*Identification of Mass, Damping and Stiffness Matrices of Mechanical Systems*", Transactions of ASME, Journal of Vibration, Acoustics, Stress and Reliability in Design, **108**, pp. 9-16.

Gardiner, A. B., 1966, "*Elimination of the Effect of Nonlinearities on Process Cross-correlation*", Electron Lett., **2**, pp. 164-165.

Gardiner, A. B., 1968, "*Determination of the Linear Output Signal of a Process Containing Single-Valued Nonlinearities*", Electron Lett., **4**, pp. 224-226.

Gifford, S. J., 1993, "*Estimation of Second and Third Order Frequency Response Functions using Truncated Models*", Mechanical Systems and Signal Processing, Vol 7(2), pp. 145-160.

Gifford, S. J. and Tomlinson, G. R., 1989, "*Recent Advances in the Application of Functional Series to Nonlinear Structures*", Journal of Sound and Vibration, **135**(2), pp. 289-317.

Haber, R., 1989, "*Structural Identification of Quadratic Block-Oriented Models Based on Estimated Volterra Kernels*", International Journal of Systems Science, **20**(8), pp. 1355-1380.

Haber, R. and Unbehauen, H., 1990, "*Structure Identification of Nonlinear Dynamic Systems-A Survey on Input/Output Approaches*", Automatica, **26**(4), pp. 651-677.

Hanagud, S. V., Meyyappa, M. and Craig, J. I., 1985, "*Method of Multiple Scales and Identification of Nonlinear Structural Dynamic Systems*", AIAA Journal, **23**(5), pp. 802-807.

Harris, G. H. and Lapidus, L., 1967, "*The Identification of Nonlinear Systems*", Industrial and Engineering Chemistry, **59**(6), pp. 66-81.

Harris, T. A., 1984, "*Rolling Bearing Analysis*", New Tork: wiley.

Hung, G. and Stark, L., 1977, "*Introductory Review: The Kernel Identification Method: Review of Theory, Calculation, Application and Interpretation*", Mathematical Biosciences, **37**, pp. 135-190.

Ibanez, P., 1973, "*Identification of Dynamic Parameters of Linear and Nonlinear Structural Models form Experimental Data"*, Nuclear Engineering and Design, **25**, pp. 30-41.

Ibanez, P., 1988, "*A General Identification of a Nonlinear Single-Degree-of-Freedom Systems under Sinusoidal Excitation*", Proceedings of 6th International Modal Analysis Conference, pp. 777-782.

Ibrahim, S. R., 1973, "*Time Domain Modal Vibration Test Techniques*", Shock and Vibration Bulletin, **43**(4), pp. 21-25.

Katzenelson, J. and Gould, L., 1962, "*The Design of Nonlinear Filtering and Control Systems*", Part I, Inf. Control, **5**, pp. 108-143.

Khan, A. A., 1999, PhD thesis on "*Parameter Estimation in Nonlinear Rotor-Bearing Systems through Volterra and Wiener Theories*", I.I.T., Kanpur.

Khan, A. A. and Vyas, N. S., 1999, *"Nonlinear Parameter Estimation using Volterra and Wiener Theories*", Journal of Sound and Vibration, **221**(5), pp. 805-821.

Khan, A. A. and Vyas, N. S., 2001, "*Nonlinear Bearing Stiffness Parameter Estimation in Flexible Rotor-Bearing Systems using Volterra and Wiener* Approach", Probabilistic Engineering Mechanics, Vol.**6** (2), pp. 137-157.

Khan, A. A. and Vyas, N. S., 2001, "*Application of Volterra and Wiener theories for Nonlinear Parameter Estimation in a Rotor-Bearing System*", Nonlinear Dynamics, Vol.**24** No. 3, pp. 285-304.

Kolmogorov, A., 1931, "*Uber Die Analytischen Methoden in Wahrsheinlicheitsrechnung*", Mathematische Annalen, **104**, pp. 415-458.

Koukoulas, P. and Kalouptsidis, N., 1995, "*Nonlinear System Identification using Gaussian Inputs*", IEEE Transactions on Signal Processing, **43**(8), pp. 1831-1841.

Koh, T. and Powers, E. J., 1985, "*Second Order Volterra Filtering and its Application to Nonlinear System Identification*", IEEE Transaction on Acoustics, Speech and Signal Processing, **ASSP-33**, pp. 1445-1455.

Korenberg, M. J., 1973, "*Identification of Nonlinear Differential Systems*", JACC, pp. 597-603.

Korenberg, M. J. and Hunter, I. W., 1990, "*The Identification of Nonlinear Boilogical Systems: Wiener Kernel Approach*", Annals of Biomedical Engineering, **18**, pp. 629-654.

Lee,G. M., 1997, " *Estimation of Nonlinear System Parameters using Higher Order Frequency Response Functions*", Mechanical Systems and Signal Processing, **11**(2), pp. 219-228.

Lee, Y. W. and Schetzen, M., 1965, "*Measurement of Wiener Kernels of Nonlinear Systems by Cross correlation*", International Journal of Control, **2**(3), pp. 237-254.

Lesiak, C. and Krener, A. J., 1978, "*Existence and Uniqueness of Volterra Series*", IEEE Transaction on Automatic Control, **AC-23**, pp. 1090-1095.

Levy, E. C., 1959, "*Complex Curve Fitting*", IRE Transaction on Automatic Control, **AC-4**, pp. 37-44.

Marmarelis, P., and Naka, K. I., 1973, "*Nonlinear analysis and Synthesis of Receptive-Field Responses in the Catfish retina-I: Horizontal Cell Ganglion Cell Chain; II: One Input White Noise Analysis; III: Two Input White Noise Analysis*", Journal of Neurophysiology, **36**, pp. 605-648.

Marmarelis, P., and Naka, K. I., 1974, "*Identification of Multi-Input Biological Systems*", IEEE Transaction on Biomedical Engineering, **BME-21**, pp. 88-101.

Marmarelis, P. Z. and Udwadia, F. E., 1976, "*The Identification of Building Structural Systems-Part II: The Nonlinear Case*", Bulletin of the Seismological Society of America, **66**, pp. 153-171.

Masri, S. F. and Caughy, T. K., 1979, "*A Nonparametric Identification Technique for Nonlinear Dynamic Problems*", Transactions of ASME, Journal of Applied Mechanics, **46**, pp. 433-447.

Masri, S. F., Sassi, H. and Caughy, T. K., 1982, "*Nonparametric Identification of Nearly Arbitrary Nonlinear Systems*", Transactions of ASME, Journal of Applied Mechanics, **49**, pp. 619-627.

Masri, S.F., Miller, R. K., Saud,A. F. and Caughy, T. K., 1987, "*Identification of Nonlinear Vibrating Structures: Part I- Formulation*", Transactions of ASME, Journal of Applied Mechanics, **54**, pp. 918-922.

Masri, S.F., Miller, R. K., Saud,A. F. and Caughy, T. K., 1987, "*Identification of Nonlinear Vibrating Structures: Part II-Applications*", Transactions of ASME, Journal of Applied Mechanics, 54, pp. 923-929.

McNiven, H. D. and Matzen, V. C., 1978, "*A Mathematical Model to Predict the Inelastic Response of a Steel Frame-Part I: Formulation of the Model; Part II: Establishment of Parameters from Shaking table Experiments*", International Journal of Earthquake Engineering and Structural Dynamics, **6**, pp. 189-202.

Mohammad, K. S., Worden, K. and Tomlinson, G. R., 1992, "*Direct Parameter Estimation for Linear and Nonlinear Structures*", Journal of Sound and Vibration, **152**(3), pp. 471-499.

Mook, D. J., 1989, "*Estimation and Identification of Nonlinear Dynamic Systems*", AIAA Journal, **27**(7), pp. 968-974.

Mottershead, J. E. and Stanway, R., 1986, "*Identification of Nth-Power Velocity Damping*", Journal of Sound and Vibration, **105**(2), pp. 309-319.

Nam, S. W., Kim, S. B. and Powers, E. J., 1990, "*Nonlinear System Identification with Random Excitation using Third Order Volterra Series*", Proceedings of 8th International Modal Analysis Conference, pp. 1278-1283.

Nayfeh, A. H., 1985, "*Parametric Identification of Nonlinear Dynamic Systems*", Computers & Structures, **20**, pp. 487-493.

Nayfeh, A. H. and Mook, D. T., 1979, "Nonlinear Oscillations", New York: John Wiley and Sons.

Odiari, E. A. and Ewins, D. J., 1992, "*Parameter Identification for Nonlinear Rotor-Stator Systems-The Volterra/Wiener Based Approach*", Proceedings of Institution of Mechanical Engineers (IMechE) Conference on Vibrations in Rotating Machineries, pp. 193-202.

Orabi, I. I. And Ahmadi, G., 1987, "*A Functional Series Expansion Method for Response Analysis of Nonlinear Systems Subjected to Random Excitations*", International Journal of Nonlinear Mechanics, **22**(6), pp. 451-465.

Palm, G. and Poggio, T., 1977, "*The Volterra Representation and Wiener Expansion: Validity and Pitfalls*", SIAM Journal of Appl. Math., 33(2), pp. 195-216.

Palm, G. and Popel, B., 1985, "Volterra Representation and Wiener like Identification of Nonlinear Systems: Scope and Limitations", Quarterly Review of Biophysics, Vol. **18**, pp. 135-164.

Planck, M., 1917, "Uber Einen Satz der Statischen Dynamik und Seine Erweiterung in der Quanten-Theorie", Sitzungber, Preuss. Akademie Weiss, pp. 324-341.

Ragulskis, K. M., Jurkauskas, A. Yu., Atstupenas, V. V., Vitkute, A. Yu. And Kulvec, A. P., 1974, "*Vibration in Bearings*", Vilnyus: Mintis Publishers.

Rice, H. J. and Fitzpatrick, J. A., 1988, "*A Generalised Technique for Spectral Analysis of Nonlinear Systems*", Mechanical Systems and Signal Processing, **2**(2), pp. 195-207.

Rice, H. J. and Fitzpatrick, J. A., 1991, "*The Measurement of Nonlinear Damping in Single-Degree-of Freedom Systems*", Transaction of ASME, Journal of Vibration and Acoustics, **113**, pp. 132-140.

Rice, H. J. and Fitzpatrick, J. A., 1991, "*A Procedure for the Identification of Linear and Nonlinear Multi-Degree-of-Freedom Systems*", Journal of Sound and Vibration, **149**(3), pp. 397-411.

Richards, C. M. and Singh, R., 1998, "*Identification Of Multi-Degree-Of-Freedom Nonlinear Systems Under Random Excitations By The Reverse Path Spectral Method*", Journal of Sound and Vibration, Vol. **213**, pp. 673-708.

Richards, C. M. and Singh, R., 1999, "*Feasibility Of Identifying Nonlinear Vibratory Systems Consisting Of Unknown Polynomial Forms*", Journal of Sound and Vibration, Vol. **220** (3), pp. 413-450.

Richards,C. M. and Singh, R., 2000,"*Comparison of Two Nonlinear System Identification Approaches Derived from 'Reverse Path' Spectral Analysis*", Journal of Sound and Vibration, Vol. **237**(2), pp. 361-376.

Rugh, W. J., 1981, "*Nonlinear System Theory: The Volterra/Wiener Approach*", John Hopkins University Press, Baltimore, Maryland.

Sandberg, I. W., 1992, "*Uniform Approximation with Doubly Finite Volterra Series*", IEEE Transactions on Signal Processing, **40**, pp. 1438-1442.

Sandberg, A. and Stark, L., 1968, "*Wiener G-Function Analysis as an Approach to Nonlinear Characteristics of Human Pupil Light Reflex*", Brain Res., **11**, pp. 194-211.

Schetzen, M., 1965, "*Measurement of the Kernels of a Nonlinear System of Finite Order*", International Journal of Control, **1**(3), pp. 251-263.

Schetzen, M., 1965a, "*Synthesis of a Class of Nonlinear Systems*", International Journal of Control, **1**(5), pp. 401-414.

Schetzen, M., 1974, "*A Theory of Nonlinear System Identification*", International Journal of Control, **20**(4), pp. 577-592

Schetzen, M., 1980, "*The Volterra and Wiener Theories of Nonlinear Systems*", New York: John Wiley and Sons.

Simpson. R. J. and Powers, H. M., 1972, "*Correlation Techniques for the Identification of Nonlinear Systems", Measurement and Control*, Vol. **5**, pp. 316-321.

Storer, D. M. and Tomlinson, G. R., 1993, "*Recent Developments in the Measurement and Interpretation of Higher Order Transfer Functions from Nonlinear Structure*", Mechanical Systems and Signal Processing, Vol 7(2), pp. 173-189.

Tiwari, R. and Vyas, N. S., 1995, "Estimation of Nonlinear Stiffness Parameters of Rolling Element Bearings from Random Response of Rotor Bearing Systems", Journal of Sound and Vibration, **187**(2), pp. 229-239.

Tiwari, R. and Vyas, N. S., 1997, "*Nonlinear Bearing Stiffness Parameter Extraction from Random Response in Flexible Rotor-Bearing Systems*", Journal of Sound and Vibration, **203**(3), pp. 389-408.

Tiwari, R. and Vyas, N. S., 1997a, "*Parameter Estimation in Imbalanced Nonlinear Rotor-Bearing Systems from Random Response*", Journal of Sound and Vibration, **208**(1), pp. 1-14

Tiwari, R. and Vyas, N. S., 1998, "*Stiffness Estimation from Random Response in Multi-Mass Rotor-Bearing Systems", Probabilistic Engineering Mechanics*, **13**(4), pp. 255-268.

Tomlinson, G. R., Manson, G. and Lee, G. M., 1996, "*A Simple Criterion for Establishing an Upper Limit to the Harmonic Excitation Level of the Duffing Oscillator using the Volterra Series*", Journal of Sound and Vibration, **190**(5), pp. 751-762.

Udwadia, F. E. and Kuo, C. P., 1981, "*Nonparametric Identification of a Class of Nonlinear Close-Coupled Dynamic systems*", Earthquake Engineering and Structural Dynamics, **9**, pp. 385-409.

Ushida, A. and Chua, L. O., 1984, "*Frequnecy-Domain Analysis of Nonlinear Circuits Driven by Multi-Tone Signals*", IEEE Transactions on Circuits and Systems, **CAS-31**(9), pp. 766-778.

Victor, J. and Shapley, R., 1980, "*A Method of Nonlinear Analysis in the Frequency Domain*", Biophysical Journal, **29**, pp. 459-484.

Volterra, V., 1930, "*Theory of Functionals*", Glasgow: Blackie and Sons.

Volterra, V., 1959, "*Theory of Functionals and of Integral and integro-Differential Equations*", New York: Dover Publications Inc.

Wiener, N., 1958, "*Nonlinear Problems in Random Theory*", New York: Wiley.

Weiner, D. D. and Spina, J. F., 1980, "Sinusoidal Analysis and Modelling of Weakly Nonlinear Systems", New York: Van Nostrand Reinhold Company.

Whitefield, A. H. and Messali, N., 1987, *"Integral-Equation approach to System Identification*", International Journal of Control, **45**(4), pp. 1431-1445.

Worden, K. and Tomlinson, G. R., 1989, "*Application of the Restoring Force Surface Method to Nonlinear Elements*", Proceedings of 7th International Modal Analysis Conference, Los Angeles, pp. 1347-1355.

Worden, K., Manson, G. and Tomlinson, G. R., 1997, "*A Harmonic Probing Algorithm for the Multi-Input Volterra Series*", Journal of Sound and Vibration, **201**(1), pp. 67-84.

Wysocki, E. M. and Rugh, W. J., 1976, "*Further Results on the Identification Problem for the Class of Nonlinear Systems* S_M", IEEE Transactions on Circuits and Systems, **CAS-23**(11), pp. 664-670.

Xiaojiang, M., Xia, Y. J. and Piede, L., 1990 , "*A New Nonlinear Modal Parameters Identification Method*", Proceedings of 8th International Modal analysis Conference, pp. 1381-1385.

Yasui, S., 1979, "*Stochastic Functional Fourier Series, Volterra Series, and Nonlinear Systems Analysis*", IEEE Transactions on Automatic Control, **AC-24**(2), pp.230-242.

Yang, Y. and Ibrahim, S. R., 1985, " *A Nonparametric Identification Technique for a Variety of Discrete Nonlinear Vibrating Systems*", ASME Journal of Vibration, Acoustics, Stress and Reliabilty in Design, **107**, pp. 60-66.

Yun, C. B. and Shinozuka, M., 1980, "*Identification of Nonlinear Structural Dynamic Systems*", Journal of Struct. Mech., **8**(2), pp. 187-203.

List of publications from the present research work

Published

1) Animesh Chatterjee and N.S.Vyas, 2000, " *Convergence Analysis of Volterra Series Response of Nonlinear Systems Subjected to Harmonic Excitation*", Journal of Sound and Vibration, Vol. **236**(2), pp. 339-358.

2) Animesh Chatterjee and N.S.Vyas, 2001, "*Stiffness Nonlinearity Classification through Structured Response Component Analysis using Volterra Series*", Mechanical Systems and Signal processing, Vol. **15**(2), pp 323-336.

3) N.S.Vyas and Animesh Chatterjee, "*Nonlinear System Identification and Volterra – Wiener Theories*", Proc. I international conference, VETOMAC, Bangalore, India, 2000.

Communicated for Publication

4) Animesh Chatterjee and N.S.Vyas, "*Nonlinear Parameter Estimation through Volterra Series using Method of Recursive Iteration* ", communicated to Journal of Sound and Vibration.

5) Animesh Chatterjee and N.S.Vyas, "*Multi-input Volterra Series and Parameter Estimation in Multi-Degree-of-Freedom Nonlinear systems*", communicated to Mechanical Systems and Signal Processing

6) Animesh Chatterjee and N.S.Vyas, " *Analytical and Experimental Investigations on Nonlinear Parameter Estimation in Rotor Bearing System using Volterra Series*", communicated to Transactions of ASME, Journal of Vibration and Acoustics.

7) Animesh Chatterjee and N. S. Vyas, "*Nonlinear Parameter Estimation using Volterra Series with Multi-Tone Excitation*", communicated for presentation in international conference of IMAC-XX, Los Angeles, 2002.